Socioeconomic and Epidemiologic Modeling: A Fractional Differintegral Approach

THESIS

Submitted in partial fulfillment of the requirements

for the degree of

DOCTOR OF PHILOSOPHY

by

Komal

ID No. 2019PHXF0041P

Under the Supervision of

Prof. Trilok Mathur

Birla Institute of Technology and Science, Pilani, Pilani Campus, India

BIRLA INSTITUTE OF TECHNOLOGY AND SCIENCE, PILANI

Pilani Campus, Rajasthan, India

2024

“Exploration of the unknown, leading to

the discovery of the known.”

W.S. Gilbert

BIRLA INSTITUTE OF TECHNOLOGY AND SCIENCE, PILANI

PILANI CAMPUS, RAJASTHAN, INDIA

CERTIFICATE

This is to certify that the thesis entitled, **"Socioeconomic and Epidemiologic Modeling: A Fractional Differintegral Approach"** submitted by **Ms. Komal** ID No. **2019PHXF0041P** for the award of Ph.D. degree of the institute embodies original work done by her under my supervision.

_____

Signature of the Supervisor

Name : **PROF. TRILOK MATHUR**

Designation : **Associate Professor**

Department of Mathematics

BITS Pilani, Pilani Campus

Date: __/__/____

Dedicated to

My Beloved Mother

Acknowledgements

A journey is undoubtedly smoother when you have companions. During my Ph.D. journey, I've been fortunate to have the company and support of numerous individuals. I am profoundly grateful to all those who have contributed to the successful completion of this doctoral journey, which would not have been possible without their unwavering support, guidance, and encouragement. First and foremost, I express my deepest gratitude to the Almighty God for granting me the strength, wisdom, and perseverance throughout this journey.

I would like to extend my heartfelt gratitude to my supervisor, Prof. Trilok Mathur, for his mentorship, insightful guidance, and invaluable feedback throughout the entire research process. His expertise and dedication have been instrumental in shaping the direction of this thesis. His passion for the subject, patience in addressing my queries, and commitment to excellence have been truly inspiring. He has not only been a guide in academia but also a source of motivation during the challenging phases. His belief in my potential has encouraged me to strive for higher standards. The collaborative atmosphere he fostered in our interactions has been instrumental in broadening my perspectives. I am grateful for the opportunity to learn under his mentorship. I truly appreciate his dedication to my intellectual growth, his willingness to invest time and effort, and his role as a constant pillar of support.

I am also thankful to all the professors of the Department of Mathematics of BITS Pilani, Pilani Campus, for their guidance and valuable suggestions in my research work. I feel fortunate to have my Doctoral Advisory Committee (DAC) members, Prof. Shivi Agarwal and Dr. Gaurav Dwivedi, for their insightful discussions, constructive criticism, and valuable suggestions that have significantly enriched the quality of this work.

I am grateful to Prof. Bhupendra Kumar Sharma (Former Head of the Department), and Prof. Devendra Kumar, Head of the Department of Mathematics, for their unwavering support. I extend my acknowledgment to all the faculty members and research scholars for

their valuable assistance and cooperation throughout my research journey. The moments we've shared hold a special corner in my heart and will be cherished for eternity. I convey my heartfelt appreciation for the valuable contribution you've made to my academic journey.

I want to express my gratitude to my parents, Mrs. Geeta Devi and Mr. Jaibhagwan, for showering me with boundless love and unwavering encouragement, which have been like a deep well of inspiration. Their invaluable guidance and wisdom have significantly shaped my academic journey. I extend my thanks to my brothers, Dikshit Bansal and Monu Goyal, for their steadfast belief in me. Their constant motivation has been an unending source of inspiration, propelling me forward in my studies. My sister, Himanshu, your unwavering support has been a steady anchor, providing relief during the highs and lows of this journey. I would also like to give my special affection to my little masters, Jiyanshi and Suryansh, your smiles have illuminated my path, reminding me of the greater purpose behind my hard work and learning.

I am thankful to my colleagues and fellow researchers, Deepak sir, Sugandha di, Barkha di, Pallav sir, Sandeep sir, Komal di, Sonali di, Parveen, and Babli whose engaging discussions and camaraderie have fostered an environment conducive to intellectual growth. Not to forget, I could not have completed this thesis without my friends, Himanshu Verma & Meghana who provided stimulating discussions and happy distractions to rest my mind outside research.

I must acknowledge the financial support provided by CSIR/UGC, which enabled me to carry out this research effectively and efficiently. I am also thankful to the office staff members who helped me with all the formalities. This journey has been a collective effort, and my deepest gratitude goes to each and every individual for helping me to reach this milestone.

Place: BITS Pilani, Pilani Campus

Date: __/__/____ **Komal**

Abstract

This thesis embarks on a journey to uncover the enigmas of fractional calculus, addressing its theoretical intricacies and practical implications. The examination will focus on the historical evolution, beginning with the pioneering works of Euler and Leibniz that laid the groundwork for traditional calculus and tracing the development of fractional calculus through Liouville, Riemann, and beyond contributions. Additionally, we will explore the mathematical properties and fundamental theorems underlying fractional calculus, shedding light on its unique characteristics that set it apart from integer-order calculus. Fractional-order mathematical modeling has emerged as a powerful tool for describing complex systems with non-integer dynamics, finding applications across a wide range of scientific disciplines. This doctoral thesis delves into the realm of fractional-order mathematical modeling, exploring its theoretical underpinnings, computational methods, and diverse applications.

Moreover, the thesis will delve into a rich array of applications, showcasing how fractional calculus has been harnessed to solve complex problems in fields such as sociology, economics, and epidemiology. The thesis begins by providing a comprehensive overview of the fundamentals of fractional calculus, elucidating the significance of fractional derivatives and integrals in capturing memory and hereditary effects in real-world systems. The subsequent segment will identify gaps in existing research to formulate the overarching objective of the thesis. The core of the thesis revolves around the applications of fractional-order mathematical modeling in diverse domains of socioeconomic and epidemiology and explores the efficacy of fractional-order models in capturing complex behaviors that elude traditional integer-order models.

Firstly, this thesis extensively explores the multifaceted dynamics of criminal behavior in the twenty-first century. Criminologists have conducted an exhaustive study covering biological, psychological, sociological, and economic aspects to comprehend the intricate factors that shape criminal conduct. A notable observation reveals that offspring of criminal parents exhibit a twofold likelihood of acquiring criminal convictions compared

to their counterparts from non-criminal families. Integer-order mathematical models cannot determine the high degree of accuracy necessary to explain the transmission process. In light of this challenge, fractional calculus emerges as a potent analytical tool capable of surpassing the limitations of integer-order models. Fractional calculus depicts and manages the retention and transmission nuances inherent in diverse materials. Consequently, fractional differential equations emerge as the novel approach employed to address the inherent complexities within this realm. By harnessing the power of fractional calculus, Chapter 2, Chapter 3, and Chapter 4 contribute to a more nuanced understanding of criminal behavior transmission processes, shedding light on the intricate interplay of factors that contribute to the persistence of criminal tendencies across generations.

Due to the alarming increase in the categories of crimes committed and the number of criminal activities around the globe, there is an urgent need to revise the current policies and models adopted by judicial institutions. Most mathematical models do not account for the offender's criminal history, which is essential for controlling crime transmission within the specified time frame. In addition, a substantial number of perpetrators have not been imprisoned due to external factors and policies. To address these societal problems, Chapter 2 proposes a fractional-order crime transmission model by clustering the extant population into four distinct groups. These groups consist of law-abiding citizens, criminally active individuals who have not been incarcerated, prisoners, and released prisoners. In addition, the proposed model is extended to the delayed model by incorporating the time-delay coefficient to account for the time gap between the offender's offense and their conviction. Until a certain point, the endemic equilibrium of the delayed model is locally asymptotically stable, after which bifurcation occurs.

Various studies present different mathematical models of ordinary and fractional differential equations to reduce delinquent behavior and encourage prosocial growth. However, these models do not consider the non-linear transmission rate, which depicts reality better than the linear transmission rate, as the relationship between non-criminals and criminals is not linear, according to the National Crime Records Bureau, Government of India. In light of this, a novel fractional-order mathematical crime propagation model

with a non-linear Beddington-DeAngelis transmission rate is proposed in Chapter 3 that divides the entire population into three clusters. The present study also compares the crime transmission models for various transmission rates, followed by an analytical investigation. In addition, this research investigates the incidence of transcritical bifurcation at the criminal-free equilibrium point. In summary, the finding of this research suggests that as the order of derivative increases, the population approaches equilibrium more swiftly, and criminals decline with time for the different orders of derivative.

Everyone is affected by crime in some manner and criminal activity spreads through peer influence and is contagious. Several mathematical models for predicting crime transmission have been proposed in various studies. However, these models do not account for an individual's logistic development, which is required to describe criminal behavior changes. As a result, Chapter 4 presents a fractional-order mathematical model of crime transmission that considers the logistic growth of law-abiding people. Numerical simulations have been performed to validate the analytical findings, further supporting our qualitative conclusions and establishing the role of different crucial parameters and variables used in the proposed model. The model with logistic growth outperforms the exponential model to capture reality. The results reveal that offenders survive as long as the coefficient of law enforcement remains below a specific threshold value. The criminals start vanishing once this value is achieved.

Another application of fractional calculus, the impact of social media on academics in sociology, is examined in Chapter 5. Due to covid pandemic and lockdown, usage of the social platform has increased not only for entertainment purposes but also for academic purposes. As a result, students are at significant risk of developing social media addiction, so techniques to control social media addiction transmission throughout society are required. There are several positive and negative ways in which social media affects the academic performance of a student. Hence, there is a pressing need to modify existing regulations and approaches. Most of the earlier systems did not include the impact of social media addiction on academics as well as memory/past history. The most common causes of social media addiction are chronic stress, trauma, mental illness, and a family

history of addiction. So, a fractional-order mathematical model is required to overcome this issue and show how memory affects the influence of the social network on students. Hence, Chapter 5 offers a fractional-order mathematical model to analyze the impact of social media on academics to solve the aforementioned societal concerns. This model is analyzed qualitatively and quantitatively and has obtained two equilibrium points. Based on an evaluation of the threshold value, the social web free equilibrium point is globally asymptotically stable whenever the threshold value is less than one. Addicted equilibrium points exist when the threshold value is more than one. Finally, numerical simulations have been performed to examine changes in population dynamics and validate analytical predictions. The primary aim of this chapter is to optimize the utilization of social media to contribute to a more promising future for students by optimizing the order of derivative.

Addressing one of the significant economic challenges, namely unemployment, involves the application of fractional differential equations. The global impact of high unemployment rates has significant economic and social consequences. To overcome this, various skill development programs are initiated by governments of developing countries. But the problem of unemployment is still increasing day by day. So, there is a pressing necessity to revise the current policies and models. The past history of a region or country has a significant impact on its current unemployment situation. The historical context profoundly affects current unemployment, considering factors like economic cycles, government policies, education, and technological advancements. Policymakers should acknowledge this history to address challenges effectively. Therefore, Chapter 6 proposes a fractional-order mathematical model that examines the impact of various skill development programs for youths. The primary goal of this research is to examine the impact of training programs aimed at enhancing the abilities of unemployed individuals, with the ultimate goal of reducing the overall unemployment rate. This chapter also explores the possibility of transcritical bifurcation and investigates the impact of skill development on the unemployment rate. The numerical simulations are conducted to validate our analytical findings, further supporting our qualitative conclusions. These simulations help illustrate the unemployment dynamics and confirm the stability and behavior of the equilibrium

points predicted by the mathematical model.

The application of fractional calculus in epidemiology is discussed in Chapter 7. Despite modern medical developments, infectious diseases continue to impact millions worldwide. Malaria, for instance, is a significant cause of mortality and suffering in developed and developing countries. The most challenging hurdle for scientists to control this disease is the parasite's propensity to develop resistance to novel medicines and treatment approaches, as mosquitoes have memory and hereditary properties. Therefore, Chapter 7 presents a novel fractional-order model of malaria transmission that integrates drug resistance development and therapy as a preventative measure. In addition, sensitivity analysis has been performed to demonstrate the variation of findings for the different parameters. The research has broad implications for healthcare, including the need to achieve high treatment and immunity development rates while minimizing the emergence of drug resistance due to treatment failure. In summary, this research sheds light on this terrible pandemic's nature by assessing the impact of treatment rates and resistance levels.

In Chapter 8, the research endeavors are synthesized, offering a thorough overview of pivotal discoveries and emphasizing prospects for forthcoming investigations.

In summary, this thesis contributes to the advancement of fractional-order mathematical modeling by providing a comprehensive exploration of its theoretical foundations, numerical methodologies, and applications across diverse scientific disciplines. The insights gained from this research have the potential to reshape how complex systems are understood, analyzed, and controlled, leading to advancements in science that capitalize on the rich dynamics captured by fractional-order models.

Keywords: Fractional calculus, Mathematical modeling, Caputo derivative, Crime transmission, Social media users, Unemployment, Malaria, Drug resistance, Equilibrium points, Stability, Bifurcation, Routh-Hurwitz Criteria, Lyapunov function.

Contents

List of Symbols

$\mathbb{N}$	Natural number
$\mathbb{R}$	Real number
$\mathbb{C}$	Complex number
$\mathbb{R}^n$	Real coordinate space of dimension n
$\mathcal{L}$	Laplace transformation
$\mathcal{C}^n[a,b]$	n time differentiable with each derivative continuous
Γ	Gamma function
$\mathbb{E}_{\eta,\gamma}$	Mittage- Leffler function
η	Order of derivative
S	Non-Criminals
C	Criminals/ Offender
R	Recovered
P	Prisoners
X	Non-Users of Social Media
S_L	Less Active Users of Social media
S_A	Active Users of Social media
H_P	High Performing Students
L_P	Low Performing Students
U	Unemployed Individuals
E	Employed Individuals
S_U	Skilled Unemployed
V	Number of Vacancy
S_h	Susceptible Human
I_h	Infected Human
R_h^I	Human with Drug Resistance Level 1

R_h^{II}	Human with Drug Resistance Level 2
R_h^{III}	Human with Drug Resistance Level 3
S_m	Susceptible Mosquitoes
I_m	Infected Mosquitoes
A	Recruitment rate of Non-Criminals
α	Rate from which people switch from S to C (crime indulgment)
ξ	Rate of moving back to society from recovered class (criminal or non-criminal class)
δ	Rate of release from prison to R
δ_1	Rate of release from prison to S
μ	Birth rate
l	Rate of law-enforcement for criminal
ϱ	Natural death rate
A_h	Recruitment rate of susceptible human population
A_m	Recruitment rate of mosquito population
β_1	Rate at which people switch from S_h to I_h
β_2	Rate at which mosquito switch from S_m to I_m
α_1	Rate that humans in I_h class acquire partial immunity and switch to S_h
α_2	Rate that humans in R_h^I class acquire partial immunity and switch to S_h
α_3	Rate that humans in R_h^{II} class acquire partial immunity and switch to S_h
α_4	Rate that humans in R_h^{III} class acquire partial immunity and switch to S_h
θ_1	Rate from which people switch from I_h to R_h^I
θ_2	Rate from which people switch from R_h^I to R_h^{II}
θ_3	Rate from which people switch from R_h^{II} to R_h^{III}
θ_4	Rate from which people switch from I_h to R_h^{II}
θ_5	Rate from which people switch from I_h to R_h^{III}
d_h	Mortality rate of human population due to malaria
d_m	Mortality rate of mosquito population due to malaria
$\tilde{A}$	Recruitment rate of non-user of social media

$\tilde{\beta}$	Rate at which student switch from the X to S_L
$\tilde{\theta_1}$	Rate from which student switch from S_L to S_A
$\tilde{\delta}$	Rate from which student switch from S_A to S_L
$\tilde{\tau_1}$	Rate of performing high by less involved users
$\tilde{\tau_2}$	Rate of performing low by less involved users
$\tilde{\alpha_1}$	Rate of performing high by active users
$\tilde{\alpha_2}$	Rate of performing low by active web users
$\tilde{\theta_2}$	Rate at which low-performing students are switched to less involved users
$\tilde{\rho_1}$	Graduation rate as a consequence of outstanding results
$\tilde{\rho_2}$	withdrawal rate as a consequence of poor performance
$\grave{\Lambda}$	Recruitment rate of unemployed individuals
$\grave{\sigma}$	Rate of unemployed individual transitions into skilled-unemployed
$\grave{\kappa_1}$	Rate of unemployed transitions into employment class
$\grave{\kappa_2}$	Rate of skilled unemployed individuals transitioning into employment class
$\grave{\beta}$	Rate of employed individuals are resigning, being fired, or dismissed from their jobs
$\grave{d_1}$	Rate of unemployed individuals migrate or pass away
$\grave{d_2}$	Rate of employed individuals migrate, retire, or pass away
$\grave{\delta}$	Diminution rate

List of Tables

List of Figures

Chapter 1

Introduction

The art of proposing a question must be held of higher value than solving it.

— Georg Cantor

Exploring certain mathematical concepts from a slightly different perspective can often unveil concealed insights. Take, for instance, the concepts of continuity and differentiability of a real-valued function $f : \mathbb{R} \to \mathbb{R}$, both rooted in limit notions, albeit defined differently. However, the latter concept divulges more intricate geometric aspects of a function than the former. This sort of abstraction not only fuels curiosity but also serves to simplify complex details and widen the spectrum of its applications. An illustrative example is the prime number theorem, a renowned theorem in number theory. Surprisingly, its initial proof ventures into the terrain of complex analysis. This exemplifies how extending a mathematical concept can breathe fresh life into it and offer novel perspectives to tackle a broader array of problems. Going back to the historical exchange between Leibniz and L'Hopital, a pivotal question was posed: "Can the framework of derivatives, traditionally reserved for integer orders, be expanded to encompass non-integer orders?" This inquiry ignited the intellectual curiosity of luminaries like Euler, Laplace, Fourier, Lacroix, Lagrange, Abel, Riemann, and Liouville, culminating in the formulation of the theory of fractional integrals and derivatives [1–3]. This theory addresses the question's profound implications, unraveling the potential of derivatives with fractional orders.

The inspiration for this thesis arises from the increasingly recognized potency of frac-

tional calculus in modeling and comprehending intricate systems [1, 3–7]. This exhaustive investigation endeavors to delve into the fundamental tenets, theoretical foundation, and diverse applications of fractional calculus across a variety of domains. This dissertation investigates the mathematical properties and fundamental theorems distinguishing fractional calculus from its integer-order counterpart. Furthermore, this thesis explores a number of applications, highlighting how fractional calculus has been utilized to solve complex socio-economic and epidemiological problems. An introductory chapter introduces key concepts, such as fractional calculus, mathematical modeling, and fractional-order mathematical modeling in various domains, such as crime transmission, unemployment, social media addiction, and Malaria transmission. In addition, this chapter provides the necessary definitions, theorems, and evaluation parameters for developing and analyzing proposed models.

1.1 Fractional Calculus

In the field of mathematical analysis, the foundations of classical calculus have played a significant role in advancing science and engineering by providing a solid mathematical framework for modeling and comprehending a wide range of natural phenomena. As the complexities of real-world systems become more apparent, it becomes clear that traditional calculus has limitations in capturing and elucidating the complex dynamics demonstrated by various processes. In response to these challenges, fractional calculus has emerged as a compelling extension of classical calculus, offering a novel perspective for characterizing and analyzing systems characterized by memory, long-range dependencies, and behaviors that extend beyond local interactions.

Fractional calculus, an applied mathematical discipline, focuses on manipulating derivatives and integrals with varying degrees. While the inception of fractional derivatives dates back more than three centuries, the advancement of fractional calculus in its initial stages could have been much better due to the lack of geometric interpretation and practical use cases. Fractional derivatives of order η can be interpreted as a generalization of integer-order derivatives to non-integer values. They describe how a function changes with

respect to the fractional order. A fractional derivative can be thought of as a process that extracts information about the local slope or curvature of a curve at a point in a more flexible manner compared to integer-order derivatives. For example, a first-order fractional derivative ($\eta = 1$) represents the slope of a curve, but a fractional derivative with $\eta \in (0, 1)$ may capture intermediate information about the curve's steepness (Figure 1.1).

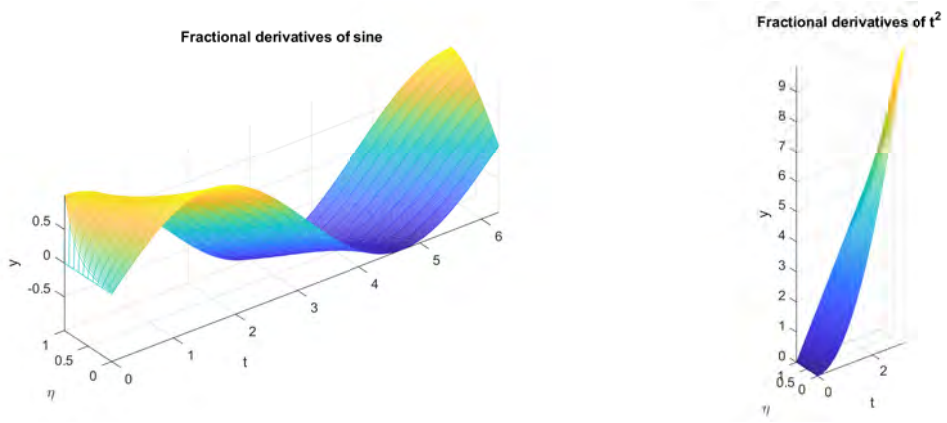

Figure 1.1: Fractional derivative of $\sin t$ and t^2 for different order of derivative.

Fractional derivatives offer a broader perspective on a system's dynamics compared to integer-order derivatives, capturing global evolution rather than just local characteristics and providing more accurate models for real-world phenomena demonstrated by Diethelm and Ford [8]. The relation between stress $\sigma(t)$ and strain $\varepsilon(t)$ in a material under the influence of external forces:

$$\sigma(t) = \alpha \frac{d}{dt} \varepsilon(t) \tag{1.1.1}$$

is Newton's law for a viscous liquid, with α the viscosity of the material and

$$\sigma(t) = E\varepsilon(t) \tag{1.1.2}$$

is Hooke's law for an elastic solid, with E the modulus of elasticity. We can rewrite

$$\sigma(t) = \nu \frac{d^\eta}{dt^\alpha} \varepsilon(t) \tag{1.1.3}$$

with $\eta = 0$ for elastic solids and $\eta = 1$ for a viscous liquid.

However, in practical situations, viscoelastic materials exhibit behavior lying between an elastic solid and a viscous liquid. In such cases, it can be useful to make sense of the operator $\frac{d^\eta}{dt^\eta}$ for $0 \leq \eta \leq 1$.

In its current phase, fractional calculus serves as a dynamic field where novel dimensions of fractional modeling and its practical applications emerge annually [4, 5, 9, 10]. Fractional calculus is expanding its scope even further, encompassing the intricate dynamics of the real world. This momentum has prompted the exploration and testing of fresh ideas using authentic data sets.

Fractional derivatives are excellent tools for describing the memory and hereditary properties of various materials and processes [11]. Memory plays a vital role in real life and we believe in learn from the past to welcome the new era, while in integer-order derivative models, such effects are neglected. The beauty of this field is that fractional derivatives (and integrals) do not have a local (or point) property [12–14]. Recently, it has been applied to successfully modeling certain physical phenomena. A number of papers in the literature have recently reported on the applications of fractional calculus [4–6, 10, 14, 15]. However, we are only just getting started with this highly capable instrument in many fields of research. Many models are still to be introduced, discussed and applied to real-world applications in various branches of science and engineering where non-locality or memory plays a crucial role. Although researchers have already reported extremely excellent results in several seminal monographs and review articles, there are still a large number of non-local phenomena unexplored and waiting to be discovered [1, 3, 6, 7, 15]. Various definitions have emerged for the differentiation and integration of arbitrary orders, each imbued with its unique attributes. Our primary objective revolves around harnessing these inherent characteristics to formulate novel algorithms and applying them to practical challenges. However, to define fractional operators, certain fundamental functions are essential to enhance the comprehension of these operators. Among these fundamental functions, two commonly employed ones are the Gamma and Mittag-Leffler functions, which are defined as follows:

1.1.1 Gamma Function

The gamma function, denoted by $\Gamma(z)$, is a mathematical function that extends the concept of factorial to real and complex numbers. It was introduced by the Swiss mathematician Leonhard Euler in the 18th century and has since found numerous applications in mathematics, physics, engineering, and other scientific disciplines.

The gamma function, $\Gamma(z)$ is the meromorphic function on $\mathbb{C}$ with simple poles at $z = 0, -1, -2, -3, \ldots$ defined by

$$\Gamma(z) = \frac{e^{-\gamma z}}{z} \prod_{n=1}^{\infty} \left(1 + \frac{z}{n}\right)^{-1} e^{z/n} \quad \text{such that } \Gamma(1) = 1. \tag{1.1.4}$$

If $Re\ z > 0$, then the Gamma function can also defined as:

$$\Gamma(z) = \int_0^{\infty} e^{-t} t^{z-1} dt. \tag{1.1.5}$$

One of the vital properties of the Gamma function is:
$\Gamma(z+1) = z\Gamma(z)$ for $z \neq 0, -1, -2, \ldots$. So, for $n = 1, 2, 3, 4, \ldots$ $\Gamma(n+1) = n!$.

1.1.2 Mittag-Leffler Function

G. M. Mittag Leffler developed the Mittag-Leffler function, which occurs naturally in the solution of fractional differential equations [16]. The one parameter generalization of the exponential function, e^z is denoted by

$$\mathbb{E}_{\eta}(z) = \sum_{k=0}^{\infty} \frac{z^k}{\Gamma(\eta k + 1)}, \quad \text{where } \eta > 0. \tag{1.1.6}$$

The two-parameter Mittag-Leffler function was introduced by Agarwal [17] and defined as

$$\mathbb{E}_{\eta,\gamma}(z) = \sum_{k=0}^{\infty} \frac{z^k}{\Gamma(\eta k + \gamma)} \quad \text{where } \eta > 0 \text{ and } \gamma > 0. \tag{1.1.7}$$

Laplace transform of the Mittag-Leffler function is [18]

$$\mathcal{L}(t^{\gamma-1}\mathbb{E}_{\eta,\gamma}(zt^{\eta})) = \frac{s^{\eta-\gamma}}{s^{\eta}-z}. \tag{1.1.8}$$

The value of the Mittag-Leffler function depends on the parameter η and the argument z. When η is between 0 and 1, and z is negative, the Mittag-Leffler function is completely monotone and bounded by one [19, 20].

Numerous definitions for fractional operators have been proposed; however, the extensively accepted definition can be summarized as follows:

1.1.3 Grünwald-Letnikov Fractional Derivative

The Grünwald–Letnikov derivative is named after its developers, Karl Grünwald and Igor Letnikov, who independently contributed to its development. The Grünwald–Letnikov derivative is a way of extending the concept of derivative to non-integer orders [21]. It is defined as a limit of a finite difference approximation of the derivative, using a binomial coefficient to weight the terms. It is one of the simplest and oldest methods of fractional calculus and functions to be k times differentiable for Grünwald–Letnikov derivative. The **generalized version** of fractional integral and derivatives for any arbitrary real or even complex number η is

$${}^{GL}D^{\eta}f(t) = \lim_{\substack{h\to 0 \\ kh=t-a}} h^{-\eta}\sum_{r=0}^{k}(-1)^{r}\binom{\eta}{r}f(t-rh) \tag{1.1.9}$$

where $\binom{\eta}{r} = \dfrac{\Gamma(\eta+1)}{\Gamma(\eta-r+1).\Gamma(r+1)}$ and suppose that $k \to \infty$ as $h \to 0$ [7].

The derivatives of an integer order η and the η fold integral of the continuous function $f(t)$ are particular cases of eq. (1.1.9), which represents the derivative of order m if $\eta = m$ and the m-fold integral if $\eta = -m$. This formula is based on recursively applying the standard definition of the derivative to get higher-order derivatives and then replacing the integer order with a real number.

1.1.4 Riemann-Liouville Fractional Integral

Let $\eta > 0$ and functions f is piecewise continuous on $(0, \infty)$ and integrable on any finite subinterval of $[0, \infty)$. Then for $t > t_0$ and $t, t_0 \in \mathbb{R}$,

$$ {}^{RL}D^{-\eta} f(t) = \frac{1}{\Gamma(\eta)} \int_{t_0}^{t} (t-\xi)^{\eta-1} f(\xi)\, d\xi \tag{1.1.10} $$

is known as the Riemann-Liouville fractional integral of order η [1]. The above eq. (1.1.10) is Riemann fractional integration if $t_0 = 0$ and Liouville fractional integration if $t_0 = -\infty$.

1.1.5 Riemann-Liouville Fractional Derivative

Suppose that $\eta > 0$, $t > t_0$. Then for $k \in \mathbb{N}$,

$$ {}^{RL}D^{\eta} f(t) = \begin{cases} \dfrac{1}{\Gamma(k-\eta)} \dfrac{d^k}{dt^k} \displaystyle\int_{t_0}^{t} \frac{f(\xi)}{(t-\xi)^{\eta+1-k}}\, d\xi, & k-1 < \eta < k \\ \dfrac{d^k}{dt^k} f(t), & \eta = k \end{cases} \tag{1.1.11} $$

is known as the Riemann-Liouville fractional derivative of order η [1, 2]. The aforementioned definition contradicts the classical derivative of the constant, as the non-integer derivative of a constant is non-zero. In 1967, Caputo suggested that the Riemann-Liouville concept of fractional derivative be amended to address this deficiency.

1.1.6 Caputo Fractional Derivative

Suppose that $\eta > 0$, $t > t_0$. Then for $k \in \mathbb{N}$,

$$ {}^{\mathrm{C}}D^{\eta} f(t) = \frac{d^{\eta} f(t)}{dt^{\eta}} = \begin{cases} \dfrac{1}{\Gamma(k-\eta)} \displaystyle\int_{t_0}^{t} \frac{f^{(k)}(\xi)}{(t-\xi)^{\eta+1-k}}\, d\xi, & k-1 < \eta < k \\ \dfrac{d^k}{dt^k} f(t), & \eta = k \end{cases} \tag{1.1.12} $$

is known as the Caputo fractional derivative of order η [22].

The Caputo fractional derivative necessitates that a function be n times differentiable, whereas the Riemann-Liouville derivative demands that a function be piecewise continuous. Consequently, functions that exhibit discontinuities, such as ECG signals or earthquake waves, cannot be differentiated using the Caputo derivative. The Caputo derivative is especially helpful for dealing with real-world phenomena since it permits standard initial and boundary conditions and the derivative of a constant is also zero [1]. Assuming that the Laplace transform $F(s)$ of the function $f(t)$ exists for n is an integer, then the Laplace transform of the Caputo fractional derivative is [3]

$$\mathcal{L}\left(\frac{d^{\eta}f(t)}{dt^{\eta}}\right) = s^{\eta}F(s) - \sum_{k=1}^{n} s^{\eta-k} f^{(k-1)}(0) \quad \text{where } n-1 < \eta \leq n. \tag{1.1.13}$$

Due to the practical applicability, Caputo fractional derivative is used throughout in this thesis.

1.1.7 Memory Property of Fractional Differentiation

Any integer-order derivative considers the only instantaneous rate of change, which is a local property. For example, the first-order derivative is written as

$$\frac{df(t)}{dt} = \lim_{\Delta t \to 0} \frac{f(t) - f(t-\Delta t)}{\Delta t}, \quad t > 0. \tag{1.1.14}$$

Due to the utilization of only two specific data points, this definition describes the short-term memory aspect of the system. Conversely, in the context of the Caputo fractional operator, the variable t encompasses all values from the system's inception. Consequently, the expression for the fractional-order derivative portrays the historical trajectory of the function under consideration. As the fractional derivative incorporates the entirety of preceding function values $f(t)$, its application to depicting a system's memory attribute captures the phenomenon of long-term memory. The memory of a dynamic system follows a power-law relationship. This relationship characterizes the current state of the system at time t and assigns a weight to past states at time t_j. The weight attributed to

these prior states is directly proportional to $(t - t_j)^{\alpha-1}$, where α falls within the range $0 < \alpha < 1$ and denotes the order of the derivative. This power-law memory system can be mathematically described through a fractional-order differential equation. The non-local nature of the fractional operator renders it suitable for incorporation into mathematical models influenced by past occurrences. In numerous mathematical transmission models, fractional operators are preferred due to the substantial influence of prior events on future occurrences. Our primary objective revolves around harnessing these distinctive qualities to forge novel mathematical models and deploy them to address real-world issues.

1.2 Mathematical Modeling

Mathematical modeling is an effective and adaptable method that allows us to describe, analyze, and predict real-world phenomena by employing mathematical principles and techniques. It acts as a link between theoretical concepts and empirical observations, enabling us to gain insight into the behavior of complex systems and make informed decisions [23, 24]. It empowers us to make informed decisions, solve complex problems, and gain deeper insights into the intricate workings of the natural and man-made systems that surround us.

At its core, mathematical modeling involves creating a simplified representation of a real-world situation using mathematical equations, relationships, and symbols. These models can take various forms, such as differential equations, algebraic equations, stochastic processes, or even computational simulations [25, 26]. The process of developing a mathematical model involves determining the relevant variables, parameters, and interactions of the system. It provides an organized structure for examining various circumstances and comprehending the underlying mechanisms that govern system behavior. By manipulating the model's variables and parameters, researchers and analysts can simulate different conditions and predict the system's behavior. This predictive capability is indispensable for making well-informed decisions, optimizing processes, and comprehending the potential outcomes of various actions.

Mathematical modeling finds applications in a wide range of fields, including physics,

engineering, biology, economics, social sciences, environmental science, and more [4, 27–29]. For instance, in physics, mathematical models describe celestial bodies' motion, fluids' behavior, and particles' interactions. In economics, models can help predict market trends, evaluate policy impacts, and analyze financial risks. In biology, models aid in understanding population dynamics, disease spread, and evolutionary processes.

1.3 Fractional-Order Mathematical Modeling

A fractional-order mathematical model is a specialized form of mathematical model that includes fractional calculus, a branch of mathematics that focuses on derivatives and integrals of non-integer orders. In contrast to traditional integer-order calculus, which uses whole numbers for differentiation and integration, fractional calculus extends these operations to non-integer orders, permitting a more flexible and detailed description of complex systems and phenomena. Models of fractional order have implications in numerous fields, including physics, engineering, biology, and economics. They provide a distinct perspective that encompasses complex behaviors and phenomena that are not adequately modeled by integer-order models [30]. In many cases, these models can provide a more accurate and realistic description of real-world processes.

The fractional-order derivatives and integrals introduce memory effects and non-local behavior into the model, which can be especially useful for systems with long-range interactions, anomalous diffusion, and complex dynamics [6, 12, 13]. Fractional-order models have been applied to phenomena such as diffusion processes in porous media, viscoelastic materials, electrochemical systems, signal processing, and even in modeling the behavior of certain biological systems. Despite their potential benefits, fractional-order mathematical models also have some challenges [6]. The non-local nature of fractional calculus can make the models more complex to analyze and solve, and obtaining accurate data for model validation may be difficult in some cases [31,32]. Applications of fractional-order mathematical models extend to diverse fields, encompassing socio-economic realms by including crime transmission, the excessive use of social media, the unemployment problem, and epidemiological contexts, and can be elucidated as follows:

1.3.1 Crime Transmission Modeling

Crime is one of the illicit ways to subjudice civilized human society. This has been an age-old problem, and it is very important to address this problem carefully. Mainly, crime can be defined as an unlawful act that is accounted for by a state or authority. Two of the pathbreaking research on criminal behavior, Wilson and Kelling's "broken window theory," introduced in 1982, discusses the implications of urban disorder signals [33]. The broken window theory interlinks the implications of unattended and mischievous bypassers to unwatched broken window [34]. Due to its unsophisticated and malleable structure, many scientists and mathematicians have widely accessed this criminologist theory to analyze labyrinthine criminal systems.

The American scientist Alfred Blumstein [35–37] suggested various methodologies in different crime-related fields such as prison population, criminal careers, deterrence, and drug enforcement to eradicate the spread of crime. Blumstein's [37, 38] criminology models were introduced in the late 20th century to restrain criminal activity. Subsequently, based on Blumstein's works, numerous researchers analyzed the chances of offenders being incarcerated, the magnitude and proceedings of offenders' retribution, and the impact of crime in society [39]. Becker's [40, 41] works help to investigate the cost of crimes committed by comparing them with similar criminal activities. The crime economics remained even after several extensions were made to the works of Becker. These extensions were explicitly based on the probability of being fined and captured [42, 43]. These models led to solicitation to evaluate maximum enforcement and solve drawbacks in Becker's model. In the same decade as Becker's studies, an alternate branch of crime literature showed how criminal activities and their forms become profitable whenever a group is engaged in similar work, leading to multiple equilibria [44–46]. From an evolutionary standpoint, Quinteros [47] investigated the dynamics and stability of the economics of crime and punishment games. Crokidakis [48] studied the police action and the risk perception regarding crimes that led to increased ownership of legal guns. Helbing *et al.* [49] focused on models of crowd disasters, crime, terrorism, war, and disease spreading

to show that conventional recipes, such as deterrence strategies, are often not effective and sufficient to contain them. Freeman *et al.* [50] focused on the rate of violence in a small location as well as the amount of money involved.

On the contrary, many of the policies designed by policymakers were criticized due to their ineffective implementation. Subsequent studies analyzed the equilibrium of crime models to eradicate and control crime spreading in society. By taking numerous paradigms, a game-theoretical approach was modeled in the field of criminology [51–55]. Snowdrift game is hired to thrust fines on non-abiding citizens [56]. An evolutionary game-based methodology was designed to assess the long-term impact on prisoners and recidivists [57]. As the most important and frequently used subclasses of evolutionary games, Sendina *et al.* [58] focused on social dilemmas and the prisoner dilemma game especially.

Criminologists looked at various reasons in the twenty-first century to understand why an individual would commit crimes. Throughout history, individuals have sought to understand why a person will commit crimes in biological, psychological, social, and economic aspects. In the transmission phase, the future condition is strongly linked to the criminal history of a person. To reduce crime dissemination, the history and experience of the judiciary are also very relevant [59]. A criminal conviction is more likely in children of criminal parents compared to non-criminal parents [60, 61]. Further, to strengthen the proper functioning of jurisdictional agencies, several mathematical models were introduced. The previous experiments were conceived as a preliminary investigation based on the ordinary differential equation (integer-order) compartmental crime models.

In 2021, Pritam *et al.* [10] used fractional-order differential equations to develop a crime propagation model to include the history of crime. In 1978-2005, an analysis of the impact of unemployment on criminal incentives and opportunities found a clear correlation between unemployment rates and property crimes such as robbery, larceny, and motor vehicle theft [62]. A shortage of work has driven many people into illegal activity, with unemployment rates increasing from 7 percent before the lockdown to 27.11 percent in April of 2020 [63, 64]. Much like infectious diseases, crime exhibits a spreading pattern. As per data from the National Crime Records Bureau of the Government of India, the

number of criminals is on the rise. The crime rate per lakh population has been consistently increasing from 1981 to 2020 (Figure 1.2).

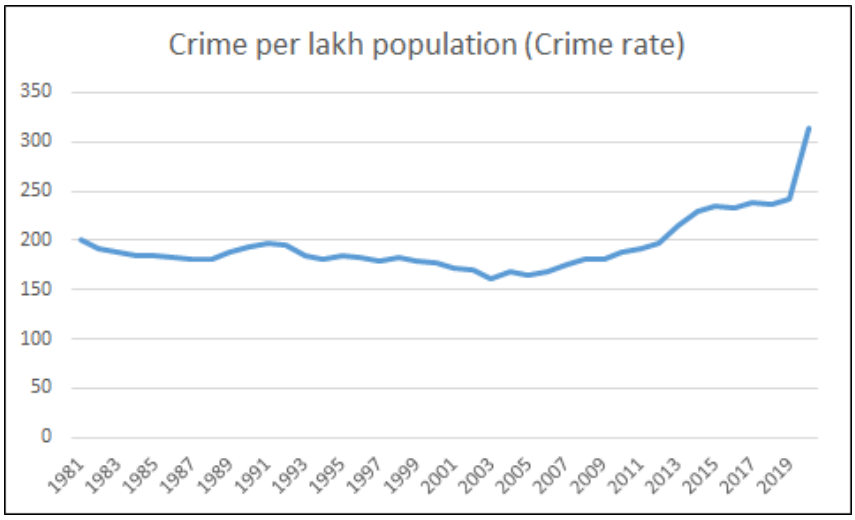

Figure 1.2: Crime rate per lakh population in India.

As a result, there is a high risk of transmission of crime and it is very important to develop tools to control crime transmission in society. Therefore, this thesis develops fractional-order mathematical models to reduce crime transmission.

1.3.2 Modeling the Excessive Use of Social Media

Each facility carries its own set of merits and drawbacks. Social media usage is consistent across various age groups, encompassing teenagers, adults, and the elderly. Nevertheless, there are instances where this social interaction transforms from a routine activity into a habit, eventually evolving into an addiction. Users find themselves ensnared in the virtual realm, which can detrimentally impact their real-life contentment in terms of relationships and individual aspirations.

Several studies found the educational group is concerned that Orbit Showtime Network is systematically lowering the confidence of the student in educational systems, which not only impacts their success but may also result in dropouts [65–67]. Ishaku *et al.* [68] analyzed the impact of the social web on academic and anti-behavioral outcomes in students and found the role of social networks on academic achievement and

organizational performance. The findings suggest that different forms of the social web have an unfavorable impact on educational outcomes while having a favorable effect on anti-behavioral outcomes. Beqiri *et al.* [69] investigated the influence of social media platforms and revealed that social network has an effect on students and is beneficial in terms of connectivity and interactivity. Mbodila *et al.* [70] studied the impact of social sites on the development of a student, focusing on the extent of interaction and communication between them when using Facebook and revealed that Facebook usually affects student teamwork and interaction. Mwadime performed a study on the adverse effect of online social networking on the academic achievement of the student [71]. According to the findings, social media harms students' academic success. The positive and negative effects of social networking sites on the habits of students were also examined by Gok [72]. Therefore, social media has a significant impact on the academics of students in both positive and negative ways.

Due to the COVID pandemic and lockdown, usage of social platforms increased not only for entertainment purposes but also for academic purposes. As a result, students are at significant risk of developing social media addiction, so techniques to control social media addiction transmission throughout society are required. Common factors contributing to social media addiction include chronic stress, trauma, mental health disorders, and a family history of addictive behaviors. Most of the earlier models overlooked the influence of social media addiction on academic performance and personal history. To address this issue and illustrate how memory impacts the influence of social networks on students, a fractional-order mathematical model becomes necessary. Hence, this thesis proposes a fractional-order social media model to depict the dynamics of interactions between social media-addicted students and individuals with less involvement or non-users.

1.3.3 Unemployment Modeling

Unemployment is a pressing global issue that affects individuals, communities, and entire economies. It refers to the situation where individuals willing and able to work cannot secure enough employment opportunities based on their skills. The consequences of high

unemployment rates are far-reaching, encompassing economic, social, and psychological aspects [73]. Youth unemployment is a critical global issue and a significant indicator of a country's economic situation. In impoverished nations, the lack of job opportunities for young individuals is often attributed to their inadequate experience and the incompatibility between their skills and the market demands [74, 75].

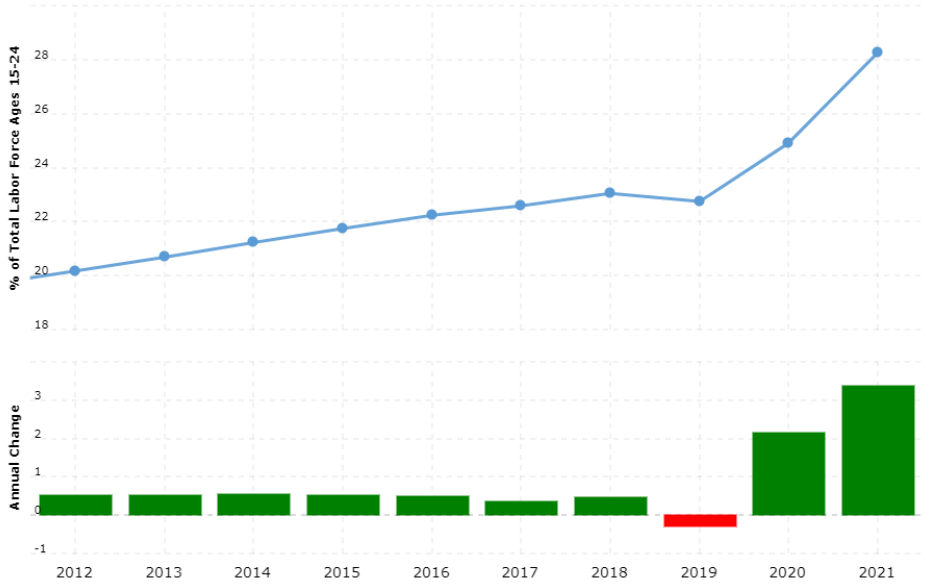

Figure 1.3: Youth unemployment: the labor force ages 15-24 without work but available for and seeking employment (Data Source: World Bank).

Notably, the introduction of mathematical models describing the unemployment problem can be attributed to Misra and Singh in 2011 [76]. In 2015, Pathan and Bhathawala [77] conducted a study investigating the influence of self-employment on the unemployment rate. Another study by Daud and Ghozali [78] in the same year developed a mathematical model incorporating two classes: employed and unemployed individuals. Building upon their previous work, Pathan and Bhathawala [29] expanded their model in 2016 by incorporating four classes: unemployed individuals, employed individuals, new migrant workers, and newly vacant positions. In 2017, Misra and Singh [79] further explored the unemployment problem by considering the influence of skill development programs provided by academic institutions. Additionally, Ashi *et al.* [80] examined the impact of

government assistance on reducing the unemployment rate in a study conducted in 2022. These studies contribute to understanding unemployment dynamics and provide insights into potential strategies and interventions to address this issue. According to Gir-Alana *et al.* [81], the unemployment rate in Turkey demonstrates long memory characteristics. The enduring nature of unemployment rates, public perceptions, past policy interventions, and the utilization of historical data for predictive analysis all underscore the significance of accounting for the impact of prior events and trends in the examination and mitigation of unemployment.

Numerous mathematical models of unemployment problem exist of integer-order derivative and these models failed to account for the non-local nature of time or dynamic memory. Even though history substantially affects unemployment, there is no study of unemployment problems with fractional differential equations. Considering the increasing youth unemployment rate (Figure 1.3), it is crucial to examine the youth unemployment problem comprehensively. Therefore, this thesis developes a fractional-order mathematical model to analyze the effect of skill development programs on youth employment.

1.3.4 Epidemic Modeling

Epidemic modeling is a crucial field in epidemiology and public health that involves understanding the spread and dynamics of infectious diseases within populations. Over the years, extensive research has been conducted to develop models that can accurately predict, analyze, and control disease outbreaks. In this thesis, we delve into the dynamics of malaria transmission.

Malaria has become more prevalent in recent years due to climate change or global warming, which is expected to have unanticipated repercussions for the disease's prevalence. The life cycles of both the vector and the parasite are affected by temperature fluctuations [82]. Mathematical models have been used for more than a century to give a clear framework for analyzing human malaria transmission patterns [83–88]. Sir Ronald Ross discovered the malaria parasite's life cycle in mosquitoes while working for the Indian Medical Service in the 1890s. He was one of the first to publish a series of studies utilizing

mathematical functions to research malaria transmission in the early 1900s [89–91]. Due to changing environmental and socio-economic circumstances, the conditions are still expanding and threaten to become a serious cause of mortality and disability. Hence, existing models must be critically evaluated and explored.

Drug resistance refers to an organism's ability to adapt and survive when exposed to a drug that would typically be lethal. It occurs due to random genetic alterations that confer the organism with the capability to withstand treatment [92]. The emergence and spread of drug-resistant malaria have prompted extensive research efforts aimed at developing innovative strategies to combat this disease [93]. In the context of disease transmission and drug resistance, the future state is intricately linked to the preceding (current as well as past) state due to hereditary factors. Integer-order models lack memory properties. Therefore, this thesis introduces a novel compartmental model for malaria transmission. This model incorporates memory effects between human-to-mosquito and mosquito-to-human transmissions, allowing for a more comprehensive analysis.

The examination of the literature has revealed the presence of the following research gaps in various real-life applications of socio-economic and epidemiology problems:

- The fractional-order modeling of crime transmission has not taken into account factors like the duration required to capture and reinforce criminals, non-linear transmission rates, and the logistic growth rate of non-criminal individuals.
- A fractional-order model addressing the impact of social media on academic outcomes has yet to be explored in research.
- A fractional-order model that examines the influence of skill development programs on youth employment has not been explored through research endeavors.
- The impact of drug resistance, a critical element in the control of malaria transmission, has yet to be investigated in fractional-order modeling.

The process of constructing a fractional-order mathematical model involves defining fractional-order derivatives or integrals that capture the specific features of the system.

This may also require specialized mathematical techniques and algorithms for solving and analyzing the resulting fractional differential equations, which are defined in the next section.

1.4 Preliminaries

1.4.1 Existence and Uniqueness Theorem

This theorem is employed to demonstrate the existence and uniqueness of solutions for fractional-order differential equations.

Theorem 1.4.1. [1] *Consider the fractional differential equation*

$$\frac{d^{\eta} f(t)}{dt^{\eta}} = y(t, x), t > t_0$$

with $0 < \eta \leq 1$ *and* $y : [t_0, \infty] \times \Omega \to \mathbb{R}^n, \Omega \in \mathbb{R}^n$. *Then, a unique solution of the above equation on* $[t_0, \infty] \times \Omega$ *exists provided* $y(t, x)$ *obeys the local Lipschitz condition with respect to* x.

1.4.2 Generalized Mean Value Theorem

The generalized mean value theorem serves as a powerful tool for understanding the intricate relationships between function properties and their derivatives, providing deeper insights into the underlying geometry and behavior of functions. This theorem is utilized to establish that solutions for fractional-order differential equations are non-negative.

Theorem 1.4.2. [94] *Let* $f(t) \in \mathcal{C}[a, b]$ *and* $\frac{d^{\eta} f(t)}{dt^{\eta}} \in \mathcal{C}[a, b]$ *for* $0 < \eta \leq 1$, *then*

$$f(t) = f(a) + \frac{1}{\Gamma(\eta)} \frac{d^{\eta} f(\epsilon)}{dt^{\eta}} (t - a)^{\eta} \;\; \textit{with} \;\; 0 \leq \epsilon \leq t, \;\; \forall \;\; t \in (a, b].$$

Lemma 1.4.1. [94] *If* $f(t) \in \mathcal{C}[0, b]$ *and* $\frac{d^{\eta} f(t)}{dt^{\eta}} \in \mathcal{C}[0, b]$ *for* $0 < \eta \leq 1$. *It is clear that if*

- $\frac{d^{\eta} f(t)}{dt^{\eta}} \geq 0 \; \forall \; t \in (0, b]$, *then* $f(t)$ *is non-decreasing*

- $\frac{d^\eta f(t)}{dt^\eta} \leq 0 \; \forall \; t \in (0, b]$, *then* $f(t)$ *is non-increasing.*

1.4.3 Equilibrium Points

Equilibrium points, also referred to as steady-state or fixed points, play a pivotal role in the analysis of dynamical systems. These points denote states where the system's behavior remains constant over time, characterized by the derivatives of the system being zero. Equilibrium points are of utmost importance in the study of dynamic systems, often representing stable states or special solutions. They can be broadly categorized into two types:

1. **Stable Equilibrium Points:** At a stable equilibrium point, the system returns to the equilibrium state when perturbed slightly. In other words, if the system starts near a stable equilibrium, it tends to remain in proximity to that point. Stable equilibrium points are frequently associated with attracting behavior.

2. **Unstable Equilibrium Points:** At an unstable equilibrium point, the system diverges from the equilibrium state when perturbed slightly. If the system commences near an unstable equilibrium, it moves away from that point. Unstable equilibrium points are commonly associated with repelling behavior.

Understanding the behavior of a system in the vicinity of its equilibrium points is vital for comprehending its stability and long-term dynamics. Stability analysis entails investigating how the system reacts to perturbations around these points and often holds a central role in fields such as physics, engineering, biology, and economics.

1.4.4 Descartes' Rule of Signs

Descartes' rule of signs is a mathematical principle used to determine the number of positive and negative roots of a polynomial equation or equilibrium points. It provides a way to estimate the number of real roots without explicitly solving the equation. The rule is named after René Descartes, a French mathematician and philosopher [95]. *The rule states that if a polynomial equation in one variable with real coefficients, the number of positive*

roots of the equation is either equal to the number of sign changes in the coefficients or less than that by an even number [96].

1.4.5 Local Stability

Local stability analysis provides a focused understanding of a system's behavior by examining how small perturbations or deviations from equilibrium points influence its trajectories in the immediate vicinity. The Routh-Hurwitz criteria is a mathematical tool used to determine the local stability of a system by examining the coefficients of its characteristic polynomial. It provides a systematic way to assess stability without explicitly solving the characteristic equation or finding the roots. The criteria are based on constructing a special table called the Routh array, which uses the coefficients of the characteristic polynomial. The Routh array allows us to evaluate the signs of certain determinants, known as the principal minors, which provide information about the stability of the system [97–99]. For fractional-order systems, the stability analysis of equilibrium points is complex and difficult due to the non-local property of fractional calculus. In this, we check the stability of an equilibrium point in its neighborhood.

Theorem 1.4.3. (Matignon Criteria) *Assume that our model can be represented in the following form*

$$\frac{d^{\eta}X(t)}{dt^{\eta}} = F(X(t)) \ ,$$

where $X(t) = (x_1(t); x_2(t); ...; x_n(t))^T; F(X(t)) = (f_1; f_2; ...; f_n)^T$ *and* $E^* = (x_1^*; x_2^*; ...; x_n^*)^T$ *is the equilibrium point. For the fractional-order system, the equilibrium points of the system are asymptotically stable if all the eigenvalues at the equilibrium* E^* *satisfy the following condition:*

$$|arg(eig(J))| = |arg(\lambda_j)| > \frac{\pi}{2}\alpha$$

where $j = 1, 2, ...n$ *and* J *is the Jacobian matrix of the system evaluated at the equilibria* E^* [100].

Theorem 1.4.4. (Routh-Hurwitz Criteria) *Let the characteristic polynomial of the Jacobin*

matrix of the form:

$$P(s) = s^n + a_1 s^{n-1} + \ldots + a_{n-1} s + a_n$$

The Routh-Hurwitz criteria involve constructing a table based on the coefficients of the polynomial. Routh-Hurwitz matrix is composed as follows.

$$H_n = \begin{bmatrix} a_1 & 1 & 0 & 0 & 0 & 0 & \cdots & 0 \\ a_3 & a_2 & a_1 & 1 & 0 & 0 & \cdots & 0 \\ a_5 & a_4 & a_3 & a_2 & a_1 & 1 & \cdots & 0 \\ \vdots & \vdots & \vdots & \vdots & \vdots & \vdots & \ddots & \vdots \\ 0 & 0 & 0 & 0 & 0 & 0 & \cdots & a_1 \end{bmatrix}$$

The principal diagonal minors of the Hurwitz matrix are given by the formulas:

$$\begin{aligned} \Delta_1 &= a_1, \\ \Delta_2 &= a_1 a_2 - a_3, \\ \Delta_3 &= \begin{vmatrix} a_1 & 1 & 0 \\ a_3 & a_2 & 1 \\ a_3 & a_4 & a_5 \end{vmatrix}, \\ &\vdots \end{aligned}$$

The roots of the auxiliary equation have negative real parts if and only if all the principal diagonal minors of the Hurwitz matrix are positive. For the most common systems of the $n = 2, 3, 4, 5$*, the following stability criteria is obtained:*

- $n = 2 : a_1 > 0,\ a_2 > 0$*,*
- $n = 3 : a_1 > 0,\ a_3 > 0,\ a_1 a_2 > a_3$*,*
- $n = 4 : a_1 > 0,\ a_2 > 0,\ a_3 > 0,\ a_4 > 0, a_1 a_2 a_3 > a_3^2 + a_1^2 a_4$*,*

- $n = 5 : a_i > 0$ *for* $i = 1, 2, 3, 4, 5,\ a_1a_2a_3 > a_3^2 + a_1^2a_4,$
  $(a_1a_4 - a_5)(a_1a_2a_3 - a_3^2 - a_1^2a_4) > a_4(a_1a_2 - a_3)^2.$

1.4.6 Global Stability

Global stability analysis takes a wide-angle view of a system's behavior, exploring whether the system, no matter where it starts, eventually settles into a stable state. A Lyapunov function is a real-valued function used to analyze the global stability of a dynamical system. It is required to be continuous, positive definite, and have a derivative that indicates stability (non-increasing or strictly decreasing) along the system trajectories. Lyapunov functions are used to assess the stability and convergence properties of dynamical systems without explicitly solving the system's equations [101, 102].

Theorem 1.4.5. *Let a fractional-order non-autonomous dynamical system have an equilibrium point E^* contained in domain $\chi \subset \mathbb{R}^n$. Then for any function $U : [0, \infty) \times \chi \to \mathbb{R}$ continuously differentiable along with the conditions $U_1(x) \leq U(t, x(t)) \leq U_2(x)$ and $\frac{d^\eta}{dt^\eta}U(t, x(t)) \leq -U_3(x)$, where $U_1(x), U_2(x)$ and $U_3(x)$ are continuous positive definite functions on the domain χ for every $\eta \in (0, 1)$, the fractional non-autonomous dynamical system is uniformly asymptotically stable* [101, 103].

1.4.7 Bifurcation Theory

When a variation in a parameter brings about a change in the fundamental behavior of the equilibrium states in a dynamic system, this occurrence is referred to as a bifurcation. The term "qualitative behavior" in this context encompasses two key aspects:

- The count of equilibrium states.
- The stability of these equilibrium states.

Several specific types of bifurcations exist, including:

- Hopf Bifurcation
- Saddle-Node Bifurcation

- Transcritical Bifurcation
- Pitchfork Bifurcation

Now, the following theorems are used to show the bifurcation type for the system. Sotomayor's theorem is employed to derive the conditions for the existence of saddle-node and transcritical bifurcations and the Center Manifold Theorem is particularly useful for understanding the behavior of systems that exhibit both stable and unstable modes around an equilibrium [104, 105].

Theorem 1.4.6. (Sotomayor's Theorem) [106–108] *Let* $f(x_0; H_0) = 0$ *and matrix* $A = Df(x_0; H_0)$ *has an eigenvalue 0 with eigenvectors* v *and* w *for*A *and* A^T *respectively. If the requirements listed below are fulfilled,*

- $\nabla_1 = \boldsymbol{w}^T f_H(x_0, H_0) = 0,$
- $\nabla_2 = \boldsymbol{w}^T [Df_H(x_0, H_0)v] \neq 0,$
- $\nabla_3 = \boldsymbol{w}^T [D^2 f(x_0, H_0)(v, v)] \neq 0$

then the system undergoes a transcritical bifurcation at the equilibrium point x_0 *as the parameter* H *varies through the bifurcation value* $H = H_0$.

Theorem 1.4.7. (Center Manifold Theorem) [104, 105]. *Assume* $A = D_x f(0, 0) = \frac{\partial f_i}{\partial x_j}(0, 0)$ *is the linearization matrix around the equilibrium 0 with* φ *evaluated at 0. Zero is a simple eigenvalue of* A *and all other eigenvalues of* A *have negative real parts. Matrix* A *has a non-negative right eigenvector* w *and a left eigenvector* v *corresponding to the zero eigenvalue. Let* f_k *be the* k*th component of* f*, and define:*

$$a = \sum_{k,i,j=1}^{n} v_k w_i w_j \frac{\partial^2 f_k}{\partial x_i \partial x_j}(0, 0),$$
$$b = \sum_{k,i=1}^{n} v_k w_i \frac{\partial^2 f_k}{\partial x_i \partial \varphi}(0, 0).$$

If $a < 0$ and $b > 0$ and φ changes from negative to positive, 0 changes its stability from stable to unstable. Correspondingly, a negative unstable equilibrium becomes positive and locally asymptotically stable.

1.4.8 Numerical Simulation

Numerical simulation is a computational technique used to model and analyze real-world phenomena or systems by simulating their behavior using mathematical models and algorithms. There are several methods to solve fractional differential equations (FDEs), like Euler method, fractional finite difference method, Laplace transform method, Adams-Bashforth-Moulton predictor-corrector and many more. The Euler method is a simple and widely used method for solving ordinary differential equations (ODEs). However, it is less suitable for FDEs because it is purely explicit and does not account for non-local fractional derivatives. Fractional finite difference methods directly discretize fractional derivatives, making them well-suited for FDEs. However, they can be computationally expensive, especially for large systems, and may require fine grids for accuracy. Laplace transform methods can be used for linear FDEs. They involve transforming the FDE into an algebraic equation, making the solution more straightforward. However, they are limited to linear problems.

The Adams-Bashforth-Moulton predictor-corrector approach is selected for solving systems of FDEs because it provides a balanced combination of accuracy and stability [109]. The explicit prediction step is followed by an implicit correction step, allowing for the handling of non-local fractional derivatives and the potential presence of stiffness in the equations. This method is versatile and can be adapted to a wide range of FDE problems, making it a valuable tool for researchers and engineers working in various fields. This approach combines explicit prediction (Adams-Bashforth) and implicit correction (Adams-Moulton) to provide an accurate and stable solution for systems of FDEs. Here's a description of the Adams-Bashforth-Moulton predictor-corrector approach for solving systems of FDEs:

1. **Adams-Bashforth Predictor**

   In the predictor step, the Adams-Bashforth method is used to estimate the values of the dependent variables at the next time step based on their current values and derivatives. This is an explicit method that provides a preliminary prediction. For a system of FDEs, the Adams-Bashforth predictor of order k uses the previous k values of the system to predict the next values. For example, for a first-order FDE with a fractional derivative of order η, the Adams-Bashforth predictor might be expressed as:

   $$x_{n+1}^{(p)} = x_n + h^\eta f(x_n) \tag{1.4.1}$$

   Here, $x_{n+1}^{(p)}$ is the predicted value, x_n is the current value, h is the time step, η is the fractional order, and $f(x_n)$ is the derivative with order η.

2. **Adams-Moulton Corrector**

   In the corrector step, the Adams-Moulton method is applied to refine the predictions made in the predictor step. The Adams-Moulton method is implicit and involves solving an equation to improve the prediction. For a system of FDEs, the Adams-Moulton corrector of order k uses the current and k predicted values to calculate the corrected values. It involves solving an equation to improve the estimate. The Adams-Moulton corrector may be written as:

   $$x_{n+1}^{(c)} = x_n + h^\eta \left[\frac{1}{\Gamma(1-\eta)} f(x_{n+1}^{(p)}) - \frac{1}{\Gamma(1-\eta)} f(x_n) \right] \tag{1.4.2}$$

   Here, $x_{n+1}^{(c)}$ is the corrected value and $\Gamma(\cdot)$ represents the gamma function.

1.5 Thesis Objectives

The primary objective of the thesis is to investigate the application of fractional calculus in various domains, including socio-economics and epidemiology, to address a recognized research gap. The subsequent objectives have been outlined in order to achieve the primary objective:

- To study the dynamics of crime transmission using fractional-order differential equations with parameters like time delay to capture criminals, non-linear transmission rate, and logistic growth of non-criminals.
- Investigate the impacts of substantial social media usage on academic achievement through the application of fractional-order differential equations.
- To explore the effects of skill development programs on youth employment using fractional differential equations.
- Apply fractional calculus approaches to analyze the dynamics of malaria infection for different drug resistance levels in the human and mosquito populations.

The first objective is addressed in Chapters 2–4, the second is discussed in Chapter 5, the third objective is addressed in Chapter 6, and the last objective is addressed in Chapter 7.

1.6 Thesis Contribution

The inception of this thesis stems from the growing recognition of the profound impact of fractional calculus on the modeling and comprehension of intricate systems characterized by substantial memory effects. This thesis attempts to bring unique insights into these under-researched areas and contribute to the progress of knowledge across different disciplines through detailed analysis, mathematical modeling, and empirical inquiry. The primary contributions of this thesis can be outlined as follows:

1. **Crime Transmission Modeling**: This research substantially advances crime transmission modeling through fractional calculus. By incorporating previously overlooked factors, such as the time required for apprehending and reinforcing criminals, non-linear transmission rates, and the logistic growth rate of non-criminal entities, the established fractional-order model provides a more accurate representation of the complex dynamics of criminal activities. This contribution not only enhances our understanding of crime propagation but also provides a basis for more informed policy-making and intervention strategies to curb criminal behaviors. According

to this research, a more robust and more effective legal system, coupled with improved living conditions and economic opportunities, can dramatically reduce the number of crimes. Though it is expected that the criminal population will decrease as the parameter law enforcement increases, a threshold value of law enforcement is obtained.

2. **Impact of Social Media on Academic Outcomes**: Through the innovative application of fractional-order modeling, this study pioneers a new approach to understanding the influence of social media on academic outcomes. This thesis presents a non-linear fractional-order model designed to investigate the impact of social media on academic performance. This innovative model accounts for both high and low-performing student classes, offering a more intricate and holistic viewpoint of the interplay between academic outcomes and social media usage. Through the integration of fractional calculus with non-linearity, this study pushes the boundaries of our comprehension of this complex relationship, setting a new standard for insight in this field. The model's predictions can aid educators, policymakers, and individuals in comprehending the implications of excessive social media use on academic performance, facilitating informed decisions and interventions.

3. **Skill Development Programs and Youth Employment**: This research recognizes the substantial economic and societal repercussions resulting from elevated unemployment rates worldwide. To tackle this challenge, governments of developing countries have initiated various skill development programs. Despite these efforts, unemployment remains a persistent issue. The thesis steps in to reassess the existing policies and models, proposing an innovative approach to shed light on this persistent concern. This study introduces a groundbreaking fractional-order mathematical model as a response to the ongoing issue of unemployment. The proposed model serves as a unique framework for evaluating the effectiveness of diverse skill development programs targeting youth. Through the incorporation of fractional-order differential equations, this model captures the intricate dynamics underlying unem-

ployment trends, offering a more comprehensive analysis compared to traditional integer-order models. This research takes a proactive stance by aiming to reduce the overall unemployment rate through the implementation of skill development programs. By assessing the outcomes of training interventions designed to empower unemployed individuals, the thesis contributes to inform decision-making regarding policy adjustments and program enhancements. Ultimately, the study aims to be a catalyst for positive change in combating unemployment challenges.

4. **Drug Resistance in Malaria Transmission**: In a world of advancing medical technologies, infectious diseases persistently affect countless lives globally. This thesis responds to the persistent challenges posed by infectious diseases, particularly focusing on malaria's impact and the development of drug resistance. Through the introduction of a novel compartmental model with memory and fractional calculus, the research strives to provide a more accurate representation of disease dynamics and the potential effects of therapeutic measures. By exploring equilibrium points and stability, the study contributes to the broader field of infectious disease modeling and offers insights into potential strategies for disease control and prevention. The early detection of drug resistance levels in individuals can aid in reducing malaria transmission by administering appropriate drug treatments. Hence, malaria tests should include an evaluation of drug resistance levels.

In summary, the main contribution of this thesis is to initiate the applications of fractional calculus in real-life problems, where memory/history plays an important role, which was overlooked in earlier models. This thesis contributes to the academic landscape through its innovative application of fractional-order modeling to diverse fields. By bridging existing research gaps, it provides a deeper understanding of complex systems and facilitates the development of informed strategies and policies across crime transmission, social media's influence on academics, skill development and youth employment, and the control of drug-resistant malaria. Through meticulous analysis, mathematical modeling, and empirical investigations, this research offers valuable insights that advance knowledge and guide

decision-making in multiple disciplines.

1.7 Thesis Organization

After elucidating the primary objective and contributions of the thesis, this section presents a concise overview of the chapter-wise road map. The thesis encompasses a total of eight chapters. The ensuing three chapters, specifically Chapters 2–4, are dedicated to crime transmission modeling and Chapter 5 address the impact of social media on academics. Moving forward, Chapter 6 delves into the realm of the youth unemployment problem, while Chapter 7 takes on the intricate subject of different drug resistance classes within malaria diseases. Each chapter starts by introducing a model, which is then thoroughly explained to understand its characteristics and then demonstrates the existence and uniqueness of the solution of the proposed model, followed by determining the equilibrium point, stability of the equilibrium point, and numerical simulation for validating theoretical findings.

Chapter 2 delves into fractional-order crime transmission modeling. The focus lies on the time required for apprehending and reinforcing criminals. Policies for law enforcement officers are devised and the well-posedness, equilibrium points, stability, and numerical simulations are meticulously examined.

Chapter 3 addressing the spread of crime through social contact and this chapter presents a fractional-order mathematical model with a non-linear transmission rate. It encompasses susceptible individuals, criminals, and prisoners, incorporating a non-linear transmission rate influenced by social backgrounds.

Chapter 4 contrasts exponential and logistic growth models within the context of crime dynamics. By modifying incarceration and criminal release, the equilibrium is studied to understand criminal behavior's societal impact. The chapter contributes to effective strategies in crime prevention through the examination of stability across various derivative orders.

Chapter 5 shifts focus to the educational arena, utilizing a non-linear fractional-order model to assess the influence of social networking sites on student academic achievement.

Chapter 6 probes the interplay between skill development programs and the youth unemployment problem. A fractional-order model is devised, emphasizing the enhancement of unemployed individuals' abilities. This chapter examines equilibrium points, stability, and numerical simulations to glean insights into unemployment dynamics.

Chapter 7 addressing the pressing issue of drug resistance in malaria transmission. This chapter presents a novel compartmental model of malaria transmission with memory between human-to-mosquito and mosquito-to-human that integrates drug resistance development and therapy as a preventative measure.

The final chapter offers a summary of the entire research journey. It encapsulates the overarching findings, contributions, and implications of the study. Moreover, it outlines potential avenues for future research and development in the explored domains.

Chapter 2

Mathematical Modeling of Crime Transmission

"Crime is a reaction, not a simple action."

— Criss Jami

A crime is a harmful act committed towards society against the wishes of the resident government territory, which is punished by a fine, imprisonment, or death upon conviction. Most governments worldwide have recommended numerous ways and predictive methodologies to combat crime, particularly crime perpetrated against diverse genders, castes, religions, and faiths. The advancement of crime in society adversely impacts various socio-economic parameters [110]. The copious forms of crime include fraud, theft, smuggling, human trafficking, and other abuse. Drunks, prostitutes, panhandlers, and loiterers are more likely to perpetrate crime than carefully and orderly patrolled ones. Although many factors determine the mechanisms of crime dissemination in society, there is no denying that crime spreads like an infectious disease in society (as the interaction of criminally active individuals can adversely affect other's actions).

Criminologists looked at various reasons in the twenty-first century to understand why an individual would commit crimes. Throughout history, individuals have sought to understand why a person will commit crimes in biological, psychological, social, and economic aspects. Greed, anger, jealousy, retribution, or vanity may contribute to a crime

being committed. Some individuals tend to commit an organized crime. In the transmission phase, the future condition is strongly linked to the criminal history of a person. To reduce crime dissemination, the history and experience of the judiciary are also very relevant [59]. Children with criminal parents have a twofold increased probability of acquiring a criminal conviction compared to those with non-criminal parents [60]. Further, to strengthen the proper functioning of jurisdictional agencies, several mathematical models were introduced. The previous experiments were conceived as a preliminary investigation based on the ordinary differential equation (integer-order) compartmental crime models. In India, the scarcity of employment opportunities has compelled a significant number of individuals to resort to illegal activities, with unemployment rates soaring from 7 percent before the lockdown to 27.11 percent in April 2020 [63, 64]. As a result, there is a high risk of transmission of crime, and it is very important to develop tools to control crime transmission in society.

This chapter is an attempt to develop a mathematical model of the nonlinear fractional-order differential equation for analyzing the dynamics of the propagation of crime. It is assumed that with proper law enforcement and subsequent treatment, the crime can be optimized. Subsequently, citizens will transform from offenders to people who have been rehabilitated. It is further believed that individuals from the recovered class will transfer to the criminal population or non-criminal population as certain offenders do not change their minds even after therapy. It takes time for criminals to be caught and reinforced. This will happen as it takes time to judge whether someone is a criminal or not. As a result, the proposed fractional-order model is upgraded with the model of capturing offenders with a delay.

2.1 Description of Crime Propagation Model

A crime propagation model shown in Figure 2.1 which is proposed by categorizing the existing population into four clusters. These clusters include law-abiding citizens (non-criminals (S)), criminally active individuals (who have not been imprisoned (C)), prisoners (P), and prisoners who completed the prison tenure (recovered (R)).

Non-criminal individuals are recruited into the community at rates of A and $(1-\epsilon)\xi$, where A is the birth or immigration rate of individuals, ξ is the rate at which individuals move from R to either C or S and $(1-\epsilon)$ is the fraction related to the movement of individual people from R to S.

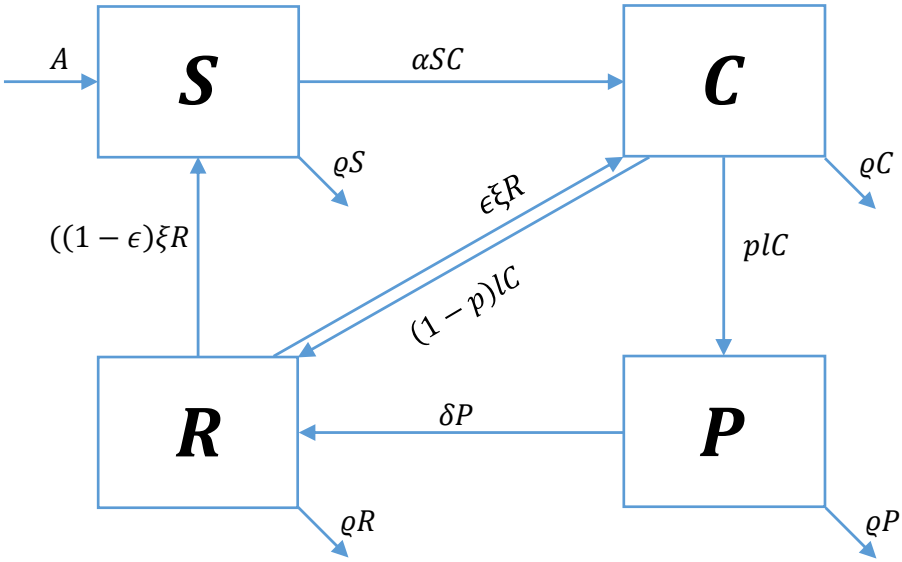

Figure 2.1: Schematic diagram of the proposed crime transmission model.

The non-criminal population is decreased at the rates of α and ϱ, where ϱ is the natural death rate and α is the transmission rate from S to C as non-criminals becoming criminals due to the interaction of criminal and non-criminal population. The criminal population increased at the rates of α, $\epsilon\xi$ and decreased at the rates of l, ϱ where ϵ the is fraction related to the movement of individual people from R to C and l is law enforcement rate and counseling for criminals. The prisoners increased at the rate pl and decreased at the rates δ, ϱ, where p is the fraction contributing to the migration of population from C to P due to enforcement laws and δ is the rate at which individuals moves from P to R after completed the prison tenure. The recovered population increased at the rates $(1-p)l$, δ and decreased at the rates ξ and ϱ.

A fractional order mathematical model, subject to non-negative initial conditions, is proposed as follows, by considering the above facts/assumptions:

$$\begin{aligned}
\frac{d^\eta S(t)}{dt^\eta} &= A^\eta - \alpha^\eta S(t)C(t) + (1-\epsilon)\xi^\eta R(t) - \varrho^\eta S(t) \\
\frac{d^\eta C(t)}{dt^\eta} &= \alpha^\eta S(t)C(t) - l^\eta C(t) + \epsilon\xi^\eta R(t) - \varrho^\eta C(t) \\
\frac{d^\eta P(t)}{dt^\eta} &= pl^\eta C(t) - \delta^\eta P(t) - \varrho^\eta P(t) \\
\frac{d^\eta R(t)}{dt^\eta} &= (1-p)l^\eta C(t) + \delta^\eta P(t) - \xi^\eta R(t) - \varrho^\eta R(t)
\end{aligned} \tag{2.1.1}$$

where $\eta \in (0, 1]$ is the order of derivative in the crime transmission model. Here, $S(t),\ C(t), P(t),\ R(t)$ and their Caputo fractional derivative are continuous at $t \geq 0$. The human population is in fractional time with dimension $t^{-\eta}$ in the LHS of the system. As mortality rate, birth rate, etc., always have dimension t^{-1}, every constant has power η in the RHS of the system to keep the system dimensionally balanced.

Table 2.1: Parameter description for proposed crime transmission model.

Parameter	Description
A	Recruitment rate in non-criminal class
α	Rate of crime indulgment
ξ	Rate of moving back to society (criminal or non-criminal class)
δ	Rate of release from prison
l	Rate of law-enforcement for criminal
ϱ	Natural death rate
p	Fraction contributing to the migration of population from C to P
ϵ	Fraction contributing to the migration of population from R to C

2.2 Dynamics of the Proposed Model

This section demonstrates that the given system has a unique, bounded, and positive solution in $\Omega\ \forall\ t \geq 0$, where

$$\Omega = \left\{ (S, C, P, R) \in \mathbb{R}^4_+ : 0 \leq S + C + P + R \leq \frac{A^\eta}{\varrho^\eta} \right\}. \tag{2.2.1}$$

Let $N(t) = S(t) + C(t) + P(t) + R(t)$

$$\frac{d^\eta N(t)}{dt^\eta} = \frac{d^\eta S(t)}{dt^\eta} + \frac{d^\eta C(t)}{dt^\eta} + \frac{d^\eta P(t)}{dt^\eta} + \frac{d^\eta R(t)}{dt^\eta} \tag{2.2.2}$$

$$\frac{d^{\eta}N(t)}{dt^{\eta}} = A^{\eta} - \varrho^{\eta}N(t) \tag{2.2.3}$$

By taking Laplace transformation (from eq. (1.1.13)),

$$N(s) = \frac{A^{\eta}s^{-1} + s^{\eta-1}N(0)}{s^{\eta} + \varrho^{\eta}}. \tag{2.2.4}$$

Now, by taking inverse Laplace transformation (from eq. (1.1.8)),

$$N(t) = \frac{A^{\eta}}{\varrho^{\eta}}[1 - \mathbb{E}_{\eta}(-\varrho^{\eta}t^{\eta})] + N(0)\mathbb{E}_{\eta}(-\varrho^{\eta}t^{\eta}) \tag{2.2.5}$$

where $\mathbb{E}_{\eta}$ is Mittag-Leffler function defined in eq. (1.1.6).

$$\text{If } 0 < \eta \leq 1, \text{then } 0 \leq \mathbb{E}_{\eta,1}(-\varrho^{\eta}t^{\eta}) \leq 1 \implies N(t) \leq \frac{A^{\eta}}{\varrho^{\eta}}. \tag{2.2.6}$$

2.2.1 Ensuring Existence and Uniqueness

Theorem 2.2.1. *Along with non-negative initial conditions, the crime propagation model has a unique and bounded solution for* $t \geq 0$.

Proof. Now let,

$$\begin{aligned}
\frac{d^{\eta}S(t)}{dt^{\eta}} &= A^{\eta} - \alpha^{\eta}S(t)C(t) + (1-\epsilon)\xi^{\eta}R(t) - \varrho^{\eta}S(t) = f_1(t,S,C,P,R)\\
\frac{d^{\eta}C(t)}{dt^{\eta}} &= \alpha^{\eta}S(t)C(t) - l^{\eta}C(t) + \epsilon\xi^{\eta}R(t) - \varrho^{\eta}C(t) = f_2(t,S,C,P,R)\\
\frac{d^{\eta}P(t)}{dt^{\eta}} &= pl^{\eta}C(t) - \delta^{\eta}P(t) - \varrho^{\eta}P(t) = f_3(t,S,C,P,R)\\
\frac{d^{\eta}R(t)}{dt^{\eta}} &= (1-p)l^{\eta}C(t) + \delta^{\eta}P(t) - \xi^{\eta}R(t) - \varrho^{\eta}R(t) = f_4(t,S,C,P,R)
\end{aligned} \tag{2.2.7}$$

where $f_i(t,S,C,P,R)$ for $i = 1,2,3,4$ are continuous and bounded for $t \geq 0$ as $S(t),\ C(t),\ P(t),\ R(t)$ are bounded by eq. (2.2.6). Here $f_i(t,S,C,P,R)$ for $i = 1,2,3,4$ are continuous and bounded and satisfies the Lipschitz condition. Then, from the existence and uniqueness theorem (Theorem 1.4.1), the solution of the proposed model for

$t \in (0, \infty)$ is not only exists but also unique and bounded. □

2.2.2 Validation of Non-Negative Solutions

As the solution of a system of eq. (2.1.1) gives non-criminal population (S), criminal population (C), prisoners (P), and recovered population (R), and the number of individuals can not be negative in real life. So, the non-negativity of solution is proved in this section. To show $(S, C, P, R) \geq 0$, let us assume that there exists some t_0 where the condition fails. Let $t_0 = inf\{t > 0 | (S(t), C(t), P(t), R(t)) \notin (\mathbb{R}_0^+)^4\}$. Since $(S(t_0), C(t_0), P(t_0), R(t_0)) \in (\mathbb{R}_0^+)^4$ then one of $S(t_0), C(t_0), P(t_0), R(t_0)$ is zero. Then,

$$\begin{aligned}
\left.\frac{d^\eta S(t)}{dt^\eta}\right|_{S(t_0)=0} &= A^\eta + (1-\epsilon)\xi^\eta R(t_0) \\
\left.\frac{d^\eta C(t)}{dt^\eta}\right|_{C(t_0)=0} &= \epsilon\xi^\eta R(t_0) \\
\left.\frac{d^\eta P(t)}{dt^\eta}\right|_{P(t_0)=0} &= pl^\eta C(t_0) \\
\left.\frac{d^\eta R(t)}{dt^\eta}\right|_{R(t_0)=0} &= (1-p)l^\eta C(t_0) + \delta^\eta P(t_0).
\end{aligned} \tag{2.2.8}$$

$$\implies \frac{d^\eta S(t)}{dt^\eta} \geq 0, \quad \frac{d^\eta C(t)}{dt^\eta} \geq 0, \quad \frac{d^\eta P(t)}{dt^\eta} \geq 0, \quad \frac{d^\eta R(t)}{dt^\eta} \geq 0. \tag{2.2.9}$$

Now, from eq. (2.2.6) and generalized mean value theorem (Theorem 1.4.2), the solution of proposed model is non-negative and $\Omega = \left\{(S, C, P, R) \in \mathbb{R}_+^4 : 0 \leq S + C + P + R \leq \frac{A^\eta}{\varrho^\eta}\right\}$ is positively invariant region.

2.3 Equilibrium Points and Criminal Generation Number

2.3.1 Crime Free Equilibrium

A crime-free equilibrium refers to a hypothetical state and often difficult to attain in practice. The crime-free equilibrium point (E_0) is the steady-state solution determined when there is

no criminal population, i.e., $(C(t) = 0)$, and it is given by $E_0 = \left(\frac{A^\eta}{\varrho^\eta}, 0, 0, 0\right)$. However, it's important to note that achieving a completely crime-free society is often considered idealistic and challenging, as some level of crime may always persist.

2.3.2 Criminal Generation Number

The criminal generation number, denoted C_g, is defined as "the estimated number of secondary cases created by a criminally active person in a fully non-criminal population [111]." If a criminal generates fewer than one new criminal individual, on average, during their period of criminal activity, the crime will not propagate. Conversely, if each criminally active person, on average, gives rise to more than one new criminal, the crime will proliferate throughout the population. To determine the criminal generation number, next-generation matrix approach [111] is employed at crime-free equilibrium. Assume $\Psi_i(t)$ denotes the rate of introduction of novel criminals in the i^{th} compartment, $\psi_i^+(t)$ denotes the rate of migration of individuals into the i^{th} compartment by all other means, and $\psi_i^-(t)$ denotes the rate of transfer of individuals out of the i^{th} compartment. It is also possible to write the proposed model (2.1.1) as

$$\left[\frac{d^\eta S(t)}{dt^\eta}, \frac{d^\eta C(t)}{dt^\eta}, \frac{d^\eta P(t)}{dt^\eta}, \frac{d^\eta R(t)}{dt^\eta}\right]^T = \Psi(t) - \psi(t) \tag{2.3.1}$$

where $\psi_i(t) = \psi_i^-(t) - \psi_i^+(t)$ and matrices $\Psi(t), \psi^-(t), \psi^+(t)$ are given by

$$\Psi(t) = \begin{bmatrix} 0 \\ \alpha^\eta S(t)C(t) \\ 0 \\ 0 \end{bmatrix},$$

$$\psi^+(t) = \begin{bmatrix} A^\eta + (1-\epsilon)\xi^\eta R(t) \\ \epsilon\xi^\eta R(t) \\ pl^\eta C(t) \\ (1-p)l^\eta C(t) + \delta^\eta P(t) \end{bmatrix}, \qquad \psi^-(t) = \begin{bmatrix} \alpha^\eta S(t)C(t) + \varrho^\eta S(t) \\ (\varrho^\eta + l^\eta)C(t) \\ (\varrho^\eta + \delta^\eta)P(t) \\ (\varrho^\eta + \xi^\eta)R(t) \end{bmatrix}.$$

The Jacobian matrix of $\Psi(t)$ and $\psi(t)$ at E_0 is given by

$$\Psi^* = \begin{bmatrix} 0 & 0 & 0 & 0 \\ 0 & \dfrac{\alpha^\eta A^\eta}{\varrho^\eta} & 0 & 0 \\ 0 & 0 & 0 & 0 \\ 0 & 0 & 0 & 0 \end{bmatrix}, \quad \psi^* = \begin{bmatrix} \varrho^\eta & \dfrac{\alpha^\eta A^\eta}{\varrho^\eta} & 0 & -(1-\epsilon)\xi^\eta \\ 0 & \varrho^\eta + l^\eta & 0 & -\epsilon\xi^\eta \\ 0 & -pl^\eta & \varrho^\eta + \delta^\eta & 0 \\ 0 & -(1-p)l^\eta & -\delta^\eta & \varrho^\eta + \xi^\eta \end{bmatrix}.$$

The spectral radius of $\Psi^*{\psi^*}^{-1}$ is equal to C_g, where,

$$C_g = \frac{A^\eta \alpha^\eta (\varrho^\eta + \xi^\eta)(\varrho^\eta + \delta^\eta)}{\varrho^\eta[(\varrho^\eta + \delta^\eta)\{\varrho^{2\eta} + \varrho^\eta(\xi^\eta + l^\eta) + \xi^\eta l^\eta(1-\epsilon)\} + p\epsilon\varrho^\eta\xi^\eta l^\eta]}. \tag{2.3.2}$$

Here, when the population is deemed free of criminality, C_g determines the number of secondary offenders that a single criminal has made in his continuing criminal life.

2.3.3 Crime Persistence/Endemic Equilibrium

A crime-persistence equilibrium describes a state or condition where crime remains at a stable, persistent level over time. In a crime persistence equilibrium, the community experiences consistent and unchanging crime rates over an extended period. This implies that despite efforts to reduce or control crime, it remains resilient and does not decrease significantly. The equilibrium point $E^* = (S^*, C^*, P^*, R^*)$ is steady state solution determined when $C > 0$. Now, set the RHS of equations in the proposed models to zero,

$$\begin{aligned} A^\eta - \alpha^\eta S(t)C(t) + (1-\epsilon)\xi^\eta R(t) - \varrho^\eta S(t) &= 0, \\ \alpha^\eta S(t)C(t) - l^\eta C(t) + \epsilon\xi^\eta R(t) - \varrho^\eta C(t) &= 0, \\ pl^\eta C(t) - \delta^\eta P(t) - \varrho^\eta P(t) &= 0, \\ (1-p)l^\eta C(t) + \delta^\eta P(t) - \xi^\eta R(t) - \varrho^\eta R(t) &= 0. \end{aligned} \tag{2.3.3}$$

On solving these equations, we have,

$$P^* = \frac{pl^\eta C^*}{\varrho^\eta + \delta^\eta}, \quad R^* = \frac{\delta^\eta P^* + (1-p)l^\eta C^*}{\varrho^\eta + \xi^\eta}, \quad S^* = \frac{A^\eta + (1-\epsilon)\xi^\eta R^*}{\alpha^\eta C^* + \varrho^\eta}, \tag{2.3.4}$$

$$C^* = \frac{(C_g - 1)[\varrho^\eta((\varrho^\eta + \delta^\eta)[\varrho^{2\eta} + \varrho^\eta(\xi^\eta + l^\eta) + \xi^\eta l^\eta(1-\epsilon)] + \epsilon\xi^\eta p\varrho^\eta l^\eta)]}{\alpha^\eta\varrho^\eta[\varrho^{2\eta} + \varrho^\eta(l^\eta + \xi^\eta + \delta^\eta) + \xi^\eta\delta^\eta + l^\eta\delta^\eta + p\xi^\eta l^\eta]}. \quad (2.3.5)$$

The above expression C^* is non-negative for $C_g \geq 1$. Therefore, the $E^* = (S^*, C^*, P^*, R^*)$ equilibrium point occurs if $C_g > 1$.

2.4 Stability Analysis of Crime Propagation Model

Theorem 2.4.1. *If $C_g < 1$, equilibrium point $E_0 = \left(\frac{A^\eta}{\varrho^\eta}, 0, 0, 0\right)$ is globally asymptotically stable, else it is unstable.*

Proof. The Jacobian matrix of eq. (2.1.1) at crime-free equilibrium point $E_0 = \left(\frac{A^\eta}{\varrho^\eta}, 0, 0, 0\right)$ is given by

$$J_0 = \begin{bmatrix} -\varrho^\eta & -\frac{\alpha^\eta A^\eta}{\varrho^\eta} & 0 & (1-\epsilon)\xi^\eta \\ 0 & \frac{\alpha^\eta A^\eta}{\varrho^\eta} - \varrho^\eta - l^\eta & 0 & \epsilon\xi^\eta \\ 0 & pl^\eta & -\varrho^\eta - \delta^\eta & 0 \\ 0 & (1-p)l^\eta & \delta^\eta & -\varrho^\eta - \xi^\eta \end{bmatrix}. \quad (2.4.1)$$

Here, one of the eigenvalues is $-\varrho^\eta$, which is negative. Now, for the rest of the eigenvalues

$$J_1 = \begin{bmatrix} \frac{\alpha^\eta A^\eta}{\varrho^\eta} - \varrho^\eta - l^\eta & 0 & \epsilon\xi^\eta \\ pl^\eta & -\varrho^\eta - \delta^\eta & 0 \\ (1-p)l^\eta & \delta^\eta & -\varrho^\eta - \xi^\eta \end{bmatrix}. \quad (2.4.2)$$

The characteristic equation corresponding to matrix J_1 is:

$$\lambda^3 + B_1\lambda^2 + B_2\lambda + B_3 = 0 \quad (2.4.3)$$

where

$$B_1 = -\left(\frac{\alpha^\eta A^\eta}{\varrho^\eta} - \varrho^\eta - l^\eta\right) + 2\varrho^\eta + \delta^\eta + \xi^\eta$$

$$B_2 = (\delta^\eta + \varrho^\eta)(\xi^\eta + \varrho^\eta) - (\frac{\alpha^\eta A^\eta}{\varrho^\eta} - \varrho^\eta - l^\eta)(2\varrho^\eta + \xi^\eta + \delta^\eta) - (1-p)\epsilon l^\eta\xi^\eta$$

$$B_3 = (1 - C_g)[(\varrho^\eta + \delta^\eta)\{\varrho^{2\eta} + \varrho^\eta(\xi^\eta + l^\eta) + \xi^\eta l^\eta(1 - \epsilon)\} + p\epsilon\varrho^\eta\xi^\eta l^\eta].$$

To show $E_0 = \left(\frac{A^\eta}{\varrho^\eta}, 0, 0, 0\right)$ is locally asymptotically stable Routh-Hurwitz criteria (Theorem 1.4.4) is employed. So, $B_3 > 0$ whenever $C_g < 1$. From eq. (2.3.2),

$$\frac{\alpha^\eta A^\eta}{\varrho^\eta} - \varrho^\eta - l^\eta \leq \epsilon\xi^\eta l^\eta\varrho^\eta(p-1) - \epsilon\xi^\eta l^\eta\delta^\eta \leq 0 \text{ for } C_g < 1$$

$$\implies B_1 > 0 \text{ for } C_g < 1.$$

All the eigenvalues will have negative real parts whenever $B_1B_2 - B_3 > 0$. Hence, the system is stable for equilibrium point $E_0 = \left(\frac{A^\eta}{\varrho^\eta}, 0, 0, 0\right)$ whenever $C_g < 1$. $(S, C, P, R) \to \left(\frac{A^\eta}{\varrho^\eta}, 0, 0, 0\right)$ as $t \to \infty$. So, the crime-free equilibrium point is globally asymptotically stable for $C_g < 1$ whenever $B_1B_2 - B_3 > 0$. This stability condition suggests that, under certain conditions on parameters represented by C_g, the system tends to evolve towards and settle at crime free equilibria regardless of its initial state and the system approaches E_0 in a continuous manner. □

Theorem 2.4.2. *The endemic equilibrium point $E^* = (S^*, C^*, P^*, R^*)$ exists and is locally asymptotically stable if $C_g > 1$.*

Proof. The Jacobian matrix of the given model (2.1.1) at nontrivial equilibrium point $E^* = (S^*, C^*, P^*, R^*)$ is obtained as follows:

$$J^* = \begin{bmatrix} -(\alpha^\eta C^* + \varrho^\eta) & -\alpha^\eta S^* & 0 & (1-\epsilon)\xi^\eta \\ \alpha^\eta C^* & \alpha^\eta S^* - \varrho^\eta - l^\eta & 0 & \epsilon\xi^\eta \\ 0 & pl^\eta & -\varrho^\eta - \delta^\eta & 0 \\ 0 & (1-p)l^\eta & \delta^\eta & -\varrho^\eta - \xi^\eta \end{bmatrix} \tag{2.4.4}$$

The characteristic equation corresponding to J^* is

$$\lambda^4 + D_1\lambda^3 + D_2\lambda^2 + D_3\lambda + D_4 = 0, \tag{2.4.5}$$

where

$$
\begin{aligned}
D_1 =& 4\varrho^{\eta} + \delta^{\eta} + \xi^{\eta} + l^{\eta} + C^*\alpha^{\eta} - S^*\alpha^{\eta} \\
D_2 =& 6\varrho^{2\eta} + 3\varrho^{\eta}[\delta^{\eta} + \xi^{\eta} + l^{\eta} + C^*\alpha^{\eta} - S^*\alpha^{\eta}] + \delta^{\eta}\xi^{\eta} + (\delta^{\eta} + \xi^{\eta})(C^*\alpha^{\eta} - S^*\alpha^{\eta}) + \\
& l^{\eta}[\delta^{\eta} + \xi^{\eta} + C^*\alpha^{\eta} - (1-p)\epsilon\xi^{\eta}] \\
D_3 =& 4\varrho^{3\eta} + 3\varrho^{2\eta}[\delta^{\eta} + \xi^{\eta} + l^{\eta} + C^*\alpha^{\eta} - S^*\alpha^{\eta}] + 2\varrho^{\eta}[\delta^{\eta}\xi^{\eta} + (\delta^{\eta} + \xi^{\eta})(C^*\alpha^{\eta} - S^*\alpha^{\eta}) + \\
& l^{\eta}(\delta^{\eta} + \xi^{\eta} + C^*\alpha^{\eta} - (1-p)\epsilon\xi^{\eta})] + \alpha^{\eta}\delta^{\eta}\xi^{\eta}(C^* - S^*) + l^{\eta}[(1-\epsilon)\delta^{\eta}\xi^{\eta} + \\
& C^*\alpha^{\eta}(\delta^{\eta} + \xi^{\eta}p)] \\
D_4 =& \varrho^{4\eta} + \varrho^{3\eta}[\delta^{\eta} + \xi^{\eta} + l^{\eta} + C^*\alpha^{\eta} - S^*\alpha^{\eta}] + \varrho^{2\eta}[\delta^{\eta}\xi^{\eta} + (\delta^{\eta} + \xi^{\eta})(C^*\alpha^{\eta} - S^*\alpha^{\eta}) + \\
& l^{\eta}(\delta^{\eta} + \xi^{\eta} + C^*\alpha^{\eta} - (1-p)\epsilon\xi^{\eta})] + \alpha^{\eta}\varrho^{\eta}\delta^{\eta}\xi^{\eta}(C^* - S^*) + \\
& \varrho^{\eta}l^{\eta}[(1-\epsilon)\delta^{\eta}\xi^{\eta} + C^*\alpha^{\eta}(\delta^{\eta}\xi^{\eta} + p)].
\end{aligned}
$$

The characteristic equation will have complex roots with negative real parts if the following conditions are met (from eq. (1.4.4)).

$$
D_1 > 0;\ D_4 > 0;\ D_1D_2 - D_3 > 0;\ D_1D_2D_3 - D_3^2 - D_4D_1^2 > 0. \tag{2.4.6}
$$

As a result, if the above conditions are met, E^* is locally asymptotically stable.

The condition $C_g > 1$ serves as a critical threshold. If the criminal generation number exceeds 1, it signifies that the endemic equilibrium point is locally stable. This suggests that the system, influenced by the transmission dynamics and parameters represented by C_g, tends to persist in a stable manner at E^*. The model settle at crime endemic equilibria regardless of its initial state and the system approaches E^* in a continuous manner. □

2.5 Delayed Model

A fractional-order delayed differential model is proposed to investigate the time gap between an individual's crime and their conviction. As we know, it takes time for criminals to be caught and reinforced. This happens as it takes time to judge whether he/she is a criminal or not. This is reflected in the class C by considering delay τ. The mathematical model subject to initial condition in $C([-\tau, 0], R_+^4)$ is as follows:

$$\begin{aligned}
\frac{d^\eta S(t)}{dt^\eta} &= A^\eta - \alpha^\eta S(t)C(t) + (1-\epsilon)\xi^\eta R(t) - \varrho^\eta S(t) \\
\frac{d^\eta C(t)}{dt^\eta} &= \alpha^\eta S(t)C(t) - l^\eta C(t-\tau) + \epsilon\xi^\eta R(t) - \varrho^\eta C(t) \\
\frac{d^\eta P(t)}{dt^\eta} &= pl^\eta C(t-\tau) - \delta^\eta P(t) - \varrho^\eta P(t) \\
\frac{d^\eta R(t)}{dt^\eta} &= (1-p)l^\eta C(t-\tau) + \delta^\eta P(t) - \xi^\eta R(t) - \varrho^\eta R(t)
\end{aligned} \tag{2.5.1}$$

where $\eta \in (0, 1]$ is the order of derivative in the crime transmission model.

2.6 Stability Analysis of Delayed Model

$E^* = (S^*, C^*, P^*, R^*)$ is the endemic equilibrium point of eq. (2.5.1) and S^*, C^*, P^*, R^* eq. (2.3.4) and eq. (2.3.3). The stability changing for the incremental rise in time delay is explored here. The characteristic equation of the system (2.5.1) at the equilibrium point $E^* = (S^*, C^*, P^*, R^*)$ is given by,

$$\left|J_{\tau_0} + e^{-\lambda\tau} J_{\tau_1} - \lambda I\right| = 0. \tag{2.6.1}$$

$$J_{\tau_0} = \begin{bmatrix} -(\alpha^\eta C^* + \varrho^\eta) & -\alpha^\eta S^* & 0 & (1-\epsilon)\xi^\eta \\ \alpha^\eta C^* & \alpha^\eta S^* - \varrho^\eta & 0 & \epsilon\xi^\eta \\ 0 & 0 & -\varrho^\eta - \delta^\eta & 0 \\ 0 & 0 & \delta^\eta & -\varrho^\eta - \xi^\eta \end{bmatrix}, \tag{2.6.2}$$

$$J_{\tau_1} = \begin{bmatrix} 0 & 0 & 0 & 0 \\ 0 & -l^\eta & 0 & 0 \\ 0 & pl^\eta & 0 & 0 \\ 0 & (1-p)l^\eta & 0 & 0 \end{bmatrix}. \tag{2.6.3}$$

After solving, we get

$$\lambda^4 + C_1\lambda^3 + C_2\lambda^2 + C_3\lambda + C_4 + e^{-\lambda\tau}[C_5\lambda^3 + C_6\lambda^2 + C_7\lambda + C_8] = 0, \tag{2.6.4}$$

where

$$
\begin{aligned}
C_1 =& 4\varrho^{\eta} + \delta^{\eta} + \xi^{\eta} + C^*\alpha^{\eta} - S^*\alpha^{\eta} \\
C_2 =& 6\varrho^{2\eta} + 3\varrho^{\eta}[\delta^{\eta} + \xi^{\eta} + C^*\alpha^{\eta} - S^*\alpha^{\eta}] + \delta^{\eta}\xi^{\eta} + (\delta^{\eta} + \xi^{\eta})(C^*\alpha^{\eta} - S^*\alpha^{\eta}) \\
C_3 =& 4\varrho^{3\eta} + 3\varrho^{2\eta}[\delta^{\eta} + \xi^{\eta} + C^*\alpha^{\eta} - S^*\alpha^{\eta}] + 2\varrho^{\eta}[\delta^{\eta}\xi^{\eta} + (\delta^{\eta} + \xi^{\eta})(C^*\alpha^{\eta} - S^*\alpha^{\eta})] + \\
& \alpha^{\eta}\delta^{\eta}\xi^{\eta}(C^* - S^*) \\
C_4 =& \varrho^{4\eta} + \varrho^{3\eta}[\delta^{\eta} + \xi^{\eta} + C^*\alpha^{\eta} - S^*\alpha^{\eta}] + \varrho^{2\eta}[\delta^{\eta}\xi^{\eta} + (\delta^{\eta} + \xi^{\eta})(C^*\alpha^{\eta} - S^*\alpha^{\eta})] + \\
& \alpha^{\eta}\varrho^{\eta}\delta^{\eta}\xi^{\eta}(C^* - S^*) \\
C_5 =& l^{\eta}, \quad C_6 = 3\varrho^{\eta}l^{\eta} + l^{\eta}[\delta^{\eta} + \xi^{\eta} + C^*\alpha^{\eta} - (1-p)\epsilon\xi^{\eta}] \\
C_7 =& 3\varrho^{2\eta}l^{\eta} + 2\varrho^{\eta}l^{\eta}[\delta^{\eta} + \xi^{\eta} + C^*\alpha^{\eta} - (1-p)\epsilon\xi^{\eta}] + l^{\eta}[(1-\epsilon)\delta^{\eta}\xi^{\eta} + C^*\alpha^{\eta}(\delta^{\eta} + \xi^{\eta}p)] \\
C_8 =& \varrho^{3\eta}l^{\eta} + \varrho^{2\eta}l^{\eta}[\delta^{\eta} + \xi^{\eta} + C^*\alpha^{\eta} - (1-p)\epsilon\xi^{\eta}] + \varrho^{\eta}l^{\eta}[(1-\epsilon)\delta^{\eta}\xi^{\eta} + C^*\alpha^{\eta}(\delta^{\eta} + \xi^{\eta}p)].
\end{aligned}
$$

It is acknowledged that there are infinitely many complex roots to the transcendental equation. In the presence of time delay (τ), it is very difficult to identify the signs of the roots. Therefore, we start our study by establishing the time delay (τ) is zero, then derive conditions of stability when $\tau > 0$. The eq. (2.6.4) becomes eq. (2.4.5) at $\tau = 0$ and condition of stability for eq. (2.4.5) already discussed.

Theorem 2.6.1. *The equilibrium point $E^* = (S^*, C^*, P^*, R^*)$ of system (2.5.1) is locally asymptotically stable for $\tau = 0$ iff condition (2.4.6) satisfied.*

The characteristic equation (2.6.4) will have an infinite number of roots if $\tau > 0$. A necessary condition for a change in the stability of E^* is that there should be purely imaginary solutions to the eq. (2.6.4). Let $i\omega_0$ be the root of the eq. (2.6.4) than we obtained,

$$\omega_0^4 - C_2\omega_0^2 + C_4 = [C_6\omega_0^2 - C_8]\cos(\omega_0\tau) + [C_5\omega_0^3 - C_7\omega_0]\sin(\omega_0\tau) \tag{2.6.5}$$

$$C_1\omega_0^3 - C_3\omega_0 = [C_6\omega_0^2 - C_8]\sin(\omega_0\tau) - [C_5\omega_0^3 - C_7\omega_0]\cos(\omega_0\tau) \tag{2.6.6}$$

Squaring and adding the above two equations,

$$\omega_0^8 + N_1\omega_0^6 + N_2\omega_0^4 + N_3\omega_0^2 + N_4 = 0 \tag{2.6.7}$$

where

$$\begin{aligned} N_1 =& C_1^2 - 2C_2 - C_5^2, \\ N_2 =& C_2^2 + 2C_4 - 2C_1C_3 - C_6^2 + 2C_7C_5, \\ N_3 =& C_3^2 - 2C_2C_4 + 2C_6C_8 - C_7^2, \\ N_4 =& C_4^2 - C_8^2 \end{aligned} \tag{2.6.8}$$

If $N_4 < 0$;, then at least one positive root of the eq. (2.6.7) and two purely imaginary roots $i\omega_0$ of the eq. (2.6.6) exists. τ is obtained by using the eq. (2.6.5),

$$\tau_k = \frac{1}{\omega_0}\cos^{-1}\left[\frac{(C_6\omega_0^2 - C_8)(\omega_0^4 - C_2\omega_0^2 + C_4) - \omega_0(C_5\omega_0^3 - C_7\omega_0)(C_1\omega_0^2 - C_3)}{(C_6\omega_0^2 - C_8)^2 + (C_5\omega_0^3 - C_7\omega_0)^2}\right] + \frac{2k\pi}{\omega_0} \tag{2.6.9}$$

Now, by differentiating the eq. (2.6.4) with respect to τ,

$$\left(\frac{d\lambda}{d\tau}\right)^{-1} = \frac{4\lambda^3 + 3C_1\lambda^2 + 2C_2\lambda + C_3}{-\lambda(\lambda^4 + C_1\lambda^3 + C_2\lambda^2 + C_3\lambda + C_4)} + \frac{3C_5\lambda^2 + 2C_6\lambda + C_7}{\lambda(C_5\lambda^3 + C_6\lambda^2 + C_7\lambda + C_8)} - \frac{\tau}{\lambda} \tag{2.6.10}$$

Let us consider

$$\begin{aligned} \left[Re\left(\frac{d\lambda}{d\tau}\right)^{-1}\right]_{\lambda=i\omega_0} =& \left\{Re\left(\frac{4\lambda^3 + 3C_1\lambda^2 + 2C_2\lambda + C_3}{-\lambda(\lambda^4 + C_1\lambda^3 + C_2\lambda^2 + C_3\lambda + C_4)}\right)\right\}_{\lambda=i\omega_0} \\ &+ \left\{Re\left(\frac{3C_5\lambda^2 + 2C_6\lambda + C_7}{\lambda(C_5\lambda^3 + C_6\lambda^2 + C_7\lambda + C_8)} - \frac{\tau}{\lambda}\right)\right\}_{\lambda=i\omega_0} \\ &= \{H_1 + H_2\}, \text{where} \end{aligned} \tag{2.6.11}$$

$$H_1 = \frac{4\omega_0^3 + \omega_0^6(3C_1^2 - 2C_2) + \omega_0^4(4B_4 - 2C_3C_1 + 2C_2^2) + \omega_0^2(C_3^2 - 2C_2C_4)}{(C_3\omega_0^2 - C_1\omega_0^4)^2 + (C_1\omega_0^3 - C_4\omega_0 - \omega_0^2)^2}$$

$$H_2 = \frac{\omega_0^4(C_5^2 - 2C_6^2 + 3C_5C_7) + \omega_0^2(2C_6C_8 - C_7C_5) - 3\omega_0^6C_5^2}{(C_5\omega_0^4 - C_7\omega_0^2)^2 + (C_8\omega_0 - C_6\omega_0^3)^2}$$

If H_1, H_2 are positive then

$$\left[Re\left(\frac{d\lambda}{d\tau}\right)^{-1}\right]_{\tau=\tau^*} = \left[Re\left(\frac{d\lambda}{d\tau}\right)^{-1}\right]_{\lambda=i\omega_0} > 0$$

so, there is a branch of periodic solutions bifurcating from the equilibrium point $E^* = (S^*, C^*, P^*, R^*)$ near $\tau = \tau^*$.

Theorem 2.6.2. *Suppose that H_1, H_2 are positive for system (2.5.1), the endemic equilibrium $E^* = (S^*, C^*, P^*, R^*)$ is locally asymptotically stable for $\tau \in [0, \tau^*)$ and unstable when $\tau > \tau^*$ and displays a Hopf bifurcation at the equilibrium point $E^* = (S^*, C^*, P^*, R^*)$ when $\tau = \tau^*$.*

2.7 Numerical Validation Through Simulation

This section presents the numerical results to illustrate the dynamic behavior of crime transmission and to validate the analytical findings for different orders of differentiation and different values of time delay.

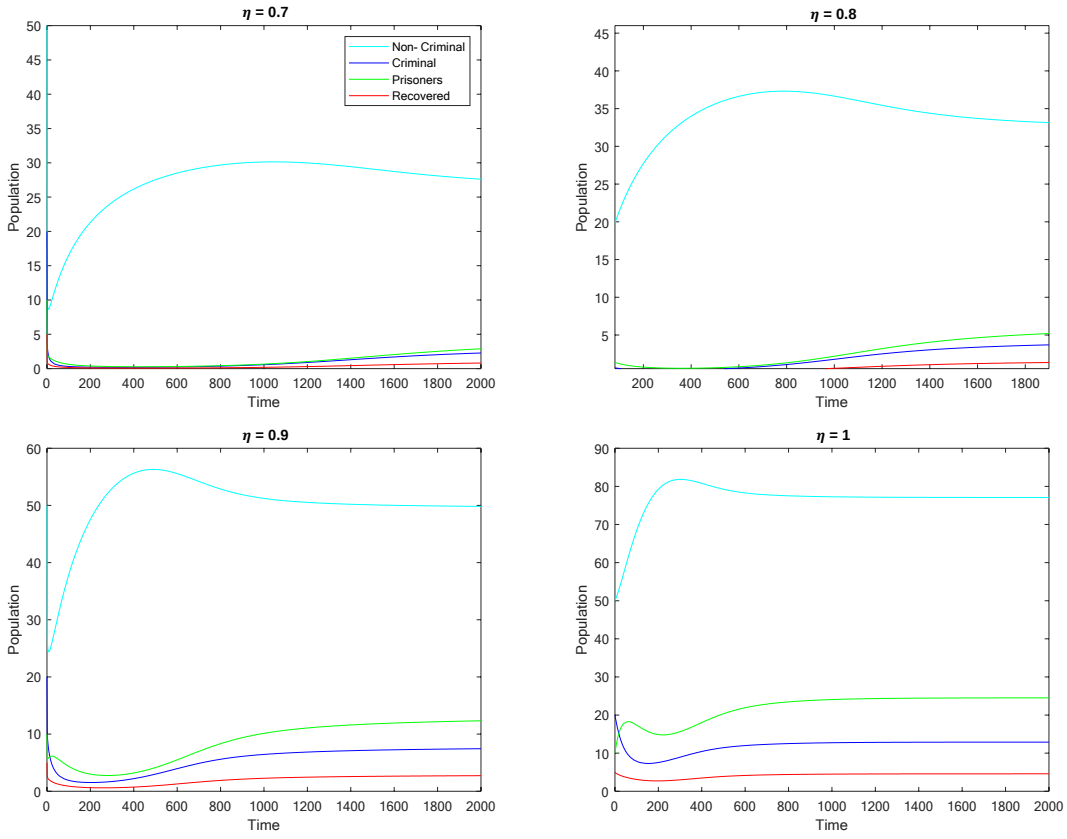

Figure 2.2: Variations of Non-Criminal population S, Criminal population C, Prisoners P, and Recovered population R with time without delay for different order η which shows criminal population C is decreasing with time when order decreases.

Table 2.1 describes the parameters used and Table 2.2 shows the initial conditions and the set of parameters used for validation, which are retrieved from [51, 112].

Table 2.2: Parameter value for crime transmission model.

Parameter	A	α	ξ	δ	l	ϱ	p	ϵ
Value	0.5	0.0005	0.1	0.01	0.045	0.00422	0.6	0.3

Population	S	C	P	R
Initial Values	50	20	10	5

Table 2.3: Variation of delay with order of derivative.

η	0.7	0.8	0.9	1
τ	29.95	29.5	27.9	25.5

In Figure 2.2, numerical simulations show that the endemic equilibrium points for the proposed fractional-order crime transmission model are asymptotically stable for $\eta = 1, 0.9, 0.8, 0.7$ and for $\eta < 0.7$ populations become negative. Trajectories of all the populations, irrespective of the order chosen, justify the stability of the proposed model. If $C_g > 1$, society cannot be crime-free, but crime declines and becomes stable after a particular time, irrespective of the order of derivative. Also, the criminal population decreases as the order of derivative decreases. From Figure 2.2, it can be noticed that each population converges faster to its equilibrium as η is increased.

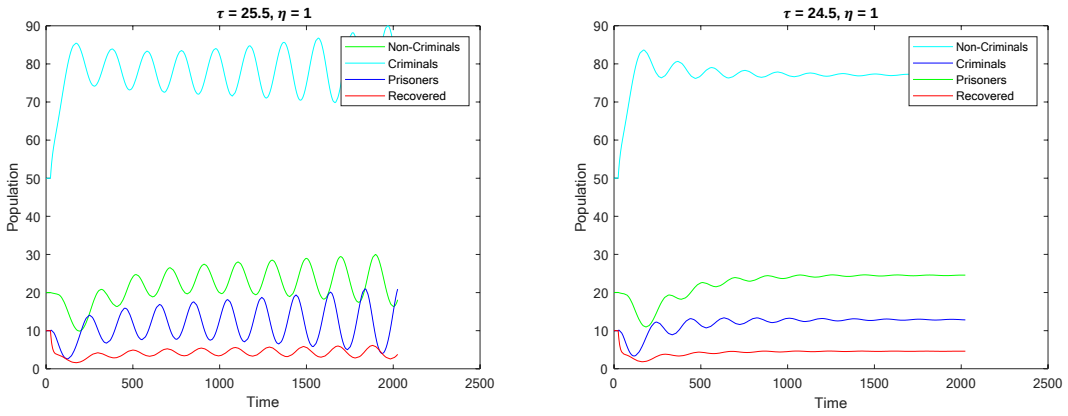

Figure 2.3: The fractional-order delayed crime model is unstable for time delay $\tau \geq \tau_1 = 25.5$ and stable for chosen time delay $\tau = 24.5$, $\eta = 1$.

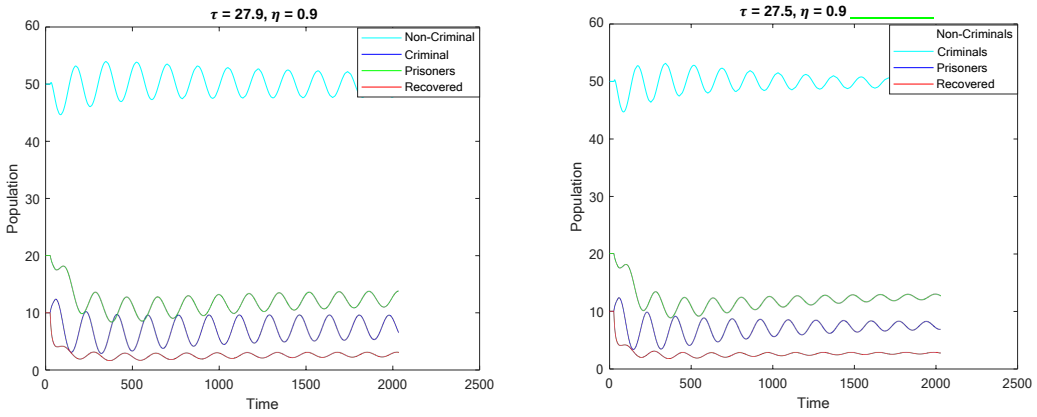

Figure 2.4: The fractional-order delayed crime model is unstable for time delay $\tau \geq \tau_{0.9} = 27.9$ and stable for chosen time delay $\tau = 27.5$, $\eta = 0.9$.

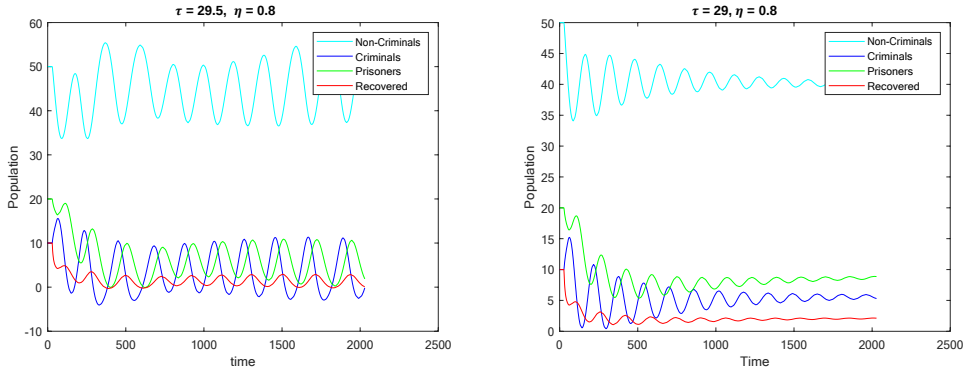

Figure 2.5: The fractional-order delayed crime model is unstable for time delay $\tau \geq \tau_{0.8} = 29.5$ and stable for chosen time delay $\tau = 29$, $\eta = 0.8$.

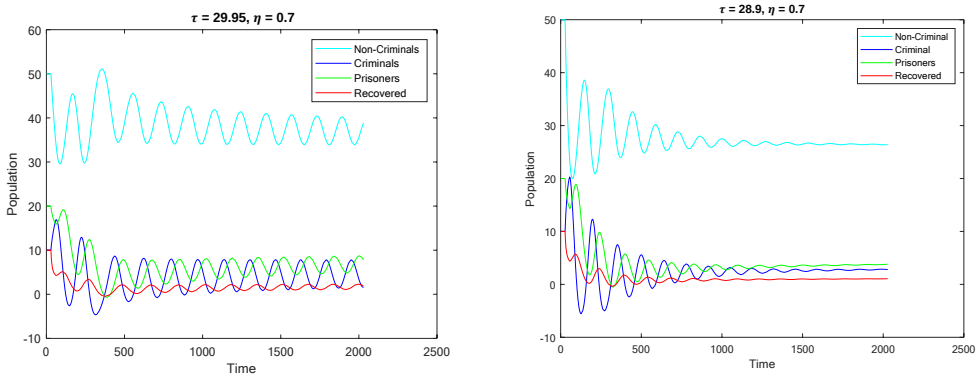

Figure 2.6: The fractional-order delayed crime model is unstable for time delay $\tau \geq \tau_{0.7} = 29.95$ and stable for chosen time delay $\tau = 28.9$, $\eta = 0.7$.

The Figures 2.3 to 2.6 illustrates the behavior of delayed crime model (2.5.1) for $\eta = 0.7, 0.8, 0.9, 1$. The graphs present the dynamics of each population for $\eta = 0.7, 0.8, 0.9, 1$ with time delay and it is clear that the system becomes unstable for $\tau \geq \tau_\eta$. The values of the delay coefficient for various values of η are shown in Table 2.3. Clearly, the Figures 2.3 to 2.6 show that the delay decreases as the order of derivative increases, indicating that the model's stability region expands. Hence, the finding reveals that law enforcement officers can have 30 weeks to apprehend criminals and ensure their convictions. In contrast, the time frame for the integer-order model is constrained to approximately 25 weeks.

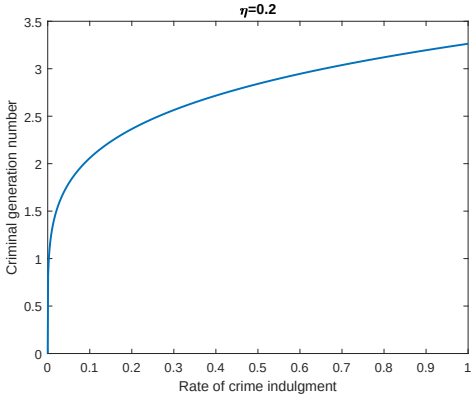

(a) Criminal generation number increasing with increase in crime indulgence rate.

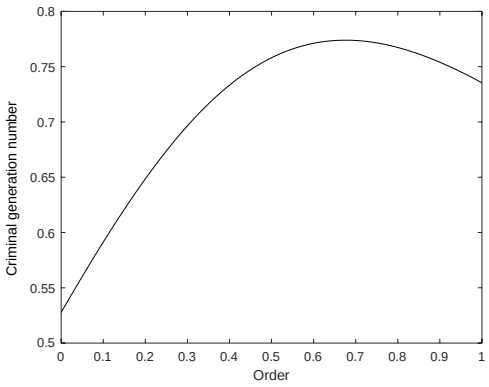

(b) Criminal generation number is increasing with the order of derivative, i.e., criminal population decreases with the order of derivative.

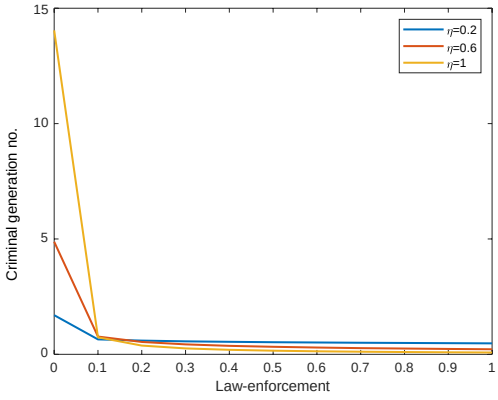

(c) Criminal generation number is inversely proportional to the rate of law enforcement.

Figure 2.7: Relation of criminal generation no. (C_g) with order of derivative (η), Law-enforcement (l), and rate of crime indulgement (α).

According to Figure 2.7, the criminal generation number increases as order (η) increases up to a certain value of η, after that, it starts decreasing. As density (the rate of indulgement (l)) increases, the criminal generation number increases, which means the criminal population increases with the rate of indulgement. Again, from Figure 2.7, crime transmission reduces as law enforcement increases for different values of the order of derivative (η). Although there is a need for a higher rate of law enforcement, the graph shows the optimal value of law enforcement lies near 0.1 irrespective of the order of differentiation, which means it will lead to crime-free equilibrium for $l > 0.1$.

2.8 Summary and Conclusions

There is great scope to enhance the existing law to capture the crime prevalent in the current society. Hence, to address this, a fractional-order crime propagation mathematical model for analyzing the dynamics of the propagation of crime by considering the criminal history is proposed. From this work, it is evident that the criminal generation number increases as the order of derivative (η) increases up to a certain value of η. Though it is expected that the criminal population will decrease as the parameter l increases, we have obtained a threshold value of l. The major findings of the present research are listed below:

- The delayed model suggests that once the delay reaches a certain threshold, the model would oscillate periodically. If the order of derivative increases from 0 to 1, the delay decreases, indicating that the stability region expands for the fractional-order model.

- According to this model, law enforcement officers are provided approximately 30 weeks to apprehend criminals and secure their convictions, whereas, in the case of the integer order model, the time frame is around 25 weeks. Hence, the fractional-order model allows law enforcement officers additional time, which is beneficial in securing a criminal's conviction, as 25 weeks to apprehend criminals and secure their convictions is practically not possible (Department of Justice, United States; National Center for State Courts, United States).

- As law enforcement increases, the criminal population declines, but until a certain point is reached, there is no longer any discernible impact on the spread of crime. Moreover, the optimal value of law enforcement lies near 0.1, as not much variation is seen in the behavior of criminal generation number beyond 0.1. If the law enforcement rate increases beyond 0.1, the adverse impact on the country's economy will be more pronounced than the benefits derived from a reduction in the crime rate.

- Incorporating memory using a fractional-order derivative in the crime transmission model results in fewer criminal generation number as the derivative order decreases. This correlation arises because the memory property diminishes as the derivative order decreases from 1. Consequently, it is observed that crime transmission reduced by decreasing the memory.

In order to effectively diminish crime, policymakers should concentrate on initiatives directed at shielding children from exposure to criminal influences and enhancing their living conditions. Establishing an environment where criminals cannot freely share their experiences becomes crucial to minimizing the transmission of criminal behavior. Hence, the proposed model accelerates to achieve a crime-free society by considering memory and hereditary property as a crucial parameters.

The substantial part of this chapter has been published in the following publications:

- *K. Bansal, S. Arora, K. S. Pritam, T. Mathur, and S. Agarwal (2022), " Dynamics of crime transmission using fractional-order differential equations." Fractals, 30(01), 2250012.*
- *K. Bansal, T. Mathur, N. S. S. Singh, and S. Agarwal (2022), "Analysis of illegal drug transmission model using fractional delay differential equations." AIMS Mathematics, 7(10), 18173-18193.*

Chapter 3

Crime Propagation Model With Non-Linear Transmission Rate

"The growth of crime is like a cancer that, unchecked, will eventually destroy society."

- E.F. Schumacher

Crime is one of the most significant challenges throughout all societies [113, 114]. Crime is an aberrant activity that deviates from established standards and ideals. The social structure of the organization has a significant impact on the propagation of crime within a community. It is a well-known fact that crime spreads across society like an infectious illness, even though a variety of factors may impact this dynamic [51, 115]. Mathematical modeling is a crucial tool for comprehending how infectious diseases propagate and are controlled [116–118]. The transmission rate is the primary consideration in modeling techniques when assessing the spread of any disease [119, 120]. There are different types of transmission rates, such as linear and non-linear. Initially, a huge population would not be feasible for the bilinear transmission rate (linear), βSI, where β is the infection rate, S stands for susceptible people, and I stands for infected people [121–123]. As we may deduce from the word SI, it is unrealistic to presume that an increase in the susceptible population will directly result in a proportional rise in the number of individuals infected per unit of time. The National Crime Records Bureau, Government of India, also reports that the relationship between non-criminals and criminals is not linear (see Figure 1.2).

As a result, the non-linear transmission rate can depict reality in a better way than the linear transmission rate. Therefore, modifying the conventional linear transmission rate is necessary to understand the infection dynamics among a vast population.

Several mathematical models with a bilinear transmission rate for the prevention of crime transmission based on ordinary differential equations and fractional differential equations have already been proposed [10, 35–37, 47, 50–54, 124–126]. Several authors proposed various kinds of non-linear transmission rates in epidemiology [121, 127–130]. In 1978 Anderson and May [128] first proposed the saturated transmission rate $\frac{\alpha SI}{1+\beta S}$ and saturation factor β has an impact on epidemic control. Li *et al.* [131] suggested a SIR model with a non-linear transmission rate $\frac{\alpha SI}{1+\gamma I}$ and saturation factor γ is inhibition effect (treatment of infected population). The number of influencing contacts between infectious and susceptible people may saturate at high infectious levels due to the crowding of infected people at this transmission rate. Baba *et al.* [132] proposed a tuberculosis model using saturated incidence rate and established the significance of the inhibitory effect. Xiao *et al.* [133] suggested that the number of effective interactions between infective and susceptible persons falls at high infective levels due to the quarantine of infective individuals or protective measures taken by susceptible individuals by utilizing the non-monotone non-linear incidence rate. Ruan *et al.* [134] also studied the dynamical behavior of an epidemic model with a non-linear incidence rate. A non-linear Beddington DeAngelis transmission rate, $\frac{\alpha SI}{1+\beta S+\gamma I}$, was independently developed by Beddington and DeAngelis in 1975 [135, 136]. The Beddington-DeAngelis transmission rate is a generalization of linear and some non-linear transmission rates. This chapter presents a mathematical crime propagation model with a Beddington-DeAngelis non-linear transmission rate contributing to a better understanding of crime transmission.

This chapter seeks to develop a fractional-order mathematical model with a non-linear transmission rate for evaluating the dynamics of crime spread. The population comprises non-criminals, criminals, and prisoners. This concept's main assumption is that crime may spread through social contact, which is impacted by social background. Contrary to reality, the bilinear transmission rate implies that criminals increased as non-criminals increased.

Therefore, the present study compares the various crime transmission model with different transmission rates.

3.1 Establishment of Crime Propagation Model

Criminal activity is still rising despite the frequent implementation of several appropriate measures (police deployment, penalty, jail, recidivism, and other laws and regulations). As a result, we must put forth a model that can help explain, anticipate, and further restrain illicit proliferation by deploying appropriate security officers and enforcing laws on the criminal behavior of the population.

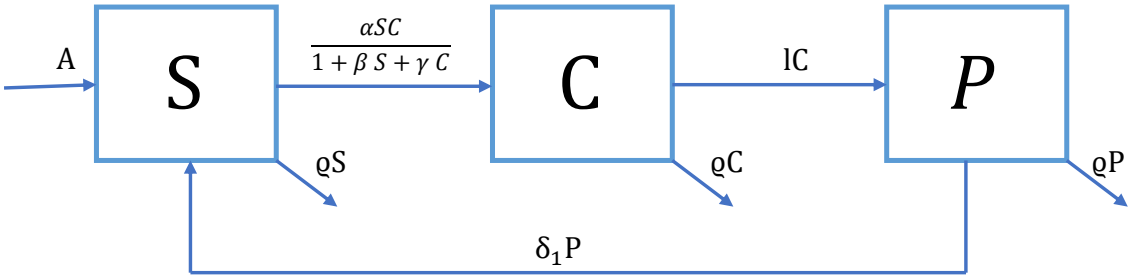

Figure 3.1: Crime propagation model for non-linear transmission rate.

Consider that the population is divided into three categories: Non-Criminals (S), Criminals (C), and Prisoners (P). Figure 3.1 depicts the suggested model's flow diagram. Let the non-criminals be recruited with the rate A, and each class's population experiences a natural death rate of ϱ. Because of the interplay of the criminal and non-criminal populations, the non-criminal population is decreasing at a rate of α as non-criminals become criminals. Criminals move to the prisoners class due to law enforcement with the rate l, and prisoners move to the non-criminals class after completing the required time in prison with the rate δ_1. With the aforementioned facts in mind and non-negative initial conditions, the proposed mathematical model is represented by the following dimensionally balanced fractional differential equations:

$$\begin{aligned}
\frac{d^\eta S(t)}{dt^\eta} &= A^\eta - \frac{\alpha^\eta S(t)C(t)}{1+\beta S(t)+\gamma C(t)} + \delta_1^\eta P(t) - \varrho^\eta S(t) \\
\frac{d^\eta C(t)}{dt^\eta} &= \frac{\alpha^\eta S(t)C(t)}{1+\beta S(t)+\gamma C(t)} - l^\eta C(t) - \varrho^\eta C(t) \\
\frac{d^\eta P(t)}{dt^\eta} &= l^\eta C(t) - \varrho^\eta P(t) - \delta_1^\eta P(t)
\end{aligned} \tag{3.1.1}$$

where $S(0) > 0,\ C(0) > 0,\ P(0) > 0$, and η is order of derivative . In the proposed model incidence rate is

$$f(S,C) = \frac{\alpha^\eta S(t)C(t)}{1+\beta S(t)+\gamma C(t)}$$

here, α stands for the transmission rate, β for the inhibition effect (preventive measures taken by non-criminal individuals), and γ for the inhibition effect (treatment of criminals). It's vital to note that the incidence rate proposed in this study may be categorized as:

- If $\beta = 0;\ \gamma = 0$, then $f(S,C) = \alpha^\eta SC$ represents linear (bilinear) incidence rate.
- If $\gamma = 0; \beta \neq 0$, then the saturation incidence rate for the non-criminal people is $f(S,C) = \dfrac{\alpha^\eta S(t)C(t)}{1+\beta S(t)}$. The prevention strategy employed to curb an epidemic's spread results in the inhibitory impact β induced by the saturation factor.
- If $\beta = 0; \gamma \neq 0$, then the saturation incidence rate for the criminal individuals $f(S,C) = \dfrac{\alpha^\eta S(t)C(t)}{1+\gamma C(t)}$. In this scenario, the interaction between criminal and non-criminal people may saturate at high infection levels due to the crowding of criminals or the preventive measures adopted by non-criminal individuals.

3.2 Basic Properties of Proposed Model

This section demonstrates that the solution of the proposed model uniquely exists as well as is non-negative and bounded.

3.2.1 Invariant Region

The set Ω is invariant if, for all the initial conditions are in Ω, the solution of the proposed model remains in Ω. As a consequence, a positively invariant set will have positive

solutions.

The dynamics of the fractional-order crime propagation model (3.1.1) are explored in a feasible region $\Omega \in \mathbb{R}^3_+$, where

$$\Omega = \left\{ (S, C, P) \in \mathbb{R}^3_+ : S + C + P \leq \frac{A^\eta}{\varrho^\eta} \right\}. \tag{3.2.1}$$

Theorem 3.2.1. *The region $\Omega \in \mathbb{R}^3_+$ is the positively invariant region with non-negative initial conditions for the proposed crime transmission model.*

Proof. Let $N(t) = S(t) + C(t) + P(t)$. Then,

$$\begin{aligned} \frac{d^\eta N(t)}{dt^\eta} &= \frac{d^\eta S(t)}{dt^\eta} + \frac{d^\eta C(t)}{dt^\eta} + \frac{d^\eta P(t)}{dt^\eta} \\ &= A^\eta - \varrho^\eta N(t). \end{aligned} \tag{3.2.2}$$

Using the Laplace transformation (from eq. (1.1.13)):

$$N(s) = \frac{\frac{A^\eta}{s} + s^{\eta-1} N(0)}{s^\eta + \varrho^\eta}. \tag{3.2.3}$$

Now, using inverse Laplace transformation (from eq. (1.1.8):

$$N(t) = \frac{A^\eta}{\varrho^\eta}[1 - \mathbb{E}_{\eta,1}(-\varrho^\eta t^\eta)] + N(0)\mathbb{E}_{\eta,1}(-\varrho^\eta t^\eta), \tag{3.2.4}$$

where $\mathbb{E}_{\eta,1}$is Mittag-Leffler function defined in eq. (1.1.7).

$$\text{If } 0 < \eta \leq 1, \text{then } 0 \leq \mathbb{E}_{\eta,1}(-\varrho^\eta t^\eta) \leq 1 \implies N(t) \leq \frac{A^\eta}{\varrho^\eta}. \tag{3.2.5}$$

$$\left.\frac{d^\eta S(t)}{dt^\eta}\right|_{S(t_0)=0} = A^\eta N + \delta_1^\eta P \geq 0, \tag{3.2.6}$$

$$\left.\frac{d^\eta C(t)}{dt^\eta}\right|_{C(t_0)=0} = 0 \geq 0, \tag{3.2.7}$$

$$\left.\frac{d^{\eta}P(t)}{dt^{\eta}}\right|_{P(t_0)=0} = \delta_1^{\eta} C \geq 0. \tag{3.2.8}$$

Now, from the generalized mean value theorem (Theorem 1.4.2), the solution of the proposed model is non-negative and lies in Ω. As a result, the region Ω is the positively invariant region, attracting all the solutions. □

3.2.2 Existence and Uniqueness

Theorem 3.2.2. *Along with non-negative initial conditions, the crime propagation model has a unique and bounded solution for* $t \geq 0$.

Proof. RHS of proposed model eq. (3.1.1) is continuous, bounded from eq. (3.2.5) and satisfy Lipschitz conditions. So, according to the existence and uniqueness theorem (Theorem 1.4.1), the solution of the proposed model (3.1.1) not only exists but is also unique and bounded. □

3.3 Dynamical Evaluation of Crime Propagation Model

This section presents the equilibrium points and the criminal generation number. Setting the right-hand sides of each equation in the proposed models to zero allows us to find equilibrium points.

3.3.1 Criminal-free Equilibria

A criminal-free equilibrium point (trivial equilibrium point) exists if the criminals become zero, i.e.,

$$E_1 = \left(\frac{A^{\eta}}{\varrho^{\eta}}, 0, 0\right).$$

3.3.2 Criminal Generation Number

The criminal generation number, denoted C_g, is defined as "the anticipated count of subsequent cases produced by an individual engaged in criminal activity within a completely non-criminal community [111]." To determine the criminal generation number, the

next-generation matrix approach [111] is utilized at criminal-free equilibrium. Let

$$\frac{d^{\eta}X}{dt^{\eta}} = \mathcal{F}(X) - \mathcal{V}(X), \tag{3.3.1}$$

where $X = [S \;\; C \;\; P]$,

$\mathcal{V}(X)$ represents the matrix of terms used for movement in and out of a class, and

$\mathcal{F}(X)$ represents the matrix of terms used for new infections.

$$F = \left(\frac{\partial \mathcal{F}}{\partial X}\right)_{E_1}, V = \left(\frac{\partial \mathcal{V}}{\partial X}\right)_{E_1}.$$

$$F = \begin{bmatrix} 0 & 0 & 0 \\ 0 & \dfrac{\alpha^{\eta}A^{\eta}}{\varrho^{\eta}+\beta A^{\eta}} & 0 \\ 0 & 0 & 0 \end{bmatrix}, \qquad V = \begin{bmatrix} \varrho^{\eta} & \dfrac{\alpha^{\eta}A^{\eta}}{\varrho^{\eta}+\beta A^{\eta}} & -\delta_1^{\eta} \\ 0 & \varrho^{\eta}+l^{\eta} & 0 \\ 0 & -l^{\eta} & \delta_1^{\eta}+\varrho^{\eta} \end{bmatrix}.$$

The spectral radius of FV^{-1} is equal to C_g, where,

$$C_g = \frac{A^{\eta}\alpha^{\eta}}{(\varrho^{\eta}+l^{\eta})(\varrho^{\eta}+A^{\eta}\beta)}. \tag{3.3.2}$$

3.3.3 Crime Persistence Equilibria

The concept of a crime persistence equilibrium refers to a situation where crime remains at a relatively stable and persistent level over time within a community or society. The crime persistence equilibrium point (endemic equilibrium point) exists if criminals become non-zero, i.e., $E_2 = (S^*, C^*, P^*)$. Now set the RHS of equations in the proposed models to zero,

$$\begin{aligned} A^{\eta} - \frac{\alpha^{\eta}S(t)C(t)}{1+\beta S(t)+\gamma C(t)} + \delta_1^{\eta}P(t) - \varrho^{\eta}S(t) &= 0, \\ \frac{\alpha^{\eta}S(t)C(t)}{1+\beta S(t)+\gamma C(t)} - l^{\eta}C(t) - \varrho^{\eta}C(t) &= 0, \\ l^{\eta}C(t) - \varrho^{\eta}P(t) - \delta_1^{\eta}P(t) &= 0. \end{aligned} \tag{3.3.3}$$

On solving these equations, we have,

$$C^* = \frac{(\varrho^\eta + l^\eta)(\varrho^\eta + \delta_1^\eta)(A^\eta\beta + \varrho^\eta)(C_g - 1)}{\varrho^\eta\gamma(\varrho^\eta + \delta_1^\eta)(\varrho^\eta + l^\eta) + \varrho^\eta(\varrho^\eta + \delta_1^\eta + l^\eta)(\alpha^\eta - \beta(\varrho^\eta + l^\eta))}.$$

$$\text{Let } C_g > 1, \frac{A^\eta\alpha^\eta}{(\varrho^\eta + l^\eta)(\varrho^\eta + A^\eta\beta)} > 1 \implies A^\eta\alpha^\eta > (\varrho^\eta + l^\eta)(\varrho^\eta + A^\eta\beta)$$

$$\implies \alpha^\eta - (\varrho^\eta + l^\eta)\beta > 0 \text{ if } C_g > 1$$

$$P^* = \frac{l^\eta C^*}{\varrho^\eta + \delta_1^\eta}, \quad S^* = \frac{(1 + \gamma C^*)(\varrho^\eta + l^\eta)}{\alpha^\eta - (\varrho^\eta + l^\eta)\beta}.$$

Hence, crime persistence equilibrium exits if $C_g > 1$. It's important to understand that achieving a persistent level of crime is not a desirable or intentionally sought-after goal for any society. While some communities may face persistent crime challenges due to complex social and economic factors, the ultimate goal remains to reduce and eliminate criminal activity rather than maintain it at a persistent level.

3.4 Stability Analysis of Proposed Model

Theorem 3.4.1. *The criminal-free equilibrium point* $E_1 = \left(\frac{A^\eta}{\varrho^\eta}, 0, 0\right)$ *of the proposed crime transmission model is stable if* $C_g < 1$.

Proof. The Jacobian matrix at E_1 is

$$J_{E_1} = \begin{bmatrix} -\varrho^\eta & -\frac{\alpha^\eta A^\eta}{\varrho^\eta + \beta A^\eta} & \delta_1^\eta \\ 0 & \frac{\alpha^\eta A^\eta}{\varrho^\eta + \beta A^\eta} - \varrho^\eta - l^\eta & 0 \\ 0 & l^\eta & -\varrho^\eta - \delta_1^\eta \end{bmatrix}.$$

Clearly, the two eigenvalues are $-\varrho^\eta, -\varrho^\eta - \delta_1^\eta$ are negative. if

$$\frac{\alpha^\eta A^\eta}{\varrho^\eta + \beta A^\eta} - \varrho^\eta - l^\eta < 0 \text{ if } C_g < 1$$

So, using Routh–Hurwitz conditions (Theorem 1.4.4), E_1 is stable. □

Theorem 3.4.2. *The criminal-free equilibrium* $E_1 = \left(\frac{A^\eta}{\varrho^\eta}, 0, 0\right)$ *of the proposed crime transmission model is globally asymptotically stable if* $C_g \leq 1$.

Proof. Let L denote the Lyapunov function described as

$$L = \frac{1}{1+\beta S_0}\left(S - S_0 - S_0\, ln\frac{S}{S_0}\right) + C + P, \text{ where } S_0 = \frac{A^\eta}{\varrho^\eta}.$$

Now, the η^{th} derivative of Lyapunov function L is given by [137]:

$$\frac{d^\eta L}{dt^\eta} \leq \frac{1}{1+\beta S_0}\left(\frac{S-S_0}{S}\right)\frac{d^\eta S}{dt^\eta} + \frac{d^\eta C}{dt^\eta} + \frac{d^\eta P}{dt^\eta},$$

$$\frac{d^\eta L}{dt^\eta} \leq -\frac{(S-S_0)^2\varrho^\eta}{S(1+\beta S_0)} + (\varrho^\eta + l^\eta)C(C_g - 1)$$

Then, clearly $\frac{d^\eta L}{dt^\eta} < 0$ if $C_g \leq 1$. □

Theorem 3.4.3. *The crime persistence equilibrium point* $E_2 = (S^*, C^*, P^*)$ *of the proposed crime transmission model exists and is locally asymptotically stable if* $C_g > 1$ *with some condition.*

Proof. The Jacobian matrix at E_2 is:

$$J_{E_2} = \begin{bmatrix} -\frac{(1+\gamma C^*)\alpha^\eta C^*}{(1+\beta S^*+\gamma C^*)^2} - \varrho^\eta & -\frac{(1+\beta S^*)\alpha^\eta S^*}{(1+\beta S^*+\gamma C^*)^2} & \delta_1^\eta \\ \frac{(1+\gamma C^*)\alpha^\eta C^*}{(1+\beta S^*+\gamma C^*)^2} & \frac{(1+\beta S^*)\alpha^\eta S^*}{(1+\beta S^*+\gamma C^*)^2} - l^\eta - \varrho^\eta & 0 \\ 0 & l^\eta & -\varrho^\eta - \delta_1^\eta \end{bmatrix}.$$

The characteristic equation for J_{E_2} is

$$\lambda^3 + Q_1\lambda^2 + Q_2\lambda + Q_3 = 0. \tag{3.4.1}$$

The root of the characteristic equation has negative real parts if $Q_1 > 0;\ Q_3 > 0;\ Q_1Q_2 > Q_3$ [138]. As a result, if the prerequisites are satisfied, $E_2 = (S^*, C^*, P^*)$ is locally asymptotically stable. □

3.5 Bifurcation Analysis

This section explores the behavior of the crime transmission model when the crime generation number is 1. A sudden qualitative shift in the system's behavior occurs when the parameter values of the system gradually change. When the equivalence $A^\eta \alpha^\eta = (\varrho^\eta + l^\eta)(\varrho^\eta + A^\eta \beta)$ is met, the two fixed points E_1 and E_2 seem to collide and change stability, giving the impression that the system is going through a transcritical bifurcation as seen in Figure 3.2.

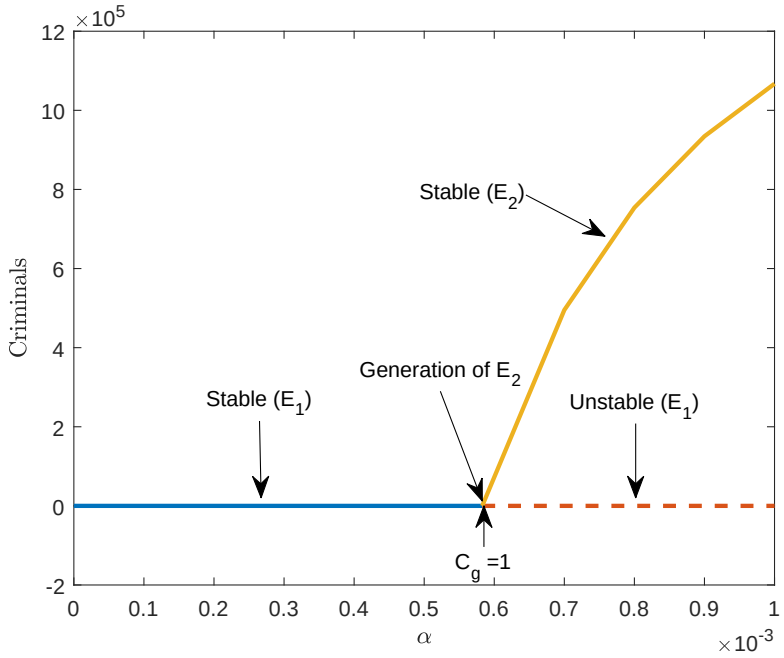

Figure 3.2: Bifurcation diagram demonstrates E_1 is stable for $C_g < 1$ and unstable for $C_g > 1$, E_2 exists and stable for $C_g > 1$.

Theorem 3.5.1. *The proposed model shows transcritical bifurcation at* $A^\eta \alpha^\eta = (\varrho^\eta + l^\eta)(\varrho^\eta + A^\eta \beta)$.

Proof. We observe that the Jacobian matrix for the proposed model derived at $C_g = 1$ and $\alpha^* = \alpha^\eta = \dfrac{(\varrho^\eta + l^\eta)(\varrho^\eta + A^\eta \beta)}{A^\eta}$ has a simple zero eigenvalue. Since the stability behavior of equilibrium points at $C_g = 1$ cannot be correctly predicted by linearization, we resort it using the center manifold theorem (Theorem 1.4.7).

Let J be Jacobian matrix at $C_g = 1$

$$J = \begin{bmatrix} -\varrho^\eta & -\varrho^\eta - l^\eta & \delta_1^\eta \\ 0 & 0 & 0 \\ 0 & l^\eta & -\varrho^\eta - \delta_1^\eta \end{bmatrix}.$$

It is simple to confirm that one of the eigenvalues is 0 as $det(J) = 0$. If $\mathcal{W}$ and $\mathcal{U}$ are the respective eigenvectors for the zero eigenvalues of the matrices J, J^T, defined as

$$\mathcal{W} = \begin{bmatrix} 0 \\ 1 \\ 0 \end{bmatrix}, \qquad \mathcal{V} = \begin{bmatrix} -\dfrac{l^\eta + \varrho^\eta + \delta_1^\eta}{l^\eta} \\ \dfrac{\varrho^\eta + \delta_1^\eta}{l^\eta} \\ 1 \end{bmatrix}$$

Then from center manifold theorem (Theorem 1.4.6), the bifurcation constants a_1 and b_1 are

$$a_1 = \sum_{i,j,k} w_k v_i v_j \left(\frac{\partial^2 f_k}{\partial x_i \partial x_j}\right)_{E_1}, \quad b_1 = \sum_{k,i} w_k v_i \left(\frac{\partial^2 f_k}{\partial x_i \partial \alpha^*}\right)_{E_1}.$$

Let $S = x_1, C = x_2, P = x_3$

$$\left(\frac{\partial^2 f_2}{\partial x_1 \partial x_2}\right)_{E_1} = \frac{\alpha^*}{(1+\beta S_0)^2}, \left(\frac{\partial^2 f_2}{\partial x_2^2}\right)_{E_1} = \frac{-2\alpha^*\gamma S_0}{(1+\beta S_0)^2}, \left(\frac{\partial^2 f_2}{\partial x_2 \partial \alpha^*}\right)_{E_1} = \frac{S_0}{(1+\beta S_0)^2}.$$

Hence $a_1 < 0, b_1 > 0$. Therefore, from Theorem 1.4.6, the criminal-free equilibrium point changes from stable to unstable when $C_g = 1$, and as C_g passes one, a positive equilibrium occurs. As a result, at $C_g = 1$, the proposed model (3.1.1) experiences transcritical bifurcation. □

The significance of transcritical bifurcation in crime modeling lies in its capacity to expose the sensitivity of crime with the variation in parameter α. This phenomenon can result in substantial shifts in equilibrium points, influencing solution stability and carrying policy implications. Identifying transcritical bifurcation serves as a crucial tool for recognizing patterns, aiding policymakers in making informed decisions, and crafting effective policies to address crime by considering the crime transmission rate α.

3.6 Numerical Illustration

The numerical simulation validates the analytical findings for various orders of derivative and illustrates the dynamic nature of the crime propagation model. The predictor-corrector approach of Adams-Bashforth-Moulton is used to solve the proposed model [109]. Table 3.1 displays the variables and parameters used for the evaluation, which are considered from several published articles such as Pritam *et al.* [10], Bansal *et al.* [125], and Partohaghighi *et al.* [126].

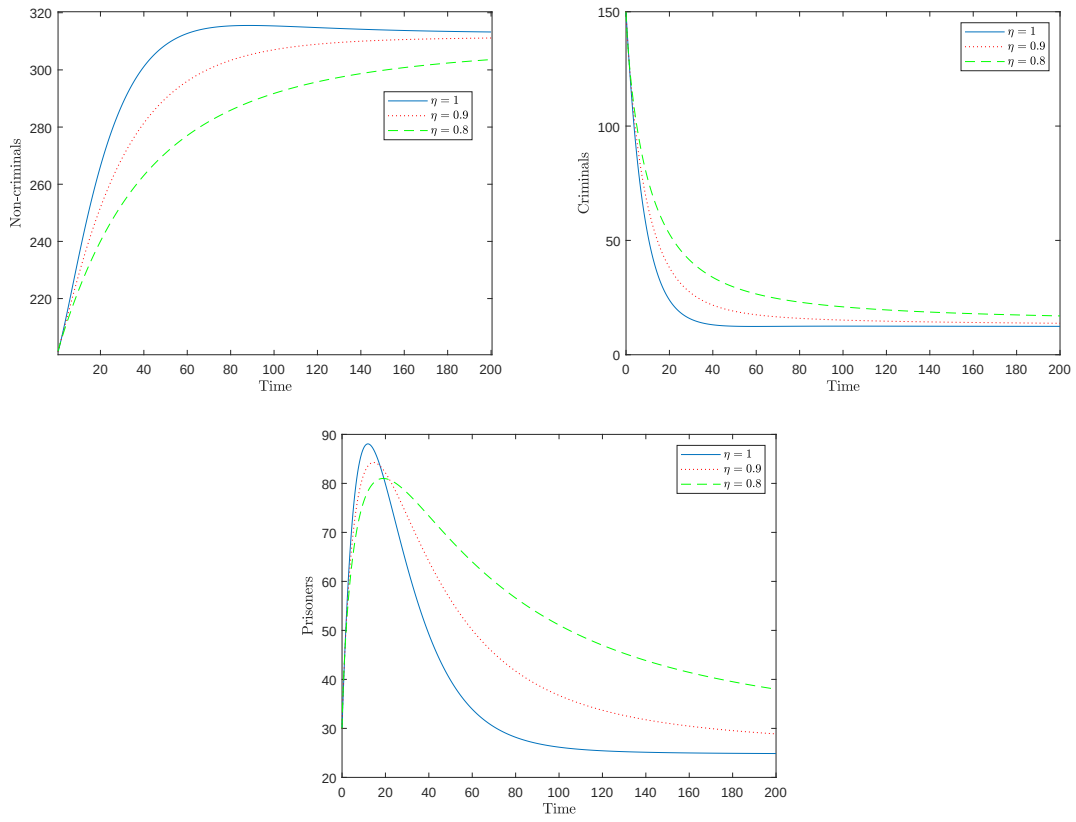

Figure 3.3: Time series plot for the dynamics of non-criminals, criminals, and prisoners for the different order of derivatives.

According to Figure 3.3, the steady states are asymptotically stable for $\eta = 0.8, 0.9,$ and 1. As η increases, the population approaches its equilibrium more swiftly, as seen in Figure 3.3. The trajectory of non-criminals, criminals, and prisoners shows the stability of

the crime propagation model for the different orders of derivative. In Figure 3.3, criminals decrease with time due to law enforcement, and the non-criminals increase and attain a steady state for the different order of derivative. Furthermore, prisoners first increase with time due to law enforcement and then start decreasing as prisoners move to the non-criminal class.

Table 3.1: Parameter description and values for crime propagation.

Parameter	Description	value
A	Recruitment rate	7
β	Inhibition effect (preventive measures by susceptible individuals)	0.002
γ	Crowding effect	0.5
ϱ	Natural death rate	0.02
δ_1	Rate from which prisoners move to non-criminal class	0.03
l	Law enforcement rate	0.1
α	Transmission rate from non-criminal to criminal class	0.003

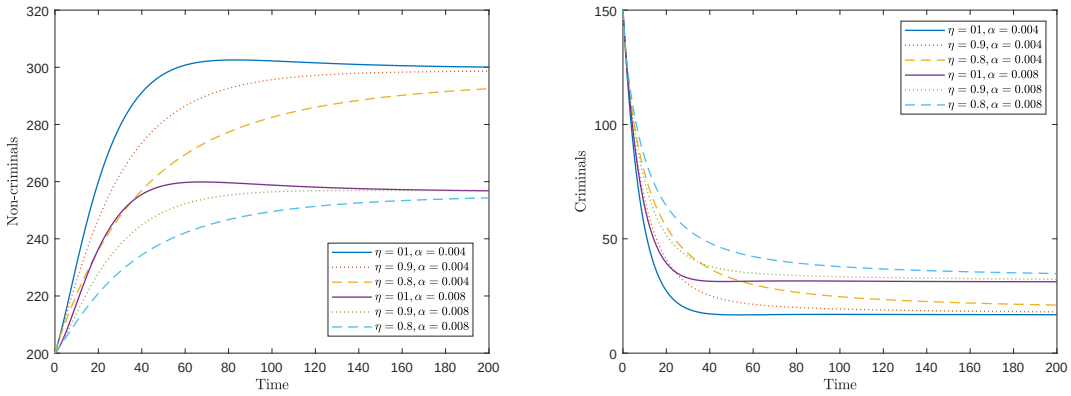

Figure 3.4: Effect of α on non-criminals and criminals for the different order of derivative.

Figure 3.4 shows the effect of α (transmission rate from non-criminal to criminal class) on non-criminals and criminals; non-criminals decrease and criminals increase with the increase in α for the different order of derivative. As we decreases the order of derivative for different value of α, non-criminals decreases and criminals showing increasing behaviour, which depict reality as shown in Figure 1.2.

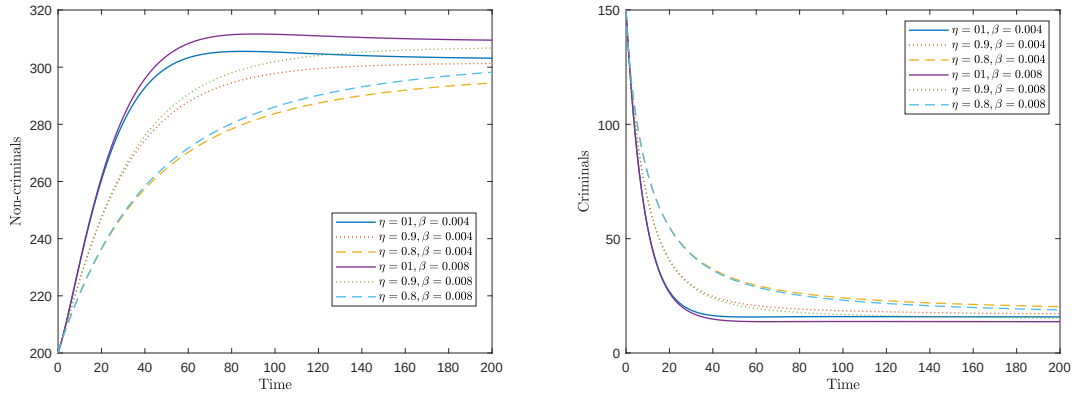

Figure 3.5: Effect of β on non-criminals and criminals for the different order of derivative.

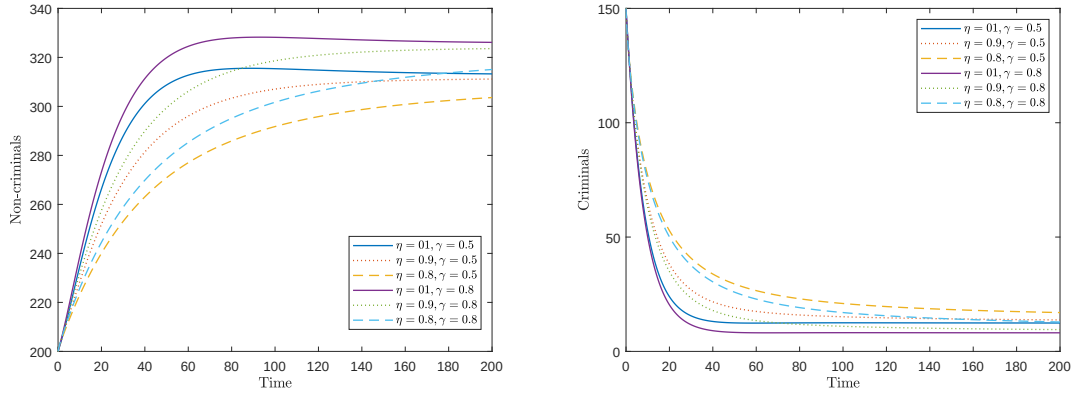

Figure 3.6: Effect of γ on non-criminals and criminals for the different order of derivative.

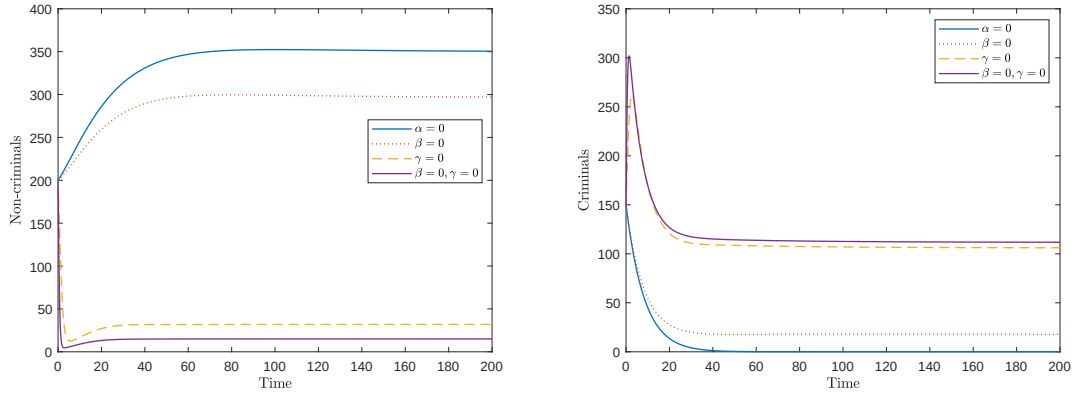

Figure 3.7: Effect of the different transmission rates (linear and non-linear) on non-criminals and criminals for integer order.

Similarly, Figure 3.5 and Figure 3.6 show the effect of β (prevention taken by non-criminals) and γ (crowding effect of criminals) on non-criminals and criminals respectively, non-criminals increases, and criminals decreases with increase in β and γ.

Figures 3.7–3.9 demonstrate the effect of different (linear, non-linear) transmission rates for the different orders of derivative. The following observations are made:

- When $\alpha = 0$, there is no transmission from the non-criminal class to the criminal class and hence, non-criminal increases and criminal decreases for the different order of derivative.

- When $\beta = 0,\ \gamma \neq 0$, non-criminal increases and criminal decreases with time for the different order of derivative due to prevention is taken by non-criminals.

- When $\gamma = 0,\ \beta \neq 0$, non-criminal initially decreases, then increases and converges to the equilibrium point. In contrast, crime initially increases then starts decreasing due to the crowding effect for the different order of derivative.

- When $\gamma = \beta = 0$, the non-linear transmission rate becomes linear, and there is a sharp increase in criminals.

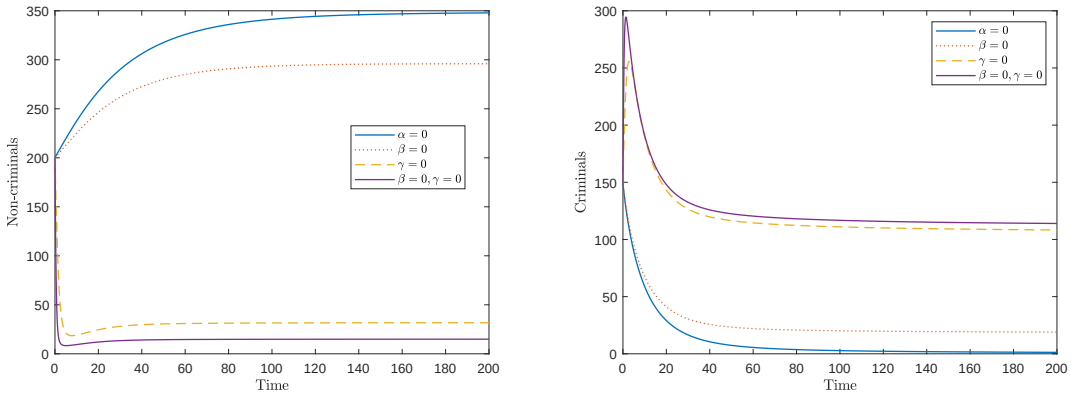

Figure 3.8: Effect of different transmission rates (linear and non-linear) on non-criminals and criminals for order of derivative $\eta = 0.9$.

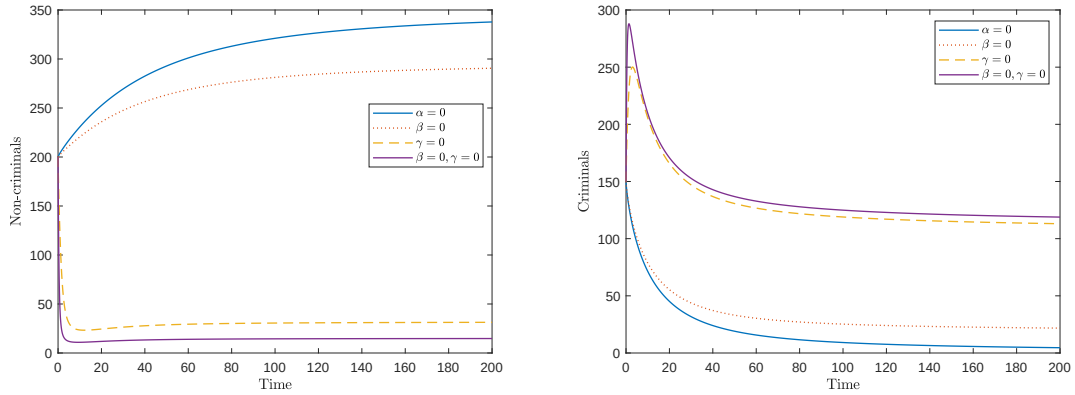

Figure 3.9: Effect of different transmission rates (linear and non-linear) on non-criminals and criminals for order of derivative $\eta = 0.8$.

On comparing the Figure 3.3 and Figures 3.7–3.9, the Beddington-DeAngelis non-linear transmission rate is better than the other discussed cases to reduce crime transmission due to the lower number of criminals under this rate..

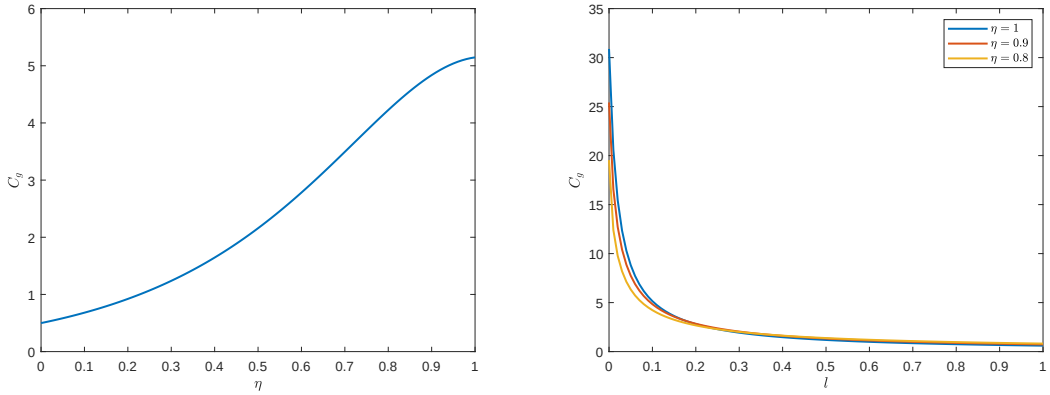

Figure 3.10: Relationship of criminal generation number (C_g) with the order of derivative (η) and law enforcement (l).

Figure 3.10 shows the relationship of criminal generation number (C_g) with order of derivative (η) and law-enforcement (l). Criminal generation number increases with the order of derivative and decreases with law enforcement. Crime transmission reduces as the order of the derivative decreases, indicating that a fractional-order model is more efficient to reduce crime transmission than an integer-order model. Furthermore, the best-fit value

for the order of derivative is close to zero as the value of C_g is 1 near the order of derivative 0.2. In spite of the fact that it is expected that the criminal population will decrease as the extent of law enforcement increases, there is not much effect on crime transmission after a threshold value, irrespective of the order of derivative.

3.7 Summary and Conclusions

This research proposes a novel fractional-order crime propagation mathematical model with Beddington-DeAngelis (non-linear) transmission rate and compares the proposed model with various transmission rates. The proposed model's solution not only exists but is also unique, bounded, and non-negative. Furthermore, the model has two non-negative equilibrium points: the criminal-free equilibrium and the crime persistence equilibrium. The crime transmission will persist if there is consistently more than one newly criminally active person generated from each criminal. The major findings of the present research are listed below:

- The Beddington-DeAngelis transmission rate is a generalization of linear and some non-linear transmission rates and the findings suggest that the Beddington-DeAngelis non-linear transmission rate is better than the other discussed cases as by considering inhibition effect (β) criminal generation number can decreases more rapidly.

- The criminal generation number (C_g) increases with the order of derivative (η), i.e., crime transmission rate decreases as the order of the derivative decreases, indicating that a fractional-order model is more efficient to reduce crime transmission rate than an integer-order model.

- The best-fit value for the order of the derivative is $\sim$0.2 to reduce crime transmission. In the fractional order model, it is found that when the various rates, including transmission rate, crowding effect, and inhibition effect, are raised to the power of 0.2, can control crime transmission more effectively.

- As memory is integrated through a fractional-order derivative in the crime transmission model, a decrease in the derivative order leads to a reduction in the number of generated criminals. Therefore, a decrease in memory has been observed to result in a decrease in the transmission of crime.

The identification of parameters such as α, β, and γ play a pivotal role in pattern recognition, assisting policymakers in informed decision-making and the formulation of effective crime-addressing policies. Policymakers should strengthen law enforcement, promote community policing, and implement deterrent programs to enhance the inhibition effect. Addressing the crowding effect caused by high population density requires thoughtful urban planning and community design. Measures such as improving public spaces, and fostering community engagement contribute to creating environments less conducive to unnoticed or unchallenged criminal activities.

The findings of this chapter are published in the following referred publication:

- *K. Bansal, T. Mathur, and S. Agarwal (2023), "Fractional-order crime propagation model with non-linear transmission rate." Chaos, Solitons & Fractals, 169, 113321.*

Chapter 4

Crime Modeling: A Comparison Between Logistic and Exponential Growth

"Society prepares the crime; the criminal commits it."

- Henry Thomas Buckle

Exponential growth mathematical model describes the rapid and unrestricted increase in the size or quantity of a population or phenomenon over time. In this model, the rate of growth is proportional to the current population size. The exponential growth is typically expressed as: $N(t) = N_0 \cdot e^{rt}$, where $N(t)$ is the population size at time t, N_0 is the initial population size at $t = 0$, r is the growth rate (a positive constant). Exponential growth assumes continuous and unbounded growth, and the population size increases without limits. It does not account for factors like limited resources or competition, which are more realistically addressed by the logistic growth model.

The logistic growth model is a modification of the exponential growth model that takes into account limitations on population growth. It assumes that as a population grows, it encounters constraints such as limited resources, competition, or environmental factors that slow down its growth rate and eventually reach a carrying capacity (K), which is the maximum sustainable population size for a given environment. The logistic growth is

typically expressed as: $N(t) = \dfrac{K}{1 + \dfrac{K - N_0}{N_0} e^{-rt}}$, where K is the carrying capacity, the maximum population size the environment can support. In the logistic growth model, the population initially grows rapidly (exponential phase) but then slows down as it approaches the carrying capacity (K). As the population size approaches K, the growth rate decreases until it levels off, resulting in a stable population size. The logistic growth model is more applicable to real-world populations and natural resources because it considers limiting factors that prevent unbounded growth.

According to the logistic growth theory, the population per capita growth rate drops when population size approaches the carrying capacity, a limit imposed by limited natural resources. The crime transmission model in previous chapter are exponential growth models. As a result, to overcome this feature of crime propagation models and reflect the significance of memory in crime propagation, a fractional mathematical model with logistic growth is required. This study analyzes the fractional crime propagation model that may be applied to dynamic processes to represent the spread of illicit activities from one criminal to another. In the current judicial system, a mathematical crime propagation model that integrates memory inheritance benefits the prevention of actual crimes and the formation of policies [59]. This crime propagation model differs from previous models discussed in Chapter 2 and Chapter 3 due to its inclusion logistic growth.

In this chapter, a comparison is drawn between various growth models, including exponential and logistic models, and the equilibrium points of the introduced fractional-order models are deduced. Furthermore, there are two equilibrium points, crime-free equilibrium and crime persistence equilibrium, for the exponential growth model, and three equilibrium points: crime-free equilibrium, crime-free axial equilibrium, and crime persistence equilibrium for the logistic growth model. By modifying critical components like incarceration and criminal release, the equilibrium may be utilized to examine the impact of criminal behavior in the community. The proposed model may help jurisdictional authorities and partners more effectively stop the spread of crime by isolation of criminals from non-criminals.

4.1 Overview of Crime Propagation Models

Even though various reasonable attempts (police deployment, punishment, incarceration, recidivism, and other rules and regulations) are made regularly at a given place, criminal activities are still on the rise. As a result, we need to propose a model that can assist in explaining, anticipating, and further curbing illegal proliferation by deploying suitable security personnel and enforcement laws. Due to the existence of two perspectives, law-abiding citizens and offenders, we may easily recognize disagreements, injustices, various forms of conflicts, and their results. Mathematical modeling is a crucial tool to address the issue of how the coexistence of two mindsets affects crime in a given region. These two mindsets will refer to two populations in this paper: the offender population (C) and the non-criminal population (S). Therefore, while taking into account the aforementioned factors, the proposed model is as follows:

4.1.1 Exponential Growth Model

The dynamics of C and S are given by the following system of fractional differential equations:

$$\begin{aligned} \frac{d^\eta S(t)}{dt^\eta} &= \mu^\eta S(t) - \alpha^\eta S(t)(C(t) - hC(t)) + l^\eta C(t) \\ \frac{d^\eta C(t)}{dt^\eta} &= \alpha^\eta S(t)(C(t) - hC(t)) - l^\eta C(t) - \varrho^\eta C(t) \end{aligned} \tag{4.1.1}$$

where η is the order of derivative and $S(0) > 0, C(0) > 0$ as the initial sizes of the populations S and C, respectively. Here, all variables $\mu, \alpha, \varrho, h, l$ are positive. The notation $\mu^\eta S$ denotes that, in the absence of an offender, a rise in S is directly proportionate to its natural growth rate μ and each parameter raised to power η (order of derivative) to dimensionally balance the model. $\alpha^\eta S(C - hC)$ denotes a decline in S due to the conversion and isolation rates. Here, α denotes the rate at which the non-criminal population transforms into the offender's population due to interaction, and h denotes the rate at which offenders are imprisoned or selected out of the general population to prevent interactions (isolation rate).

The offender transforms into the non-criminal population due to law enforcement (l). $\varrho^\eta C$ is the decrease in the offenders due to the natural mortality rate of C.

4.1.2 Logistic Growth Model

Exponential growth does not happen in the real world. A population may increase exponentially for a brief period, but ultimately, it will reach its resource limit. The logistic growth hypothesis states that the population growth rate per person decreases as population size approaches the carrying capacity, a constraint imposed by the availability of natural resources. Hence, the temporal dynamics of C and S with logistic growth are given by the following system of fractional differential equations:

$$\begin{aligned} \frac{d^\eta S(t)}{dt^\eta} &= \mu^\eta \left(1 - \frac{S(t)}{K}\right) S(t) - \alpha^\eta S(t)(C(t) - hC(t)) + l^\eta C(t) \\ \frac{d^\eta C(t)}{dt^\eta} &= \alpha^\eta S(t)(C(t) - hC(t)) - l^\eta C(t) - \varrho^\eta C(t) \end{aligned} \tag{4.1.2}$$

where K represents the carrying capacity of law-abiding citizens in the absence of the offender population. The rate of growth reduces to zero when S approaches K.

4.2 Analysis of the Proposed Models

4.2.1 Equilibrium Points

By setting the right-hand sides of each equation in the proposed model to zero, we can determine the equilibrium points.

Exponential Growth Model

There are two equilibrium points for the exponential growth model (4.1.1):

- A crime-free steady state exists if offenders become zero, i.e., $E_1 = (0, 0)$. It is the starting point of any civilization. It's important to note that achieving and maintaining a crime-free equilibrium is an ideal scenario and is not often fully realized in practice.

- Crime persistence steady state exists if both non-criminals and offenders become

non-zero, i.e.,

$$E_2 = (S^*, C^*) = \left(\frac{\varrho^\eta + l^\eta}{\alpha^\eta H}, \frac{\mu^\eta(\varrho^\eta + l^\eta)}{\alpha^\eta H \varrho^\eta} \right), \quad \text{where } (1-h) = H.$$

A crime persistence equilibrium point describes a scenario where a community experiences a consistent and enduring level of criminal activity over time. This equilibrium point is characterized by stable crime rates, recurring criminal behavior, and resilient social factors, making it challenging to reduce crime significantly despite intervention efforts.

Logistic Growth Model

There are three equilibrium points for the logistic growth model (4.1.2):

- A crime-free steady state exists if offenders become zero, i.e., $L_1 = (0, 0)$.
- Crime-free axial equilibrium exists if only offenders become zero, i.e., $L_2 = (K, 0)$. An equilibrium point in which non-criminals exist, while criminals are nonexistent (zero), represents a state in which the community or society has achieved a condition of zero criminal activity. In this equilibrium, the population consists only of individuals who do not engage in criminal behavior, resulting in a crime-free state. It signifies a highly desirable situation where law and order prevail, and crime has been effectively eliminated. It's important to note that achieving and maintaining this equilibrium is an ideal scenario and is not often fully realized in practice.
- Crime persistence steady state exists if both population non-criminals and offenders become non-zero, i.e.,

$$L_3 = (S^*, C^*) = \left(\frac{\varrho^\eta + l^\eta}{\alpha^\eta H}, \frac{\mu^\eta(\varrho^\eta + l^\eta)}{K\alpha^{2\eta} H^2 \varrho^\eta} (KH\alpha^\eta - \varrho^\eta - l^\eta) \right),$$

where $(1-h) = H$, L_3 would exist if $KH\alpha^\eta > \varrho^\eta + l^\eta$.

Achieving a persistent level of crime is not a desirable or intentionally sought-after goal for any society.

4.2.2 Stability Analysis

Exponential Growth Model

Theorem 4.2.1. *The crime-free equilibrium point* $E_1 = (0, 0)$ *of the system* (4.1.1) *is unstable (saddle point).*

Proof. The Jacobian matrix at E_1 is

$$J_{E_1} = \begin{bmatrix} \mu^\eta & l^\eta \\ 0 & -\varrho^\eta - l^\eta \end{bmatrix}.$$

Clearly, the two eigenvalues are $\mu^\eta, -\varrho^\eta - l^\eta$ and one is positive. So, using Routh–Hurwitz conditions (Theorem 1.4.4), E_1 is unstable. □

Theorem 4.2.2. *The crime persistence equilibrium point* E_2 *of the system* (4.1.1) *is locally asymptotically stable.*

Proof. The Jacobian matrix at E_2 is

$$J_{E_2} = \begin{bmatrix} \mu^\eta - \alpha^\eta C^* H & -\alpha^\eta S^* H + l^\eta \\ \alpha^\eta C^* H & \alpha^\eta S^* H - \varrho^\eta - l^\eta \end{bmatrix} = \begin{bmatrix} \mu^\eta - \alpha^\eta C^* H & -\alpha^\eta S^* H + l^\eta \\ \alpha^\eta C^* H & 0 \end{bmatrix}.$$

Hence, the characteristic equation can be written as $\lambda^2 + P_1\lambda + P_2 = 0$ where $P_1 = $ -trace(J_{E_2}), $P_2 = \det(J_{E_2})$. Clearly,

$$P_1 = -(\mu^\eta - \alpha^\eta C^* H) = -\left(\mu^\eta - \alpha^\eta \frac{\mu^\eta(\varrho^\eta + l^\eta)}{\alpha^\eta H \varrho^\eta} H\right) = \frac{\mu^\eta l^\eta}{\varrho^\eta} > 0,$$

$$P_2 = \alpha^\eta C^* H(\alpha^\eta S^* H 0 - l^\eta) = \mu^\eta(\varrho^\eta + l^\eta) > 0.$$

So, using Routh–Hurwitz conditions (Theorem 1.4.4), E_2 is stable. □

Logistic Growth Model

Theorem 4.2.3. *The crime-free equilibrium point* $L_1 = (0, 0)$ *of the system* (4.1.2) *is unstable (saddle point).*

Proof. The proof is trivial and similar to Theorem 4.2.1. □

Theorem 4.2.4. *The crime-free axial equilibrium point $L_2 = (K, 0)$ of the system (4.1.2) is locally asymptotically stable when $KH\alpha^\eta < \varrho^\eta + l^\eta$.*

Proof. The Jacobian matrix at L_2 is

$$J_{L_2} = \begin{bmatrix} -\mu^\eta & -\alpha^\eta KH + l^\eta \\ 0 & \alpha^\eta KH - \varrho^\eta - l^\eta \end{bmatrix}.$$

Clearly, the two eigenvalues are $-\mu^\eta, \alpha^\eta KH - \varrho^\eta - l^\eta$. So, using Routh–Hurwitz conditions (Theorem 1.4.4) L_2 is stable iff $\alpha^\eta KH - \varrho^\eta - l^\eta < 0 \implies KH\alpha^\eta < \varrho^\eta + l^\eta$. □

Theorem 4.2.5. *The crime persistence equilibrium point L_3 of the system (4.1.2) is locally asymptotically stable when $KH\alpha^\eta > \varrho^\eta + l^\eta$.*

Proof. The Jacobian matrix at L_3 is

$$J_{L_3} = \begin{bmatrix} \mu^\eta - \dfrac{2\mu^\eta S^*}{K} - \alpha^\eta C^* H & -\alpha^\eta S^* H + l^\eta \\ \alpha^\eta C^* H & \alpha^\eta S^* H - \varrho^\eta - l^\eta \end{bmatrix}$$

$$= \begin{bmatrix} -\dfrac{l^\eta C^*}{S^*} - \dfrac{\mu^\eta S^*}{K} & -\alpha^\eta S^* H + l^\eta \\ \alpha^\eta C^* H & 0 \end{bmatrix}.$$

Hence, the characteristic equation can be written as

$$\lambda^2 + P_1\lambda + P_2 = 0 \text{ where } P_1 = \text{-trace}(J_{L_3}), \quad P_2 = \det(J_{L_3})$$

Clearly,

$$P_1 = -\left(-\frac{l^\eta C^*}{S^*} - \frac{\mu^\eta S^*}{K}\right) > 0 \quad \text{if} \quad KH\alpha^\eta > \varrho^\eta + l^\eta,$$

$$P_2 = \alpha^\eta C^* H(\alpha^\eta S^* H - l^\eta) = \frac{\mu^\eta(\varrho^\eta + l^\eta)}{K\alpha^\eta H}(KH\alpha^\eta - \varrho^\eta - l^\eta) > 0 \quad \text{if} \quad KH\alpha^\eta > \varrho^\eta + l^\eta.$$

So, using Routh–Hurwitz conditions (Theorem 1.4.4) L_3 is stable if $KH\alpha^\eta > \varrho^\eta + l^\eta$. □

4.2.3 Validation Through Phase Portrait

Now, let the following set of parameters taken from previously published articles such as Pritam *et al.* [10], Bansal *et al.* [125], and Partohaghighi *et al.* [126] to validate our analytical result for different values of h:

$\mu = 1.3, \alpha = 0.4, l = 0.2, \varrho = 1.9, K = 10.$

$h = 0.6 \implies KH\alpha^{\eta} < \varrho^{\eta} + l^{\eta}$

$h = 0.3 \implies KH\alpha^{\eta} > \varrho^{\eta} + l^{\eta}$

for different order of derivative i.e. $\eta = 0.85,\ 0.9,\ 0.95,$ and 1. The proposed fractional order models have two and three equilibrium points for exponential growth and logistic growth, respectively. The stability analysis of equilibrium points with different orders of derivative ($\eta = 0.85,\ 0.9,\ 0.95,$ and 1) satisfying conditions $KH\alpha^{\eta} < \varrho^{\eta} + l^{\eta}$ and $KH\alpha^{\eta} > \varrho^{\eta} + l^{\eta}$ for the both proposed models shown in Figures 4.1–4.4 respectively. For both proposed models, the trivial equilibrium point is always unstable for different orders of derivatives.

The crime-persistence equilibrium is unconditionally stable for the exponential growth model (Figures 4.1(a)–4.4(a)) while for the logistic growth model, this equilibrium point exists and is stable if $KH\alpha^{\eta} > \varrho^{\eta} + l^{\eta}$ (Figures 4.1(b)–4.4(b)). Also, the crime-free axial equilibrium point exists for only the logistic growth model and stable if $KH\alpha^{\eta} < \varrho^{\eta} + l^{\eta}$ (Figures 4.1(b)–4.4(b)). The stability analysis of equilibrium points with different orders of derivative ($\eta = 0.85,\ 0.9,\ 0.95,$ and 1) for both proposed models is shown in Tables 4.1–4.8 for $KH\alpha^{\eta} < \varrho^{\eta} + l^{\eta}$, and $KH\alpha^{\eta} > \varrho^{\eta} + l^{\eta}$.

Table 4.1: Stability analysis for $h = 0.6$, $KH\alpha^{\eta} < \varrho^{\eta} + l^{\eta};\ \eta = 0.85$.

	Equilibrium point	Stability
Exponential model	(0,0) (10.787,7.813)	Saddle Point Stable Spiral
Logistic model	(0,0) (10,0) (10.787,-0.615)	Saddle Point Stable Node Saddle Point

Table 4.2: Stability analysis for $h = 0.3$, $KH\alpha^{\eta} > \varrho^{\eta} + l^{\eta};\ \eta = 0.85$.

	Equilibrium point	Stability
Exponential model	(0,0) (6.164,4.465)	Saddle Point Stable Spiral
Logistic model	(0,0) (6.164,1.713) (10,0)	Saddle Point Stable Spiral Saddle Point

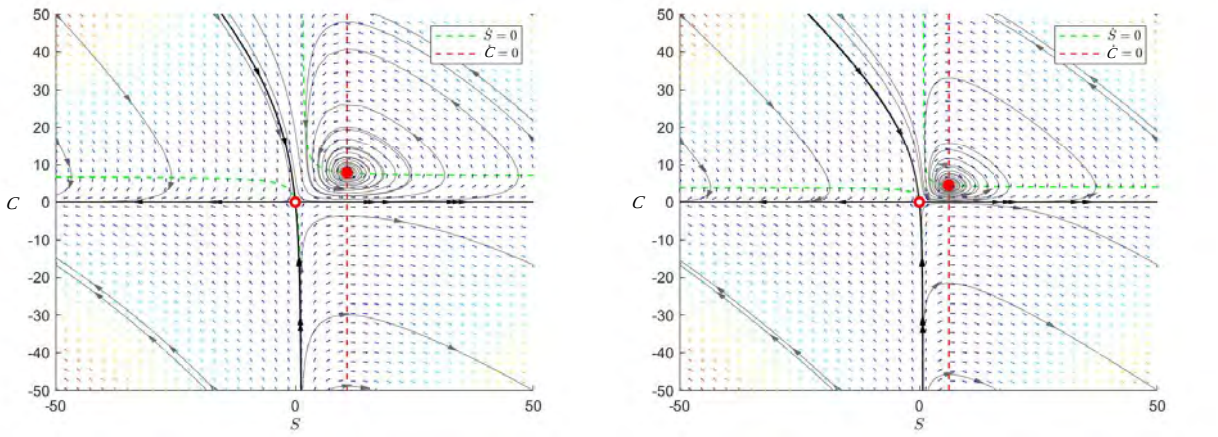

(a) Phase portrait for exponential growth for two sets of parameters satisfying conditions $KH\alpha^{\eta} < \varrho^{\eta} + l^{\eta}$ and $KH\alpha^{\eta} > \varrho^{\eta} + l^{\eta}$ respectively.

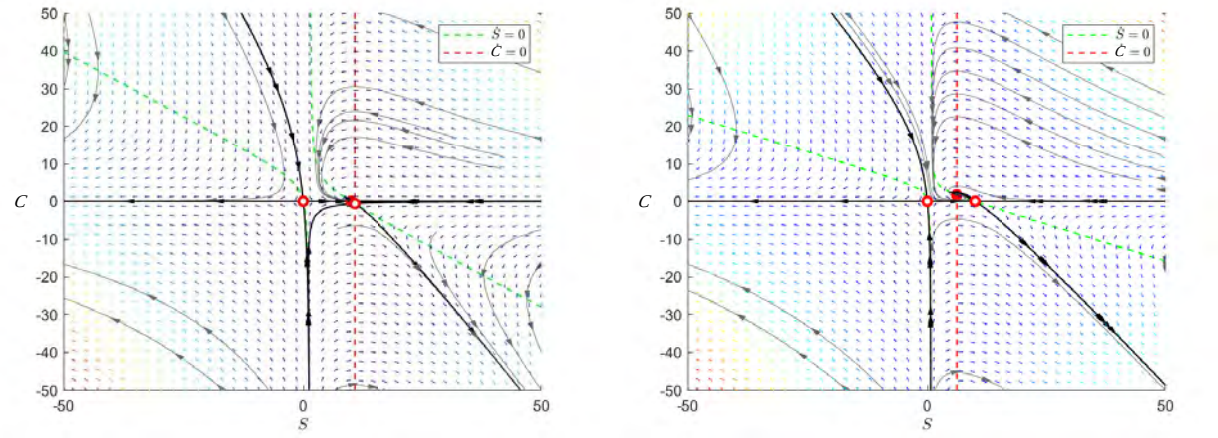

(b) Phase portrait for logistic growth for two sets of parameters satisfying conditions $KH\alpha^{\eta} < \varrho^{\eta} + l^{\eta}$ and $KH\alpha^{\eta} > \varrho^{\eta} + l^{\eta}$ respectively.

Figure 4.1: Phase portrait for stability analysis of the proposed models with an order of derivative 0.85.

Table 4.3: Stability analysis for $h = 0.6$, $KH\alpha^{\eta} < \varrho^{\eta} + l^{\eta}$; $\eta = 0.9$.

	Equilibrium point	Stability
Exponential model	(0,0) (11.501,8.174)	Saddle Point Stable Spiral
Logistic model	(0,0) (10,0) (11.501,-1.227)	Saddle Point Stable Node Saddle Point

Table 4.4: Stability analysis for $h = 0.3$, $KH\alpha^{\eta} > \varrho^{\eta} + l^{\eta}$; $\eta = 0.9$.

	Equilibrium point	Stability
Exponential model	(0,0) (6.572,4.671)	Saddle Point Stable Spiral
Logistic model	(0,0) (6.572,1.601) (10,0)	Saddle Point Stable Spiral Saddle Point

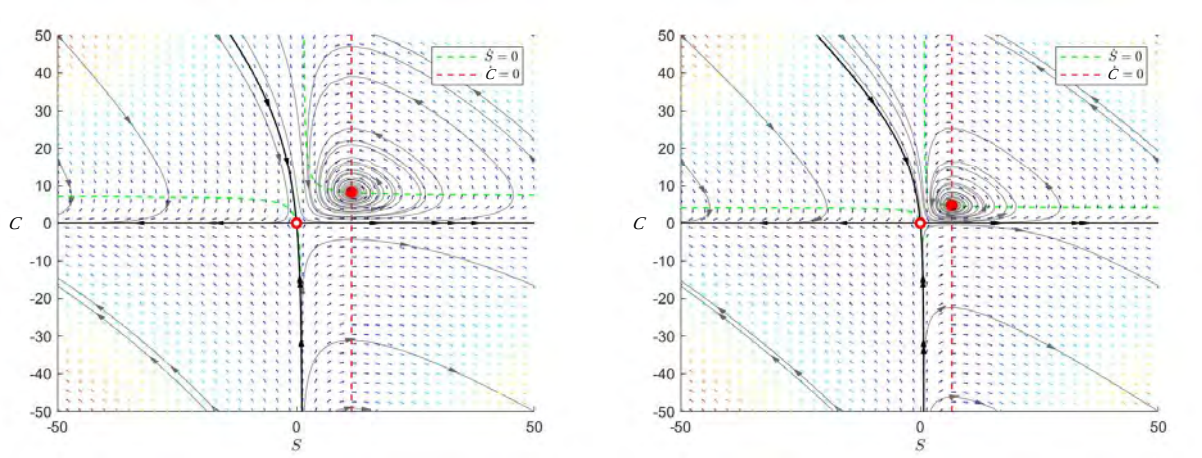

(a) Phase portrait for exponential growth for two sets of parameters satisfying conditions $KH\alpha^{\eta} < \varrho^{\eta} + l^{\eta}$ and $KH\alpha^{\eta} > \varrho^{\eta} + l^{\eta}$ respectively.

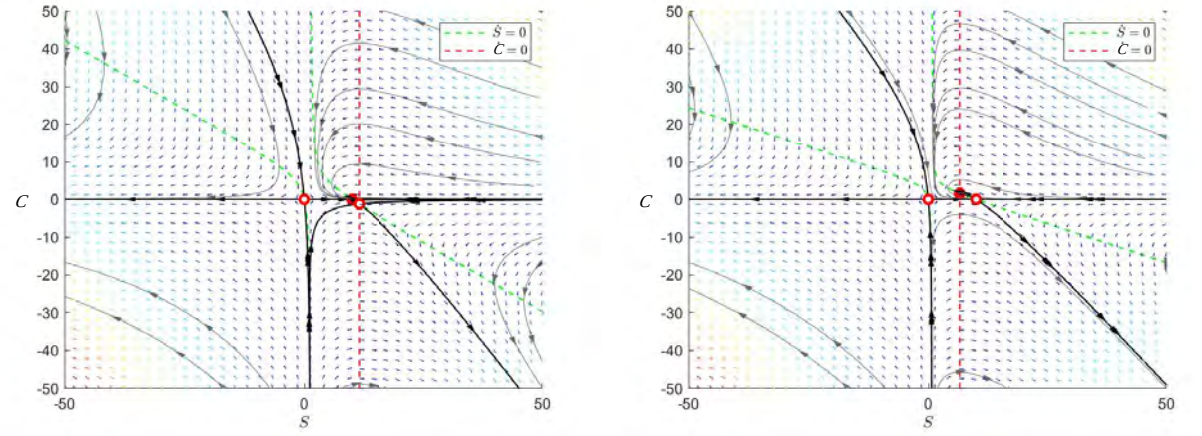

(b) Phase portrait for logistic growth for two sets of parameters satisfying conditions $KH\alpha^{\eta} < \varrho^{\eta} + l^{\eta}$ and $KH\alpha^{\eta} > \varrho^{\eta} + l^{\eta}$ respectively.

Figure 4.2: Phase portrait for stability analysis of the proposed models with an order of derivative 0.9.

Table 4.5: Stability analysis for $h = 0.6$, $KH\alpha^{\eta} < \varrho^{\eta} + l^{\eta};\ \eta = 0.95$.

	Equilibrium point	Stability
Exponential model	(0,0) (12.279,8.562)	Saddle Point Stable Spiral
Logistic model	(0,0) (10,0) (12.279,-1.951)	Saddle Point Stable Node Saddle Point

Table 4.6: Stability analysis for $h = 0.3$, $KH\alpha^{\eta} > \varrho^{\eta} + l^{\eta};\ \eta = 0.95$.

	Equilibrium point	Stability
Exponential model	(0,0) (7.017,4.893)	Saddle Point Stable Spiral
Logistic model	(0,0) (7.017,1.46) (10,0)	Saddle Point Stable Spiral Saddle Point

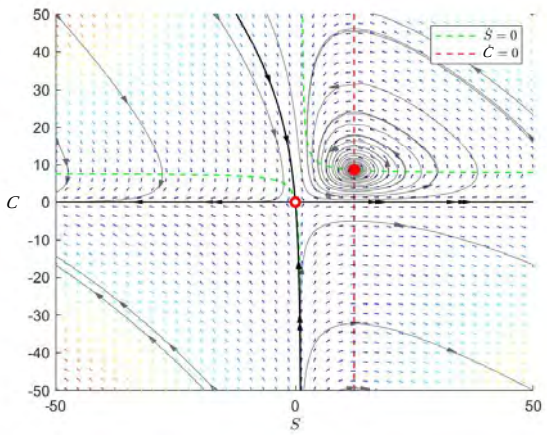

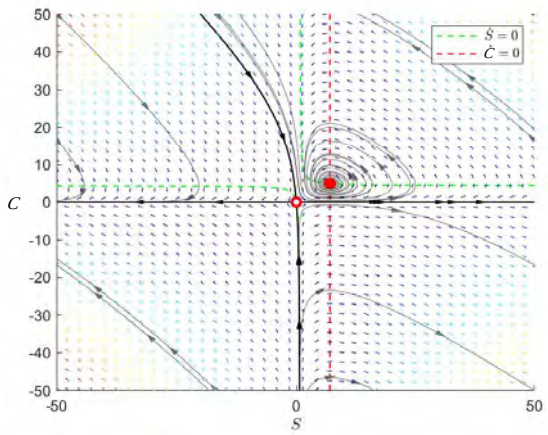

(a) Phase portrait for exponential growth for two sets of parameters satisfying conditions $KH\alpha^{\eta} < \varrho^{\eta} + l^{\eta}$ and $KH\alpha^{\eta} > \varrho^{\eta} + l^{\eta}$ respectively.

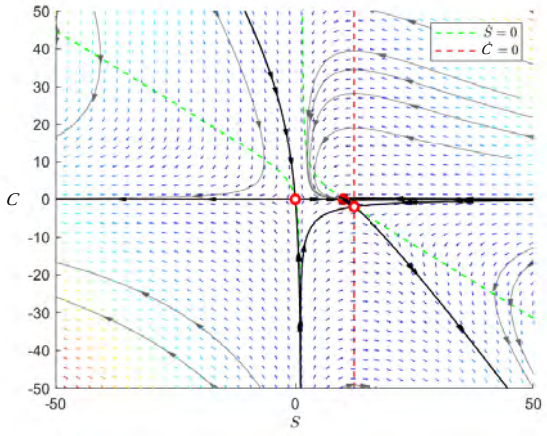

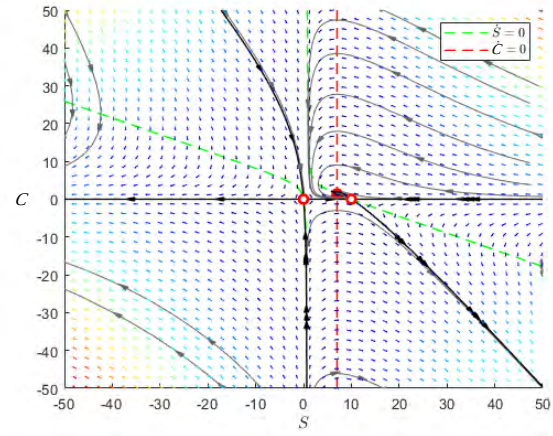

(b) Phase portrait for logistic growth for two sets of parameters satisfying conditions $KH\alpha^{\eta} < \varrho^{\eta} + l^{\eta}$ and $KH\alpha^{\eta} > \varrho^{\eta} + l^{\eta}$ respectively.

Figure 4.3: Phase portrait for stability analysis of the proposed models with an order of derivative 0.95.

Table 4.7: Stability analysis for $h = 0.6$, $KH\alpha^{\eta} < \varrho^{\eta} + l^{\eta};\ \eta = 1$.

	Equilibrium point	Stability
Exponential model	(0,0) (13.125,8.98)	Saddle Point Stable Spiral
Logistic model	(0,0) (10,0) (13.125,-2.806)	Saddle Point Stable Node Saddle Point

Table 4.8: Stability analysis for $h = 0.3$, $KH\alpha^{\eta} > \varrho^{\eta} + l^{\eta};\ \eta = 1$.

	Equilibrium point	Stability
Exponential model	(0,0) (7.5,1.283)	Saddle Point Stable Spiral
Logistic model	(0,0) (7.5,1.283) (10,0)	Saddle Point Stable Spiral Saddle Point

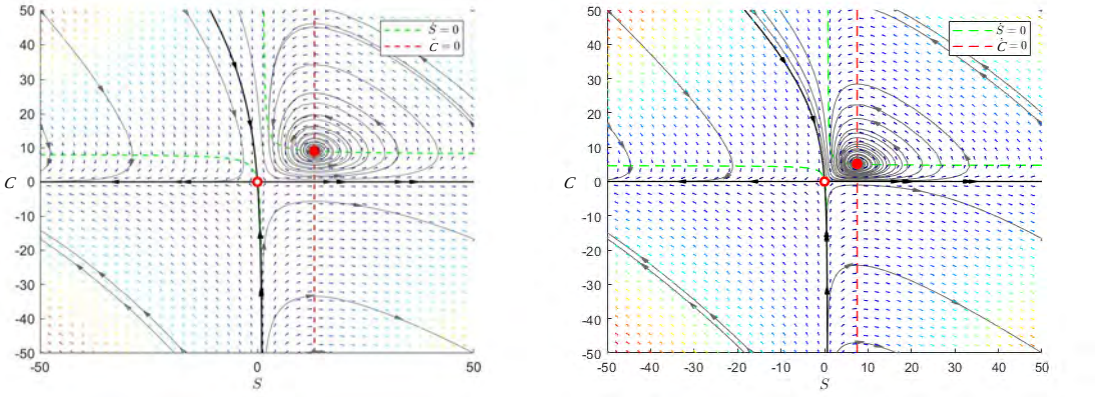

(a) Phase portrait for exponential growth for two sets of parameters satisfying conditions $KH\alpha^{\eta} < \varrho^{\eta} + l^{\eta}$ and $KH\alpha^{\eta} > \varrho^{\eta} + l^{\eta}$ respectively.

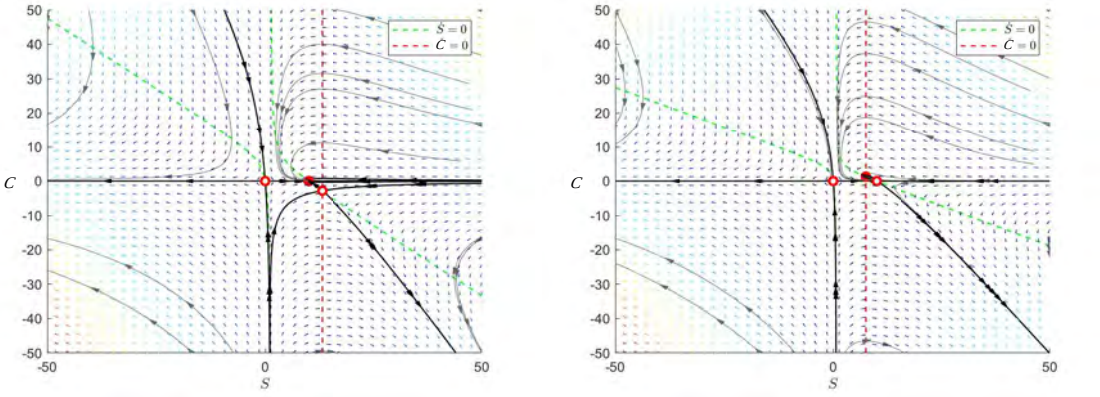

(b) Phase portrait for logistic growth for two sets of parameters satisfying conditions $KH\alpha^{\eta} < \varrho^{\eta} + l^{\eta}$ and $KH\alpha^{\eta} > \varrho^{\eta} + l^{\eta}$ respectively.

Figure 4.4: Phase portrait for stability analysis of the proposed models with an order of derivative 1.

4.3 Transcritical Bifurcation

In the exponential growth model, there are two equilibrium points. The trivial equilibrium is always unstable, whereas the crime persistence equilibrium is globally stable. But in the logistic growth model, when $KH\alpha^{\eta} > \varrho^{\eta} + l^{\eta}$, we can observe that the logistic growth model has three equilibrium points. The trivial equilibrium and crime-free axial equilibrium are unstable saddle points, while crime persistence equilibrium is a stable node. However, L_2 turns out to be stable, whereas L_3 appears to be unstable when

$KH\alpha^\eta < \varrho^\eta + l^\eta$. Consequently, when the system's parameter values gradually change and satisfy the equivalence $KH\alpha^\eta = \varrho^\eta + l^\eta$, a sudden qualitative shift in its behavior takes place. This shift causes the two fixed points, L_2 and L_3, to appear as if they are colliding and undergoing a change in stability, resembling a transcritical bifurcation.

Theorem 4.3.1. *The proposed logistic growth model* (4.1.2) *shows transcritical bifurcation at* $KH\alpha^\eta = \varrho^\eta + l^\eta$.

Proof. To verify the transversality condition necessary for the occurrence of a transcritical bifurcation, we employ Sotomayor's theorem (Theorem 1.4.6). One of the eigenvalues is $\lambda = 0$ since $det(J_{L_2}) = \lambda_1\lambda_2 = 0$. Assuming that v and w represent the eigenvectors corresponding to the zero eigenvalues of matrices J_{L_2} and $J_{L_2}^T$ respectively, defined as

$$v = \begin{bmatrix} \frac{-\varrho^\eta}{\mu^\eta} \\ 1 \end{bmatrix}, \qquad w = \begin{bmatrix} 0 \\ 1 \end{bmatrix}.$$

The proposed model (4.1.2) is given by:

$$f = \begin{bmatrix} \mu^\eta \left(1 - \frac{S}{K}\right) S - \alpha^\eta S(C - hC) + l^\eta C \\ \alpha^\eta S(C - hC) - l^\eta C - \varrho^\eta C \end{bmatrix}, \quad f_H = \begin{bmatrix} \alpha^\eta SCH \\ \alpha^\eta SCH \end{bmatrix}.$$

At $E_2 = (K, 0)$, $f_H = 0 \implies \nabla_1 = \mathbf{w}^T f_H(x_0, H_0) = 0$. Now,

$$Df_H = \begin{bmatrix} \alpha^\eta C & \alpha^\eta S \\ -\alpha^\eta C & -\alpha^\eta S \end{bmatrix},$$

$$[D^2 f(x_0, H_0)(v, v)] = \begin{bmatrix} \frac{-2\varrho^{2\eta}}{\mu^\eta K} + \frac{-2\alpha^\eta H\varrho^\eta}{\mu^\eta} \\ \frac{-2\alpha^\eta H\varrho^\eta}{\mu^\eta} \end{bmatrix}.$$

Hence,

$$\nabla_2 = \mathbf{w}^T[Df_H(x_0, H_0)v] = -\alpha^\eta K \neq 0$$

$$\nabla_3 = \mathbf{w}^T[D^2 f(x_0, H_0)(v, v)] = \frac{-2\alpha^\eta H\varrho^\eta}{\mu^\eta} \neq 0.$$

The system meets all three requirements for transcritical bifurcation. Transcritical bifurcation at H_0 is thus demonstrated. It provides insights into the coexistence of stable crime states, the sensitivity to parameter variations, and the potential for abrupt shifts in criminal activity. This understanding can inform crime prevention strategies, law enforcement efforts, and policy decisions to better address and manage crime in a given area. □

4.4 Validation Through Numerical Simulation

The analytical findings for different orders of derivatives and growth models are supported by the numerical data presented in this section.

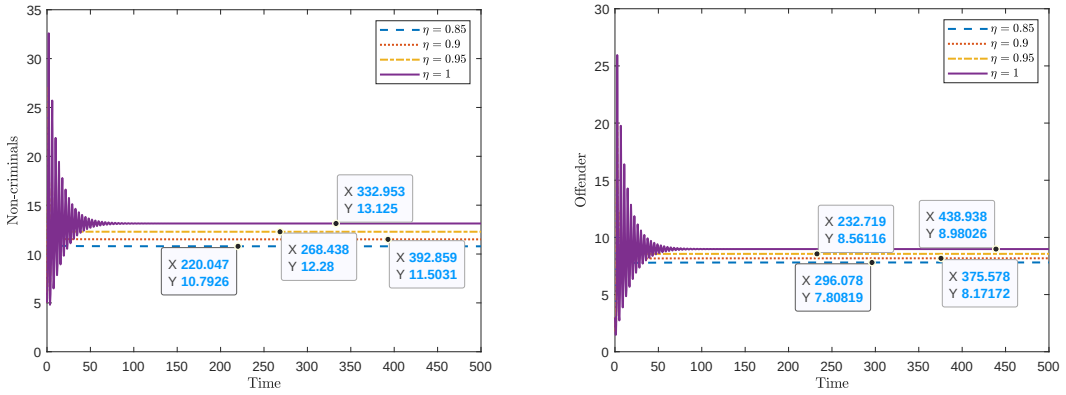

(a) Time series plot for the dynamics of non-criminals and offenders for exponential growth.

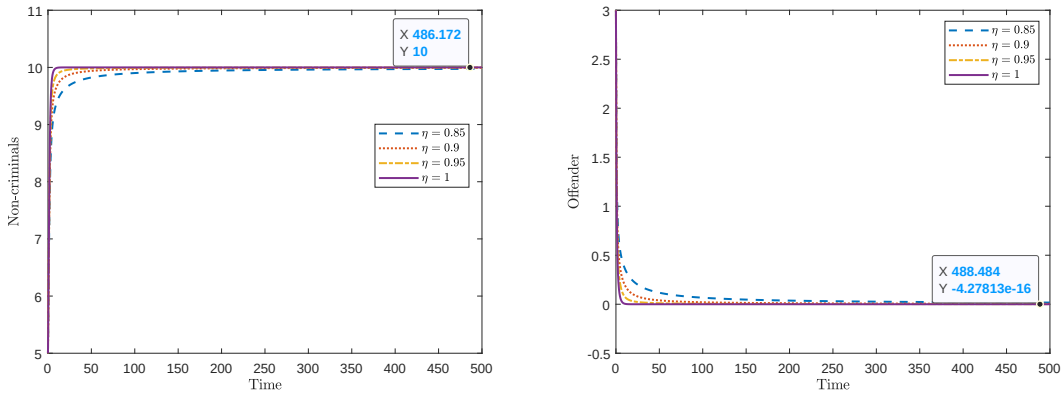

(b) Time series plot for the dynamics of non-criminals and offenders for logistic growth.

Figure 4.5: Dynamics of non-criminals and criminals for the set of parameters satisfying $KH\alpha^{\eta} < \varrho^{\eta} + l^{\eta}$ for different order of derivative.

To solve the proposed model, the Adams-Bashforth-Moulton predictor-corrector method is employed [109]. Figure 4.5(a) and Figure 4.6(a) show that the crime persistence equilibrium point for the proposed exponential growth model is asymptotically stable unconditionally for different derivative orders (η). It is also observed that the offender population decreases with the derivative order, and the equilibrium point is achieved faster in the fractional-order model compared to the integer-order model.

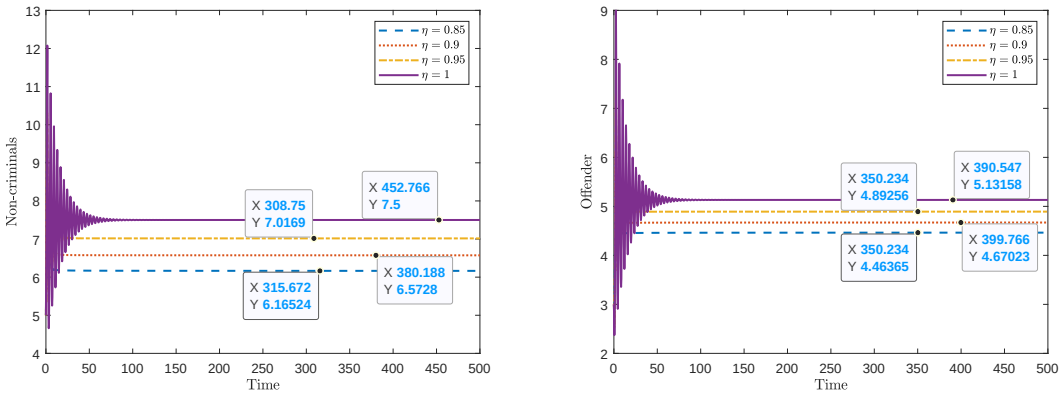

(a) Time series plot for the dynamics of non-criminals and offenders for exponential growth.

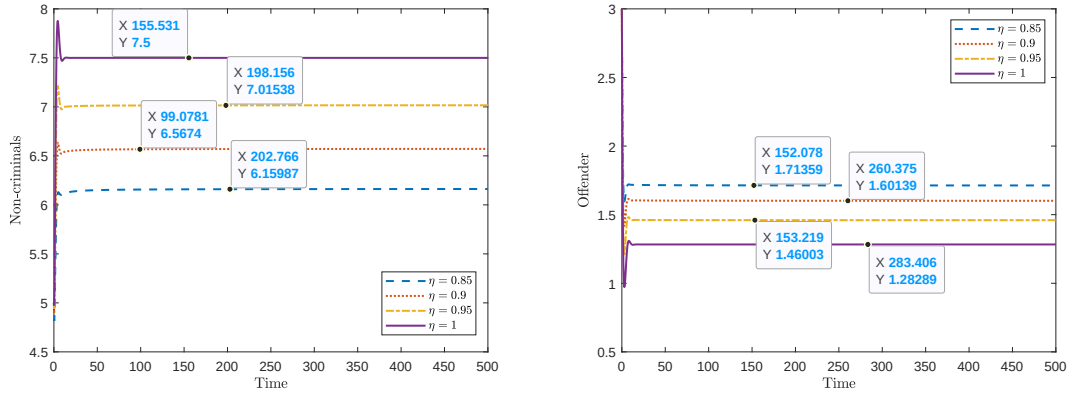

(b) Time series plot for the dynamics of non-criminals and offenders for logistic growth.

Figure 4.6: Dynamics of non-criminals and criminals for the set of parameters satisfying $KH\alpha^{\eta} > \varrho^{\eta} + l^{\eta}$ for the different order of derivative.

The study also demonstrates that the logistic growth model's offenders ultimately reach zero when $KH\alpha^{\eta} < \varrho^{\eta} + l^{\eta}$ (Figure 4.5(b)). The axial crime equilibrium exists and is stable when $KH\alpha^{\eta} < \varrho^{\eta} + l^{\eta}$ for the logistic growth model only. This is because

the population of offenders who are dying (ϱ) and becoming non-criminals (l) is greater than those who can become offenders (α). Due to increased resource availability and law enforcement development, the maximum population of non-criminals who turn into offenders is reduced, and offenders are more likely to convert to non-criminals, resulting in a society free from crime. The crime persistence equilibrium exists and is stable when $KH\alpha^{\eta} > \varrho^{\eta}+l^{\eta}$ for the logistic growth model. This is because the population of offenders who are dying (d) and becoming non-criminals (l) is smaller than those who can become offenders (α). When $KH\alpha^{\eta} > \varrho^{\eta}+l^{\eta}$ (Figure 4.6(b)), the incoming flux into the offenders is larger than the outgoing flux from the offenders at a particular time. The natural growth factor would first cause the non-criminal population to rise and reach its peak. There is a net gain in the offender population when the non-criminal population is at its highest point because the conversion of non-criminals into offenders rises, reaches its maximal, and outperforms the decline in the offender population caused by deaths and conversion to non-criminality.

4.5 Results and Discussion

This research investigated an exploiter-victim model system using the predator-prey interaction system. It is a fairly simple model, and more complex ones may be developed by incorporating a variety of real-world possibilities. Offenders stand for the predator type, whereas non-criminals represent the prey type. The exponential growth model (4.1.1) shows that the offender and non-criminal population can exist simultaneously as the trivial equilibrium point is unstable (saddle point). Furthermore, any slight modification to the system does not lead to a significant change while both populations are at a positive level (Figures 4.1(a)–4.6(a)). Additionally, as the number of non-criminals rises, the population of offenders also increases for exponential growth (Tables 4.1–4.8). It is also observed that the offender population decreases as the order of derivatives decreases. Hence, the fractional-order exponential model demonstrates that offenders increase with non-criminals and decrease with the order of derivatives.

According to this study, in the logistic model, as the order of derivatives increases, the

non-criminal population increases, and the offender population declines. In the integer-order model, the non-criminal population is maximized while the offender population is minimized, which is beneficial to society. However, according to the National Crime Records Bureau, Government of India, the criminal population is increasing as the crime rate per lakh population rises from 1981 to 2020 (Figure 1.2). As a result, the fractional-order logistic model reflects reality as compared to the integer-order model.

According to the analysis of the logistic growth model (4.1.2), the criminally inclined community can either cohabit with the law-abiding citizens (Figure 4.6(b)) or go extinct (Figure 4.5(b)). Whether the offender coheres with the law-abiding citizens or decreases to zero depends on isolation term h and law enforcement l. Our findings reveal that the offender increases when both h and l are decreased. However, the offender rapidly declines and wipes out when either of these two hits a threshold number. At the threshold values of h and l, the investigated logistic growth model exhibits bifurcation centered on an internal equilibrium point L_3. Therefore, the findings suggest that constructing a stronger and more effective legal system or providing better living circumstances that isolates the criminals from non-criminals can significantly lower the number of criminal acts. A community may not always be able to increase law enforcement and offer the necessary resources simultaneously. This research demonstrates that a society may be free from crime even if only one of the requirements is satisfied.

4.6 Summary and Conclusions

A fractional-order crime transmission mathematical model with logistic growth and isolation rate is developed in this work, which considers essential links and behavioral changes among the population. This study compares the exponential and logistic growth models. In an exponential growth model, there are only two equilibrium points, while in the logistic growth model, there are three equilibrium points. Crime-free axial equilibrium exists only in logistic growth and is stable when $KH\alpha^{\eta} < \varrho^{\eta} + l^{\eta}$ otherwise unstable. For the logistic growth model, the integer-order model maximizes the population of law-abiding people while minimizing the population of criminals, which is advantageous for society but not

practically possible. Hence, the fractional-order logistic model depicts reality in a better way than integer-order models. We discover that the offender population increases when both h and l are decreased. However, the criminal population rapidly declines and is wiped out when either of these two hits a threshold number. Numerical simulations were used to validate the theoretical conclusions. Finally, this study demonstrated the importance of having a trustworthy subset of law enforcement in society to lower crime. Below, we summarize the key points of this chapter:

- A fractional-order mathematical model of crime transmission is proposed by including the logistic growth and isolation rate and this study compares the exponential and logistic growth crime transmission models for different order of derivatives.
- Analytical findings are validated by phase portraits and numerical simulations for different order of derivatives.
- The incidence of transcritical bifurcation is investigated including law enforcement and the finding reveals that the fractional-order logistic models better reflect reality than integer-order models.

Based on this research, a stronger and more efficient legal system, in conjunction with enhanced living conditions that can isolates criminals and noncriminals has the potential to significantly decrease the incidence of crimes. It's important to note that a community might not always have the capacity to simultaneously bolster law enforcement and provide the necessary resources. Hence, this chapter demonstrates that a society can achieve a crime-free environment even if only one of these conditions is fulfilled.

This chapter has been communicated as follows:

- *K. Bansal and T. Mathur, "Fractional-order crime propagation model: A comparison between logistic and exponential growth." (Communicated)*

Chapter 5

Impact of Social Media on Academics

"We don't have a choice on whether we do social media;
the question is how well we do it."
- Erik Qualman

India is the world's third-largest internet user, and social media has become a playground for the young generation. Social media's popularity has grown exponentially over the past few decades. Social networking services such as Twitter and Facebook have become popular in recent years [27]. Social media can both, positively and negatively impact academics [139]. On the positive side, it can facilitate collaboration, information sharing, educational resources, exposure to diverse perspectives, and networking among students and researchers. It can also serve as a platform for educational content and discussions. However, the negative aspects include distractions, reduced focus, and the potential for misinformation [140]. Excessive use of social media might lead to decreased study time and even impact mental well-being [141, 142]. It's important for individuals to find a balance that enhances their academic pursuits while minimizing the drawbacks of social media. In some cases, students are more obsessed with social media or social networks than with the classroom teaching, due to which students affect their academic performance. The unfavorable consequences of using social networking sites overbalance the opportunities. Any facility comes with its own set of benefits and drawbacks. However, as the individual becomes immersed in the digital world, social networking becomes an addiction, and

this enthusiasm costs real-life happiness in terms of relationships and personal ambitions. In summary, social media can be a valuable tool for academics, but its usage should be approached with caution. Students and researchers need to be mindful of the potential distractions and negative effects, and make deliberate efforts to strike a balance between online engagement and their academic pursuits.

Due to covid pandemic and lockdown, usage of social platforms increases not only for entertainment purposes but also for academic purposes. As a result, students are at significant risk of developing social media addiction, so techniques to control social media addiction transmission throughout society are required. Early exposure, traumatic events, positive and negative memories, peer influence, and past behavioral patterns can shape addiction tendencies. Positive reinforcement, emotional attachment, and memories of social connections can make it difficult to disengage from social media. Understanding these historical factors is essential for addressing and managing social media addiction effectively. As a preliminary investigation, all prior experiments have used integer-order compartmental structures [143–148]. Furthermore, fractional-order derivatives outperform integer-order derivatives in several applications of sciences where memory plays an important role [4, 125, 149–152].

As a result, in 2021, Kongson *et al.* [5] proposed a nonlinear fractional social media addiction model utilizing Atangana Baleanu Caputo derivative. However, the above mentioned studies did not include the impact of social media addiction on academics as well as memory/past history. The most common causes of social media addiction are chronic stress, trauma, mental illness, and a family history of addiction. As a result, a fractional-order mathematical model is required to overcome this issue and show how memory affects the influence of the social network on students. Hence, a fractional-order social media model is suggested in this study to represent the interaction of social media-addicted students with less involved or non-user individuals.

5.1 Development of Mathematical Model

This section proposes a model that involves the following assumptions:

- There are two groups of students: non-users of the social web and users of the social web. Students who are users of the social web can be less involved or active users. As a result, we categorize the overall student population N into five distinct categories:
  - X : Non-users of the social web,
  - S_L : Less involved users (less active),
  - S_A : Active users,
  - L_P : Users performing low,
  - H_P : Users performing high.

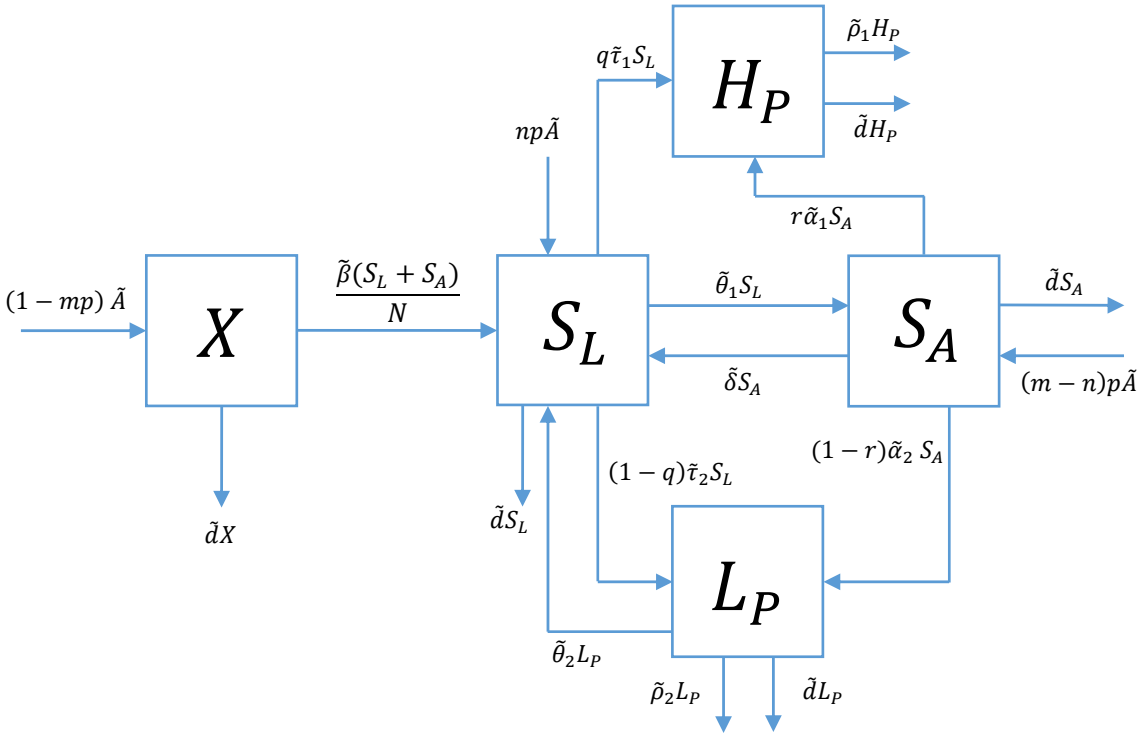

Figure 5.1: Schematic diagram of the proposed model.

- Since the overall likelihood is one, suppose the possibility of students in the non-users compartment is $1 - mp$, the possibility of students being in the less involved compartment is np, and the possibility of students being in the active compartment of the social web be $(m - n)p$.

- As we classified the students in terms of social web users, all three groups should have a recruitment rate. Students will be recruited at the rates of $(1 - mp)\tilde{A}$ for $X(t)$, $np\tilde{A}$ for $S_L(t)$, and $(m - n)p\tilde{A}$ for $S_A(t)$ where $\tilde{A}$ is recruitment rate.

- Users who do not use the social web interact with less involved or active users and eventually develop an interest in using it, leading them to join as less involved users with the rate of transmission $\dfrac{\tilde{\beta}X(t)[S_L(t) + S_A(t)]}{N(t)}$.
  A student who joins the social web nowadays is not perceived as an obsessive person and is assigned to the compartment of less involved pupils.

- Students in the less involved compartment switch to the active compartment at a rate of $\tilde{\theta}_1 S_L(t)$, whereas active social media users switch to the less involved compartment at a rate of $\tilde{\delta} S_A(t)$.

- Students in the less involved compartment may perform high or low at the rate $q\tilde{\tau}_1 S_L(t)$, $(1 - q)\tilde{\tau}_2 S_L(t)$ respectively, with the likelihood of students performing high and low is q and $(1 - q)$, respectively.

- Additionally, students in the active compartment can perform either high or low at the rate $r\tilde{\alpha}_1 S_A(t)$, $(1 - r)\tilde{\alpha}_2 S_A(t)$ respectively, with the likelihood of students performing high and low is r and $(1 - r)$ respectively.

- Students with poor grades may opt to move to a less involved class at a rate of $\tilde{\theta}_2 L_P(t)$ if not removed. Students who perform low may die naturally at a rate of $\tilde{d}$ or be removed at a rate of $\tilde{\rho}_2 L_P(t)$, whereas students who perform high graduate at a rate of $\tilde{\rho}_1 H_P(t)$ or die naturally at a rate of $\tilde{d}$.

5.1.1 Model Equations

This section establishes a mathematical model, which is a system of nonlinear fractional order differential equations with non-negative initial conditions, based on above assumptions and Figure 5.1:

$$\begin{aligned}
\frac{d^\eta X(t)}{dt^\eta} &= (1-mp)\tilde{A}^\eta - \frac{\tilde{\beta}^\eta X(t)[S_L(t)+S_A(t)]}{N(t)} - \tilde{d}^\eta X(t)\\
\frac{d^\eta S_L(t)}{dt^\eta} &= np\tilde{A}^\eta + \frac{\tilde{\beta}^\eta X(t)[S_L(t)+S_A(t)]}{N(t)} + \tilde{\theta}_2^\eta L_P(t) + \tilde{\delta}^\eta S_A(t)\\
&\quad - (\tilde{d}^\eta + \tilde{\theta}_1^\eta + q\tilde{\tau}_1^\eta + (1-q)\tilde{\tau}_2^\eta)S_L(t) \qquad (5.1.1)\\
\frac{d^\eta S_A(t)}{dt^\eta} &= (m-n)p\tilde{A}^\eta + \tilde{\theta}_1^\eta S_L(t) - (\tilde{d}^\eta + r\tilde{\alpha}_1^\eta + (1-r)\tilde{\alpha}_2^\eta + \tilde{\delta}^\eta)S_A(t)\\
\frac{d^\eta H_P(t)}{dt^\eta} &= q\tilde{\tau}_1^\eta S_L(t) + r\tilde{\alpha}_1^\eta S_A(t) - \tilde{\rho}_1^\eta H_P(t) - \tilde{d}^\eta H_P(t)\\
\frac{d^\eta L_P(t)}{dt^\eta} &= (1-q)\tilde{\tau}_2^\eta S_L(t) + (1-r)\tilde{\alpha}_2^\eta S_A(t) - (\tilde{\rho}_2^\eta + \tilde{d}^\eta + \tilde{\theta}_2^\eta)L_P(t).
\end{aligned}$$

$$X(0) = X_0,\ S_L(0) = S_{L0},\ S_A(0) = S_{A0},\ H_P(0) = H_{P0},\ L_P = L_{P0}. \qquad (5.1.2)$$

Here $N(t) = X(t) + S_L(t) + S_A(t) + H_P(t) + L_P(t)$ and $\eta \in (0, 1]$ is order of derivative. Parameters raised to power η to balance the dimension of system.

5.2 Dynamical Behaviour of Proposed Model

This section demonstrates the existence and uniqueness of the solution and then also prove that the solution is non-negative and bounded.

5.2.1 Existence and Uniqueness of Solution

Theorem 5.2.1. *There is a unique solution* $\Phi(t) = [X(t), S_L(t), S_A(t), H_P(t), L_P(t)]$ *for the initial value problem given by eq.* (5.1.1) *along initial conditions* (5.1.2) *on* $t \geq 0$. *Furthermore, all solutions are bounded.*

Proof. Let

$$D^\eta y(t) = A_1 y(t) + \gamma A_2 y(t) + A_3 = f(t, y(t)) \qquad (5.2.1)$$

where

$$y(t) = [X(t), S_L(t), S_A(t), H_P(t), L_P(t)]^T,$$

$$\gamma = \frac{S_L + S_A}{N} \leq 1,$$

$$A_1 = \begin{bmatrix} -\tilde{d}^\eta & 0 & 0 & 0 & 0 \\ 0 & -(\tilde{\theta}_1^\eta + \tilde{d}^\eta + q\tilde{\tau}_1^\eta) & \tilde{\delta}^\eta & 0 & \tilde{\theta}_2^\eta \\ & -(1-q)\tilde{\tau}_2^\eta & & & \\ 0 & \tilde{\theta}_1^\eta & -(\tilde{d}^\eta + r\tilde{\alpha}_1^\eta) & 0 & 0 \\ & & -(1-r)\tilde{\alpha}_2^\eta + \tilde{\delta}^\eta & & \\ 0 & q\tilde{\tau}_1^\eta & r\tilde{\alpha}_1^\eta & -\tilde{\rho}_1^\eta - \tilde{d}^\eta & 0 \\ 0 & (1-q)\tilde{\tau}_2^\eta & (1-r)\tilde{\alpha}_2^\eta & 0 & -\tilde{\rho}_2^\eta - \tilde{d}^\eta - \tilde{\theta}_2^\eta \end{bmatrix}$$

$$A_2 = \begin{bmatrix} -\tilde{\beta}^\eta & 0 & 0 & 0 & 0 \\ \tilde{\beta}^\eta & 0 & 0 & 0 & 0 \\ 0 & 0 & 0 & 0 & 0 \\ 0 & 0 & 0 & 0 & 0 \\ 0 & 0 & 0 & 0 & 0 \end{bmatrix}, \qquad A_3 = \begin{bmatrix} (1-mp)\tilde{A}^\eta \\ np\tilde{A}^\eta \\ (m-n)p\tilde{A}^\eta \\ 0 \\ 0 \end{bmatrix}.$$

Eq. (5.2.1) represents the system of eq. (5.1.1) of the proposed model.

$$\begin{aligned} ||D^\eta y(t)|| = ||f(t, y(t))|| &= ||A_1 y(t) + \gamma A_2 y(t) + A_3|| \\ &\leq ||A_1||.||y(t)|| + ||A_2||.||y(t)|| + ||A_3|| \\ &= (||A_1|| + ||A_2||)||y(t)|| + ||A_3||. \end{aligned} \tag{5.2.2}$$

Now as,

$$\begin{aligned} N(t) &= X(t) + S_L(t) + S_A(t) + H_P(t) + L_P(t), \\ \frac{d^\eta N(t)}{dt^\eta} &= \frac{d^\eta X(t)}{dt^\eta} + \frac{d^\eta S_L(t)}{dt^\eta} + \frac{d^\eta S_A(t)}{dt^\eta} + \frac{d^\eta H_P(t)}{dt^\eta} + \frac{d^\eta L_P(t)}{dt^\eta}, \\ \frac{d^\eta N(t)}{dt^\eta} &= \tilde{A}^\eta + \tilde{d}^\eta N(t) - \tilde{\rho}_1^\eta H_P - \tilde{\rho}_2^\eta L_P, \\ &\leq \tilde{A}^\eta + \tilde{d}^\eta N(t). \end{aligned} \tag{5.2.3}$$

By taking Laplace transformation (from eq. (1.1.13)),

$$N(s) = \frac{\frac{\tilde{A}^\eta}{s} + s^{\eta-1}N(0)}{s^\eta + \tilde{d}^\eta}. \tag{5.2.4}$$

Now, by taking inverse Laplace transformation (from eq. (1.1.8)),

$$N(t) = \frac{\tilde{A}^\eta}{\tilde{d}^\eta}[1 - \mathbb{E}_\eta(-\tilde{d}^\eta t^\eta)] + N(0)\mathbb{E}_\eta(-\tilde{d}^\eta t^\eta) \tag{5.2.5}$$

where $\mathbb{E}_\eta$ is Mittag-Leffler function defined in eq. (1.1.6) and $0 \leq \mathbb{E}_\eta(-\tilde{d}^\eta t^\eta) \leq 1$.

$$\implies N(t) \leq \frac{\tilde{A}^\eta}{\tilde{d}^\eta} \tag{5.2.6}$$

According to existence and uniqueness theorem (Theorem 1.4.1) the solution on $t \in (0, \infty)$ of the proposed model (5.1.1) not only exists but also unique and bounded. □

5.2.2 Non-Negative Solution

From 1^{st} equation of proposed model (5.1.1),

$$\frac{d^\eta X(t)}{dt^\eta} \geq -\left(\tilde{\beta}^\eta \frac{S_L(t) + S_A(t)}{N(t)} + \tilde{d}^\eta\right) X(t)$$

$$\implies X(t) \geq X(0)\mathbb{E}_\eta[-(\tilde{\beta}^\eta\gamma + \tilde{d}^\eta)t^\eta] \tag{5.2.7}$$

$$\implies X(t) \geq 0. \tag{5.2.8}$$

Similarly,

$$S_L(t) \geq 0,\ S_A(t) \geq 0,\ H_P(t) \geq 0,\ L_P(t) \geq 0. \tag{5.2.9}$$

5.2.3 Identifying the Invariant Set

The set Ω is an invariant set, if the initial conditions are in Ω, the solution of model always remains in Ω. As a consequence, a positively invariant set will have positive solutions. Hence, from eq. (5.2.6)–eq. (5.2.9)

$$\Omega = \left\{ (X, S_L, S_A, H_P, L_P) \in \mathbb{R}^4_+ : 0 \leq X + S_L + S_A + H_P + L_P \leq \frac{\tilde{A}^\eta}{d^\eta} \right\}$$

is a positively invariant region.

5.3 Assessment of Equilibrium Points and Reproduction Number

There are two equilibrium points exist for the proposed model eq. (5.1.1):

- Social Web Free equilibrium: When there are no social web users (less involved users and active users).
- Endemic Equilibrium: When the number of social web users are not zero.

5.3.1 Social Web Free Equilibrium

The social web free equilibrium point exists when less involved and active users are zero. Students who sought admission to an educational institution were either denied admission, or got an acceptance letter but had not enrolled/were still registering, or had registered but had yet to begin utilizing social media for academic reasons. As a result, $E_0 = \left(\frac{\tilde{A}^\eta}{\tilde{d}^\eta}, 0, 0, 0, 0 \right)$.

5.3.2 Reproduction Number

The reproduction number, denoted R_0, is defined as "the estimated number of secondary cases created by an infective person in a fully susceptible population [111]." The proposed model has two infected groups (less involved users (S_L), active users (S_A)) and a force of infection $\tilde{\beta}^\eta \frac{S_L(t) + S_A(t)}{N(t)}$. To determine the reproduction number the next-generation matrix approach is employed at social web free equilibrium.

$$\frac{d^\eta Z}{dt^\eta} = \mathcal{F}(Z; Y) - \mathcal{V}(Z; Y)$$

$$\frac{d^{\eta}Y}{dt^{\eta}} = \mathcal{W}(Z;Y)$$

$\mathcal{F}(Z;Y)$: New infection rates (flows from Y to Z)

$\mathcal{V}(Z;Y)$: All other rates (not new infection).

$$F = \left(\frac{\partial \mathcal{F}}{\partial X}\right)_{E_0}, V = \left(\frac{\partial \mathcal{V}}{\partial X}\right)_{E_0}$$

$$F = \begin{bmatrix} \tilde{\beta}^{\eta} & \tilde{\beta}^{\eta} \\ 0 & 0 \end{bmatrix}, \qquad V = \begin{bmatrix} \tilde{\theta}_1^{\eta} + \tilde{d}^{\eta} + q\tilde{\tau}_1^{\eta} + (1-q)\tilde{\tau}_2^{\eta} & -\tilde{\delta}^{\eta} \\ -\tilde{\theta}_1^{\eta} & \tilde{d}^{\eta} + r\tilde{\alpha}_1^{\eta} + (1-r)\tilde{\alpha}_2^{\eta} + \tilde{\delta}^{\eta} \end{bmatrix}$$

Let $B_1 = \tilde{\theta}_1^{\eta} + \tilde{d}^{\eta} + q\tilde{\tau}_1^{\eta} + (1-q)\tilde{\tau}_2^{\eta}, \qquad B_2 = \tilde{d}^{\eta} + r\tilde{\alpha}_1^{\eta} + (1-r)\tilde{\alpha}_2^{\eta} + \tilde{\delta}^{\eta}$

The spectral radius of FV^{-1} is equal to R_0, and

$$R_0 = \frac{\tilde{\beta}^{\eta}(B_2 + \tilde{\theta}_1^{\eta})}{B_1 B_2 - \tilde{\delta}^{\eta}\tilde{\theta}_1^{\eta}}.$$

$$R_0 = \frac{\tilde{\beta}^{\eta}[\tilde{d}^{\eta} + r\tilde{\alpha}_1^{\eta} + (1-r)\tilde{\alpha}_2^{\eta} + \tilde{\delta}^{\eta} + \tilde{\theta}_1^{\eta}]}{(\tilde{\theta}_1^{\eta} + \tilde{d}^{\eta} + q\tilde{\tau}_1^{\eta} + (1-q)\tilde{\tau}_2^{\eta})(\tilde{d}^{\eta} + r\tilde{\alpha}_1^{\eta} + (1-r)\tilde{\alpha}_2^{\eta} + \tilde{\delta}^{\eta}) - \tilde{\delta}^{\eta}\tilde{\theta}_1^{\eta}}. \tag{5.3.1}$$

5.3.3 Endemic Equilibrium Point

Theorem 5.3.1. *The positive endemic equilibrium exists and is unique if* $R_0 > 1$.

Proof. Let $E^* = (X^*, S_L^*, S_A^*, H_P^*, L_P^*)$ be the endemic equilibrium point of model (5.1.1) then E^* satisfies eq. (5.1.1), $N^* = X^* + S_L^* + S_A^* + H_P^* + L_P^*$, and $\gamma^* = \dfrac{\tilde{\beta}^{\eta}[S_A^* + S_L^*]}{N^*}$

Thus from eq. (5.1.1), we have

$$X^* = \frac{(1-mp)\tilde{A}^{\eta}}{\tilde{d}^{\eta} + \gamma^*}, \quad H_P^* = \frac{q\tilde{\tau}_1^{\eta}S_L^* + r\tilde{\alpha}_1^{\eta}S_A^*}{\tilde{\rho}_1^{\eta} + \tilde{d}^{\eta}}, \quad L_P^* = \frac{(1-q)\tilde{\tau}_2^{\eta}S_L^* + (1-r)\tilde{\alpha}_2^{\eta}S_A^*}{\tilde{\rho}_2^{\eta} + \tilde{d}^{\eta} + \tilde{\theta}_2^{\eta}}$$

$$S_L^* = \frac{\gamma^* A + B(\gamma^* + \tilde{d}^{\eta})}{(\gamma^* + \tilde{d}^{\eta})Q}, \quad S_A^* = \frac{\gamma^* D + E(\gamma^* + \tilde{d}^{\eta})}{(\gamma^* + \tilde{d}^{\eta})Q}$$

where $A = B_2B_8(1-mp)\tilde{A}^{\eta}, \quad B = [nB_2B_8 + (m-n)(\tilde{\theta}_2^{\eta}B_7 + \tilde{\delta}^{\eta}B_8)]p\tilde{A}^{\eta},$

$D = B_8\tilde{\theta}_1^{\eta}(1-mp)\tilde{A}^{\eta}, E = [n\tilde{\theta}_1^{\eta}B_8 + (m-n)(B_1B_8 - \tilde{\theta}_2^{\eta}B_6)]p\tilde{A}^{\eta},$

$Q = B_1B_2B_8 - \tilde{\delta}^{\eta}\tilde{\theta}_1^{\eta}B_8 - \tilde{\theta}_1^{\eta}\tilde{\theta}_2^{\eta}B_7 - \tilde{\theta}_2^{\eta}B_2B_6$

and

$B_3 = q\tilde{\tau}_1^{\eta}, \quad B_4 = r\tilde{\alpha}_1^{\eta}, \quad B_5 = \tilde{\rho}_1^{\eta} + \tilde{d}^{\eta}, \quad B_6 = (1-q)\tilde{\tau}_2^{\eta}, \quad B_7 = (1-r)\tilde{\alpha}_2^{\eta}, B_8 = \tilde{\rho}_2^{\eta} + \tilde{d}^{\eta} + \tilde{\theta}_2^{\eta}.$

Now, let $F = A + B$ and $G = D + E$,

then

$$S_L^* = \frac{\gamma^* F + B\tilde{d}^{\eta}}{(\gamma^* + \tilde{d}^{\eta})Q}, \quad S_A^* = \frac{\gamma^* G + E\tilde{d}^{\eta}}{(\gamma^* + \tilde{d}^{\eta})Q}, \quad H_P^* = \frac{\gamma^* FB_3 + \gamma^* GB_4 + (BB_3 + EB_4)\tilde{d}}{(\gamma^* + \tilde{d}^{\eta})QB_5}$$

$$L_P^* = \frac{\gamma^* FB_6 + \gamma^* GB_7 + (BB_6 + EB_7)\tilde{d}}{(\gamma^* + \tilde{d}^{\eta})QB_8}, \qquad N^* = \frac{\gamma^* A_0 + T}{(\gamma^* + \tilde{d}^{\eta})B_5B_8Q}$$

where

$$A_0 = B_5B_8F + B_5B_8G + B_3B_8F + B_4B_8G + B_5B_6F + B_5B_7F,$$

$$T = B_5B_8Q(1-mp)\tilde{A}^{\eta} + B_5B_8B\tilde{d}^{\eta} + B_5B_8E\tilde{d}^{\eta} + B_8(BB_3 + EB_4)\tilde{d}^{\eta} + B_5(BB_6 + EB_7)\tilde{d}^{\eta}$$

We have,

$$\gamma^{*2}A_0 + \gamma^* A_1 - A_2 = 0, \tag{5.3.2}$$

where

$$A_1 = T - B_5B_8\tilde{\beta}^{\eta}(F + G), \qquad A_2 = \frac{\tilde{\beta}^{\eta}\tilde{d}^{\eta}B_5B_8(B + E)(B_1B_2 - \tilde{\delta}^{\eta}\tilde{\theta}_1^{\eta})}{\tilde{\beta}^{\eta}(B_2 - \tilde{\theta}_1^{\eta}) - (B_1B_2 - \tilde{\delta}^{\eta}\tilde{\theta}_1^{\eta})}(R_0 - 1).$$

According to Descartes rule of signs this polynomial has exactly one positive root if $R_0 > 1$. □

5.4 Stability Analysis of Proposed Model

Theorem 5.4.1. *The social web free equilibrium point* $E_0 = \left(\frac{\tilde{A}^{\eta}}{\tilde{d}^{\eta}}, 0, 0, 0, 0\right)$ *of the system* (5.1.1) *is globally asymptotically stable under some restriction on parameters when* $R_0 < 1$*; otherwise it is unstable.*

Proof. Jacobian matrix at E_0 is

$$J_{E_0} = \begin{bmatrix} -\tilde{d^\eta} & -\tilde{\beta}^\eta & -\tilde{\beta}^\eta & 0 & 0 \\ 0 & \tilde{\beta}^\eta - (\tilde{\theta}_1^\eta + \tilde{d}^\eta + q\tilde{\tau}_1^\eta) & \tilde{\beta}^\eta + \tilde{\delta}^\eta & 0 & \tilde{\theta}_2^\eta \\ & -(1-q)\tilde{\tau}_2^\eta & & & \\ 0 & \tilde{\theta}_1^\eta & -(\tilde{d}^\eta + r\tilde{\alpha}_1^\eta) & 0 & 0 \\ & & -(1-r)\tilde{\alpha}_2^\eta + \tilde{\delta}^\eta & & \\ 0 & q\tilde{\tau}_1^\eta & r\tilde{\alpha}_1^\eta & -\tilde{\rho}_1^\eta - \tilde{d}^\eta & 0 \\ 0 & (1-q)\tilde{\tau}_2^\eta & (1-r)\tilde{\alpha}_2^\eta & 0 & -\tilde{\rho}_2^\eta - \tilde{d}^\eta - \tilde{\theta}_2^\eta \end{bmatrix}.$$

Clearly, two eigen-values are $-\tilde{d^\eta}, -\tilde{\rho}_1^\eta - \tilde{d}^\eta$ lie in 2^{nd} quadrant.

To examine the stability of the system, it is necessary to assess the remaining eigenvalues. To accomplish this, we take into account the following:

$$J_{E_0} = \begin{bmatrix} \tilde{\beta}^\eta - (\tilde{\theta}_1^\eta + \tilde{d}^\eta) & \tilde{\beta}^\eta + \tilde{\delta}^\eta & \tilde{\theta}_2^\eta \\ -(q\tilde{\tau}_1^\eta + (1-q)\tilde{\tau}_2^\eta) & & \\ \tilde{\theta}_1^\eta & -(\tilde{d}^\eta + r\tilde{\alpha}_1^\eta) & 0 \\ & -((1-r)\tilde{\alpha}_2^\eta + \tilde{\delta}^\eta) & \\ (1-q)\tilde{\tau}_2^\eta & (1-r)\tilde{\alpha}_2^\eta & -\tilde{\rho}_2^\eta - \tilde{d}^\eta - \tilde{\theta}_2^\eta \end{bmatrix}.$$

The characteristic equation of above matrix is given by

$$\lambda^3 + C_1\lambda^2 + C_2\lambda + C_3 = 0$$

where $C_1 = -\tilde{\beta}^\eta + \tilde{\theta}_1^\eta + \tilde{d}^\eta + q\tilde{\tau}_1^\eta + (1-q)\tilde{\tau}_2^\eta + \tilde{d}^\eta + r\tilde{\alpha}_1^\eta + (1-r)\tilde{\alpha}_2^\eta + \tilde{\delta}^\eta + \tilde{\rho}_2^\eta + \tilde{d}^\eta + \tilde{\theta}_2^\eta$

For

$$R_0 = \frac{\tilde{\beta}^\eta(B_2 + \tilde{\theta}_1^\eta)}{B_1B_2 - \tilde{\delta}^\eta\tilde{\theta}_1^\eta} < 1 \implies \tilde{\beta}^\eta - B_1 < 0.$$

$$\implies C_1 = -\tilde{\beta}^\eta + B_1 + B_2 + \tilde{\rho}_2^\eta + \tilde{d}^\eta + \tilde{\theta}_2^\eta > 0 \text{ whenever } R_0 < 1$$

$C_2 = B_2(\tilde{\rho}_2^\eta + \tilde{d}^\eta + \tilde{\theta}_2^\eta) - (\tilde{\beta}^\eta - B_1)(\tilde{\rho}_2^\eta + \tilde{d}^\eta + \tilde{\theta}_2^\eta) - (1-q)\tilde{\tau}_2^\eta\tilde{\theta}_2^\eta - (\tilde{\beta}^\eta - B_1)B_2 - \tilde{\theta}_1^\eta(\tilde{\beta}^\eta + \tilde{\delta}^\eta)$

$$= (B_2 - (\tilde{\beta}^\eta - B_1))(\tilde{\rho}_2^\eta + \tilde{d}^\eta + \tilde{\theta}_2^\eta) - (1-q)\tilde{\tau}_2^\eta\tilde{\theta}_2^\eta + B_1B_2 - \tilde{\delta}^\eta\tilde{\theta}_1^\eta(1-R_0)$$

$$C_3 = (B_1B_2 - \tilde{\delta}^\eta\tilde{\theta}_1^\eta)(1-R_0)((\tilde{\rho}_2^\eta + \tilde{d}^\eta + \tilde{\theta}_2^\eta) - \tilde{\theta}_2^\eta[(1-q)\tilde{\tau}_2^\eta B_2 + (1-r)\tilde{\alpha}_2^\eta\tilde{\theta}_1^\eta]$$

By using Routh-Hurwitz criteria (Theorem 1.4.4), if $C_1,\ C_3,\ C_1C_2 - C_3$ are greater than zero; then the eigenvalues will have negative real parts. Therefore, the proposed model (5.1.1) is stable if $R_0 < 1$. Here $(S_L(t), S_A(t), H_P(t), L_P(t)) \to (0,0,0,0)$ as $t \to \infty$, so, $(X(t), S_L(t), S_A(t), H_P(t), L_P(t)) \to \left(\frac{\tilde{A}^\eta}{\tilde{d}^\eta}, 0, 0, 0, 0\right)$ as $t \to \infty$. Hence, E_0 is globally asymptotically stable for $R_0 < 1$ if $C_1,\ C_3,\ C_1C_2 - C_3$ are greater than zero. □

Theorem 5.4.2. *The $E^* = (X^*, S_L^*, S_A^*, H_P^*, L_P^*)$ is locally asymptotically stable if $R_0 > 1$.*

Proof. The characteristic equation corresponding to the Jacobian matrix of the proposed model at $E^* = (X^*, S_L^*, S_A^*, H_P^*, L_P^*)$ is

$$D_4 + D_3\lambda + D_2\lambda^2 + D_1\lambda^3 + \lambda^4 = 0 \tag{5.4.1}$$

The characteristics equation will have complex roots with negative real parts if $D_1,\ D_4,\ D_1D_2 - D_3,\ D_1D_2D_3 - D_3^2 - D_4D_1^2$ are greater than zero. As a consequence, $E^* = (X^*, S_L^*, S_A^*, H_P^*, L_P^*)$ is locally asymptotically stable if the preceding conditions are satisfied. □

5.5 Dataset and Methodology

The COVID-19 pandemic has accelerated and magnified the role of social media in our lives, affecting both the positive and negative aspects of our interactions with these platforms. While social media can serve as a valuable tool for connection and information-sharing, it's important to be mindful of the potential for addictive behaviors and to find a healthy balance between online and offline activities. Despite the substantial advantages social media brings to academia, it is prudent to adopt a careful approach. In this regard, the primary aim of this study is to optimize the utilization of social media to contribute to a more promising future for students in real-life situations. For this, to collect data, Google

Forms circulated as a questionnaire to students of various institutions in Punjab, Haryana, and Rajasthan states in India namely, BITS Pilani, Pilani campus; Chaudhary Devi Lal College; Galgotia College of Engineering and Technology; Amity University; Maharshi Dayanand University; Guru Jambheshwar University of Science and Technology; and Banasthali Vidyapith.

Table 5.1: Initial value for different categories of social media users.

Population	X	S_L	S_A	H_P	L_P
Initial Values	200	100	50	80	50

Table 5.2: Parameter description and values for social media addiction.

Parameter	Description	Value
$\tilde{A}$	Recruitment rate	500
$\tilde{\beta}$	Rate at which people switch from the non-users to less involved users	0.7
$\tilde{\theta}_1$	Rate from which people switch from less involved users to active users	0.1
$\tilde{\delta}$	Rate from which people switch from active users to less involved users	0.1
$\tilde{\tau}_1$	Rate of performing high by less involved users	0.68
$\tilde{\tau}_2$	Rate of performing low by less involved users	0.32
$\tilde{\alpha}_1$	Rate of performing high by active users	0.78
$\tilde{\alpha}_2$	Rate of performing low by active web users	0.28
$\tilde{\theta}_2$	Rate at which low-performing students are switched to less involved users	0.4
$\tilde{\rho}_1^{\eta}$	Graduation rate as a consequence of outstanding results	0.5
$\tilde{\rho}_2^{\eta}$	withdrawal rate as a consequence of poor performance	0.3
$\tilde{d}$	Natural death rate	0.019
mp	Possibility of students being in the non-users compartment	0.6
np	Possibility of students being in the less involved compartment	0.2

Students in higher education are chosen since they are more likely to use smartphones and computers. According to the findings, the most popular reason for using social media is to keep in touch with friends, immediately followed by reasons like socializing with more people, enjoying oneself, professional issues, and many more. As a result of the COVID-19 pandemic, the bulk of time spent on social media networking sites is approximately three hours each day for academic objectives. Consequently, within the scope of this current research, students who allocate up to three hours to social media

are categorized as non-users of social platforms. Those who spend between three to five hours on social media are considered less active users, while those who invest more than five hours are regarded as active social media users. Students achieving a 60% and above are classified as high-performing students, while those falling below this threshold are categorized as low-performing students. Subsequently, the collected data is employed to compute various parameters for further analysis. The initial conditions and values of parameters used for verification are shown in Tables 5.1–5.2.

5.6 Numerical Experiment

The numerical simulation supports the analytical results for different derivative orders and illustrates the relevance of the threshold value (R_0).

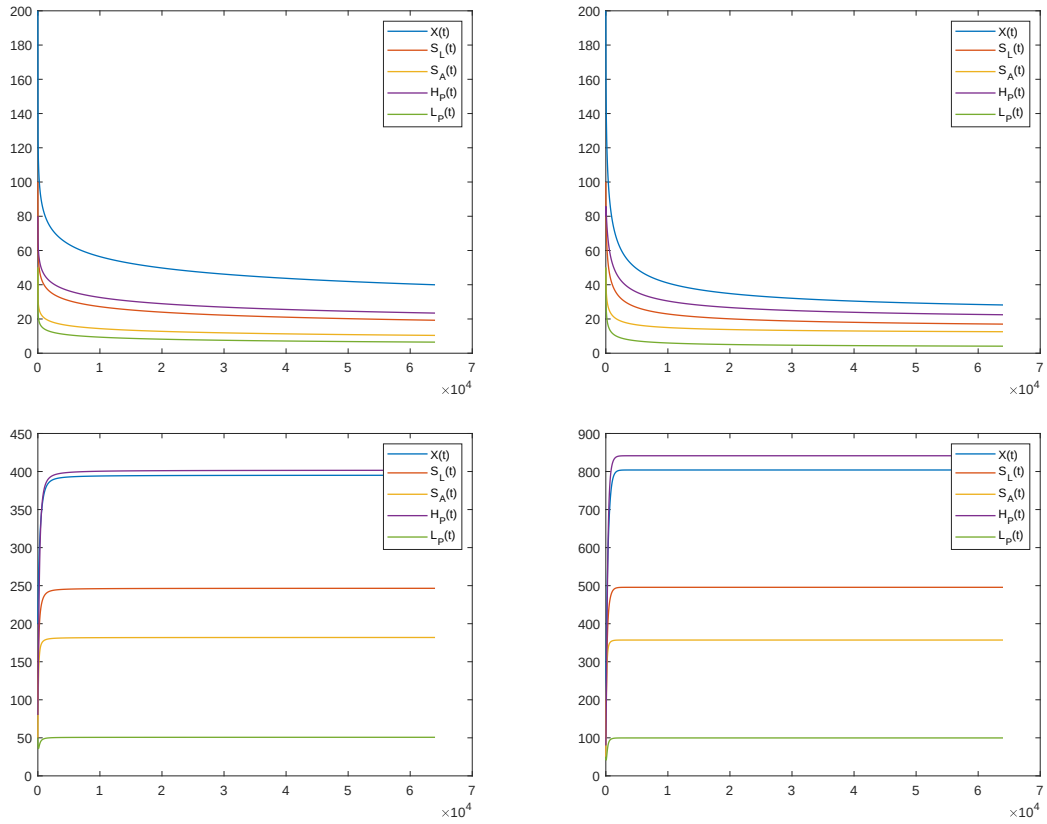

Figure 5.2: Variations of Non-Users X, Less-Involved users S_L, Active Users S_A, Users performing high H_P, and Users performing low L_P with time for the different order of derivatives, 0.25, 0.5, 0.75, and 1 respectively.

These simulations also help us to understand better how different groups of individuals interact. The predictor-corrector approach of Adams-Bashforth-Moulton is used to solve the proposed model [109].

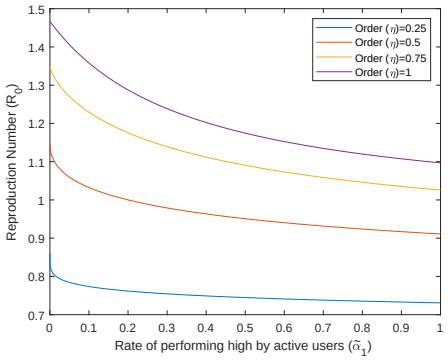

(a) Variation of R_0 with $\tilde{\alpha}_1$ is shown for the different order of derivatives, reproduction number decreasing with increase in the rate of performing high by active users.

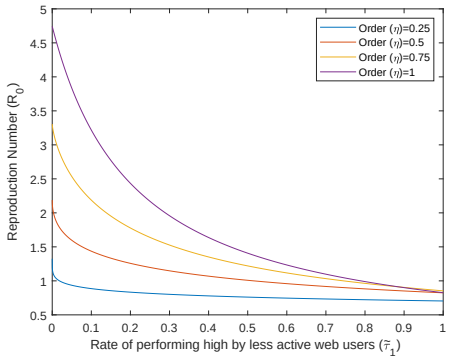

(b) Variation of R_0 with $\tilde{\tau}_1$ is shown for the different order of derivatives, reproduction number decreasing with increase in the rate of performing high by less active users.

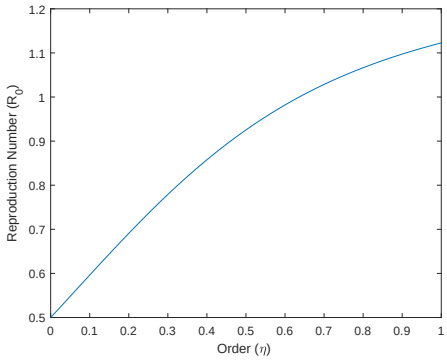

(c) Reproduction number is increasing with the order of derivative, i.e., active users increase with the order of derivative.

Figure 5.3: Relation of reproduction no. (R_0) with rate of performing high by active users ($\tilde{\alpha}_1$), users performing high by less active users ($\tilde{\tau}_1$), and order of derivative (η).

Figure 5.2 shows that the social web free and endemic steady state of the proposed model is asymptotically stable for various values of the order of derivative (η). Trajectories of all the compartments decrease for orders less than equal to 0.5 and show increasing behavior for orders greater than 0.5. From Figure 5.2, Figure 5.4, and Figure 5.5, it can be shown that as η increases, each population converges faster to its equilibrium. If $R_0 > 1$,

the society cannot be social media-free, but it can reduce its usage and become stable over a certain period, irrespective of the order of derivative.

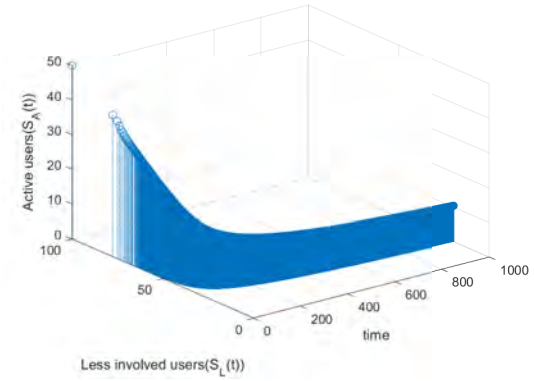

(a) For $\eta = 0.25$, S_L, S_A decreasing with time to attain the stable state.

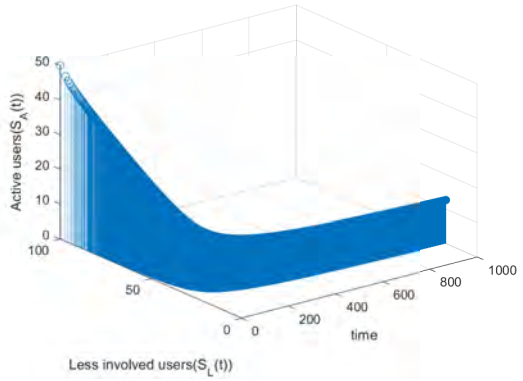

(b) For $\eta = 0.5$, S_L, S_A decreasing with time to attain the stable state.

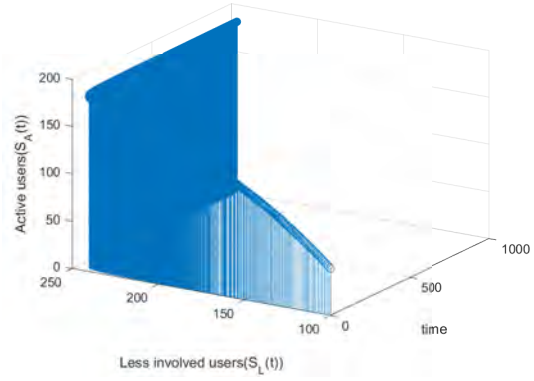

(c) For $\eta = 0.75$, S_L, S_A increasing with time to attain the stable state.

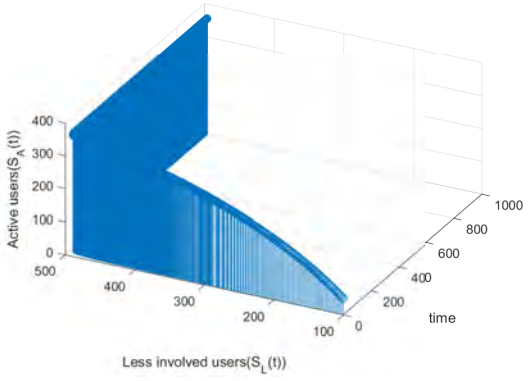

(d) For $\eta = 1$, S_L, S_A, increases with time to attain the stable state.

Figure 5.4: Variation of Less active users (S_L), Active users (S_A), with different order of derivative 0.25, 0.5, 0.75, and 1 respectively.

Figure 5.3(a) shows that the socially addicted population S_A decreases as the reproduction number decreases with time when the rate of performing high by active users increases. Figure 5.3(b) shows that the socially addicted population S_A is decreasing with time when the rate of performing high by less active web users increases. Figure 5.3(c) shows that the socially addicted population S_A is decreasing with time as the reproduction number decreases when order decreases from 1 to 0. Hence, the reproduction number decreases with the rate of high-performance users increasing irrespective of the order of

derivative and validates the stability of the fractional-order model.

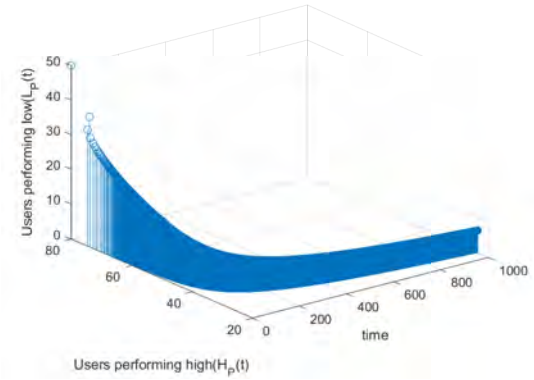

(a) For $\eta = 0.25$, H_P, L_P decreasing with time to attain the stable state.

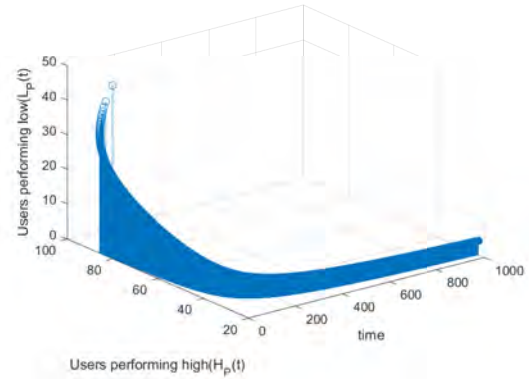

(b) For $\eta = 0.5$, H_P, L_P decreasing with time to attain the stable state.

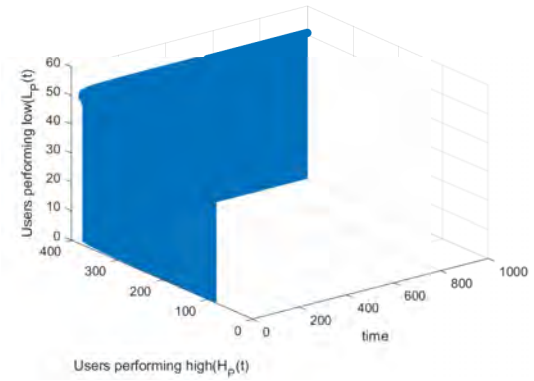

(c) For $\eta = 0.75$, H_P, L_P increasing with time to attain the stable state.

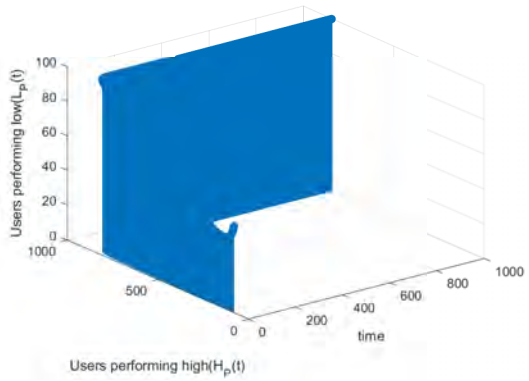

(d) For $\eta = 1$, H_P, L_P increasing with time to attain the stable state.

Figure 5.5: Variation of Users performing high (H_P), Users performing low (L_P) with different order of derivative 0.25, 0.5, 0.75, and 1 respectively.

For the set of parameters given in Tables 5.1–5.2, it is found that for the order of derivative (η) less than 0.5, the reproduction number (R_0) is less than 1. The solution of the suggested model converges to social web free equilibrium point $\eta \leq 0.5$ indicating for $\eta \leq 0.5$ social media addiction converse to zero. The rate of performing high increases as the order of derivative decreases. As the derivative order decreases, the reproduction number also decreases. When reducing the derivative order from 1, the system exhibits an increased memory effect, leading to decrease in social media addiction. This suggests that the fractional order model outperforms the integer order model. The social web

free equilibrium point does not exist in reality, and the primary objective is to use social networking sites for students' benefit. Hence, the optimal value of the order of derivative lies in the neighborhood of 0.5, where the reproduction number is one (Figure 5.3(c)).

5.7 Conclusion

The nonlinear fractional differential equations are proposed to describe the impact of social networking sites on student academic achievement. The social web free and endemic equilibrium point exists for the proposed model. The reproduction number R_0 differentiates the social web free and socially addicted equilibrium points. According to the study, the social web free steady state is locally asymptotically stable when the reproduction number is less than one and unstable otherwise. The significant findings of the present research are listed below:

- The model proposed in this chapter differs from previous models as the social web-free equilibrium point is not beneficiary for society. The primary objective of this chapter is to show the existence and stability of endemic equilibria.

- All population trajectories demonstrate decreasing behavior for the order of derivative less than or equal to 0.5 and increasing behavior for orders greater than 0.5. The primary aim of this study is to optimize the utilization of social media to contribute to a more promising future for students in real-life situations. Hence, the optimal value for the order of the derivative is $\sim$0.5 to optimize the utilization of social media.

- As memory is integrated through a fractional-order derivative, a decrease in the derivative order leads to a reduction in the reproduction number. This highlights the significance of memory and demonstrates the high efficiency of a fractional-order model over an integer-order model.

- The reproduction number diminishes as the prevalence of high-performance users rises. Consequently, the frequency of high-performance occurrences increases as

the derivative order decreases to incorporate memory.

Implementing educational programs with the aim of informing students about the impact of social media on academic performance and fostering a perspective that sees social media as a tool for academic enhancement, rather than a distraction, can significantly enhance students' academic achievements.

The findings of this chapter are published in the following referred publication:

- *K. Bansal, T. Mathur, T. Mathur, S. Agarwal, and R.D. Sharma, "Impact of social media on academics: A fractional order mathematical model." International Journal of Modelling and Simulation.*

Chapter 6

Impact of Skills Development on Youth Unemployment

"Addressing unemployment requires a holistic approach that integrates education, skills development, and job creation."

- Nelson Mandela

Unemployment is a pressing global issue that affects individuals, communities, and entire world economies. It refers to the situation where individuals willing and able to work cannot secure enough employment opportunities based on their skills. The consequences of high unemployment rates are far-reaching, encompassing economic, social, and psychological aspects [73]. The social impact of unemployment is profound. It can lead to social exclusion, a loss of self-esteem, and a sense of hopelessness among the unemployed population [153]. The lack of job opportunities can exacerbate inequality and social divisions, as certain groups, such as youth and marginalized communities, are disproportionately affected. Additionally, unemployment can lead to increased crime rates and social unrest, posing significant challenges to the overall stability and well-being of societies [154–156]. Addressing the unemployment problem requires a comprehensive understanding of its causes, dynamics, and potential solutions.

Youth unemployment is a critical global issue and a significant indicator of a country's economic situation. In impoverished nations, the lack of job opportunities for young indi-

viduals is often attributed to their inadequate experience and the incompatibility between their skills and the market demands [74,75]. Consequently, several governments, including India, have taken steps to address this challenge through initiatives focused on skills development for the unemployed [155]. One notable program is the "Pradhan Mantri Kaushal Vikas Yojana (PMKVY)" or the "Skill India" program. This program aims to provide skill training to a large number of Indian youth to make them job-ready and enhance their employability. It offers a wide range of skill development courses and certifications across various industries and sectors. Furthermore, the World Bank Group has been striving to make sure that people have opportunities for high-quality education and training through collaboration with several nations and development partners. Simultaneously, they also support employers in identifying and accessing the required skills. Overall, addressing unemployment and bridging the skills gap is crucial for promoting economic growth and reducing the disparities in job availability. Governments, international organizations, and development partners are actively involved in initiatives to equip individuals with the necessary skills for employment and facilitate cooperation between job seekers and employers.

Unemployment is influenced by a multitude of causative factors, including economic conditions, labor market dynamics, government policies, education levels, technological changes, and more. Mathematical models can incorporate these factors to provide insights into the drivers of unemployment. Mathematical modeling provides a valuable tool for analyzing and predicting the behavior of unemployment rates and evaluating the effectiveness of various policy interventions. By formulating mathematical models that capture the complexities of the unemployment problem, researchers and policymakers can gain insights into the underlying mechanisms, identify key factors influencing unemployment dynamics, and explore strategies to mitigate its adverse effects. Recently several researchers have focused on mathematical modeling of the unemployment problem [29,76,78–80,156–163]. Notably, the introduction of mathematical models describing the unemployment problem can be attributed to Misra and Singh in 2011 [76]. In 2015, Pathan and Bhathawala [77] investigated the influence of self-employment on the unemployment rate. Another study

by Daud and Ghozali [78] in the same year developed a mathematical model incorporating two classes: employed and unemployed individuals. Building upon their previous work, Pathan and Bhathawala [29] expanded their model in 2016 by incorporating four classes: unemployed individuals, employed individuals, new migrant workers, and newly vacant positions. In 2017, Misra and Singh [79] further explored the unemployment problem by considering the influence of skill development programs provided by academic institutions. In 2018, another study highlighted the importance of creating more job opportunities through increased employment rates and reduced diminution rates to address unemployment effectively [157]. Additionally, Ashi *et al.* [80] examined the impact of government assistance on reducing the unemployment rate in a study conducted in 2022. These studies contribute to understanding unemployment dynamics and provide insights into potential strategies and interventions to address this issue. By utilizing mathematical models, researchers have shed light on various factors influencing unemployment and proposed measures to mitigate its impact.

According to Gir-Alana *et al.* [81] the unemployment rate in Turkey demonstrates long memory characteristics. Specifically, the non-agricultural and rural unemployment exhibit long memory, indicating a non-locality of time or dynamic memory. The persistence of unemployment rates, public perceptions and expectations, previous policy interventions, and the use of historical data for forecasting demonstrate the importance of considering the influence of past events and trends when studying and addressing unemployment. The past history of a region or country has a significant impact on its current unemployment situation. Factors such as economic cycles, structural changes, government policies, education, demographics, historical events, technological advancements, globalization, and social and cultural factors influence the current state of unemployment. Understanding this historical context is vital for policymakers and economists when addressing unemployment challenges and promoting job creation. It highlights the need for policies that consider the long-term consequences of past events and trends on the labor market. Hence, fractional order derivatives provide a more suitable approach for modeling unemployment compared to integer-order derivative models. While several unemployment models have been

developed over the years using integer-order derivatives, these models failed to account for the non-local nature of time or dynamic memory [76, 79, 80, 157, 158]. The authors of the aforementioned studies predominantly relied on traditional integer-order derivatives, which often fail to capture the persistence and inherent characteristics of real-world dynamic events. Therefore, embracing fractional order derivatives and modeling techniques is imperative to better capture the complexities and dynamic memory of unemployment, ultimately leading to more precise depictions and predictions of real-world dynamics.

Considering the increasing youth unemployment rate (Figure 1.3), it is crucial to examine the youth unemployment problem comprehensively. This chapter aims to understand the impact of fractional order derivatives on modeling unemployment and explore the effect of the skill development program. In summary, modeling socio-economic phenomena like unemployment provides valuable insights into the underlying dynamics and allows policymakers to devise appropriate policy implications. By leveraging mathematical and statistical models, researchers and policymakers can gain a deeper understanding of the causes and consequences of unemployment, identify effective interventions, and work towards creating a more prosperous and inclusive society.

6.1 Mathematical Model Formulation of Unemployment

This section proposes the unemployment model that involves the following assumptions:

- The overall population consists of three distinct categories: individuals without employment (U), skilled individuals who are currently unemployed (S_U), and those who are employed (E). It's important to note that not all members of the unemployed group possess the necessary qualifications and skill set to secure a job.

- The proportion of unemployed individuals motivated to enhance their skills is directly related to the size of the unemployed population moving to the S_U class.

- There is a possibility that certain individuals who are currently unemployed may transition into employment. The rate at which individuals move from unemployment

to employment depends on the number of unemployed and available job vacancies (V).

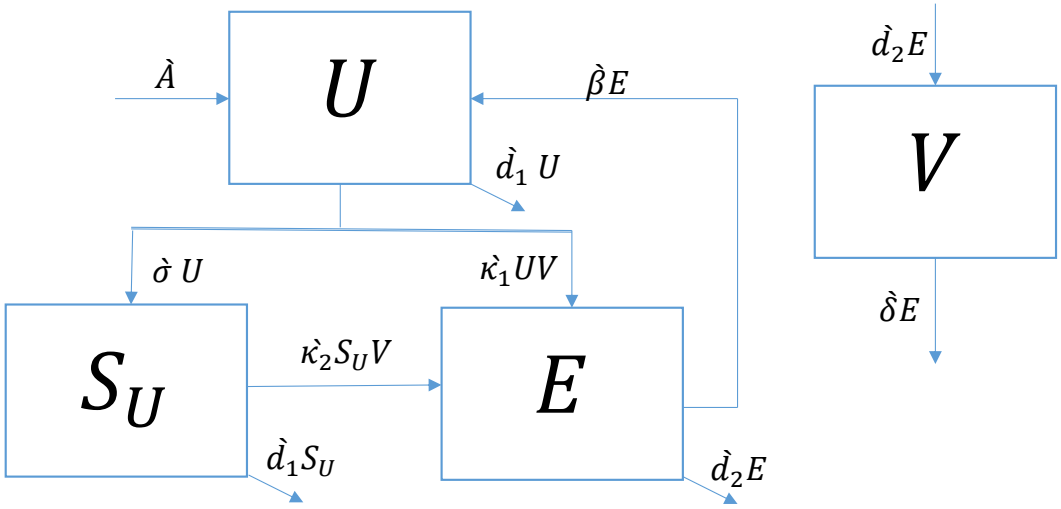

Figure 6.1: Schematic diagram of the proposed model.

- The rate of employment for skilled individuals who are unemployed is significantly higher than the rate for unskilled individuals.

- Various factors can influence the number of employed individuals. Some employers may terminate or lay off employees, while others may resign voluntarily. In either case, these individuals will transition from being employed to becoming part of the unemployed population.

- It is assumed that the rate at which individuals migrate or pass away is directly proportional to the size of the population. The creation of vacancies solely occurs due to employed individuals retiring, passing away, or migrating.

Figure 6.1 is a flowchart that is used to analyze how people move with the social hierarchy of the human population, and the following set of dimensionally balanced fractional

differential equations characterizes the corresponding model:

$$\begin{aligned}
\frac{d^{\eta}U}{dt^{\eta}} &= \grave{A}^{\eta} - \grave{\kappa}_1^{\eta}UV + \grave{\beta}^{\eta}E - \grave{\sigma}^{\eta}U - \grave{d}_1^{\eta}U \\
\frac{d^{\eta}S_U}{dt^{\eta}} &= -\grave{\kappa}_2^{\eta}S_UV + \grave{\sigma}^{\eta}U - \grave{d}_1^{\eta}S_U \\
\frac{d^{\eta}E}{dt^{\eta}} &= \grave{\kappa}_1^{\eta}UV + \grave{\kappa}_2^{\eta}UV - \grave{\beta}^{\eta}E - \grave{d}_2^{\eta}E \\
\frac{d^{\eta}V}{dt^{\eta}} &= \grave{d}_2^{\eta}E - \grave{\delta}^{\eta}V
\end{aligned} \tag{6.1.1}$$

where $\grave{A}, \grave{\sigma}, \grave{\kappa}_1, \grave{\kappa}_2, \grave{\beta}, \grave{d}_1, \grave{d}_2, \grave{\delta}$, and η are positive constants that are defined as follows:

- $\grave{A}$: The rate at which the number of unemployed individuals is increasing.
- $\grave{\sigma}$: The rate at which the number of unemployed individuals transitions into skilled-unemployed individuals.
- $\grave{\kappa}_1$: The rate at which the number of unemployed individuals transitions into employment class.
- $\grave{\kappa}_2$: The rate at which the number of skilled unemployed individuals transitioning into employment class.
- $\grave{\beta}$: The rate at which employed individuals are resigning, being fired, or dismissed from their jobs.
- $\grave{d}_1$: The rate at which unemployed individuals migrate or pass away.
- $\grave{d}_2$: The rate at which employed individuals migrate, retire, or pass away.
- $\grave{\delta}$: The rate at which available vacancies decrease due to insufficient government funds (Diminution rate).
- η : Order of derivative.

6.2 Qualitative Properties of Proposed Model

This section analyzes the fundamental properties of the proposed model, including its existence, uniqueness, non-negativity, and boundedness of solution.

6.2.1 Invariant Region

The behavior of the proposed unemployment model (6.1.1) is examined in the region $\Omega \in \mathbb{R}^4_+$, where

$$\Omega = \left\{ (U, S_U, E, V) \in \mathbb{R}^4_+ : U + S_U + E + V \leq \frac{\grave{A}^\eta}{\lambda^\eta} \left(1 + \frac{\grave{d}_2^\eta}{\grave{\delta}^\eta} \right) \right\}$$

and $\lambda = min(\grave{d}_1, \grave{d}_2)$.

Theorem 6.2.1. *The region $\Omega \in \mathbb{R}^4_+$ is the positively invariant region for the unemployment model.*

Proof. Let $N(t) = U(t) + S_U(t) + E(t)$ represent the entire population at any given instant. Then,

$$\begin{aligned} \frac{d^\eta N(t)}{dt^\eta} &= \frac{d^\eta U(t)}{dt^\eta} + \frac{d^\eta S_U(t)}{dt^\eta} + \frac{d^\eta E(t)}{dt^\eta} \\ &\leq \grave{A}^\eta - \lambda^\eta N(t), \quad \text{where } \lambda = min(\grave{d}_1, \grave{d}_2). \end{aligned} \tag{6.2.1}$$

By taking Laplace's transformation (from eq. (1.1.13)),

$$N(s) = \frac{\frac{\grave{A}^\eta}{s} + s^{\eta-1} N(0)}{s^\eta + \lambda^\eta}. \tag{6.2.2}$$

Now, by taking the inverse Laplace transformation (from eq. (1.1.8)),

$$N(t) \leq \frac{\grave{A}^\eta}{\lambda^\eta} [1 - \mathbb{E}_\eta(-\lambda^\eta t^\eta)] + N(0) \mathbb{E}_\eta(-\lambda^\eta t^\eta). \tag{6.2.3}$$

Similarly,

$$V(t) \leq \frac{\grave{d}_2^{\eta}\grave{A}^{\eta}}{\grave{\delta}^{\eta}\grave{\lambda}^{\eta}}[1 - \mathbb{E}_{\eta}(-\grave{\delta}^{\eta}t^{\eta})] + V(0)\mathbb{E}_{\eta}(-\grave{\delta}^{\eta}t^{\eta}).$$

$\mathbb{E}_{\eta}$ is Mittage -Leffler function defined in eq. (1.1.6) and $0 \leq \mathbb{E}_{\eta}(-\grave{\delta}^{\eta}t^{\eta}) \leq 1$

$$\implies U + S_U + E + V \leq \frac{\grave{A}^{\eta}}{\grave{\lambda}^{\eta}}\left(1 + \frac{\grave{d}_2^{\eta}}{\grave{\delta}^{\eta}}\right). \tag{6.2.4}$$

To demonstrate that the solution of the suggested model (6.1.1) is non-negative, we have:

$$\begin{aligned}
\frac{d^{\eta}U(t)}{dt^{\eta}}\bigg|_{U(t_0)=0} &= \grave{A}^{\eta} + \grave{\beta}^{\eta}E \geq 0,\\
\frac{d^{\eta}S_U(t)}{dt^{\eta}}\bigg|_{S_U(t_0)=0} &= \grave{\sigma}^{\eta}U \geq 0,\\
\frac{d^{\eta}E(t)}{dt^{\eta}}\bigg|_{E(t_0)=0} &= \grave{\kappa}_1^{\eta}UV + \grave{\kappa}_2^{\eta}UV \geq 0,\\
\frac{d^{\eta}V(t)}{dt^{\eta}}\bigg|_{V(t_0)=0} &= \grave{d}_2^{\eta}E.
\end{aligned} \tag{6.2.5}$$

Now from Generalized mean value theorem (Theorem 1.4.2) the solution of the unemployment model (6.1.1) is non-negative. As Ω contains the positive solution to the proposed model assuming non-negative initial conditions, Ω is the positively invariant region. □

6.2.2 Existence and Uniqueness

Theorem 6.2.2. *There exists a unique solution along with the given initial conditions of the proposed model* (6.1.1) *on* $t \geq 0$.

Proof. The right-hand side of the proposed model (6.1.1) is continuous, bounded according to eq. (6.2.4) and satisfies the Lipschitz condition. So, from existence and uniqueness theorem (Theorem 1.4.1), it is established that the solution of model (6.1.1) with given initial conditions, not only exists but is also unique for $t > 0$. □

6.3 Analysis of Equilibrium Points

This section calculates the equilibrium points and threshold parameter (Reproduction number) for the proposed model. The equilibrium point is calculated by taking the right-hand side of the proposed model equal to zero. The proposed model have the following two equilibrium points:

- Employment-free equilibrium: This equilibrium exists when there is no employed person and no vacancy.

  So, $E = 0, V = 0$. Therefore, employment-free equilibrium point is given by

$$Q_0 = \left(\frac{\grave{A}^\eta}{\grave{\sigma}^\eta + \grave{d}_1^\eta}, \frac{\grave{\sigma}^\eta \grave{A}^\eta}{\grave{d}_1^\eta(\grave{\sigma}^\eta + \grave{d}_1^\eta)}, 0, 0 \right).$$

- Employment-persistence equilibrium: This equilibrium exists when the employed person and vacancy are not zero and is given by $Q^* = (U^*, S_U^*, E^*, V^*)$.

Here,

$$E^* = \frac{\grave{\delta}^\eta V^*}{\grave{d}_2^\eta}, \quad S_U^* = \frac{\grave{\sigma}^\eta \grave{\delta}^\eta (\grave{\beta}^\eta + \grave{d}_2^\eta)}{\grave{d}_2^\eta (\grave{\kappa}_1^\eta \grave{d}_1^\eta + \grave{\kappa}_1^\eta \grave{\kappa}_2^\eta V^* + \grave{\kappa}_2^\eta \grave{\sigma}^\eta)}, \quad U^* = \frac{\grave{\delta}^\eta (\grave{\beta}^\eta + \grave{d}_2^\eta)(\grave{d}_1^\eta + \grave{\kappa}_2^\eta V^*)}{\grave{d}_2^\eta (\grave{\kappa}_1^\eta \grave{d}_1^\eta + \grave{\kappa}_1^\eta \grave{\kappa}_2^\eta V^* + \grave{\kappa}_2^\eta \grave{\sigma}^\eta)}$$

and to find V^* substitute E^* and U^* in $\dfrac{d^\eta U(t)}{dt^\eta}$ of model (6.1.1) which reflect in the quadratic equation as:

$$P_1 {V^*}^2 + P_2 V^* + P_3 = 0, \tag{6.3.1}$$

where, $P_1 = \grave{\kappa}_1^\eta \grave{\kappa}_2^\eta \grave{d}_2^\eta \grave{\delta}^\eta > 0$, $P_2 = \grave{\kappa}_1^\eta \grave{\kappa}_2^\eta \grave{A}^\eta \grave{d}_2^\eta + \grave{d}_2^\eta \grave{\delta}^\eta (\grave{d}_1^\eta \grave{\kappa}_1^\eta + \grave{\sigma}^\eta \grave{\kappa}_2^\eta) + (\grave{d}_2^\eta + \grave{\beta}^\eta) \grave{\delta}^\eta \grave{d}_1^\eta \grave{\kappa}_2^\eta$, $P_3 = \grave{d}_1^\eta \grave{\delta}^\eta (\grave{d}_1^\eta + \grave{\sigma}^\eta)(\grave{d}_2^\eta + \grave{\beta}^\eta)(1 - R) < 0$ iff $R > 1$ and

$$R = \frac{\grave{A}^\eta \grave{d}_2^\eta (\grave{\kappa}_1^\eta \grave{d}_1^\eta + \grave{\kappa}_2^\eta \grave{\sigma}^\eta)}{\grave{\delta}^\eta \grave{d}_1^\eta (\grave{d}_2^\eta + \grave{\beta}^\eta)(\grave{d}_1^\eta + \grave{\sigma}^\eta)} \tag{6.3.2}$$

is calculated by next generation matrix approach [111]. Now, by taking three possibilities into account to examine the values of V^* (it is important to note that P_1 is always greater

than zero and $\grave{\kappa}_2$ is greater than $\grave{\kappa}_1$ as assumed in the model):

1. If $R > 1$, then $P_3 < 0$. According to Descartes' rule of signs proposed model has only one positive equilibrium.

2. If $R < 1$, then $P_3 > 0$ and

   I if $P_2 < 0$, then according to Descartes' rule of signs proposed model has two positive equilibrium.

   II if $P_2 > 0$, then the proposed model has no positive equilibrium.

3. If $R = 1$, then $P_3 = 0$ and

   I if $P_2 < 0$, then according to Descartes' rule of signs proposed model has one positive equilibrium.

   II if $P_2 > 0$, then the proposed model has no positive equilibrium.

However, It is important to note the existence of the employment-persistence equilibrium point in part (I) of the last two cases is not established as

$$R \leq 1 \implies \grave{d}_2^{\eta}\grave{A}^{\eta} \leq \frac{\grave{\delta}^{\eta}\grave{d}_1^{\eta}(\grave{d}_2^{\eta}+\grave{\beta}^{\eta})(\grave{d}_1^{\eta}+\grave{\sigma}^{\eta})}{(\grave{\kappa}_1^{\eta}\grave{d}_1^{\eta}+\grave{\kappa}_2^{\eta}\grave{\sigma}^{\eta})},$$

$$P_2 \leq 0 \implies \grave{d}_2^{\eta}\grave{A}^{\eta} \leq \frac{\grave{\delta}^{\eta}\grave{d}_1^{\eta}(\grave{\kappa}_1^{\eta}\grave{d}_1^{\eta}+\grave{\kappa}_2^{\eta}\grave{\sigma}^{\eta})+\grave{d}_1^{\eta}\grave{\delta}^{\eta}\grave{\sigma}^{\eta}(\grave{d}_2^{\eta}+\grave{\beta}^{\eta})}{\grave{\kappa}_1^{\eta}\grave{\kappa}_2^{\eta}},$$

$$\implies \grave{\delta}^{\eta}\grave{d}_2^{\eta}(\grave{d}_1^{\eta}\grave{\kappa}_1^{\eta}+\grave{\kappa}_2^{\eta}\grave{\sigma}^{\eta})^2+\grave{\kappa}_2^{\eta}\grave{\delta}^{\eta}\grave{d}_1^{\eta}\grave{\sigma}^{\eta}(\grave{d}_2^{\eta}+\grave{\beta}^{\eta})(\grave{\kappa}_2^{\eta}-\grave{\kappa}_1^{\eta}) < 0,$$

this deviates from our presumptions that $\grave{\kappa}_2$ is greater than $\grave{\kappa}_1$, and all parameters are positive. Consequently, when R is greater than 1, the proposed model (6.1.1) has only one employment-persistence equilibrium point.

6.4 Stability Analysis of Unemployment Model

This section explores the stability of the employment-free and employment-persistence equilibrium points locally and globally. The linearization approach employ to analyze the

local stability, while the Lyapunov function is utilized to assess the global stability of these equilibrium points.

Theorem 6.4.1. *The employment-free equilibrium point* $Q_0 = \left(\frac{\grave{A}^\eta}{\grave{\sigma}^\eta + \grave{d}_1^\eta}, \frac{\grave{\sigma}^\eta \grave{A}^\eta}{\grave{d}_1^\eta(\grave{\sigma}^\eta + \grave{d}_1^\eta)}, 0, 0\right)$ *of the proposed model (6.1.1) is locally and globally asymptotically stable when* $R < 1$.

Proof. The Jacobian matrix of the proposed model at Q_0 is

$$J_{Q_0} = \begin{bmatrix} -(\grave{\sigma}^\eta + \grave{d}_1^\eta) & 0 & \grave{\beta}^\eta & \frac{-\grave{\kappa}_1^\eta \grave{A}^\eta}{\grave{d}_1^\eta + \grave{\sigma}^\eta} \\ \grave{\sigma}^\eta & -\grave{d}_1^\eta & 0 & \frac{-\grave{\kappa}_2^\eta \grave{A}^\eta \grave{\sigma}^\eta}{\grave{d}_1^\eta(\grave{d}_1^\eta + \grave{\sigma}^\eta)} \\ 0 & 0 & -(\grave{d}_2^\eta + \grave{\beta}^\eta) & \frac{\grave{A}^\eta(\grave{\kappa}_1^\eta \grave{d}_1^\eta + \grave{\kappa}_2^\eta \grave{\sigma}^\eta}{\grave{d}_1^\eta(\grave{d}_1^\eta + \grave{\sigma}^\eta)} \\ 0 & 0 & \grave{d}_2^\eta & -\grave{\delta}^\eta \end{bmatrix}.$$

Clearly, two eigen-values are $-\grave{d}_1^\eta$ and $-(\grave{\sigma}^\eta + \grave{d}_1^\eta)$ which are lie in 2nd quadrant. Next, let us consider the following to examine the remaining eigenvalues:

$$J_{2\times 2} = \begin{bmatrix} -(\grave{d}_2^\eta + \grave{\beta}^\eta) & \frac{\grave{A}^\eta(\grave{\kappa}_1^\eta \grave{d}_1^\eta + \grave{\kappa}_2^\eta \grave{\sigma}^\eta}{\grave{d}_1^\eta(\grave{d}_1^\eta + \grave{\sigma}^\eta)} \\ \grave{d}_2^\eta & -\grave{\delta}^\eta \end{bmatrix}.$$

The characteristic equation for the aforementioned matrix is expressed as follows:

$$\lambda^2 + A_1\lambda + A_2 = 0 \tag{6.4.1}$$

where $A_1 = \grave{d}_2^\eta + \grave{\beta}^\eta + \grave{\delta}^\eta > 0$ and $A_2 = (\grave{d}_2^\eta + \grave{\beta}^\eta)\grave{\delta}^\eta(1 - R) > 0$ for $R < 1$.
By using Routh-Hurwitz criteria, if A_1, A_2 are greater than zero, then the eigenvalues will have negative real parts. Since Ω is a positively invariant set for the proposed model (6.1.1), Q_0 is globally asymptotically stable, as

$$(U, S_U, E, V) \to Q_0 = \left(\frac{\grave{A}^\eta}{\grave{\sigma}^\eta + \grave{d}_1^\eta}, \frac{\grave{\sigma}^\eta \grave{A}^\eta}{\grave{d}_1^\eta(\grave{\sigma}^\eta + \grave{d}_1^\eta)}, 0, 0\right) \text{ when } t \to \infty.$$

Therefore, the proposed model (6.1.1) is locally and globally asymptotically stable if $R < 1$. □

Theorem 6.4.2. *The employment-persistence equilibrium point $Q^* = (U^*, S_U^*, E^*, V^*)$ of the proposed model (6.1.1) is locally asymptotically stable when $R > 1$; otherwise, it is unstable.*

Proof. The Jacobian matrix of the proposed model at Q^* is

$$J_{Q^*} = \begin{bmatrix} -(\grave{\kappa}_1^{\eta} V^* + \grave{\sigma}^{\eta} + \grave{d}_1^{\eta}) & 0 & \grave{\beta}^{\eta} & -\grave{\kappa}_1^{\eta} U^* \\ \grave{\sigma}^{\eta} & -(\grave{\kappa}_2^{\eta} V^* + \grave{d}_1^{\eta}) & 0 & -\grave{\kappa}_2^{\eta} S_U^* \\ \grave{\kappa}_1^{\eta} V^* & \grave{\kappa}_2^{\eta} V^* & -(\grave{\beta}^{\eta} + \grave{d}_2^{\eta}) & \grave{\kappa}_1^{e} taV^* + \grave{\kappa}_2^{\eta} S_U^* \\ 0 & 0 & \grave{d}_2^{\eta} & -\grave{\delta}^{\eta} \end{bmatrix}.$$

The characteristic equation of J_{Q^*} is given by

$$\lambda^4 + B_1\lambda^3 + B_2\lambda^2 + B_3\lambda + B_4 = 0, \tag{6.4.2}$$

where

$B_1 = (\grave{\kappa}_1^{\eta} + \grave{\kappa}_2^{\eta})V^* + 2\grave{d}_1^{\eta} + \grave{\sigma}^{\eta} + \grave{d}_2^{\eta} + \grave{\beta}^{\eta} + \grave{\delta}^{\eta}$,

$B_2 = (\grave{\kappa}_1^{\eta} V^* + \grave{d}_1^{\eta} + \grave{\sigma}^{\eta})(\grave{\kappa}_2^{\eta} V^* + \grave{d}_1^{\eta}) + \grave{\kappa}_1^{\eta} V^*(\grave{d}_2^{\eta} + \grave{\delta}^{\eta}) + (\grave{d}_2^{\eta} + \grave{\beta}^{\eta} + \grave{\delta}^{\eta})(\grave{\kappa}_2^{\eta} V^* + 2\grave{d}_1^{\eta} + \grave{\sigma}^{\eta})$,

$B_3 = \grave{d}_2^{\eta}\grave{\kappa}_2^{\eta} S_U^* V^*(\grave{\kappa}_2^{\eta} - \grave{\kappa}_1^{\eta}) + (\grave{d}_2^{\eta} + \grave{\delta}^{\eta})(\grave{\kappa}_1^{\eta} V^* + \grave{d}_1^{\eta} + \grave{\sigma}^{\eta})(\grave{\kappa}_2^{\eta} V^* + \grave{d}_1^{\eta}) + \grave{\beta}^{\eta}\grave{d}_1^{\eta}(\grave{\kappa}_2^{\eta} V^* + \grave{d}_1^{\eta} + \grave{\sigma}^{\eta}) + \grave{\kappa}_1^{\eta}\grave{\delta}^{\eta}\grave{d}_2^{\eta} V^*$,

$B_4 = \grave{d}_2^{\eta}\grave{\kappa}_2^{\eta}\grave{d}_1^{\eta} S_U^* V^*(\grave{\kappa}_2^{\eta} - \grave{\kappa}_1^{\eta}) + \grave{d}_2^{\eta}\grave{\delta}^{\eta} V^*(\grave{\kappa}_1^{\eta}\grave{d}_1^{\eta} + \grave{\kappa}_1^{\eta}\grave{\kappa}_2^{\eta} V^* + \grave{\kappa}_2^{\eta}\grave{\sigma})$.

Here, $B_1 > 0, B_3 > 0,$, $B_4 > 0$, and $B_3(B_1B_2 - B_3) - B_1^2 B_4 > 0$ provided that $R > 1$ and $\grave{\kappa}_2 > \grave{\kappa}_1$. Consequently, all eigenvalues possess a negative real part, indicating that the positive equilibrium point Q^* exhibits local asymptotic stability. □

Theorem 6.4.3. *The employment-persistence equilibrium point $Q^* = (U^*, S_U^*, E^*, V^*)$ of the proposed model (6.1.1) is globally asymptotically stable for $\grave{d}_2 = \grave{d}_1$.*

Proof. Consider the positive semi-definite Lyapunov function denoted as L, which is

defined as follows:

$$L = \frac{1}{2}\left[U(t) - U^* + S_U - S_U^* + E(t) - E^*\right]^2. \tag{6.4.3}$$

Now, the η^{th} derivative of the Lyapunov function L can be expressed as [137]:

$$\frac{d^\eta L}{dt^\eta} = \left[U(t) - U^* + S_U - S_U^* + E(t) - E^*\right]\left[\grave{A}^\eta - \grave{d}_1^\eta(U + S_U) - \grave{d}_2^\eta E\right]. \tag{6.4.4}$$

$$\frac{d^\eta L}{dt^\eta} = \left[U(t) - U^* + S_U - S_U^* + E(t) - E^*\right]\left[-\grave{d}_1^\eta(U(t) - U^* + S_U - S_U^*) - \grave{d}_2^\eta(E(t) - E^*)\right].$$

Then, clearly $\frac{d^\eta L}{dt^\eta} = -\grave{d}_1^\eta\left[U(t) - U^* + S_U - S_U^* + E(t) - E^*\right]^2 \leq 0$ if $\grave{d}_2 = \grave{d}_1$. Hence, the employment-persistence equilibrium point $Q^* = (U^*, S_U^*, E^*, V^*)$ of the proposed model (6.1.1) is globally asymptotically stable for $\grave{d}_2 = \grave{d}_1$. □

6.5 Transcritical Bifurcation Analysis

This section investigates how the unemployment model behaves when the reproduction number R is 1. The proposed model (6.1.1) exhibits two equilibrium point: employment-free Q_0 and employment-persistence Q^*. When R is less than 1, the employment-free equilibrium is asymptotically stable, but it is no longer stable when R is more than 1. On the other hand, the employment-persistence equilibrium point occurs and is asymptotically stable for R values greater than 1. It is worth noting that the theoretical existence of Q^* persists even for $R < 1$, although it may not have positive coordinates.

A qualitative change in the system's behavior happens when parameter values are gradually altered. The following equivalences demonstrate this change:

$$\grave{A}^\eta \grave{d}_2^\eta(\grave{\kappa}_1^\eta \grave{d}_1^\eta + \grave{\kappa}_2^\eta \grave{\sigma}^\eta) = \grave{\delta}^\eta \grave{d}_1^\eta(\grave{d}_2^\eta + \grave{\beta}^\eta)(\grave{d}_1^\eta + \grave{\sigma}^\eta). \tag{6.5.1}$$

At this point, the two fixed points Q_0 and Q^* appear to collide and undergo a change in stability. This phenomenon resembles a transcritical bifurcation, as depicted in Figure 6.2. The impact of transcritical bifurcation is characterized by its ability to reveal how

sensitive the labor market is to parameter changes. It can lead to significant shifts in equilibrium points, affect the stability of solutions, and has policy implications. Recognizing transcritical bifurcation can serve as an early warning regarding no. of job vacancy and skilled unemployed individuals for policymakers, helping them make informed decisions and design effective labor market policies.

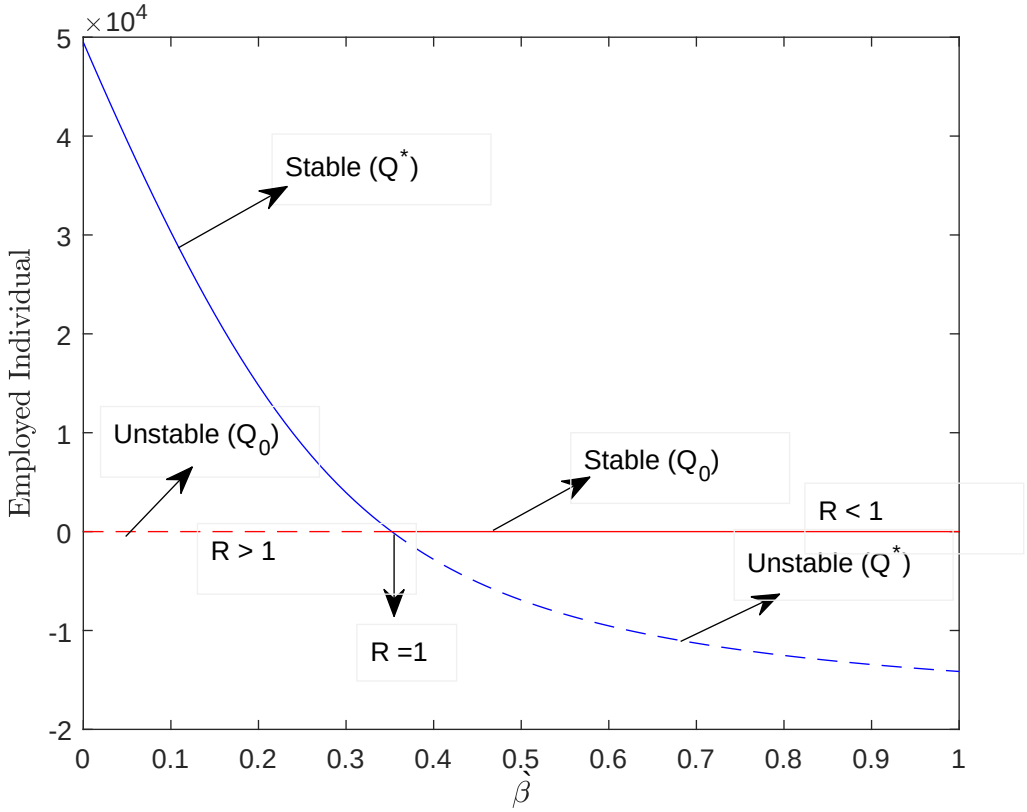

Figure 6.2: Bifurcation diagram demonstrates stability of equilibrium point for $R < 1$ and $R > 1$.

6.6 Numerical Simulation

Numerical simulation is utilized to demonstrate the dynamic nature of the unemployment model, validating the analytical findings across different orders of derivatives. The model is solved by employing the Adams-Bashforth-Moulton predictor-corrector technique [109]. Table 6.1 presents the variables and parameters employed for the numerical solution of the proposed model [80].

Table 6.1: Description of variables and parameters of unemployment.

Parameter	$\grave{\kappa}_1$	$\grave{\kappa}_2$	$\grave{A}$	$\grave{d}_1$	$\grave{\sigma}$	$\grave{d}_2$	$\grave{\beta}$	$\grave{\delta}$
Value	8.64×10^{-6}	1.728×10^{-5}	3000	0.048	0.1	0.05	0.01	0.1125

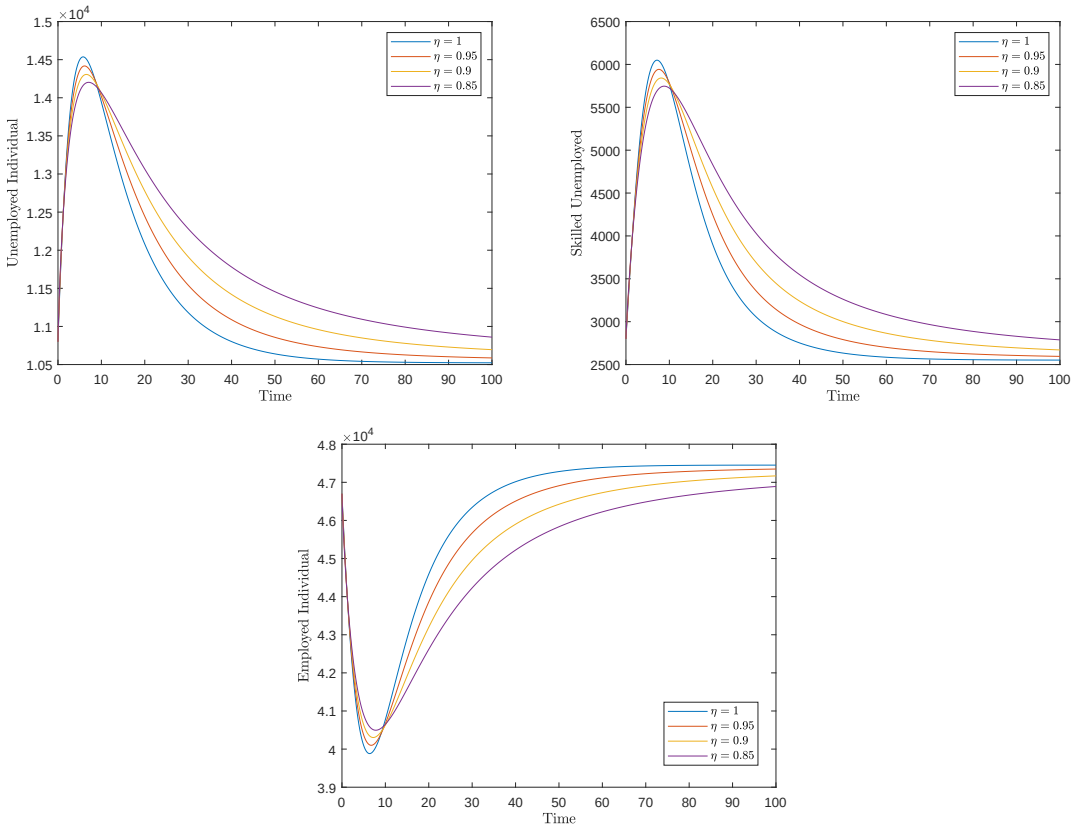

Figure 6.3: Variations of the Unemployed (U), Skilled Unemployed (S_U), and Employed individual (E) for various order of derivative (η), which shows the path of all the classes irrespective of the order of derivative validates the stability of the model.

Figure 6.3 illustrates the asymptotic stability of the steady states for values of η equal to 0.8, 0.9, 0.95, and 1. The trajectory of all categories confirms the stability of the proposed model across different derivative orders. Figure 6.3 is plotted using the values provided in Table 6.1, with an initial R value greater than 1. The trajectories converge towards an employment-persistence equilibrium point. Over time, the number of employed individuals initially decreases and then starts to increase, while the unemployed and skilled unemployed populations exhibit different trends, initially increasing and then decreasing. As the order of derivative decreases, the employed population decreases and converges to

a specific point, while the unemployed and skilled unemployed populations increase and also converge to a specific point.

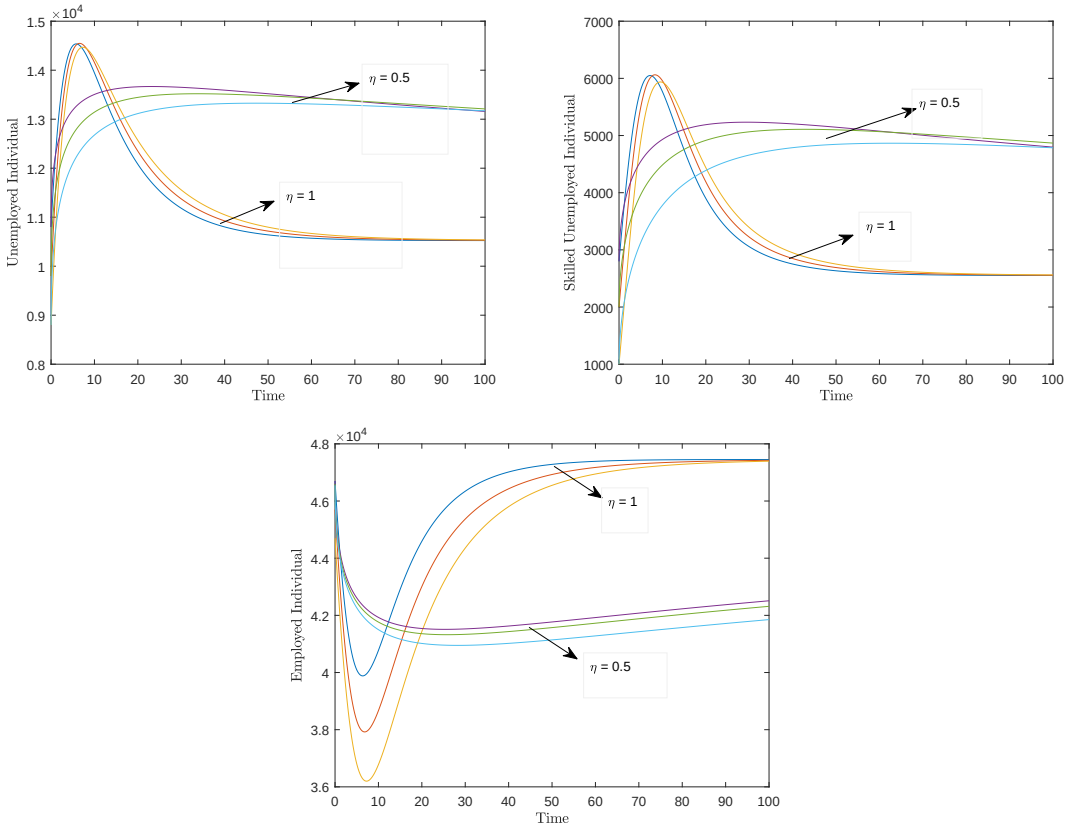

Figure 6.4: Variations of the Unemployed (U), Skilled Unemployed (S_U), and Employed individual (E) for the different initial conditions and various order of derivative (η), which shows the path of all classes irrespective of the order of derivative validates the stability of the model.

From Figure 6.4, it is clear that unemployment rate increasing trend for order of derivative 0.5 and decreasing trend for integer-order derivative. Hence, the unemployed individuals increases as order of derivative decreases. It is also observed that, in reality, the unemployed population increases with time (Figure 1.3), indicating that the fractional order model can better capture the reality. The convergence of all population trajectories towards the employment persistence equilibrium point across various initial conditions and derivative orders indicates the stability of the equilibrium point when $R > 1$ (Figure 6.4).

6.7 Sensitivity Analysis

To effectively address the issue of unemployment, it is essential to comprehensively understand the relative significance of the numerous factors contributing to unemployment. The reproduction number denoted as R, is directly associated with various variables and parameters. Sensitivity analyses are often necessary to assess the stability of the parameter values employed in model predictions. To evaluate the suitability of each parameter elasticity is utilized, which represents the partial derivative of R. The results of a sensitivity analysis conducted on the threshold parameter R are summarized in Table 6.2.

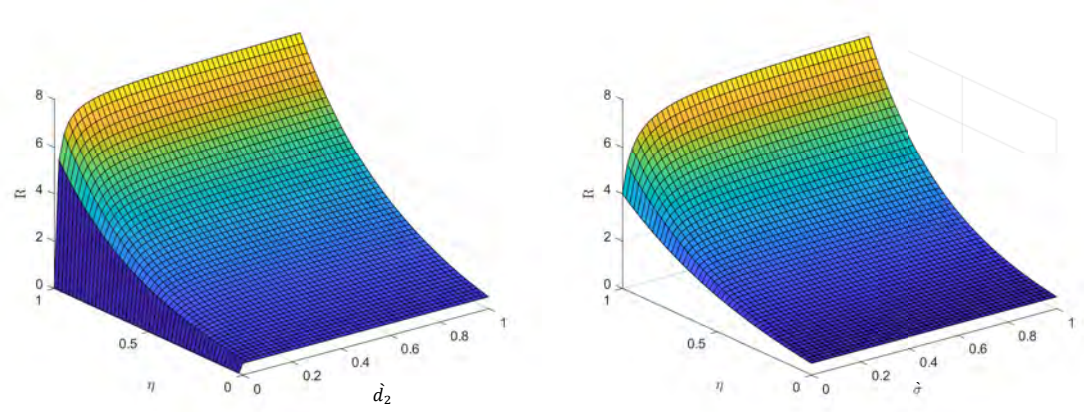

Figure 6.5: Relation of R with $\grave{d}_2$ and $\grave{\sigma}$ for different order of derivative.

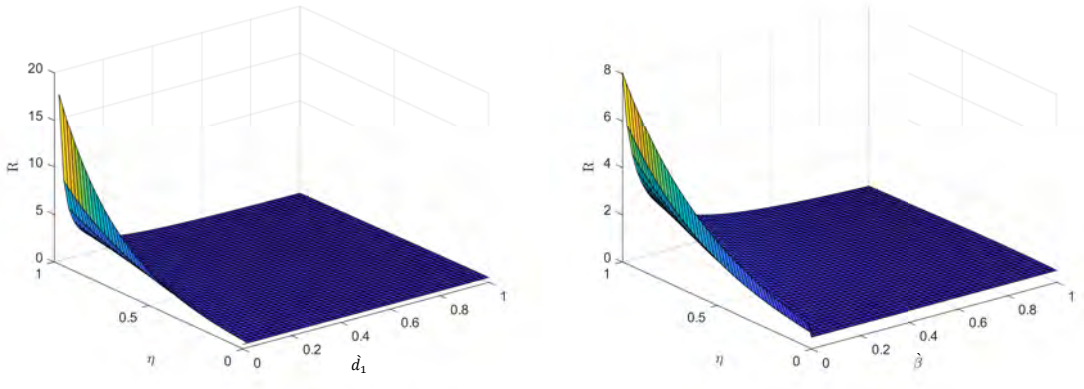

Figure 6.6: Relation of R with $\grave{d}_1$ and $\grave{\beta}$ for different order of derivative.

Table 6.2: Sensitivity analysis results for the threshold parameter R.

Parameter	$\grave{\kappa}_1$	$\grave{\kappa}_2$	A	$\grave{d}_1$	$\grave{\sigma}$	$\grave{d}_2$	$\grave{\beta}$	η	$\grave{\delta}$
Sensitivity index sign	154	315	0.22	-15.7	87.655	22.34	–11.7	13.09	-59.57

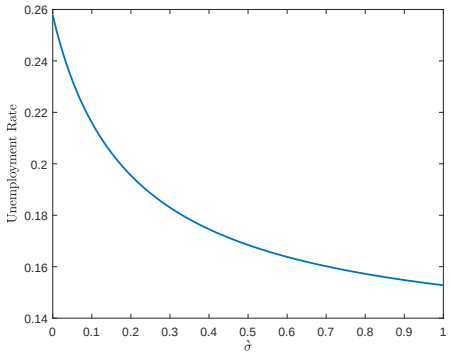

(a) Unemployment rate decreases with $\grave{\sigma}$.

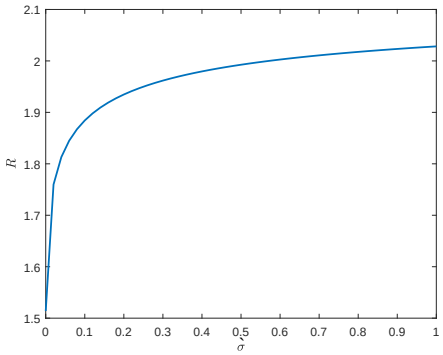

(b) Reproduction number increases with $\grave{\sigma}$.

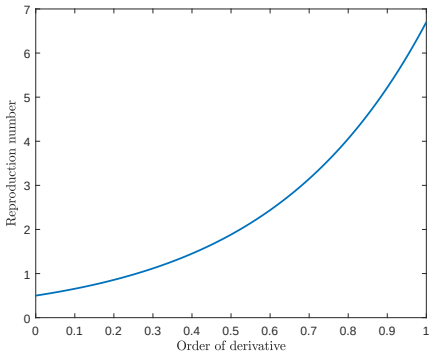

(c) Reproduction number increases with order of derivative.

Figure 6.7: Relation of unemployment rate with R, $\grave{\sigma}$ and η i.e. unemployment rate decreases with R and η.

The relationship between R and its parameters can be summarized as follows: R is directly proportional to $\grave{\kappa}_1$, $\grave{\kappa}_2$, and $\grave{\Lambda}$, and inversely proportional to $\grave{\beta}$. Hence, an increase in $\grave{\kappa}_1$, $\grave{\kappa}_2$, or $\grave{\Lambda}$ leads to an increase in R, while an increase in $\grave{\beta}$ results in a decrease in R. Additionally, when considering the effects of other parameters, it is observed that R increases with $\grave{d}_2$ and $\grave{\sigma}$ for different orders of derivatives (Figure 6.5). On the other hand, R decreases with $\grave{d}_1$ and $\grave{\beta}$ (Figure 6.6). These relationships demonstrate that changes in $\grave{d}_2$ and $\grave{\sigma}$ positively impact R, while variations in $\grave{d}_1$ and $\grave{\beta}$ have a negative effect on

R. From Figure 6.7, it is also observed that unemployment decreases with increase in R and η and the most sensitive parameters are $\grave{\kappa}_1$, $\grave{\sigma}$ and $\grave{\kappa}_2$ i.e. enhancing individual skill development and addressing job vacancies have more positive impact on employment than other parameters.

6.7.1 Impact of Order of Derivative

The findings depicted in Figure 6.7 indicate a clear relationship between the unemployment rate $\left(\frac{U+S_U}{U+S_U+E}\right)$ and the parameter $\grave{\sigma}$: as $\grave{\sigma}$ increases, the unemployment rate decreases. Additionally, a positive correlation exists between the R and $\grave{\sigma}$, meaning that as $\grave{\sigma}$ increases, the R also increases. Consequently, it is observed that the unemployment rate decreases as the R increases.

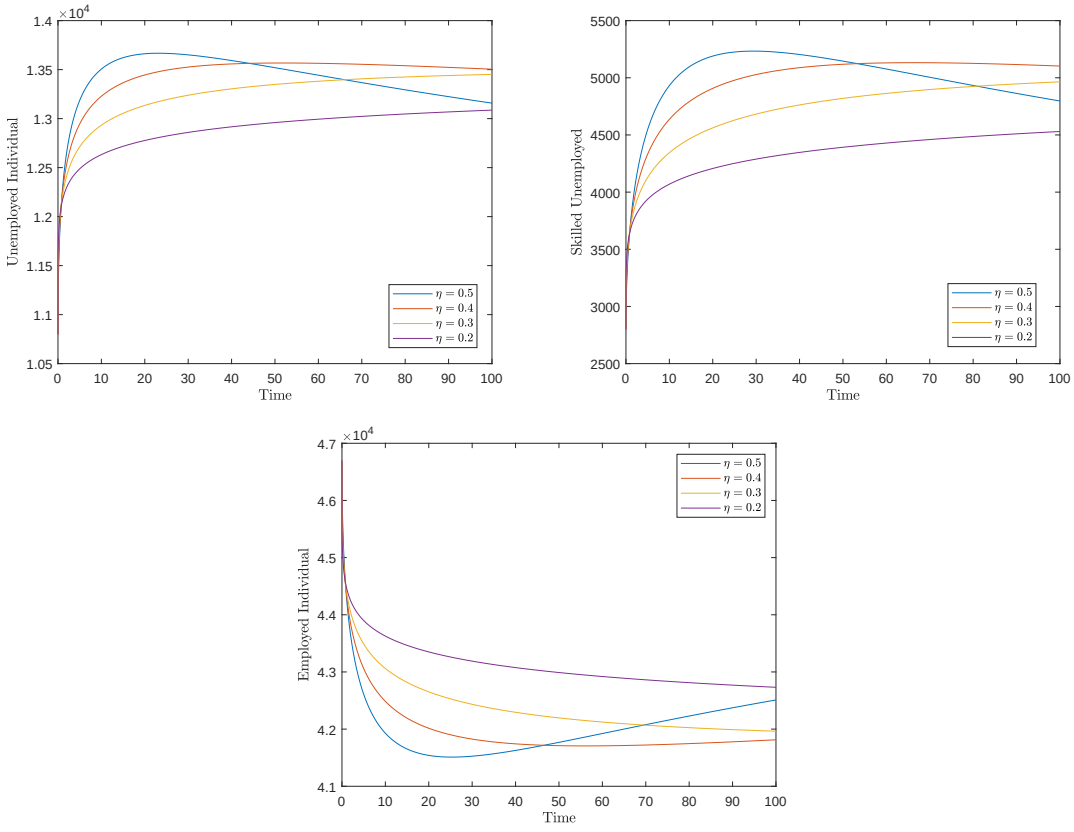

Figure 6.8: Variations of the Unemployed (U), Skilled Unemployed (S_U), and Employed individual (E) for various order of derivative (η), which shows the path of all the classes irrespective of the order of derivative validates the stability of the model.

Moreover, considering the impact of the derivative order, it is evident that as the order of derivative increases, the R also increases. Consequently, the unemployment rate decreases with increasing order of derivative. An increase in the R can be attributed to higher orders of derivative. As the parameter η increases, so does R, resulting in a subsequent decrease in the unemployment rate. By observing Figure 6.3 and Figure 6.8, it becomes evident that the order of derivative significantly influences the unemployment rate. Specifically, the unemployment rate decreases as the order of derivative increases. However, in reality, the unemployment rate is observed to be increasing. Moreover, according to the model, the unemployment rate increases for the order of derivatives less than 0.5. Here, the objective is to minimize the unemployment rate by considering real-life situations. In this context, the optimum value of the order of derivative is $\sim$0.5.

6.7.2 Effects of Skill Enhancement

The rise in the reproduction number R is partly influenced by a higher rate $\grave{\sigma}$ of unemployed individuals with improved skills. As $\grave{\sigma}$ rises, so does R, resulting in a subsequent decrease in the unemployment rate. However, providing skill development opportunities for all unemployed individuals can pose financial challenges, particularly for governments in impoverished countries. These governments often have competing economic priorities, such as addressing education and healthcare needs. Therefore, the objective of this section is to determine the threshold parameter for $\grave{\sigma}$, representing the minimum value required for skill development programs to have a substantial impact on decreasing the unemployment rate. This analysis will help to assess the government's capacity for sustaining effective support in training programs. Let's denote the rate of employment of individuals with developed skills as $\grave{\kappa}_2 = b\grave{\kappa}_1$, where $b > 1$ as $\grave{\kappa}_2 > \grave{\kappa}_1$.

$$R(\grave{\sigma}) = \frac{\grave{A}^\eta \grave{d}_2^\eta(\grave{\kappa}_1^\eta \grave{d}_1^\eta + \grave{\kappa}_2^\eta \grave{\sigma}^\eta)}{\grave{\delta}^\eta \grave{d}_1^\eta(\grave{d}_2^\eta + \grave{\beta}^\eta)(\grave{d}_1^\eta + \grave{\sigma}^\eta)} = \frac{(\grave{d}_1^\eta + b\grave{\sigma}^\eta)R_0}{\grave{d}_1^\eta + \grave{\sigma}^\eta}, \text{ where } R_0 = \frac{\grave{A}^\eta \grave{d}_2^\eta \grave{\kappa}_1^\eta}{\grave{\delta}^\eta \grave{d}_1^\eta(\grave{d}_2^\eta + \grave{\beta}^\eta)}. \tag{6.7.1}$$

It is evident that if $\grave{\sigma} > 0$, then $R_0 < R(\grave{\sigma}) < R_\infty$, where $\lim_{\grave{\sigma}\to\infty} R(\grave{\sigma}) = bR_0 = R_\infty$. Additionally, when $\grave{\sigma} = 0$, we have $R(\grave{\sigma}) = R_0$. By setting $R(\grave{\sigma}) = 1$, the threshold rate

$\grave{\sigma}_c$ is calculated by using the following formula: $\grave{\sigma}_c = \dfrac{\grave{d}_1^{\eta}(1 - R_0)}{R_\infty - 1}$.

It's important to note that $\grave{\sigma}_c$ will be greater than 0 if $R_0 < 1 < R_\infty$. In this scenario, two cases can arise:

- When $\grave{\sigma} < \grave{\sigma}_c$, it is observed that $R_0 < R(\grave{\sigma}) < 1 < R_\infty$. In this scenario, the employment persistence equilibrium does not exist, and the employment-free steady state is asymptotically stable.

- When $\grave{\sigma} > \grave{\sigma}_c$, it is observed that $R_0 < 1 < R(\grave{\sigma}) < R_\infty$. In this scenario, the equilibrium for the employment-free state is unstable. As a result, we may draw the conclusion that in this situation, the unemployment rate can be significantly decreased.

These findings indicate that when $\grave{\sigma}$ exceeds the threshold $\grave{\sigma}_c$, the impact on reducing unemployment becomes more pronounced (Figure 6.6).

6.8 Summary

This chapter proposes a fractional-order mathematical model that focuses on the issue of youth unemployment in resource-limited countries. The primary objective of this research is to investigate the influence of fractional order derivatives on unemployment modeling. Additionally, this research examine the impact of a skill development program for different order of derivative on mitigating the issue of unemployment. The existence and uniqueness of the model are demonstrated. The threshold parameter R is calculated to analyze the effect of the skill development program on unemployment. The equilibrium points of the model, namely the employment-free and employment-persistence equilibrium points, are determined, and their stability is analyzed. The research investigates how changes in the model's parameters impact individual behavior. The key findings of this chapter are outlined below:

- The reproduction number (R) displays an ascending pattern in tandem with the order of the derivative (η). As a result, a reduction in the derivative order corresponds to

an escalation in unemployment. Nevertheless, empirical evidence, as illustrated in Figure 1.3, contradicts this expectation by demonstrating an increasing unemployment rate. On the other hand, the proposed model posits that the unemployment rate rises when the order of derivatives is less than or equal to 0.5. This suggests that a fractional-order model is more adept at reflecting reality and surpasses the capabilities of an integer-order model.

- The findings suggest that when the skill development rate ($\grave{\sigma}$) surpasses a critical threshold value, denoted as $\grave{\sigma}_c$, representing the minimum level required for skill development programs to substantially influence the reduction of unemployment, the impact of decreasing unemployment becomes more pronounced. As $\grave{\sigma}$ continues to increase, there is a noticeable decline in the unemployed population. This analysis proves valuable in assessing the government's capacity to sustain effective support for training programs.

- The system's memory is integrated through a fractional order, and in the context of real-world scenarios, an optimal value for η that significantly reduces unemployment is $\sim$0.5.

- The parameters most sensitive to change are $\grave{\kappa}_1$, $\grave{\sigma}$, and $\grave{\kappa}_2$. This implies that working for skill development programs and addressing job vacancies have a more substantial positive impact on employment compared to other parameters.

These findings contribute to a better understanding of unemployment dynamics in resource-limited countries and provide insights into effective strategies for reducing unemployment rates through skill development programs like develop programs that focus on identifying skills anticipated to be in demand in the future job market.

This chapter has been communicated as follows:

- *K. Bansal, and T. Mathur, "Impact of skills development on youth unemployment: A fractional order mathematical model." (Communicated)*

Chapter 7

Analysis of the Drug Resistance Level for Malaria Disease

"Malaria is not a disease of the past. It still kills a child every 30 seconds."

- Ray Chambers, United Nations Special Envoy for Malaria

Malaria is a febrile disease caused by plasmodium parasites, which is transmitted to humans from infected female Anopheles mosquito bites. The five parasite species that cause human malaria are P. falciparum, P. malariae, P. ovale, P. vivax, and P. knowlesi, particularly P. falciparum and P. vivax being the most deadly [164,165]. Malaria symptoms, such as fever, headache, and chills, develop 10–15 days after the infective mosquito bite and may be mild and difficult to identify from other infections [166]. If this disease from P. falciparum is left untreated, it can cause significant illness and death in as little as 24 hours [167,168]. By 2020, malaria has reached nearly half of the world's population [169]. Infants, children, pregnant women, HIV/AIDS patients, and others with weakened immune systems who travel to malaria-endemic areas are at a higher risk of catching malaria [170]. According to the recent world malaria report, 241 million malaria cases were registered in 2020, an additional 14 million over the previous year. Malaria-related casualties were reported at 627,000 in 2020, with an increase of 69,000 from 2019 [169,170]. Malaria has become more prevalent in recent years due to climate change or global warming, which is expected to have unanticipated repercussions for the disease's prevalence. The life cycles

of both the vector and the parasite are affected by temperature fluctuations [82]. Due to changing environmental and socioeconomic circumstances, the conditions are still expanding and threaten to become a serious cause of mortality and disability. Consequently, there is a significant need to revise the prevailing malaria transmission control strategies and model.

The rise and spread of drug resistant[1] P. falciparum and P. vivax hinder worldwide attempts to eradicate malaria. The most often recommended treatment for the P. falciparum and P. vivax parasite is chloroquine [172, 173]. Chloroquine-resistant P. falciparum appeared independently in three to four areas in Southeast Asia, Oceania, and South America in the late 1950s and early 1960s. Resistance to chloroquine has subsequently spread to almost every region where falciparum malaria is transmitted [174]. In 1989, Australians living in or visiting Papua New Guinea were first infected with chloroquine-resistant P. vivax malaria. In Southeast Asia, Ethiopia, and Madagascar, chloroquine resistance in P. vivax has been identified. According to one of the WHO publications, P. vivax chloroquine resistance has been documented in all WHO regions. Chloroquine resistance was found in 28 countries, including India [28]. A widespread resistance scenario might result in an annual excess of 22 million treatment failures, 116,000 fatalities, and expenses, including an estimated USD 130 million to adjust treatment policy [175]. As a result of the emergence and spread of drug-resistant malaria, many scientists have concentrated their efforts on discovering new strategies to combat the disease [93]. Discoveries in drugs and vaccines are constantly being incorporated into research. Furthermore, educating the general population on the need for correct medicine use can help to reduce the frequency with which resistance develops [176].

Combination therapy is successful as the parasite is unlikely to develop resistance to two or more medications simultaneously. Combination treatment, on the other hand, is

[1]Drug resistance is the ability of an organism to change so that it can stay alive after being exposed to a drug that would usually kill it. A random genetic alteration causes drug resistance, allowing the organism to endure treatment [92]. An organism may undergo a spontaneous mutation during replication. If the mutation renders the treatment ineffective, the mutated microorganisms continue to reproduce and live while their non-mutated counterparts die during treatment [171].

more costly, which can nullify much of its effectiveness [177]. The frontline treatments for P. falciparum malaria are artemisinin combination therapies (ACTs) [177]. Even though these therapies are effective in many parts of the world, there is a great fear that malaria parasites are acquiring broad resistance to this critical medication once again.

While malaria is not directly contagious from person to person like the common cold or the flu, there are situations where the parasite can be transmitted through blood transfusions or the sharing of needles among drug users. However, the primary mode of transmission is through the bite of infected mosquitoes. Hence, several mathematical models have been used for more than a century to analyze the human malaria transmission patterns [83–88]. Sir Ronald Ross discovered the malaria parasite's life cycle in mosquitoes while working for the Indian Medical Service in 1890. In the early 1900s, he published some of the earliest research papers using mathematical functions to study the spread of malaria [89–91]. Memory and genetic traits are present in the majority of biological systems. Memory in biological systems is not only shown by the ability to incorporate new information from the past but also by the immune response of immune cells [178]. For disease transmission, the drug resistance level future state is highly related to the previous (present) state due to heredity property, and the classical (Ordinary differential equation) models don't have memory properties as it consider only two points t and $t - \Delta t$. The malaria transmission in a region can be influenced by the historical background, as both humans and mosquitoes carry inherited traits that are shaped by biological factors. This influence encompasses aspects such as acquired immunity, relapses, mosquito populations, resistance, environmental changes, historical control efforts, imported cases, and sociopolitical factors. Understanding this historical context is vital for designing effective malaria control and elimination strategies. It helps policymakers consider the legacy of past efforts and challenges in their current actions against the disease. Preventing mosquito bites and controlling mosquito populations are essential strategies for malaria prevention. As a result, various fractional-order mathematical models are analyzed to control malaria transmission [15, 179–183]. However, the above studies do not consider the drug resistance effect, which is a crucial factor in controlling malaria transmission.

In light of this, a novel compartmental fractional-order model is proposed and analyzed that integrates the different drug resistance levels and therapy as a preventative measure of malaria transmission with memory between human-to-mosquito and mosquito-to-human. These Drug resistance levels are given by WHO and can be defined as:

- **R-I Resistance**: Recrudescence after parasite clearance (at least two consecutive days with no detectable asexual parasites within seven days of therapy initiation).
- **R-II Resistance**: Asexual parasitemia is cleared more than 75% within 48 hours.
- **R-III Resistance**: Asexual parasitemia is cleared less than 75% within 48 hours.

7.1 Mathematical Model Development

Although malaria incidence changes based on variables like rainfall and temperature, for modeling reasons, we consider that infections are transmitted consistently throughout the year. Drug resistance, which may be broken down into three distinct types, is the central focus of the present study. Mutations in the parasite's DNA or natural selection in response to repeated, sublethal doses of the medicine may contribute to developing drug resistance. One possible cause of drug resistance is ineffective therapy.

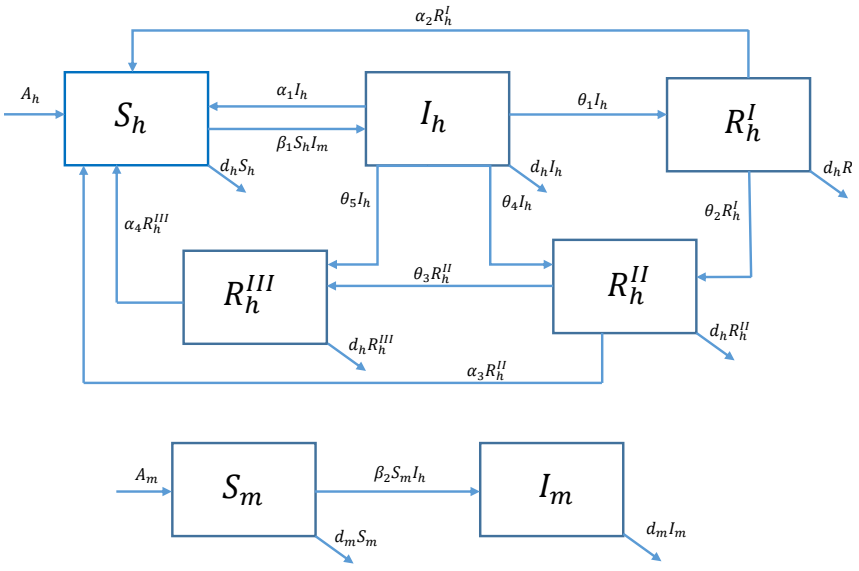

Figure 7.1: Schematic diagram of the proposed model.

Hence, a fractional-order mathematical model for analyzing drug resistance levels in malaria transmission by categorizing the human population into five sub classes and the mosquito population into two sub classes is presented. Each of the seven classes in this paradigm interacts with the other. Humans and mosquitoes are the two most prominent types of populations. The mosquito population is divided into two categories, Susceptible (S_m) and Infected (I_h). The human population is further divided into five groups: Susceptible (S_h), Infected (I_h), and Resistance classes R-I, R-II, R-III are $R_h^I, R_h^{II}, R_h^{III}$ respectively.

Those who have never been infected with malaria or completely recovered without remaining immunity from a prior infection are susceptible. All people who have ever had malaria symptoms, which are brought on by the reproduction of parasites within red blood cells, belong to the infected group. Individuals who have attempted therapy without seeing positive outcomes are said to be resistant. Level of drug resistance is measured by a reduction in asexual parasitemia. Figure 7.1 is a flowchart that is used to analyze how people move with the social hierarchy of the human population, and the following set of fractional differential equations (7.1.1) characterizes the corresponding model:

$$\begin{aligned}
\frac{d^\eta S_h}{dt^\eta} &= A_h^\eta - \beta_1^\eta S_h I_m + \alpha_1^\eta I_h + \alpha_2^\eta R_h^I + \alpha_3^\eta R_h^{II} + \alpha_4^\eta R_h^{III} - d_h^\eta S_h \\
\frac{d^\eta I_h}{dt^\eta} &= \beta_1^\eta S_h I_m - \alpha_1^\eta I_h - \theta_1^\eta I_h - \theta_4^\eta I_h - \theta_5^\eta I_h - d_h^\eta I_h \\
\frac{d^\eta R_h^I}{dt^\eta} &= \theta_1^\eta I_h - \theta_2^\eta R_h^I - \alpha_2^\eta R_h^I - d_h^\eta R_h^I \\
\frac{d^\eta R_h^{II}}{dt^\eta} &= \theta_2^\eta R_h^I + \theta_4^\eta I_h - \theta_3^\eta R_h^{II} - \alpha_3^\eta R_h^{II} - d_h^\eta R_h^{II} \\
\frac{d^\eta R_h^{III}}{dt^\eta} &= \theta_3^\eta R_h^{II} + \theta_5^\eta I_h - \alpha_4^\eta R_h^{III} - d_h^\eta R_h^{III} \\
\frac{d^\eta S_m}{dt^\eta} &= A_m^\eta - \beta_2^\eta S_m I_h - d_m^\eta S_m \\
\frac{d^\eta I_m}{dt^\eta} &= \beta_2^\eta S_m I_h - d_m^\eta I_m.
\end{aligned} \tag{7.1.1}$$

Susceptible human and mosquito populations are constantly recruiting at a rate of A_h and A_m, respectively. Infected mosquito bites malaria-prone susceptible people and

susceptible people become infected with the rate β_1. Susceptible mosquitoes become infected after biting an infected person with the rate β_2. Now, the infected population transfers to the different drug resistance class, i.e., $R_h^I, R_h^{II}, R_h^{III}$ according to the reduction in asexual parasitemia with rates $\theta_1, \theta_4, \theta_5$ respectively. People with drug resistance of level R-I can transfer to class R_h^{II} with the rate θ_2 and people with drug resistance of level R-II at any moment can transfer to class R_h^{III} with the rate θ_3. All classes of the infected population $(I_h, R_h^I, R_h^{II}, R_h^{III})$ get treatment and become susceptible with rate $\alpha_1, \alpha_2, \alpha_3, \alpha_4$ respectively. d_h and d_m are the natural mortality rate of the human and mosquitoes population. Each parameter is raised to power η to balance the model dimensionally, and η is the order of derivative.

7.2 Dynamical Evaluation of Proposed Model

This section analyzes the basic properties of the proposed model's solution, like existence and uniqueness, non-negative, and boundedness.

7.2.1 Defining the Invariant Region

The behavior of the proposed fractional-order model (7.1.1) is explored in a feasible region $\Omega \in \mathbb{R}_+^7$, where

$$\Omega = \left\{ (S_h, I_h, R_h^I, R_h^{II}, R_h^{III}, S_m, I_m) \in \mathbb{R}_+^7 : S_h + I_h + R_h^I + R_h^{II} + R_h^{III} + S_m + I_m \leq \frac{A_h^\eta}{d_h^\eta} + \frac{A_m^\eta}{d_m^\eta} \right\}.$$

Theorem 7.2.1. *The region $\Omega \in \mathbb{R}_+^7$ is the positively invariant region for the proposed fractional-order model.*

Proof. Let $N_h(t) = S_h(t) + I_h(t) + R_h^I(t) + R_h^{II}(t) + R_h^{III}(t)$ represent the entire human population at any given instant. Then,

$$\begin{aligned} \frac{d^\eta N_h(t)}{dt^\eta} &= \frac{d^\eta S_h}{dt^\eta} + \frac{d^\eta I_h}{dt^\eta} + \frac{d^\eta R_h^I}{dt^\eta} + \frac{d^\eta R_h^{II}}{dt^\eta} + \frac{d^\eta R_h^{III}}{dt^\eta} \\ &= A_h^\eta - d_h^\eta N(t). \end{aligned} \tag{7.2.1}$$

By taking Laplace's transformation (from eq. (1.1.13)),

$$N_h(s) = \frac{\frac{A_h^\eta}{s} + s^{\eta-1}N(0)}{s^\eta + d_h^\eta} \tag{7.2.2}$$

Now, by taking the inverse Laplace transformation (from eq. (1.1.8)),

$$N_h(t) = \frac{A_h^\eta}{d_h^\eta}[1 - \mathbb{E}_\eta(-d_h^\eta t^\eta)] + N(0)\mathbb{E}_\eta(-d_h^\eta t^\eta). \tag{7.2.3}$$

Similarly, let $N_m(t) = S_m(t) + I_m(t)$ represent the entire mosquito population at any given instant. Then,

$$N_m(t) = \frac{A_m^\eta}{d_m^\eta}[1 - \mathbb{E}_\eta(-d_m^\eta t^\eta)] + N(0)\mathbb{E}_\eta(-d_m^\eta t^\eta) \tag{7.2.4}$$

where $\mathbb{E}_\eta$ is Mittage-Leffler function defined in eq. (1.1.6) and $0 \leq \mathbb{E}_\eta(-d_h^\eta t^\eta) \leq 1$.

$$\implies N_h(t) + N_m(t) \leq \frac{A_h^\eta}{d_h^\eta} + \frac{A_m^\eta}{d_m^\eta}. \tag{7.2.5}$$

To demonstrate that the solution of the suggested model (7.1.1) is non-negative, we have:

$$\begin{aligned}
\left.\frac{d^\eta S_h(t)}{dt^\eta}\right|_{S_h(t_0)=0} &= A_h^\eta + \alpha_1^\eta I_h + \alpha_2^\eta R_h^I + \alpha_3^\eta R_h^{II} + \alpha_4^\eta R_h^{III} \geq 0,\\
\left.\frac{d^\eta I_h(t)}{dt^\eta}\right|_{I_h(t_0)=0} &= \beta_1^\eta S_h I_m \geq 0,\\
\left.\frac{d^\eta R_h^I(t)}{dt^\eta}\right|_{R_h^I(t_0)=0} &= \theta_1^\eta I_h \geq 0,\\
\left.\frac{d^\eta R_h^{II}(t)}{dt^\eta}\right|_{R_h^{II}(t_0)=0} &= \theta_2^\eta R_h^I + \theta_4^\eta I_h \geq 0,\\
\left.\frac{d^\eta R_h^{III}(t)}{dt^\eta}\right|_{R_h^{III}(t_0)=0} &= \theta_3^\eta R_h^{II} + \theta_5^\eta I_h \geq 0,
\end{aligned}$$

$$\left.\frac{d^\eta S_m(t)}{dt^\eta}\right|_{S_h(t_0)=0} = A_m^\eta \geq 0,$$
$$\left.\frac{d^\eta I_m(t)}{dt^\eta}\right|_{I_h(t_0)=0} = \beta_2^\eta S_m I_h \geq 0.$$

Now from Generalized mean value theorem (Theorem 1.4.2) the solution of the proposed model (7.1.1) is non-negative. As Ω contains the positive solution to the proposed model assuming non-negative initial conditions, Ω is the positively invariant area that attracts all solutions. □

7.2.2 Existence and Uniqueness

Theorem 7.2.2. *There exists a unique solution of the proposed model* (7.1.1) *along with the given initial conditions on* $t \geq 0$.

Proof. RHS of the proposed model eq. (7.1.1) is continuous, bounded from eq. (7.2.5) and satisfies Lipschitz condition. From existence and uniqueness theorem (Theorem 1.4.1) the solution of the model (7.1.1) along with given initial conditions for $t > 0$ not only exists but is also unique. □

7.3 Feasible Equilibrium Points and Stability Analysis

This section calculates the equilibrium points and threshold parameter (Reproduction number) to control malaria disease transmission.

7.3.1 Equilibrium Points

The proposed model's equilibrium point is calculated by taking the right-hand side of the proposed model equal to zero.

- Diseases-free equilibrium: This equilibrium exists when no infected human and mosquito population exists in society.

  So, $I_h = 0, I_m = 0$. Therefore, diseases free equilibrium point is given by

$$E^0 = \left(\frac{A_h^\eta}{d_h^\eta}, 0, 0, 0, 0, \frac{A_m^\eta}{d_m^\eta}, 0\right).$$

- Endemic equilibrium: This equilibrium exists when the infected human and mosquito populations are not zero and is given by

$$E^e = (S_h^e, I_h^e, R_h^{Ie}, R_h^{IIe}, R_h^{IIIe}, S_m^e, I_m^e)$$

where,

$$R_h^{Ie} = \frac{\theta_1^\eta I_h^e}{\alpha_2^\eta + \theta_2^\eta + d_h^\eta},$$

$$R_h^{IIe} = \frac{\theta_2^\eta R_h^{Ie} + \theta_4^\eta I_h^e}{\theta_3^\eta + \alpha_3^\eta + d_h^\eta} = \frac{[\theta_2^\eta\theta_1^\eta + (\alpha_2^\eta + \theta_2^\eta + d_h^\eta)\theta_4^\eta]I_h^e}{(\alpha_2^\eta + \theta_2^\eta + d_h^\eta)(\theta_3^\eta + \alpha_3^\eta + d_h^\eta)},$$

$$R_h^{IIIe} = \frac{\theta_3^\eta R_h^{IIe} + \theta_5^\eta I_h^e}{\alpha_4^\eta + d_h^\eta} = \frac{[\theta_3^\eta\theta_2^\eta\theta_1^\eta + (\alpha_2^\eta + \theta_2^\eta + d_h^\eta)[\theta_3^\eta\theta_4^\eta + (\theta_3^\eta + \alpha_3^\eta + d_h^\eta)\theta_5^\eta]]\, I_h^e}{(\alpha_2^\eta + \theta_2^\eta + d_h^\eta)(\theta_3^\eta + \alpha_3^\eta + d_h^\eta)(\alpha_4^\eta + d_h^\eta)},$$

$$S_m{}^e = \frac{A_m^\eta}{\beta_2^\eta I_h^e + d_m^\eta},$$

$$I_m^e = \frac{\beta_2^\eta S_m^e I_h^e}{d_m^\eta} = \frac{\beta_2^\eta I_h^e}{d_m^\eta}\left(\frac{A_m^\eta}{\beta_2^\eta I_h^e + d_m^\eta}\right),$$

$$S_h^e = \frac{A_h^\eta + \alpha_1^\eta I_h^e + \alpha_2^\eta R_h^{Ie} + \alpha_3^\eta R_h^{IIe} + \alpha_4^\eta R_h^{IIIe}}{\beta_1^\eta I_m^e + d_h^\eta}$$

$$I_h^e = \frac{\beta_1^\eta S_h^e I_m^e}{\alpha_1^\eta + \theta_1^\eta + \theta_4^\eta + \theta_5^\eta + d_h^\eta} = \frac{d_h^\eta d_m^{2\eta}[R_0 - 1]}{d_h^\eta d_m^\eta \beta_2^\eta + \beta_1^\eta\beta_2^\eta A_m^\eta Z},$$

where

$Z = [(\alpha_2^\eta + \theta_2^\eta + d_h^\eta)(\theta_3^\eta + \alpha_3^\eta + d_h^\eta)d_h^\eta(\theta_5^\eta + (\alpha_4^\eta + d_h^\eta)) + (\alpha_2^\eta + \theta_2^\eta + d_h^\eta)\theta_4^\eta d_h^\eta(\theta_3^\eta + \alpha_4^\eta + d_h^\eta) + (\alpha_4^\eta + d_h^\eta)\theta_1^\eta d_h^\eta(\theta_3^\eta + \alpha_3^\eta + d_h^\eta + \theta_2^\eta) + \theta_1^\eta\theta_2^\eta d_h^\eta\theta_3^\eta]/(\alpha_2^\eta + \theta_2^\eta + d_h^\eta)(\theta_3^\eta + \alpha_3^\eta + d_h^\eta)(\alpha_4^\eta + d_h^\eta)$, and

$$R_0 = \frac{\beta_1^\eta\beta_2^\eta A_m^\eta A_h^\eta}{(\alpha_1^\eta + \theta_1^\eta + \theta_4^\eta + \theta_5^\eta + d_h^\eta)d_m^{2\eta}d_h^\eta}.$$

When $R_0 = 1$ endemic equilibrium point become the disease-free equilibrium, and if $R_0 < 1$, infected human become negative, due to which all population becomes negative. As the population cannot be negative, endemic equilibrium exists if $R_0 > 1$.

7.3.2 Stability Analysis of Proposed Model

Theorem 7.3.1. *The diseases-free equilibrium point* $\left(\frac{A_h^\eta}{d_h^\eta}, 0, 0, 0, 0, \frac{A_m^\eta}{d_m^\eta}, 0\right)$ *of the system* (7.1.1) *is locally and globally asymptotically stable when* $R_0 < 1$*; otherwise, it is unstable.*

Proof. The Jacobian matrix of the proposed model is J_{E^0}

$$\begin{bmatrix} -\beta_1^\eta I_m - d_h^\eta & \alpha_1^\eta & \alpha_2^\eta & \alpha_3^\eta & \alpha_4^\eta & 0 & -\beta_1^\eta S_h \\ \beta_1^\eta I_m & -\alpha_1^\eta - \theta_1^\eta - \theta_4^\eta & 0 & 0 & 0 & 0 & \beta_1^\eta S_h \\ & -\theta_5^\eta - d_h^\eta & & & & & \\ 0 & \theta_1^\eta & -\alpha_2^\eta - \theta_2^\eta - d_h^\eta & 0 & 0 & 0 & 0 \\ 0 & \theta_4^\eta & \theta_2^\eta & -\theta_3^\eta - \alpha_3^\eta - d_h^\eta & 0 & 0 & 0 \\ 0 & \theta_5^\eta & 0 & \theta_3^\eta & -\alpha_4^\eta - d_h^\eta & 0 & 0 \\ 0 & -\beta_2^\eta S_m & 0 & 0 & 0 & -d_m^\eta & 0 \\ 0 & \beta_2^\eta S_m & 0 & 0 & 0 & 0 & -d_m^\eta \end{bmatrix}.$$

The Jacobian matrix of the proposed model at E^0 is J_{E^0}

$$\begin{bmatrix} -d_h^\eta & \alpha_1^\eta & \alpha_2^\eta & \alpha_3^\eta & \alpha_4^\eta & 0 & -\beta_1^\eta \frac{A_h^\eta}{d_h^\eta} \\ 0 & -\alpha_1^\eta - \theta_1^\eta - \theta_4^\eta & 0 & 0 & 0 & 0 & \beta_1^\eta \frac{A_h^\eta}{d_h^\eta} \\ & -\theta_5^\eta - d_h^\eta & & & & & \\ 0 & \theta_1^\eta & -\alpha_2^\eta - \theta_2^\eta - d_h^\eta & 0 & 0 & 0 & 0 \\ 0 & \theta_4^\eta & \theta_2^\eta & -\theta_3^\eta - \alpha_3^\eta - d_h^\eta & 0 & 0 & 0 \\ 0 & \theta_5^\eta & 0 & \theta_3^\eta & -\alpha_4^\eta - d_h^\eta & 0 & 0 \\ 0 & -\beta_2^\eta \frac{A_m^\eta}{d_m^\eta} & 0 & 0 & 0 & -d_m^\eta & 0 \\ 0 & \beta_2^\eta \frac{A_m^\eta}{d_m^\eta} & 0 & 0 & 0 & 0 & -d_m^\eta \end{bmatrix}.$$

Clearly, five eigen-values are $-d_h^\eta, -d_m^\eta, -\alpha_4^\eta - d_h^\eta, -\theta_3^\eta - \alpha_3^\eta - d_h^\eta, -\alpha_2^\eta - \theta_2^\eta - d_h^\eta$ which are in 2^{nd} quadrant. Now, to check the stability of the proposed model let us assume that $J_{E^0} = \begin{bmatrix} -\alpha_1^\eta - \theta_1^\eta - \theta_4^\eta - \theta_5^\eta - d_h^\eta & \beta_1^\eta \frac{A_h^\eta}{d_h^\eta} \\ \beta_2^\eta \frac{A_m^\eta}{d_m^\eta} & -d_m^\eta \end{bmatrix}$. The characteristics equation of the above

matrix is given by

$$\lambda^2 + A_1\lambda + A_2 = 0 \tag{7.3.1}$$

where $A_1 = \alpha_1^\eta + \theta_1^\eta + \theta_4^\eta + \theta_5^\eta + d_h^\eta + d_m^\eta > 0$ and

$$A_2 = (\alpha_1^\eta + \theta_1^\eta + \theta_4^\eta + \theta_5^\eta + d_h^\eta)d_m^\eta - \beta_1^\eta\beta_2^\eta\frac{A_h^\eta}{d_h^\eta}\frac{A_m^\eta}{d_m^\eta}.$$

$$A_2 = (\alpha_1^\eta + \theta_1^\eta + \theta_4^\eta + \theta_5^\eta + d_h^\eta)d_m^\eta\left[1 - \frac{\beta_1^\eta\beta_2^\eta A_h^\eta A_m^\eta}{(\alpha_1^\eta + \theta_1^\eta + \theta_4^\eta + \theta_5^\eta + d_h^\eta)d_h^\eta d_m^{2\eta}}\right].$$

$$A_2 = (\alpha_1^\eta + \theta_1^\eta + \theta_4^\eta + \theta_5^\eta + d_h^\eta)d_m^\eta\left[1 - R_0\right].$$

By using Routh-Hurwitz criteria (Theorem 1.4.4), if A_1, A_2 are greater than zero, then the eigenvalues will have negative real parts. Since Ω is a positively invariant set for the proposed model, E^0 is globally asymptotically stable, as $(S_h, I_h, R_h^I, R_h^{II}, R_h^{III}, S_m, I_m) \to E^0 = \left(\frac{A_h^\eta}{d_h^\eta}, 0, 0, 0, 0, \frac{A_m^\eta}{d_m^\eta}, 0\right)$ when $t \to \infty$. Therefore, the proposed model (7.1.1) is locally and globally asymptotically stable if $R_0 < 1$. □

Theorem 7.3.2. *The endemic equilibrium point $E^e = (S_h^e, I_h^e, R_h^{Ie}, R_h^{IIe}, R_h^{IIIe}, S_m^e, I_m^e)$ of the system (7.1.1) is locally asymptotically stable when $R_0 > 1$; otherwise, it is unstable.*

Proof. The Jacobian matrix of the proposed model is J_{E^e}

$$\begin{bmatrix}
-\beta_1^\eta I_m^e - d_h^\eta & \alpha_1^\eta & \alpha_2^\eta & \alpha_3^\eta & \alpha_4^\eta & 0 & -\beta_1^\eta S_h^e \\
\beta_1^\eta I_m^e & -\alpha_1^\eta - \theta_1^\eta - \theta_4^\eta & 0 & 0 & 0 & 0 & \beta_1^\eta S_h^e \\
 & -\theta_5^\eta - d_h^\eta & & & & & \\
0 & \theta_1^\eta & -\alpha_2^\eta - \theta_2^\eta - d_h^\eta & 0 & 0 & 0 & 0 \\
0 & \theta_4^\eta & \theta_2^\eta & -\theta_3^\eta - \alpha_3^\eta - d_h^\eta & 0 & 0 & 0 \\
0 & \theta_5^\eta & 0 & \theta_3^\eta & -\alpha_4^\eta - d_h^\eta & 0 & 0 \\
0 & -\beta_2^\eta S_m^e & 0 & 0 & 0 & -d_m^\eta & 0 \\
0 & \beta_2^\eta S_m^e & 0 & 0 & 0 & 0 & -d_m^\eta
\end{bmatrix}.$$

One eigen value is $-d_m^\eta$, then for remaining eigen values we have J_{E^e}:

$$\begin{bmatrix} -\beta_1^\eta I_m^e - d_h^\eta & \alpha_1^\eta & \alpha_2^\eta & \alpha_3^\eta & \alpha_4^\eta & -\beta_1^\eta S_h^e \\ \beta_1^\eta I_m^e & -\alpha_1^\eta - \theta_1^\eta - \theta_4^\eta & 0 & 0 & 0 & \beta_1^\eta S_h^e \\ & -\theta_5^\eta - d_h^\eta & & & & \\ 0 & \theta_1^\eta & -\alpha_2^\eta - \theta_2^\eta - d_h^\eta & 0 & 0 & 0 \\ 0 & \theta_4^\eta & \theta_2^\eta & -\theta_3^\eta - \alpha_3^\eta - d_h^\eta & 0 & 0 \\ 0 & \theta_5^\eta & 0 & \theta_3^\eta & -\alpha_4^\eta - d_h^\eta & 0 \\ 0 & \beta_2^\eta S_m^e & 0 & 0 & 0 & -d_m^\eta \end{bmatrix}.$$

The characteristic equation of J_{E^e} is given by

$$\lambda^6 + B_1\lambda^5 + B_2\lambda^4 + B_3\lambda^3 + B_4\lambda^2 + B_5\lambda + B_6 \tag{7.3.2}$$

The Hurwitz determinants, H_i, where $i = 1, 2...6$, must all be positive for the Routh-Hurwitz criteria to satisfy the necessary and sufficient requirements for the local asymptotic stability of the equilibrium point E^e [99]. For a polynomial of degree six, these conditions are provided:

$H_1 = B_1 > 0, H_2 = B_1B_2 - B_3 > 0, H_3 = B_3(B_1B_2 - B_3) - B_1(B_1B_4 - B_5) > 0,$

$H_4 = B_6B_1^2B_2 - B_1^2B_4^2 - B_1B_2^2B_5 + B_1B_2B_3B_4 - B_6B_1B_3 + 2B_1B_4B_5 + B_2B_3B_5 - B_3^2B_4 - B_5^2 > 0,$

$H_5 = -B_1^3B_6^2 + 2B_1^2B_2B_5B_6 + B_1^2B_3B_4B_6 - B_1^2B_4^2B_5 - B_1B_2^2B_5^2 - B_1B_2B_3^2B_6 + B_1B_2B_3B_4B_5 - 3B_1B_3B_5B_6 + 2B_1B_4B_5^2 + B_2B_3B_5^2 + B_3^3B_6 - B_3^2B_4B_5 - B_5^3 > 0,$

$H_6 = B_6H_5 > 0.$ □

7.4 Sensitivity Analysis

To establish the most effective means of reducing human malaria-related mortality and morbidity, it is crucial to have a firm grasp of the relative importance of the many factors contributing to the disease's transmission and prevalence. The rate of initial disease transmission, R_0, is directly linked to the different variables and parameters. The present research investigates how changing the model's parameters affects the behavior of many

individuals. The threshold parameter R_0 in the model is shown to have an impact on disease spread. To assess the appropriateness of each parameter, the elasticity is utilized, which is a partial derivative of R_0. If the partial derivative is positive, then R_0 will increase when the parameter is increased. If the partial derivative is negative, R_0 will decrease when the parameter increases. Table 7.1 summarises the findings of a sensitivity analysis performed on the value of the threshold parameter R_0. Preventing mosquito bites and controlling mosquito populations are more sensitive strategies for malaria prevention.

Table 7.1: Sensitivity analysis results for the threshold parameter R_0.

Parameter	β_1	β_2	A_h	A_m	α_1	θ_1	θ_4	θ_5	d_h	d_m
Sensitivity index	14.39	2.48	0.09	0.01	-0.23	-0.27	-0.49	-0.78	-0.24	-0.16

Table 7.2: Description of variables and parameters for malaria diseases.

Parameter	Description	Value
A_h	Recruitment rate of human population	5.5333
A_m	Recruitment rate of mosquito population	39
β_1	Rate at which people switch from the susceptible to infected	0.0038
β_2	Rate at which mosquito switch from the S_h to I_h	0.022
α_1	Rate that humans in I_h class acquire partial immunity and switch to S_h	0.0055
α_2	Rate that humans in R_h^I class acquire partial immunity and switch to S_h	0.05
α_3	Rate that humans in R_h^{II} class acquire partial immunity and switch to S_h	0.055
α_4	Rate that humans inR_h^{III} class acquire partial immunity and switch to S_h	0.05
θ_1	Rate from which people switch from I_h to R_h^I	0.2
θ_2	Rate from which people switch from R_h^I to R_h^{II}	0.01
θ_3	Rate from which people switch from R_h^{II} to R_h^{III}	0.02
θ_4	Rate from which people switch from I_h to R_h^{II}	0.01
θ_5	Rate from which people switch from I_h to R_h^{III}	0.001
d_h	Mortality rate of human population	0.016
d_m	Mortality rate of mosquito population	0.83

7.5 Numerical Validation Through Simulation

The dynamic aspect of the malaria drug resistance model is shown by numerical data, validating the analytical conclusions for different orders of derivatives. The suggested model is solved using the Adams-Bashforth-Moulton predictor-corrector method [109].

Table 7.2 displays the variables and parameters used for the evaluation [184]. For the set of parameters listed in Table 7.2; R_0 is $6.78, 5.94, 5.19, 4.52$ for $\eta = 1, 0.9, 0.8, 0.7$, respectively.

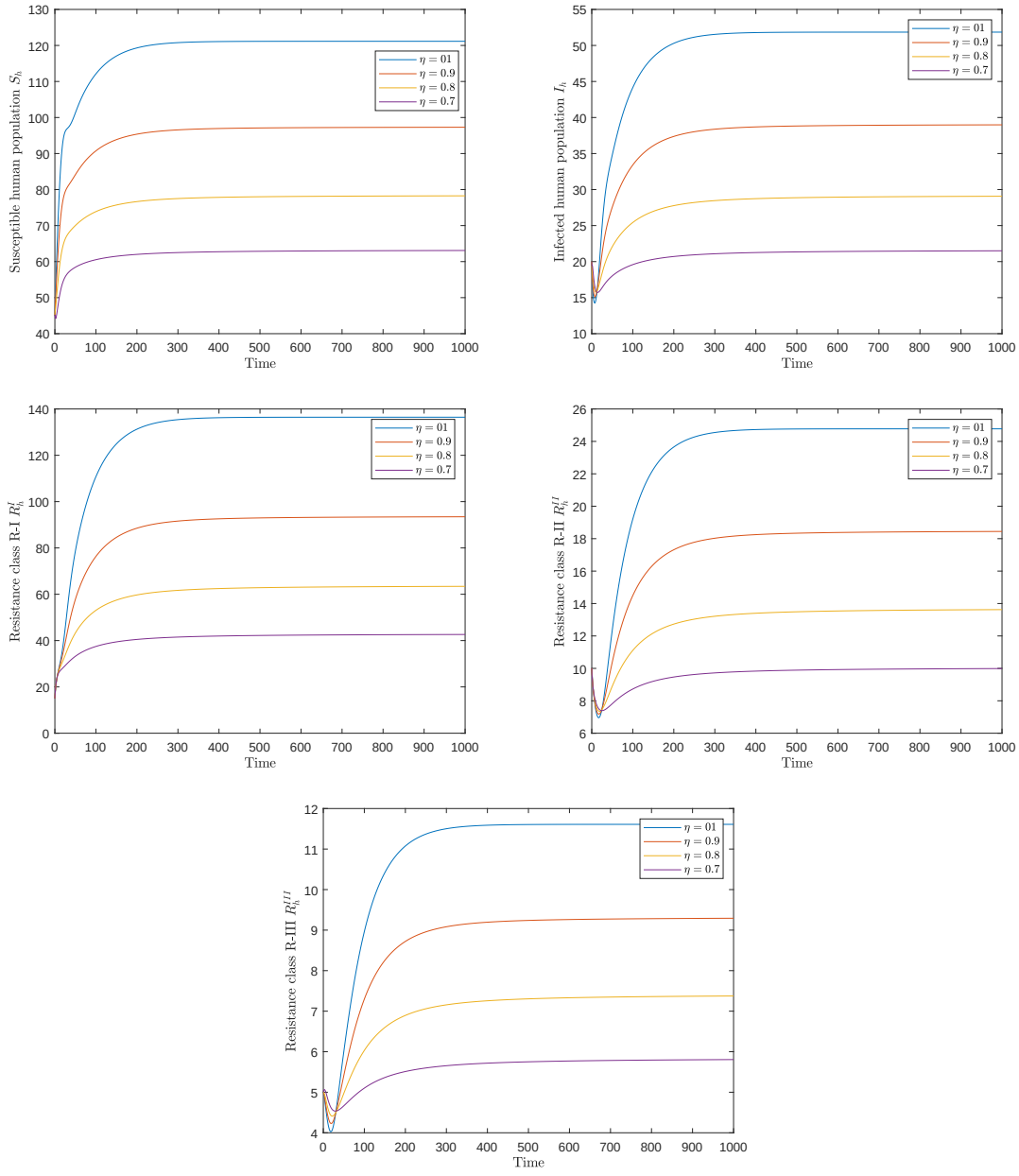

Figure 7.2: Variations of the Susceptible (S_h), Infected (I_h), Resistance classes $R_h^I, R_h^{II}, R_h^{III}$ of human for the different order of derivative (η), which shows the path of all the classes irrespective of the order of derivative validates the stability of the model.

According to Figure 7.2 and Figure 7.3, the steady states are asymptotically stable for $\eta = 0.7, 0.8, 0.9$, and 1. The trajectory of all categories, Susceptible (S_m) and Infected (I_m) mosquitoes, and Susceptible (S_h), Infected (I_h), Resistance classes R-I, R-II, R-III are $R_h^I, R_h^{II}, R_h^{III}$ of human shows the stability of the drug resistance model for the different orders of derivatives. Figure 7.2 and Figure 7.3 plotted for the values given in Table 7.2, having $R_0 > 1$, and trajectories converges to endemic equilibrium point. Each category of human population increases with time, but the mosquito population shows different trends, like susceptible mosquito decreases with time and infected mosquito increases with time. As the order of derivatives decreases, each population decreases and converges to a point.

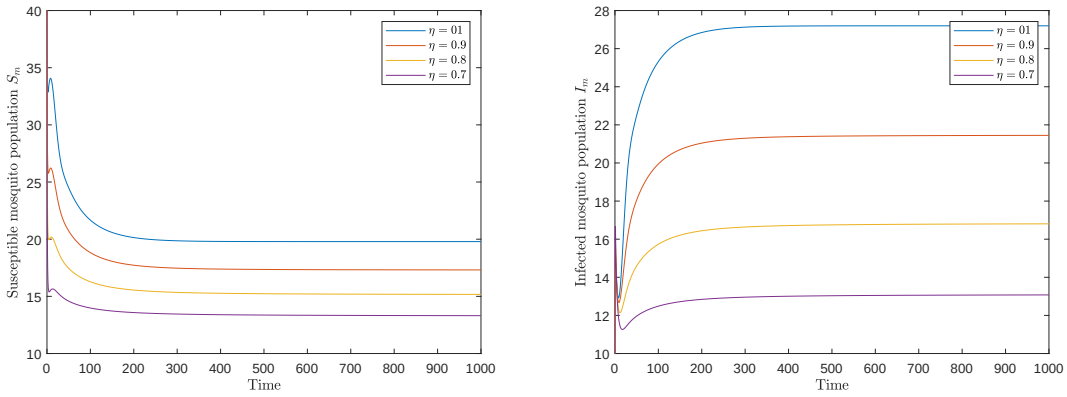

Figure 7.3: Variations of the Susceptible (S_m), Infected (I_m) mosquitoes for the different order of derivative (η), which shows the path of all the classes irrespective of the order of derivative validates the stability of the model.

Table 7.3: Different set of parameters.

Parameter	β_1	β_2	α_1	α_2	α_3	α_4
value (For $R_0 < 1$)	0.0005	0.022	0.0055	0.05	0.055	0.05
value (For $R_0 > 1$)	0.0008	0.022	0.0055	0.05	0.055	0.05

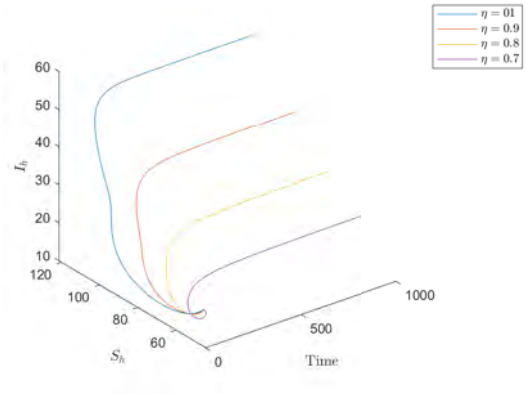

(a) Relation of S_h with I_h

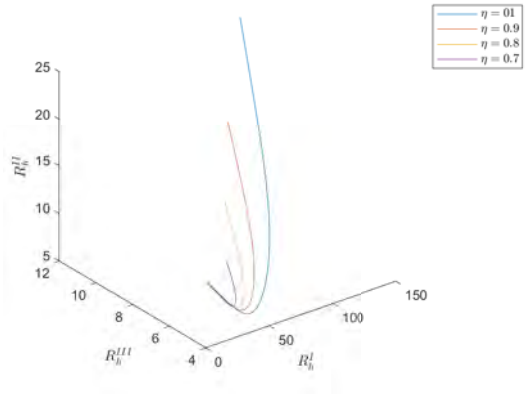

(b) Relation of R_h^I, R_h^{II} and R_h^I

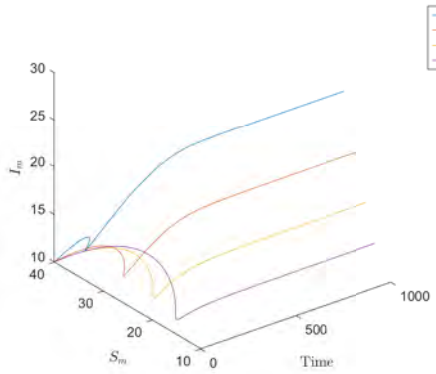

(c) Relation of S_m with I_m

Figure 7.4: Relation between the different classes of the proposed model for the set of parameters listed in Table 7.2.

Figure 7.4 shows the relation between the different classes of the proposed model. Figure 7.4(a) shows that the infected human population increases with the susceptible human population but with different ratios for the different order of derivative, and this ratio decreases with the order of derivative. Figure 7.4(b) shows the relationship between different drug resistance classes; R_h^I increases with time and R_h^{II} and R_h^{III} first decreases then start increasing with R_h^I. Figure 7.4(c) shows that the number of infected mosquitoes increases and the susceptible mosquito population decrease with time.

In this chapter, two sets of parameters, one having $R_0 < 1$ and another having $R_0 > 1$ are assumed and shown in Table 7.3. Figure 7.5 and Figure 7.8 are for $R_0 < 1$, and the

trajectories converge to disease-free equilibrium. Figure 7.6 and Figure 7.9 are for $R_0 > 1$, and the trajectories converge to endemic equilibrium.

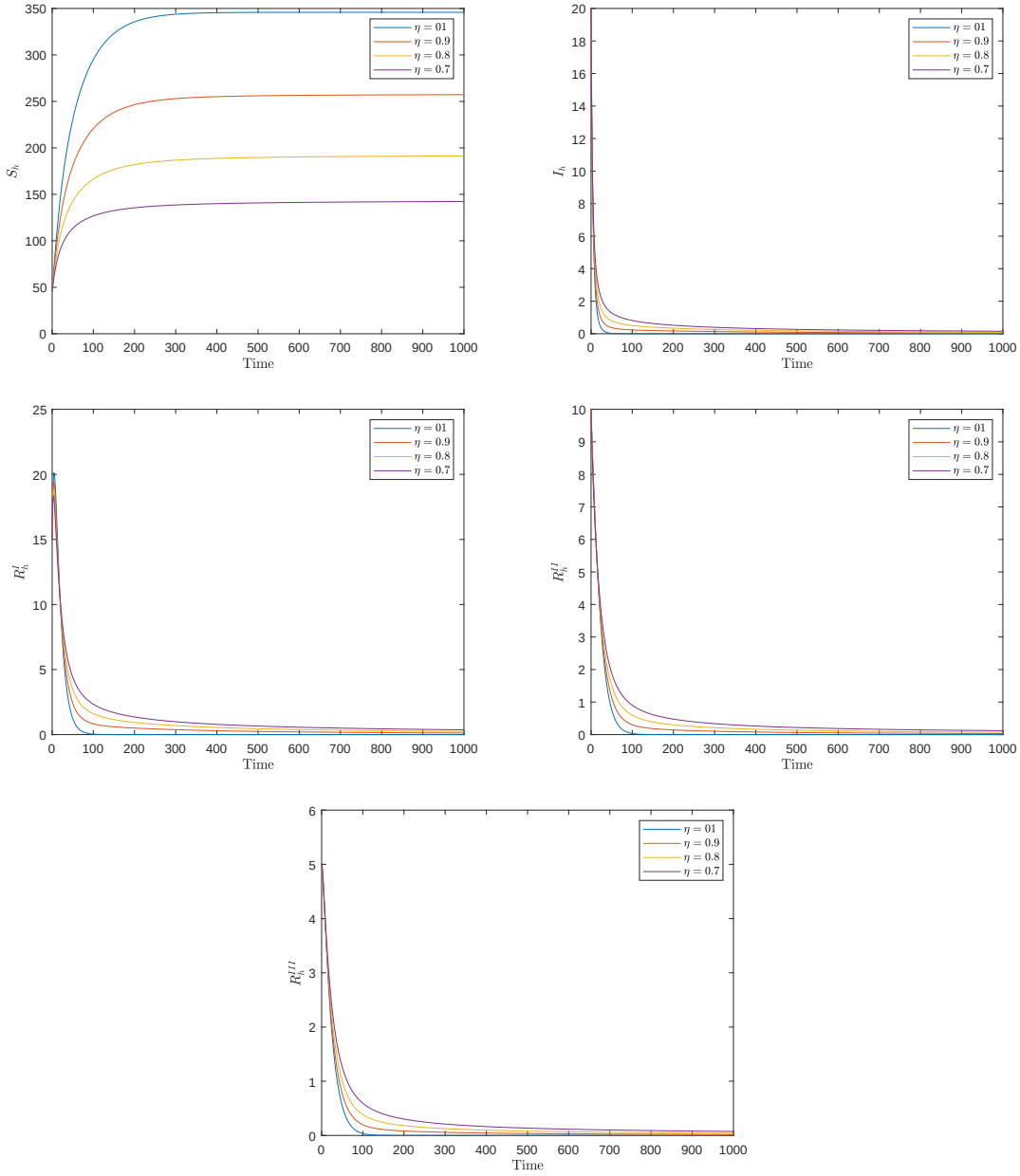

Figure 7.5: Variations of the Susceptible (S_h), Infected (I_h), Resistance classes $R_h^I, R_h^{II}, R_h^{III}$ of human for the different order of derivative (η), which shows the path of all the classes irrespective of the order of derivative validates the stability of the model. For the parameters listed in Table 7.3 ($R_0 < 1$), R_0 is $0.8918, 0.8653, 0.8368, 0.8063$ for $\eta = 1, 0.9, 0.8, 0.7$, respectively.

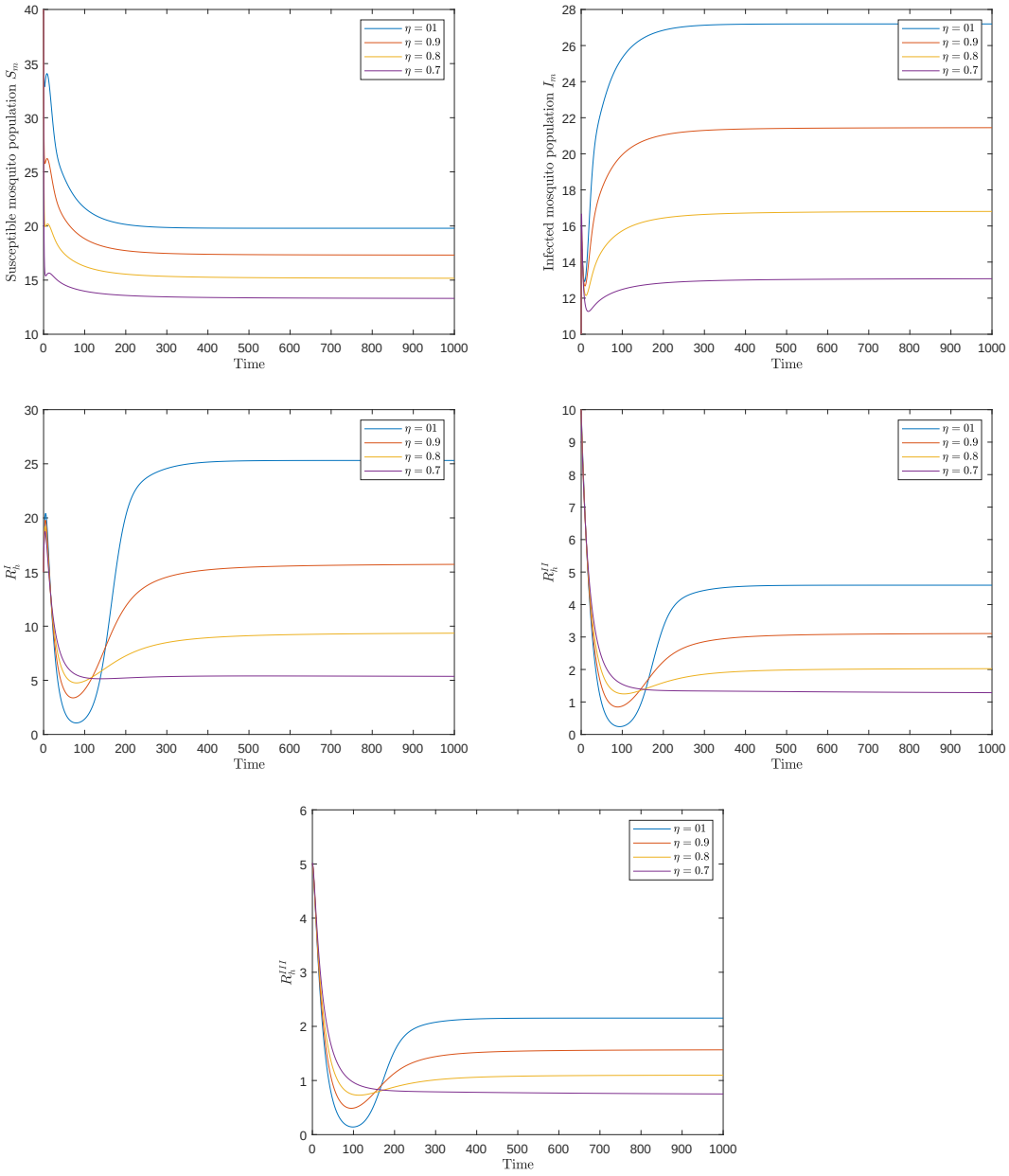

Figure 7.6: Variations of the Susceptible (S_h), Infected (I_h), Resistance classes $R_h^I, R_h^{II}, R_h^{III}$ of human for different values of the order of derivative (η), which shows the path of all classes irrespective of the order of derivative validates the stability of the model. For the parameters listed in Table 7.3 ($R_0 > 1$), R_0 is $1.4268, 1.3523, 1.2774, 1.2023$ for $\eta = 1, 0.9, 0.8, 0.7$, respectively.

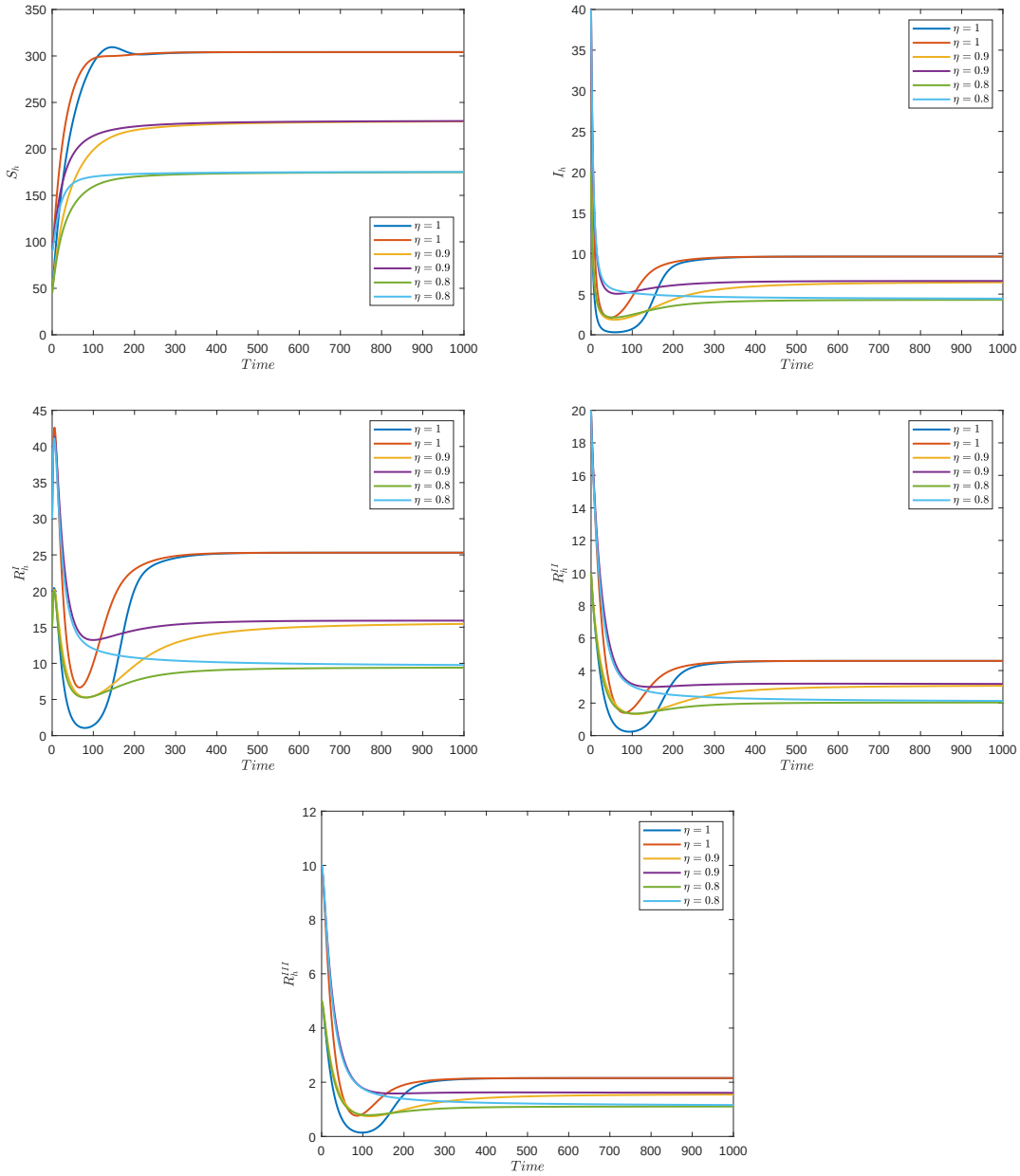

Figure 7.7: Variations of the Susceptible (S_h), Infected (I_h), Resistance classes $R_h^I, R_h^{II}, R_h^{III}$ of human for the different initial conditions and order of derivative (η), which shows the path of all classes irrespective of the order of derivative validates the stability of the model. For the parameters listed in Table 7.3 ($R_0 > 1$), R_0 is $1.4268, 1.3523, 1.2774, 1.2023$ for $\eta = 1, 0.9, 0.8, 0.7$, respectively.

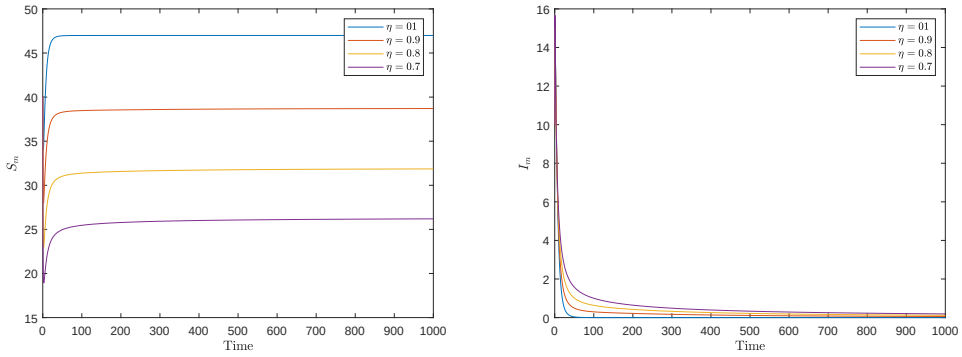

Figure 7.8: Variations of the Susceptible (S_m), Infected (I_m) mosquitoes for the parameters listed in Table 7.3 ($R_0 < 1$), R_0 is $0.8918, 0.8653, 0.8368, 0.8063$ for $\eta = 1, 0.9, 0.8, 0.7$, respectively.

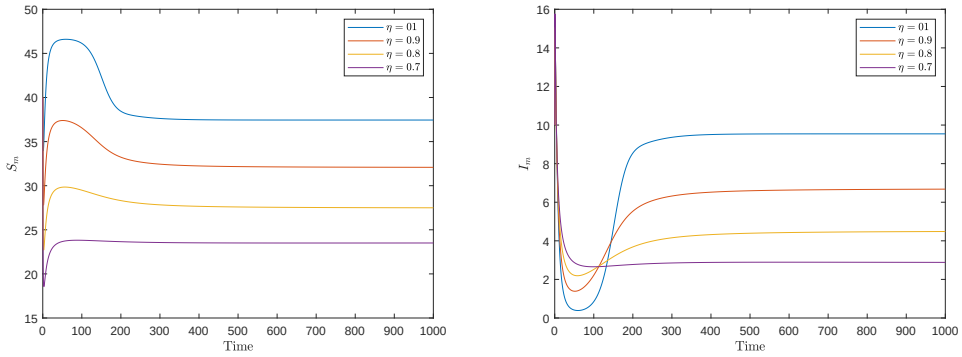

Figure 7.9: Variations of the Susceptible (S_m), Infected (I_m) mosquitoes for the parameters listed in Table 7.3 ($R_0 > 1$), R_0 is $1.4268, 1.3523, 1.2774, 1.2023$ for $\eta = 1, 0.9, 0.8, 0.7$, respectively.

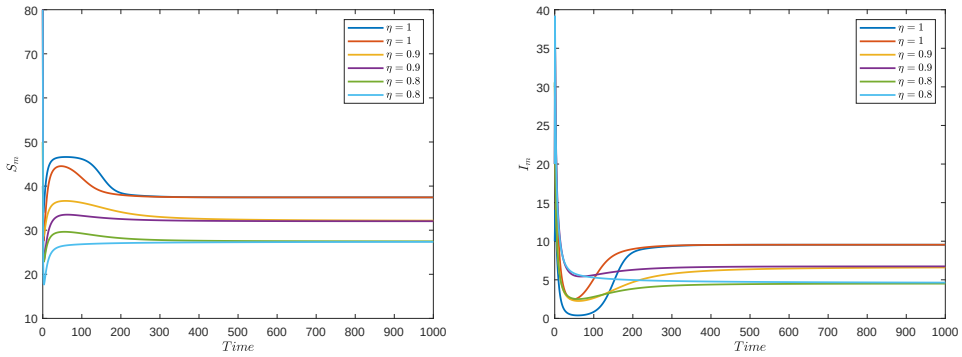

Figure 7.10: Variations of the Susceptible (S_m), Infected (I_m) mosquitoes for the different initial conditions and order of derivative (η).

In Figure 7.6 susceptible human population first increases with time and then starts decreasing for a different order of derivative, and the infected human population first decreases with time and then starts increasing. All drug resistance classes first decrease and then start increasing and converge to a specific point. Figure 7.7 and Figure 7.10 show the global stability of the endemic equilibrium point for $R_0 > 1$. For different initial conditions and orders of derivatives, all populations' paths converge to the endemic equilibrium point.

7.6 Summary

The dynamics of malaria infection for different drug resistance levels in the human and mosquito populations are investigated in this research. The mosquito population thought to be the major cause of this kind of illness, influences how far it spreads. This study presents a novel compartmental model of malaria transmission with memory between human-to-mosquito and mosquito-to-human that integrates drug resistance development and therapy as a preventative measure. The threshold parameter R_0 is calculated to analyze the impact on disease spread. The diseases- free and endemic equilibrium points are calculated, and their stability at each equilibrium point is worked out. The findings also suggest that if a doctor knows the level of drug resistance at an early stage then the transmission of malaria can be reduced by providing adequate drug to the patient (as R_0 decreases as $\theta_1, \theta_4, \theta_5$ increases). Moreover, several graphs have shown global asymptotic stability by significantly altering the initial condition. The key findings of this chapter are outlined below:

- The research investigates how changing model parameters affects the behavior of individuals within the population, shedding light on the dynamics of malaria transmission. Key preventive measures for malaria prevention include preventing mosquito bites and controlling mosquito populations as these parameters are more sensitive in spread of malaria.

- As the order of the derivative decreases from one, influenced by the memory ef-

fect within the system, there is an observed decrease in the reproduction number, resulting in a reduction in malaria transmission. India has a vision of achieving a malaria-free status by 2027 and complete elimination by 2030. Therefore, if the parameters utilized in the proposed model are raised to the power of less than 0.7 could significantly support India's goal of eradicating malaria as level of drug resistance decreases as order of derivative decreases from 1 to 0.7 (Figure 7.2).

- The results indicate that early identification of drug resistance levels in individuals can assist in decreasing malaria transmission through the administration of suitable drug treatments. Therefore, malaria tests should encompass an assessment of drug resistance levels as well.

This chapter has been communicated as follows:

- *K. Bansal, and T. Mathur, "Analysis of the drug resistance level of malaria disease: A fractional-order model." (Communicated)*

Chapter 8

Conclusions and Future Scope

This thesis elucidates diverse implementations of fractional-order differential equations within the realms of socio-economic studies and epidemiology. Employing fractional operators, this research precisely characterizes the propagation of crime, the influences of social media, unemployment dynamics, and malaria spread. Notably, the memory attribute of fractional derivatives proves instrumental in effectively capturing the intricacies of these domains, enabling the modeling and scrutiny of intricate systems manifesting long-term inter-dependencies and nonlinear tendencies. After comparing the results with the existing literature, a comparative analysis provides evidence of the superiority of the findings compared to previous efforts. The following section comprehensively describes the deduced conclusions for each application, coupled with a contemplation of the future prospects engendered by this research undertaking.

8.1 Conclusions

8.1.1 Crime Transmission Modeling

Unlike existing crime transmission modeling, the proposed fractional order models help to investigate the duration required to capture and reinforce criminals, non-linear transmission rates, isolation rate of criminals from non-criminals and the logistic growth rate of non-

criminal individuals.

The inclusion of the delay coefficient (τ) in the fractional-order crime transmission mathematical model serves the specific purpose of exploring the temporal interval between an individual's engagement in criminal activity and the legal process leading to their conviction. The outcomes derived from the delayed model present a compelling insight: when the delay surpasses a predetermined threshold, the model undergoes periodic oscillations. Notably, under this framework, law enforcement officers are granted an approximately 30-week window for the apprehension of criminals and the securing of their convictions. In contrast, the integer order model imposes a more stringent temporal constraint, limiting this interval to approximately 25 week. Additionally, a noteworthy phenomenon arises with the escalation of the derivative order from 0 to 1, characterized by a reduction in the delay. Hence, the fractional-order model allows law enforcement officers additional time, which proves beneficial in securing the conviction of a criminal as in real life scenario, simple and straightforward matters may be resolved relatively quickly, possibly within a month. This leads to an expansion of the model's stability region in the fractional-order domain.

Utilizing the Beddington-DeAngelis non-linear transmission rate, a versatile framework encompassing both linear and specific non-linear counterparts, uncovers profound insights. The results strongly affirm its superior effectiveness in curtailing crime transmission when contrasted with alternative methods. Notably, a significant trend emerges: as the derivative order decreases memory is incorporated in system and crime transmission experiences a marked reduction. This phenomenon underscores the enhanced efficiency of a fractional-order model in quelling crime transmission, surpassing the capabilities of conventional integer-order models. In the pursuit of an optimal solution, the quest leads to the discovery of the best-fit derivative order value, which converges at approximately 0.2. This parameter proves pivotal in the endeavor to reduce crime. Within the realm of fractional-order models, the strategic exponentiation of various factors, including transmission rate, crowding effect, and inhibition effect, to the power of 0.2 emerges as a formidable approach, significantly bolstering their effectiveness in combatting crime

transmission.

The introduction of a fractional-order mathematical model for crime transmission, incorporating logistic growth and isolation rates, sets the stage for a critical examination. Based on this research, a stronger and more efficient legal system, in conjunction with enhanced living conditions that can isolates criminals and noncriminals has the potential to significantly decrease the incidence of crimes. It's important to note that a community might not always have the capacity to simultaneously bolster law enforcement and provide the necessary resources. However, this study demonstrates that a society can achieve a crime-free environment even if only one of these conditions is fulfilled. Additionally, it is imperative to note that with an increase in law enforcement efforts, there is a corresponding decline in the criminal population. However, until a specific threshold is reached, there is no discernible impact on the spread of criminal activities. The optimal value for the level of law enforcement is situated near 0.1, as the variation in criminal generation remains relatively unchanged beyond this point.

The strategy proposed here accelerates establishing a crime-free society by considering crucial criteria.

8.1.2 Modeling of Excessive Use of Social Media

The proposed mathematical framework introduces nonlinear fractional differential equations to elucidate the influence of social networking platforms on the academic performance of students. Within this framework, equilibrium points representing states of both social web-free and endemic conditions are identified, with the distinction being governed by the reproduction number, denoted as R_0. This model apart from its predecessors is its deviation from the notion of a socially web-free equilibrium point as a societal benefit. Instead, the primary focus is placed on achieving endemic equilibria, which can more accurately depict real-world dynamics. A significant trend emerges in the behavior of population trajectories. When the derivative order is less than or equal to 0.5, all trajectories exhibit a declining pattern. However, for orders exceeding 0.5, an increasing trend is observed. The core objective of the study is optimizing the utilization of social media to

enhance the prospects of students in practical scenarios. Consequently, the optimal value for the derivative order is estimated at around 0.5, signifying its role in mitigating social media addiction. Intriguingly, the reproduction number R_0 exhibits an upward trend in conjunction with η. This trend indicates that a decrease in η corresponds to a reduction in social media addiction, showcasing the heightened efficiency of the fractional-order model when compared to the integer-order model.

8.1.3 Youth Unemployment Modeling

This thesis introduces a fractional-order mathematical model designed to address the pressing issue of youth unemployment in resource-limited nations. The primary aim is to scrutinize the impact of fractional-order derivatives on unemployment modeling. Furthermore, the investigation delves into the effectiveness of skill development programs across varying orders of derivatives in alleviating the unemployment challenge. The results further unveil a critical threshold, denoted as $\grave{\sigma}_c$, in the skill development rate ($\grave{\sigma}$). Beyond this threshold, which represents the minimum requirement for skill development programs to notably impact unemployment reduction, the effect becomes more pronounced. With increasing $\grave{\sigma}$, the population of the unemployed experiences a decline. This analysis holds significant relevance in evaluating the government's ability to sustain effective support for training programs. In light of the practical context, the research identifies an optimal value for η approximately 0.5 as the key to effectively curbing unemployment. This insight carries substantial implications for policy making and program implementation in the realm of youth unemployment. A notable finding is the upward trajectory of the reproduction number (R) in conjunction with the order of derivative (η). An increase in the order of derivative corresponds to an decrease in unemployment. However, empirical observations from real-world data, as depicted in Figure 1.3, contradict this trend by revealing a surge in unemployment rates. The model, in turn, suggests that unemployment increases when the order of derivatives is less than or equal to 0.5. This finding underscores the superior capacity of a fractional-order model to align with real-world scenarios, outperforming its integer-order counterpart.

These findings enhance our understanding of unemployment in resource-limited nations. They provide valuable insights into reducing unemployment rates, especially through skill development programs. This understanding helps policymakers and organizations design more effective programs to address unemployment challenges and improve workforce employability, which is crucial in competitive job markets. Ultimately, these findings inform the development and implementation of policies and initiatives to combat unemployment and enhance economic prospects in resource-limited regions.

8.1.4 Malaria Transmission Modeling

The dynamics of malaria infection for different drug resistance levels in the human and mosquito populations are investigated. The mosquito population thought to be the major cause of this kind of illness, influences how far it spreads. The thesis introduces an innovative compartmental model for malaria transmission, incorporating memory effects between humans and mosquitoes. This model accounts for drug resistance development and therapy as preventive measures. The threshold parameter, known as R_0, is computed to evaluate its impact on the spread of the disease. This study investigates how altering the model's parameters affects the behavior of individuals within the population, shedding light on the intricate dynamics of malaria transmission. Essential preventive measures for malaria include measures such as preventing mosquito bites and managing mosquito populations. As the derivative order decreases from one, influenced by the system's memory effect, there is an observable decrease in the reproduction number. This reduction correlates with a decrease in malaria transmission. India has set an ambitious goal of achieving a malaria-free status by 2027 and complete elimination by 2030. In this context, modifying the model's parameters raised to power 0.7 and below could significantly support India's mission to eradicate malaria. The results emphasize the importance of early identification of drug resistance levels in individuals. This identification can aid in reducing malaria transmission by ensuring the administration of appropriate drug treatments. Consequently, malaria tests should incorporate an evaluation of drug resistance levels to enhance the effectiveness of prevention and control efforts.

8.2 Future Scope

In the future, the proposed models can be extended to higher dimensions by considering several other factors affecting the spread of crime, malaria and many more. The optimal value of the fractional order of derivative can be obtained using different algorithms. The simulation results can be validated with real-life criminal data of different regions.

- Additional influences such as the impact of fear, the Allee effect, diverse growth rates, the variability of carrying capacity, criminal competition, and different treatment rates can all be incorporated into the crime propagation model. Artificial intelligence (AI) can play a pivotal role in predictive policing, using historical data to forecast crime trends and allocate resources more efficiently. Hence, Advanced AI algorithms can incorporate to analyze patterns in criminal behavior, aiding in the development of more accurate criminal profiles and early intervention strategies.

- Factors such as varying growth rates, the adaptable carrying capacity, and the engagement of professional individuals with social media can all be taken into account within the framework of a model for social media addiction.

- Additional factors including various growth rates, fluctuations in carrying capacity, diminution rate, and migration factor can all be integrated into the unemployment model.

- The malaria transmission model can be enhanced by including additional factors such as the Allee effect, various growth rates, fluctuations in carrying capacity, and diverse treatment rates.

Comprehensively, the optimal value for the fractional order model by employing heuristic optimization algorithms like Particle Swarm Optimization, Genetic Algorithms, and Quantum Optimization, which can lead to faster convergence. Additionally, we have the opportunity to relax constraints on parameters, allowing for an expansion of the number of stages. This opens the door to constructing higher-dimensional fractional-order models.

As a result, fractional calculus will continue to evolve as a potent tool for modeling and analyzing complex systems across various fields. Its applications are an ongoing exploration, with the potential to uncover new avenues for research and development.

References

[1] I. Podlubny, *Fractional differential equations: An introduction to fractional derivatives, fractional differential equations, to methods of their solution and some of their applications*. Elsevier, 1998.

[2] K. Oldham and J. Spanier, *The fractional calculus theory and applications of differentiation and integration to arbitrary order*. Elsevier, 1974.

[3] K. S. Miller and B. Ross, *An introduction to the fractional calculus and fractional differential equations*. Wiley, 1993.

[4] T. Sardar, S. Rana, and J. Chattopadhyay, "A mathematical model of dengue transmission with memory," *Communications in Nonlinear Science and Numerical Simulation*, vol. 22, no. 1-3, pp. 511–525, 2015.

[5] J. Kongson, W. Sudsutad, C. Thaiprayoon, J. Alzabut, and C. Tearnbucha, "On analysis of a nonlinear fractional system for social media addiction involving Atangana–Baleanu–Caputo derivative," *Advances in Difference Equations*, vol. 2021, no. 1, pp. 1–29, 2021.

[6] I. Petráš and J. Terpák, "Fractional calculus as a simple tool for modeling and analysis of long memory process in industry," *Mathematics*, vol. 7, no. 6, p. 511, 2019.

[7] B. Ross, *Fractional calculus and its applications: proceedings of the international conference held at the University of New Haven, June 1974*, vol. 457. Springer, 2006.

[8] K. Diethelm and N. J. Ford, "Analysis of fractional differential equations," *Journal of Mathematical Analysis and Applications*, vol. 265, no. 2, pp. 229–248, 2002.

[9] S. Arora, T. Mathur, and K. Tiwari, "A fractional-order model to study the dynamics of the spread of crime," *Journal of Computational and Applied Mathematics*, vol. 426, p. 115102, 2023.

[10] K. S. Pritam, Sugandha, T. Mathur, and S. Agarwal, "Underlying dynamics of crime transmission with memory," *Chaos, Solitons & Fractals*, vol. 146, p. 110838, 2021.

[11] M. Du, Z. Wang, and H. Hu, "Measuring memory with the order of fractional derivative," *Scientific Reports*, vol. 3, no. 1, pp. 1–3, 2013.

[12] J.-L. Wang and H.-F. Li, "Surpassing the fractional derivative: Concept of the memory-dependent derivative," *Computers & Mathematics with Applications*, vol. 62, no. 3, pp. 1562–1567, 2011.

[13] Y. Wei, Y. Chen, S. Cheng, and Y. Wang, "A note on short memory principle of fractional calculus," *Fractional Calculus and Applied Analysis*, vol. 20, no. 6, p. 1382, 2017.

[14] I. Petráš, "Modeling and numerical analysis of fractional-order Bloch equations," *Computers & Mathematics with Applications*, vol. 61, no. 2, pp. 341–356, 2011.

[15] C. M. Pinto and J. T. Machado, "Fractional model for malaria transmission under control strategies," *Computers & Mathematics with Applications*, vol. 66, no. 5, pp. 908–916, 2013.

[16] T. Abdeljawad and D. Baleanu, "Monotonicity analysis of a nabla discrete fractional operator with discrete Mittag-Leffler kernel," *Chaos, Solitons & Fractals*, vol. 102, pp. 106–110, 2017.

[17] P. Humbert and R. P. Agarwal, "Sur la fonction de Mittag-Leffler et quelques-unes de ses généralisations," *Bulletin des Sciences Mathematiques*, vol. 77, no. 2, pp. 180–185, 1953.

[18] L. Kexue and P. Jigen, "Laplace transform and fractional differential equations," *Applied Mathematics Letters*, vol. 24, no. 12, pp. 2019–2023, 2011.

[19] M. Kurulay and M. Bayram, "Some properties of the Mittag-Leffler functions and their relation with the Wright functions," *Advances in Difference Equations*, vol. 2012, no. 1, pp. 1–8, 2012.

[20] F. Mainardi, "On some properties of the Mittage-Leffler function $E_\alpha(-t^\alpha)$, completely monotone for $t > 0$ with $0 < \alpha < 1$," *Discrete & Continuous Dynamical Systems-Series B*, vol. 19, no. 7, 2014.

[21] H. Jalalinejad, A. Tavakoli, and F. Zarmehi, "A simple and flexible modification of Grünwald–Letnikov fractional derivative in image processing," *Mathematical Sciences*, vol. 12, no. 3, pp. 205–210, 2018.

[22] M. Caputo, "Linear models of dissipation whose Q is almost frequency independent—II," *Geophysical Journal International*, vol. 13, no. 5, pp. 529–539, 1967.

[23] F. Brauer, C. Castillo-Chavez, and Z. Feng, *Mathematical models in epidemiology*. Springer, 2019.

[24] M. Meerschaert, *Mathematical modeling*. Academic Press, 2013.

[25] W. J. Meyer, *Concepts of mathematical modeling*. Courier Corporation, 2004.

[26] D. D. Mooney and R. J. Swift, *A course in mathematical modeling*. American Mathematical Society, 2021.

[27] S. A. Veronica and A. U. Samuel, "Social media addiction among adolescents with special reference to Facebook addiction," *IOSR Journal of Humanities and Social Science (IOSR-JHSS)*, vol. 4, pp. 72–76, 2015.

[28] R. Docampo, J. M. Sá, J. L. Chong, and T. E. Wellems, "Malaria drug resistance: New observations and developments," *Essays in Biochemistry*, vol. 51, pp. 137–160, 2011.

[29] G. Pathan and P. Bhathawala, "Unemployment-discussion with a mathematical model," *International Journal of Business Management and Economic Research*, vol. 3, pp. 19–27, 2016.

[30] E. Tlelo-Cuautle, A. D. Pano-Azucena, O. Guillén-Fernández, and A. Silva-Juárez, *Analog/digital implementation of fractional order chaotic circuits and applications*. Springer, 2020.

[31] A. T. Azar, A. G. Radwan, and S. Vaidyanathan, *Mathematical techniques of fractional order systems*. Elsevier, 2018.

[32] R. Caponetto, *Fractional order systems: Modeling and control applications*, vol. 72. World Scientific, 2010.

[33] J. Q. Wilson and G. L. Kelling, "Broken windows," *Atlantic Monthly*, vol. 249, no. 3, pp. 29–38, 1982.

[34] M. R. D'Orsogna and M. Perc, "Statistical physics of crime: A review," *Physics of Life Reviews*, vol. 12, pp. 1–21, 2015.

[35] A. Blumstein, "Science and technology and the President's Crime Commission: Past and future," *Criminology & Public Policy*, vol. 17, no. 2, pp. 271–282, 2018.

[36] A. Blumstein, "Youth, guns, and violent crime," *The Future of Children*, vol. 12, no. 2, pp. 39–53, 2002.

[37] A. Blumstein and R. Larson, "Models of a total criminal justice system," *Operations Research*, vol. 17, no. 2, pp. 199–232, 1969.

[38] A. Blumstein, "Prison populations: A system out of control?," *Crime and Justice*, vol. 10, pp. 231–266, 1988.

[39] A. Chalfin and J. McCrary, "Criminal deterrence: A review of the literature," *Journal of Economic Literature*, vol. 55, no. 1, pp. 5–48, 2017.

[40] G. S. Becker, "Crime and punishment: An economic approach," in *The economic dimensions of crime*, pp. 13–68, Springer, 1968.

[41] G. S. Becker and G. J. Stigler, "Law enforcement, malfeasance, and compensation of enforcers," *The Journal of Legal Studies*, vol. 3, no. 1, pp. 1–18, 1974.

[42] A. S. Malik, "Avoidance, screening and optimum enforcement," *The RAND Journal of Economics*, vol. 21, no. 3, pp. 341–353, 1990.

[43] A. M. Polinsky and S. Shavell, "The optimal tradeoff between the probability and magnitude of fines," *The American Economic Review*, vol. 69, no. 5, pp. 880–891, 1979.

[44] D. Acemoglu, "Reward structures and the allocation of talent," *European Economic Review*, vol. 39, no. 1, pp. 17–33, 1995.

[45] R. K. Sah, "Social osmosis and patterns of crime," *Journal of Political Economy*, vol. 99, no. 6, pp. 1272–1295, 1991.

[46] G. Aldashev, I. Chaara, J.-P. Platteau, and Z. Wahhaj, "Formal law as a magnet to reform custom," *Economic Development and Cultural Change*, vol. 60, no. 4, pp. 795–828, 2012.

[47] M. J. Quinteros and M. J. Villena, "On the dynamics and stability of the crime and punishment game," *Complexity*, vol. 2022, 2022.

[48] N. Crokidakis, "Modeling the impact of civilian firearm ownership in the evolution of violent crimes," *Applied Mathematics and Computation*, vol. 429, p. 127256, 2022.

[49] D. Helbing, D. Brockmann, T. Chadefaux, K. Donnay, U. Blanke, O. Woolley-Meza, M. Moussaid, A. Johansson, J. Krause, S. Schutte, and M. Perc, "Saving human lives: What complexity science and information systems can contribute," *Journal of Statistical Physics*, vol. 158, no. 3, pp. 735–781, 2015.

[50] S. Freeman, J. Grogger, and J. Sonstelie, "The spatial concentration of crime," *Journal of Urban Economics*, vol. 40, no. 2, pp. 216–231, 1996.

[51] A. K. Srivastav, M. Ghosh, and P. Chandra, "Modeling dynamics of the spread of crime in a society," *Stochastic Analysis and Applications*, vol. 37, no. 6, pp. 991–1011, 2019.

[52] D. McMillon, C. P. Simon, and J. Morenoff, "Modeling the underlying dynamics of the spread of crime," *Plos One*, vol. 9, no. 4, p. e88923, 2014.

[53] S.-J. Wang, R. Batta, and C. M. Rump, "Stability of a crime level equilibrium," *Socio-Economic Planning Sciences*, vol. 39, no. 3, pp. 229–244, 2005.

[54] M. B. Short, M. R. D'orsogna, V. B. Pasour, G. E. Tita, P. J. Brantingham, A. L. Bertozzi, and L. B. Chayes, "A statistical model of criminal behavior," *Mathematical Models and Methods in Applied Sciences*, vol. 18, no. 1, pp. 1249–1267, 2008.

[55] M. B. Short, P. J. Brantingham, and M. R. D'orsogna, "Cooperation and punishment in an adversarial game: How defectors pave the way to a peaceful society," *Physical Review E*, vol. 82, no. 6, p. 066114, 2010.

[56] L.-L. Jiang, M. Perc, and A. Szolnoki, "If cooperation is likely punish mildly: Insights from economic experiments based on the snowdrift game," *Plos One*, vol. 8, no. 5, p. e64677, 2013.

[57] B. Berenji, T. Chou, and M. R. D'Orsogna, "Recidivism and rehabilitation of criminal offenders: A carrot and stick evolutionary game," *Plos One*, vol. 9, no. 1, p. e85531, 2014.

[58] I. Sendiña-Nadal, I. Leyva, M. Perc, D. Papo, M. Jusup, Z. Wang, J. Almendral, P. Manshour, and S. Boccaletti, "Diverse strategic identities induce dynamical states in evolutionary games," *Physical Review Research*, vol. 2, no. 4, p. 043168, 2020.

[59] M. L. Howe and L. M. Knott, "The fallibility of memory in judicial processes: Lessons from the past and their modern consequences," *Memory*, vol. 23, no. 5, pp. 633–656, 2015.

[60] R. Hjalmarsson and M. J. Lindquist, "Like godfather, like son exploring the intergenerational nature of crime," *Journal of Human Resources*, vol. 47, no. 2, pp. 550–582, 2012.

[61] S. Besemer, *Intergenerational transmission of criminal and violent behaviour*. Sidestone Press, 2012.

[62] M. Costantini, I. Meco, and A. Paradiso, "Do inequality, unemployment and deterrence affect crime over the long run?," *Regional Studies*, vol. 52, no. 4, pp. 558–571, 2018.

[63] P. Uppal, "Covid-19 will lead to increased crime rates in India," *International Journal of Research-Granthaalayah*, vol. 8, no. 4, pp. 72–78, 2020.

[64] P. Jha and M. Kumar, "Labour in India and the COVID-19 pandemic," *The Indian Economic Journal*, vol. 68, no. 3, pp. 417–437, 2020.

[65] V. Tinto, "Dropout from higher education: A theoretical synthesis of recent research," *Review of Educational Eesearch*, vol. 45, no. 1, pp. 89–125, 1975.

[66] V. Tinto, *Leaving college: Rethinking the causes and cures of student attrition.* ERIC, 1987.

[67] J. P. Bean, "Dropouts and turnover: The synthesis and test of a causal model of student attrition," *Research in Higher Education*, vol. 12, no. 2, pp. 155–187, 1980.

[68] A. Ishaku, B. S. Musa, A. Sanda, and A. M. Bakoji, "Mathematical assessment of social media impact on academic performance of students in higher institution," *IOSR Journal of Mathematics (IOSR-JM)*, vol. 14, no. 1, pp. 72–79, 2018.

[69] G. Beqiri, "The impact of social media on higher education in Kosovo: The student's perspective," *Academic Journal of Interdisciplinary Studies*, vol. 3, no. 2, p. 155, 2014.

[70] M. Mbodila, C. Ndebele, and K. Muhandji, "The effect of social media on student's engagement and collaboration in higher education: A case study of the use of Facebook at a South African university," *Journal of Communication*, vol. 5, no. 2, pp. 115–125, 2014.

[71] E. M. Mwadime, *An investigation on the impact of online social networking on academic performance among high school students in urban areas: A case study of Westlands sub-county, Nairobi*. PhD thesis, University of Nairobi, 2015.

[72] T. Gok, "The effects of social networking sites on students' studying and habits," *International Journal of Research in Education and Science*, vol. 2, no. 1, pp. 85–93, 2016.

[73] N. T. Feather, *The psychological impact of unemployment*. Springer Science & Business Media, 2012.

[74] C. E. Okojie, "Employment creation for youth in Africa: The gender dimension," *Jobs for Youth: National Strategies for Employment Promotion*, pp. 15–16, 2003.

[75] M. Pletscher, "Youth unemployment in Uganda: Roots of the problem and possible ways to mitigate them," *Fontes Foundation's Youth Program*, 2015.

[76] A. Misra and A. K. Singh, "A mathematical model for unemployment," *Nonlinear Analysis: Real World Applications*, vol. 12, no. 1, pp. 128–136, 2011.

[77] G. Pathan and P. Bhathawala, "A mathematical model for unemployment with effect of self employment," *IOSR Journal of Mathematics*, vol. 11, no. 1, pp. 37–43, 2015.

[78] A. A. M. Daud, "Stability analysis of a simple mathematical model for unemployment," *Caspian Journal of Applied Sciences Research*, vol. 4, no. 2, pp. 15–18, 2015.

[79] A. Misra, A. K. Singh, and P. K. Singh, "Modeling the role of skill development to control unemployment," *Differential Equations and Dynamical Systems*, vol. 30, pp. 1–13, 2017.

[80] H. Ashi, R. M. Al-Maalwi, and S. Al-Sheikh, "Study of the unemployment problem by mathematical modeling: Predictions and controls," *The Journal of Mathematical Sociology*, vol. 46, no. 3, pp. 301–313, 2022.

[81] L. A. Gil-Alana, Z. A. Ozdemir, and A. Tansel, "Long memory in Turkish unemployment rates," *Emerging Markets Finance and Trade*, vol. 55, no. 1, pp. 201–217, 2019.

[82] S. E. Eikenberry and A. B. Gumel, "Mathematical modeling of climate change and malaria transmission dynamics: A historical review," *Journal of Mathematical Biology*, vol. 77, no. 4, pp. 857–933, 2018.

[83] S. Mandal, R. R. Sarkar, and S. Sinha, "Mathematical models of malaria-A review," *Malaria Journal*, vol. 10, no. 1, pp. 1–19, 2011.

[84] N. Chitnis, J. M. Cushing, and J. Hyman, "Bifurcation analysis of a mathematical model for malaria transmission," *SIAM Journal on Applied Mathematics*, vol. 67, no. 1, pp. 24–45, 2006.

[85] D. L. Smith, J. Dushoff, and F. E. McKenzie, "The risk of a mosquito-borne infection in a heterogeneous environment: Supplementary material," *Plos Biology*, vol. 20368, 2004.

[86] W. Gu, C. M. Mbogo, J. I. Githure, J. L. Regens, G. F. Killeen, C. M. Swalm, G. Yan, and J. C. Beier, "Low recovery rates stabilize malaria endemicity in areas of low transmission in coastal Kenya," *Acta Tropica*, vol. 86, no. 1, pp. 71–81, 2003.

[87] F. E. McKenzie, "Why model malaria?," *Parasitology Today*, vol. 16, no. 12, pp. 511–516, 2000.

[88] G. F. Killeen, F. E. McKenzie, B. D. Foy, C. Schieffelin, P. F. Billingsley, and J. C. Beier, "A simplified model for predicting malaria entomologic inoculation rates based on entomologic and parasitologic parameters relevant to control," *The American Journal of Tropical Medicine and Hygiene*, vol. 62, no. 5, p. 535, 2000.

[89] R. Ross, *The prevention of malaria*. John Murray, 1911.

[90] R. Ross, "An application of the theory of probabilities to the study of a priori pathometry.—Part I," *Proceedings of the Royal Society of London. Series A, Containing Papers of a Mathematical and Physical Character*, vol. 92, no. 638, pp. 204–230, 1916.

[91] R. Ross and H. P. Hudson, "An application of the theory of probabilities to the study of a priori pathometry.—Part II," *Proceedings of the Royal Society of London. Series A, Containing Papers of a Mathematical and Physical Character*, vol. 93, no. 650, pp. 212–225, 1917.

[92] J. Davies and D. Davies, "Origins and evolution of antibiotic resistance," *Microbiology and Molecular Biology Reviews*, vol. 74, no. 3, pp. 417–433, 2010.

[93] A. M. Thu, A. P. Phyo, J. Landier, D. M. Parker, and F. H. Nosten, "Combating multidrug-resistant plasmodium falciparum malaria," *The FEBS Journal*, vol. 284, no. 16, pp. 2569–2578, 2017.

[94] P. A. Naik, J. Zu, and K. M. Owolabi, "Global dynamics of a fractional order model for the transmission of HIV epidemic with optimal control," *Chaos, Solitons & Fractals*, vol. 138, p. 109826, 2020.

[95] A. Armitage, "René Descartes (1596-1650) and the early Royal Society," *Notes and Records of the Royal Society of London*, vol. 8, no. 1, pp. 1–19, 1950.

[96] B. Anderson, J. Jackson, and M. Sitharam, "Descartes' rule of signs revisited," *The American Mathematical Monthly*, vol. 105, no. 5, pp. 447–451, 1998.

[97] M. S. Tavazoei and M. Haeri, "A note on the stability of fractional order systems," *Mathematics and Computers in Simulation*, vol. 79, no. 5, pp. 1566–1576, 2009.

[98] E. X. DeJesus and C. Kaufman, "Routh-hurwitz criterion in the examination of eigenvalues of a system of nonlinear ordinary differential equations," *Physical Review A*, vol. 35, no. 12, p. 5288, 1987.

[99] E. Ahmed, A. El-Sayed, and H. A. El-Saka, "On some Routh–Hurwitz conditions for fractional order differential equations and their applications in Lorenz, Rössler, Chua and Chen systems," *Physics Letters A*, vol. 358, no. 1, pp. 1–4, 2006.

[100] E. Ahmed, A. El-Sayed, and H. A. El-Saka, "Equilibrium points, stability and numerical solutions of fractional-order predator–prey and rabies models," *Journal of Mathematical Analysis and Applications*, vol. 325, no. 1, pp. 542–553, 2007.

[101] N. Aguila-Camacho, M. A. Duarte-Mermoud, and J. A. Gallegos, "Lyapunov functions for fractional order systems," *Communications in Nonlinear Science and Numerical Simulation*, vol. 19, no. 9, pp. 2951–2957, 2014.

[102] M. A. Duarte-Mermoud, N. Aguila-Camacho, J. A. Gallegos, and R. Castro-Linares, "Using general quadratic Lyapunov functions to prove Lyapunov uniform stability for fractional order systems," *Communications in Nonlinear Science and Numerical Simulation*, vol. 22, no. 1-3, pp. 650–659, 2015.

[103] Y. Li, Y. Chen, and I. Podlubny, "Stability of fractional-order nonlinear dynamic systems: Lyapunov direct method and generalized Mittag–Leffler stability," *Computers & Mathematics with Applications*, vol. 59, no. 5, pp. 1810–1821, 2010.

[104] S. Sastry, *Nonlinear systems: Analysis, stability, and control*, vol. 10. Springer Science & Business Media, 2013.

[105] C. Castillo-Chavez and B. Song, "Dynamical models of tuberculosis and their applications," *Mathematical Biosciences & Engineering*, vol. 1, no. 2, p. 361, 2004.

[106] M. Haque, "Ratio-dependent predator-prey models of interacting populations," *Bulletin of Mathematical Biology*, vol. 71, no. 2, pp. 430–452, 2009.

[107] J. Sotomayor, "Generic bifurcations of dynamical systems," in *Dynamical Systems*, pp. 561–582, Elsevier, 1973.

[108] L. Perko, *Differential equations and dynamical systems*, vol. 7. Springer Science & Business Media, 2013.

[109] K. Diethelm and A. D. Freed, "The fracPECE subroutine for the numerical solution of differential equations of fractional order," *Forschung und Wissenschaftliches Rechnen*, vol. 1999, pp. 57–71, 1998.

[110] M. Mittal, L. M. Goyal, J. K. Sethi, and D. J. Hemanth, "Monitoring the impact of economic crisis on crime in India using machine learning," *Computational Economics*, vol. 53, no. 4, pp. 1467–1485, 2019.

[111] P. Van den Driessche and J. Watmough, "Reproduction numbers and sub-threshold endemic equilibria for compartmental models of disease transmission," *Mathematical Biosciences*, vol. 180, no. 1-2, pp. 29–48, 2002.

[112] S. Abbas, J. P. Tripathi, and A. Neha, "Dynamical analysis of a model of social behavior: Criminal vs non-criminal population," *Chaos, Solitons & Fractals*, vol. 98, pp. 121–129, 2017.

[113] J. C. Nuno, M. A. Herrero, and M. Primicerio, "A triangle model of criminality," *Physica A: Statistical Mechanics and its Applications*, vol. 387, no. 12, pp. 2926–2936, 2008.

[114] L. G. Alves, H. V. Ribeiro, and R. S. Mendes, "Scaling laws in the dynamics of crime growth rate," *Physica A: Statistical Mechanics and its Applications*, vol. 392, no. 11, pp. 2672–2679, 2013.

[115] J. P. Tripathi, S. Bugalia, K. Burdak, and S. Abbas, "Dynamical analysis and effects of law enforcement in a social interaction model," *Physica A: Statistical Mechanics and its Applications*, vol. 567, p. 125725, 2021.

[116] R. M. Anderson and R. M. May, *Infectious diseases of humans: Dynamics and control*. Oxford University Press, 1992.

[117] N. T. Bailey, *The mathematical theory of infectious diseases and its applications*. Charles Griffin & Company Ltd, 5a Crendon Street, High Wycombe, Bucks HP13 6LE, 1975.

[118] F. Brauer and C. Castillo-Chávez, "Basic ideas of mathematical epidemiology," in *Mathematical Models in Population Biology and Epidemiology*, pp. 275–337, Springer, 2001.

[119] J. Shukla, V. Singh, and A. Misra, "Modeling the spread of an infectious disease with bacteria and carriers in the environment," *Nonlinear Analysis: Real World Applications*, vol. 12, no. 5, pp. 2541–2551, 2011.

[120] M. Ghosh, P. Chandra, P. Sinha, and J. Shukla, "Modelling the spread of carrier-dependent infectious diseases with environmental effect," *Applied Mathematics and Computation*, vol. 152, no. 2, pp. 385–402, 2004.

[121] Z. Zhonghua and S. Yaohong, "Qualitative analysis of a SIR epidemic model with saturated treatment rate," *Journal of Applied Mathematics and Computing*, vol. 34, no. 1, pp. 177–194, 2010.

[122] W. O. Kermack and A. G. McKendrick, "A contribution to the mathematical theory of epidemics," *Proceedings of the Royal Society of London. Series A, Containing Papers of a Mathematical and Physical Character*, vol. 115, no. 772, pp. 700–721, 1927.

[123] H. W. Hethcote, "The mathematics of infectious diseases," *SIAM Review*, vol. 42, no. 4, pp. 599–653, 2000.

[124] J. M. Miller and A. Blumstein, "Crime, justice & the COVID-19 pandemic: Toward a national research agenda," *American Journal of Criminal Justice*, vol. 45, no. 4, pp. 515–524, 2020.

[125] K. Bansal, S. Arora, K. S. Pritam, T. Mathur, and S. Agarwal, "Dynamics of crime transmission using fractional-order differential equations," *Fractals*, vol. 30, p. 2250012, 2022.

[126] M. Partohaghighi, V. Kumar, and A. Akgül, "Comparative study of the fractional-order crime system as a social epidemic of the USA scenario," *International Journal of Applied and Computational Mathematics*, vol. 8, no. 4, pp. 1–17, 2022.

[127] J.-Z. Zhang, Z. Jin, Q.-X. Liu, and Z.-Y. Zhang, "Analysis of a delayed SIR model with nonlinear incidence rate," *Discrete Dynamics in Nature and Society*, vol. 2008, 2008.

[128] R. Anderson and R. M. May, "Regulation and stability of host-parasite population interactions," *Journal of Animal Ecology*, vol. 47, no. 1, pp. 219–247, 1978.

[129] R. Xu and Z. Ma, "Stability of a delayed SIRS epidemic model with a nonlinear incidence rate," *Chaos, Solitons & Fractals*, vol. 41, no. 5, pp. 2319–2325, 2009.

[130] C. Wei and L. Chen, "A delayed epidemic model with pulse vaccination," *Discrete Dynamics in Nature and Society*, vol. 2008, 2008.

[131] X.-Z. Li, W.-S. Li, and M. Ghosh, "Stability and bifurcation of an SIR epidemic model with nonlinear incidence and treatment," *Applied Mathematics and Computation*, vol. 210, no. 1, pp. 141–150, 2009.

[132] I. A. Baba, R. A. Abdulkadir, and P. Esmaili, "Analysis of tuberculosis model with saturated incidence rate and optimal control," *Physica A: Statistical Mechanics and its Applications*, vol. 540, p. 123237, 2020.

[133] D. Xiao and S. Ruan, "Global analysis of an epidemic model with nonmonotone incidence rate," *Mathematical Biosciences*, vol. 208, no. 2, pp. 419–429, 2007.

[134] S. Ruan and W. Wang, "Dynamical behavior of an epidemic model with a nonlinear incidence rate," *Journal of Differential Equations*, vol. 188, no. 1, pp. 135–163, 2003.

[135] J. R. Beddington, "Mutual interference between parasites or predators and its effect on searching efficiency," *The Journal of Animal Ecology*, vol. 44, no. 1, pp. 331–340, 1975.

[136] D. L. DeAngelis, R. Goldstein, and R. V. O'Neill, "A model for tropic interaction," *Ecology*, vol. 56, no. 4, pp. 881–892, 1975.

[137] A. Boukhouima, K. Hattaf, E. M. Lotfi, M. Mahrouf, D. F. Torres, and N. Yousfi, "Lyapunov functions for fractional-order systems in biology: Methods and applications," *Chaos, Solitons & Fractals*, vol. 140, p. 110224, 2020.

[138] S. Bourafa, M. Abdelouahab, and A. Moussaoui, "On some extended Routh–Hurwitz conditions for fractional-order autonomous systems of order in $\alpha \in (0, 2)$ and their applications to some population dynamic models," *Chaos, Solitons & Fractals*, vol. 133, p. 109623, 2020.

[139] M. Habes, M. Alghizzawi, R. Khalaf, S. A. Salloum, and M. A. Ghani, "The relationship between social media and academic performance: Facebook perspective,"

International Journal of Information Technology and Language Studies, vol. 2, no. 1, pp. 12–18, 2018.

[140] D. Miller, J. Sinanan, X. Wang, T. McDonald, N. Haynes, E. Costa, J. Spyer, S. Venkatraman, and R. Nicolescu, *How the world changed social media*. UCL Press, 2016.

[141] N. McCarroll and K. Curran, "Social networking in education," *International Journal of Innovation in the Digital Economy*, vol. 4, no. 1, pp. 1–15, 2013.

[142] T. Kamal, M. Ishtiaq, K. Nawab, and M. Idrees, "An investigation into the negative impacts of social media on academic performance of youth," *New Media and Mass Communication*, vol. 34, pp. 50–56, 2015.

[143] H. T. Alemneh and N. Y. Alemu, "Mathematical modeling with optimal control analysis of social media addiction," *Infectious Disease Modelling*, vol. 6, pp. 405–419, 2021.

[144] N. Guelmami, M. ben Khalifa, N. Chalghaf, J. D. Kong, T. Amayra, J. Wu, F. Azaiez, and N. L. Bragazzi, "Preliminary development of the social media disinformation scale (SMDS-12) and its association with social media addiction and mental health: COVID-19 as a pilot case study," *JMIR Formative Research*, vol. 5, no. 6, p. e27280, 2021.

[145] N. Al-Qaysi, N. Mohamad-Nordin, and M. Al-Emran, "A systematic review of social media acceptance from the perspective of educational and information systems theories and models," *Journal of Educational Computing Research*, vol. 57, no. 8, pp. 2085–2109, 2020.

[146] A. Arora, S. Bansal, C. Kandpal, R. Aswani, and Y. Dwivedi, "Measuring social media influencer index-insights from Fcebook, Twitter and Instagram," *Journal of Retailing and Consumer Services*, vol. 49, pp. 86–101, 2019.

[147] W. M. Al-Rahmi and A. M. Zeki, "A model of using social media for collaborative learning to enhance learners' performance on learning," *Journal of King Saud University-Computer and Information Sciences*, vol. 29, no. 4, pp. 526–535, 2017.

[148] M. Mahdi, "Undergraduate students' perceptions toward social media usage and academic performance: A study from Saudi Arabia.," *International Journal of Emerging Technologies in Learning*, vol. 14, no. 3, 2019.

[149] K. Bansal, T. Mathur, N. S. S. Singh, and S. Agarwal, "Analysis of illegal drug transmission model using fractional delay differential equations," *AIMS Mathematics*, vol. 7, no. 10, pp. 18173–18193, 2022.

[150] K. Bansal, T. Mathur, and S. Agarwal, "Fractional-order crime propagation model with non-linear transmission rate," *Chaos, Solitons & Fractals*, vol. 169, p. 113321, 2023.

[151] P. Ramesh, M. Sambath, M. H. Mohd, and K. Balachandran, "Stability analysis of the fractional-order prey-predator model with infection," *International Journal of Modelling and Simulation*, vol. 41, no. 6, pp. 434–450, 2021.

[152] P. Panja, "Dynamics of a fractional order predator-prey model with intraguild predation," *International Journal of Modelling and Simulation*, vol. 39, no. 4, pp. 256–268, 2019.

[153] A. H. Goldsmith, J. R. Veum, and W. Darity Jr, "The psychological impact of unemployment and joblessness," *The Journal of Socio-Economics*, vol. 25, no. 3, pp. 333–358, 1996.

[154] R. Tarling, "Unemployment and crime," *Home Office Research Bulletin*, vol. 14, pp. 28–33, 1982.

[155] R. L. Jin, C. P. Shah, and T. J. Svoboda, "The impact of unemployment on health: A review of the evidence," *CMAJ: Canadian Medical Association Journal*, vol. 153, no. 5, p. 529, 1995.

[156] S. Sundar, A. Tripathi, and R. Naresh, "Does unemployment induce crime in society? A mathematical study," *American Journal of Applied Mathematics and Statistics*, vol. 6, no. 2, pp. 44–53, 2018.

[157] R. M. Al-Maalwi, H. Ashi, and S. Al-sheikh, "Unemployment model," *Applied Mathematical Sciences*, vol. 12, no. 21, pp. 989–1006, 2018.

[158] S. Al-Sheikh, R. Al-Maalwi, and H. Ashi, "A mathematical model of unemployment with the effect of limited jobs," *Comptes Rendus Mathematique*, vol. 359, no. 3, pp. 283–290, 2021.

[159] R. Al-Maalwi, S. Al-Sheikh, H. Ashi, and S. Asiri, "Mathematical modeling and parameter estimation of unemployment with the impact of training programs," *Mathematics and Computers in Simulation*, vol. 182, pp. 705–720, 2021.

[160] A. Galindro and D. F. Torres, "A simple mathematical model for unemployment: A case study in Portugal with optimal control," *Statistics, Optimization & Information Computing*, vol. 6, no. 1, pp. 116–129, 2018.

[161] S. B. Munoli and S. Gani, "Optimal control analysis of a mathematical model for unemployment," *Optimal Control Applications and Methods*, vol. 37, no. 4, pp. 798–806, 2016.

[162] S. B. Munoli, S. Gani, and S. R. Gani, "A mathematical approach to employment policies: An optimal control analysis," *International Journal of Statistics and Systems*, vol. 12, no. 3, pp. 549–565, 2017.

[163] G. Pathan and P. Bhathawala, "Mathematical model for unemployment control-A numerical study," *International Journal of Mathematics Trend and Technology*, vol. 49, no. 4, pp. 253–259, 2017.

[164] P. Olumese, "Epidemiology and surveillance: Changing the global picture of malaria–myth or reality?," *Acta Tropica*, vol. 95, no. 3, pp. 265–269, 2005.

[165] R. W. Snow, C. A. Guerra, A. M. Noor, H. Y. Myint, and S. I. Hay, "The global distribution of clinical episodes of plasmodium falciparum malaria," *Nature*, vol. 434, no. 7030, pp. 214–217, 2005.

[166] E. Kondilis, S. Giannakopoulos, M. Gavana, I. Ierodiakonou, H. Waitzkin, and A. Benos, "Economic crisis, restrictive policies, and the population's health and health care: The Greek case," *American Journal of Public Health*, vol. 103, no. 6, pp. 973–979, 2013.

[167] W. H. Organization, *International travel and health: Situation as on 1 January 2007*. World Health Organization, 2007.

[168] J. Tumwiine, S. D. Hove-Musekwa, and F. Nyabadza, "A mathematical model for the transmission and spread of drug sensitive and resistant malaria strains within a human population," *International Scholarly Research Notices*, vol. 2014, 2014.

[169] W. H. Organization, *World malaria report 2020: 20 years of global progress and challenges*. World Health Organization, 2020.

[170] W. H. Organization, *World malaria report 2021*. World Health Organization, 2021.

[171] H. S. Gold and R. C. Moellering Jr, "Antimicrobial-drug resistance," *New England Journal of Medicine*, vol. 335, no. 19, pp. 1445–1453, 1996.

[172] J. K. Baird, "Chloroquine resistance in plasmodium vivax," *Antimicrobial Agents and Chemotherapy*, vol. 48, no. 11, pp. 4075–4083, 2004.

[173] J. K. Baird, N. Valecha, S. Duparc, N. J. White, and R. N. Price, "Diagnosis and treatment of plasmodium vivax malaria," *The American Journal of Tropical Medicine and Hygiene*, vol. 95, no. 6, p. 35, 2016.

[174] P. B. Bloland and W. H. Organization, "Drug resistance in malaria," tech. rep., World Health Organization, 2001.

[175] Y. Lubell, A. Dondorp, P. J. Guérin, T. Drake, S. Meek, E. Ashley, N. P. Day, N. J. White, and L. J. White, "Artemisinin resistance–modelling the potential human and economic costs," *Malaria Journal*, vol. 13, no. 1, pp. 1–10, 2014.

[176] K. U. Jansen, C. Knirsch, and A. S. Anderson, "The role of vaccines in preventing bacterial antimicrobial resistance," *Nature Medicine*, vol. 24, no. 1, pp. 10–19, 2018.

[177] N. J. White, "Antimalarial drug resistance," *The Journal of Clinical Investigation*, vol. 113, no. 8, pp. 1084–1092, 2004.

[178] J. Huo, H. Zhao, and L. Zhu, "The effect of vaccines on backward bifurcation in a fractional order HIV model," *Nonlinear Analysis: Real World Applications*, vol. 26, pp. 289–305, 2015.

[179] N. Sweilam, S. AL-Mekhlafi, and A. Albalawi, "Optimal control for a fractional order malaria transmission dynamics mathematical model," *Alexandria Engineering Journal*, vol. 59, no. 3, pp. 1677–1692, 2020.

[180] A. Carvalho and C. M. Pinto, "A delay fractional order model for the co-infection of malaria and HIV/AIDS," *International Journal of Dynamics and Control*, vol. 5, no. 1, pp. 168–186, 2017.

[181] D. Pawar, W. Patil, and D. Raut, "Analysis of malaria dynamics using its fractional order mathematical model," *Journal of Applied Mathematics & Informatics*, vol. 39, no. 1_2, pp. 197–214, 2021.

[182] W. Ma, C. Li, Y. Wu, and Y. Wu, "Synchronization of fractional fuzzy cellular neural networks with interactions," *Chaos: An Interdisciplinary Journal of Nonlinear Science*, vol. 27, no. 10, p. 103106, 2017.

[183] W. Ma, C. Li, and J. Deng, "Synchronization in tempered fractional complex networks via auxiliary system approach," *Complexity*, vol. 2019, 2019.

[184] J. M. Tchuenche, C. Chiyaka, D. Chan, A. Matthews, and G. Mayer, "A mathematical model for antimalarial drug resistance," *Mathematical Medicine and Biology: A Journal of the IMA*, vol. 28, no. 4, pp. 335–355, 2011.

List of Research Publications

1. **Komal Bansal**, Sugandha Arora, Kocherlakota Satya Pritam, Trilok Mathur, and Shivi Agarwal (2022), " Dynamics of crime transmission using fractional-order differential equations." *Fractals*, 30(01), 2250012. (I.F.- 4.7, SCI-Q1)
   DOI: 10.1142/S0218348X22500128

2. **Komal Bansal**, Trilok Mathur, Narinderjit Singh Sawaran Singh, and Shivi Agarwal (2022), "Analysis of illegal drug transmission model using fractional delay differential equations." *AIMS Mathematics*, 7(10), 18173-18193. (I.F.- 2.2, SCI-Q2)
   DOI:10.3934/math.20221000

3. **Komal Bansal**, Trilok Mathur, and Shivi Agarwal (2023), "Fractional-order crime propagation model with non-linear transmission rate." *Chaos, Solitons & Fractals*, 169, 113321. (I.F.- 7.8, SCI-Q1)
   DOI: 10.1016/j.chaos.2023.113321

4. **Komal Bansal**, Trilok Mathur, and Shivi Agarwal (2023), "The LADM approach to analyze the fractional order model for smoking habits including memory." In *AIP Conference Proceedings*, 2819(1). AIP Publishing. (Scopus)
   DOI:10.1063/5.0136966

5. **Komal Bansal**, Tripti Mathur, Trilok Mathur, Shivi Agarwal, and R.D. Sharma, "Impact of social media on academics: A fractional order mathematical model." *International Journal of Modelling and Simulation*. (I.F.- 3.1, ESCI/Scopus-Q2)
   DOI:10.1080/02286203.2023.2286419

6. Neelu Pareek, **Komal Bansal**, Arvind Gupta, Ruchi Mathur, Trilok Mathur, and Shivi Agarwal, "LVIM approach to analyze the fractional order model for childhood diseases." *Journal of Health Management*. (I.F.-2.3, ESCI/Scopus-Q3) (*Accepted*)

7. **Komal Bansal** and Trilok Mathur, "Fractional-order crime propagation model: A comparison between logistic and exponential growth." (*Communicated*)

8. **Komal Bansal**, and Trilok Mathur, "Impact of skills development on youth unemployment: A fractional order mathematical model." (*Communicated*)

9. **Komal Bansal**, and Trilok Mathur, "Analysis of the drug resistance level of malaria disease: A fractional-order model." (*Communicated*)

10. **Komal Bansal**, Trilok Mathur, and Shivi Agarwal, "Modeling crime transmission with fear effect: A fractional-order approach for effective crime control strategies." (*Communicated*)

11. Savita Rathee, Yogeeeta Narwal, **Komal Bansal**, and Trilok Mathur, "Analyzing unemployment dynamics with real data: A fractional-order mathematical model." (*Communicated*)

Conferences/Workshops

Conferences

1. **International Conference and 22nd Annual Convention of Vijñāna Parishad of India on Advances in Operations Research, Statistics and Mathematics (AOSM-2019)** Organized by Department of Mathematics, BITS Pilani, Pilani Campus, Pilani-333031, India (28/12/2019–30/12/2019).

2. **International Conference on Advances in Differential Equations and Numerical Analysis (ADENA-2020)** Organized by Department of Mathematics, IIT-Guwahati, India (12/10/2020–15/10/2020). (Presented)

3. **International Conference on Fractional Calculus (ICFC-2022)** Organized by School of Mathematics and Statistics, University of Hyderabad, India (18/01/2022–19/01/2022). (Presented)

4. **International Conference on Advances in Mechanics, Modelling, Computing and Statistics (ICAMMCS-2022)** Organized by Department of Mathematics, BITS Pilani, Pilani Campus, Rajasthan (19/03/2022–21/03/2022).

5. **Applied Mathematics in Science and Engineering (AMSE-2022)** Organized by Centre for Data Science Siksha 'O' Anusandhan Bhubaneswar, Odisha, India (24/03/2022–26/03/2022). (Presented)

Workshops

1. **International Workshop on Stochastic Simulation and Its Applications (WSSA-2019)** organized by Department of Mathematics, BITS Pilani, Pilani Campus, Pilani-333031, India (24/12/2019–27/12/2019).

2. A Three Day National Webinar on **Covid-19 & Indian Economy** organized by School of Social Sciences, Central University of Gujarat, in collaboration with Students for Holistic Development of Humanity (SHoDH) & Knowledge Partner ICSSR (06/06/2020–11/06/2020).

3. Short Term Training Programme (STTP) On **Fractional Calculus: Foundations to Frontiers (FCFF-2020)** in association with Center for Continuing Education (CCE), SVNIT Organized by Department of Applied Mathematics & Humanities, SVNIT, Surat (28/12/2020–01/01/2021).

4. Short Term Training Programme (STTP) on **Mathematical Modelling & Control System Design** organized by the Department of Electronics Engineering, Ramrao Adik Institute of Technology, D Y Patil Deemed To Be University, Navi Mumbai (28/06/2021–03/07/2021).

5. **International Workshop on Recent Advancements in Data Envelopment Analysis and Applications (IWRADEAA-2021)** organized by Department of Mathematics, BITS Pilani, Pilani Campus, India (10/07/2021–11/07/2021).

6. **International Workshop on Fractional Derivatives: Theory & Computations with Applications (FDTCA-2021)** held at Department of Mathematical Sciences, Indian Institute of Technology (BHU) Varanasi (12/11/2021–14/12/2021).

7. Workshop on **Artificial Intelligence Application for Elecro-Optical (EO) Sensors** organized jointly by BITS Pilani, Pilani Campus and IRDE Dehradun, India (on 04/02/2022).

Biography of the Candidate

Ms. Komal completed her B.Sc. from Maharshi Dayanand University, Rohtak, and subsequently her M.Sc. in Mathematics from Guru Jambheshwar University of Science & Technology, Hisar. She has qualified the CSIR-UGC Junior Research Fellowship (JRF) test and the National Eligibility Test (NET) in Mathematical Sciences in December 2018. Her academic journey led her to embark on a full-time Ph.D. program in 2019 within the Department of Mathematics at BITS Pilani, Pilani Campus, India under the guidance of Prof. Trilok Mathur. Her primary interests encompass Fractional Calculus, Fractional Differential Equations, Delay Differential Equations, Mathematical Modeling, Stability Analysis, and Bifurcation Analysis. She has also been delving into the practical applications of fractional calculus within the realms of sociology, economics and epidemiology, showcasing the interdisciplinary nature of her work. Beyond her research endeavors, she has actively contributed to the academic environment at BITS Pilani, Pilani Campus by serving as a teaching assistant for various mathematics courses. For a deeper exploration of her research contributions, her profile on ResearchGate offers valuable insights: https://www.researchgate.net/profile/Komal-Bansal-3. To connect with her directly contact at komalbansal600@gmailcom.

Biography of the Supervisor

Prof. Trilok Mathur is an associate professor in the Department of Mathematics at Birla Institute of Technology and Science Pilani, Pilani campus. Prior to this, he served as an Assistant Professor at BITS Pilani for over a decade, from 2008 to 2021. His dedication to education extended to Banasthali University, where he held the position of Assistant Professor from 2005 to 2008. He received his Ph.D. in 2005 under the esteemed guidance of Prof. S.P. Goyal, Emeritus Professor at the Department of Mathematics, University of Rajasthan, Jaipur. His doctoral thesis, titled "A study of certain properties of generalized special functions and a general class of polynomials with applications," demonstrated his early dedication to specialized mathematical areas. His interests encompass a wide spectrum of mathematical domains, reflecting his multi-faceted approach to the discipline. His expertise in Fractional Calculus based Mathematical Modeling, Special Functions, Geometric Function Theory, Fuzzy Logic, Neural Networks, Image Processing, Artificial Intelligence, Data Envelopment Analysis, and Multi Criteria Decision Making Techniques underscores his versatile contributions to the field. He has published more than 40 research papers and articles in various refereed journals of international repute and presented his work at many international conferences. He visited many universities of international repute like VSB Technical University of Ostrava, Ostrava, Leshan Normal University, China, Ivan Frankov National University, Ukrain, Imperial College, London, U.K., University of Malaya, Malaysia, Waseda University, Tokyo, Japan to present his research work. For a deeper exploration of his research contributions, his profile on ResearchGate offers valuable insights: https://universe.bits-pilani.ac.in/pilani/tmathur/Profile. To connect with him directly contact him at tmathur@pilani.bits-pilani.ac.in.